QoS-Based Power Management Techniques for Uplink W-CDMA Cellular Systems

By

Ting-Chen Song

Studyleader: Professor L.P. Linde & Professor X. Xia

Submitted in partial fulfillment of the requirements for the degree

Master of Engineering (Electronics)

in the

Department of Electrical, Electronic & Computer Engineering, Built Environment & Information Technology

in the

School of Engineering

in the

Faculty of Engineering, Built Environment & Information Technology

UNIVERSITY OF PRETORIA

December 2002

SUMMARY

QoS-Based Power Management Techniques for Uplink W-CDMA Cellular Systems

by

Ting-Chen Song

Studyleader: Professor L.P. Linde & Professor X. Xia

Department of Electrical, Electronic & Computer Engineering

Master of Engineering (Electronics)

In the past, the design of PC algorithms for CDMA systems has remained at the physical layer to compensate for slow and fast channel impairments (known as fast PC and slow PC). The TDMA/FDMA manages inter-cell interference at the beginning of the radio planning process. In SS technology, real time adaptive PC and power management algorithms would need to work coherently to ensure reliable multi-media services, and the need for this real-time hybrid structure of PC and power management has only been shown recently. The emphasis in this dissertation is therefore on the design of a QoS-based PC structure in W-CDMA applications, the ultimate goal being to evaluate the new QoS-based PC structure by means of a Monte Carlo computer simulation; a multi-user, multimedia W-CDMA simulation package. Before the design of the QoS-based PC structure, this dissertation examines and proposes a new power-sensitive model that addresses factors affecting the W-CDMA system capacity. Consequently, PC problems are put into a framework for various optimization criteria. Finally the design of a QoS-based PC structure by means of Monte Carlo computer simulation is described and evaluate.

The first problem is closely related to the fact that W-CDMA is a design of a power management network architecture. The power management can co-exist in every layer of operation with different specific time scale and optimization objectives. The solution to this problem is therefore to introduce a general and mathematically tractable *power-sensitive model* to identify factors that influence the capacity of W-CDMA cellular systems and then

articulate the general power sensitive model to form a PC framework aimed at finding a common systematic treatment for different schools of thought on PC algorithms. This dissertation proves the benefits of layered PC operation for guaranteed QoS transmission and also shows that this research coincides with and extend the literature on PC management by categorizing PC algorithms according to various optimization objectives and time scales.

The **second** problem is to evaluate the new QoS-based PC structure in a channel coded and RAKE combining uplink UMTS/UTRA cellular environment using the Monte Carlo simulation package. The UMTS radio channel models are described in terms of frequency-selective Rayleigh fading: *Indoor-Office*, *Outdoor and Pedestrian* and *Vehicular* environments. The package is simulated in Matlab. The influence of the number of multipath components, of Doppler Spread, the number of received antenna, the coding scheme and multi-access interference are discussed in the dissertation. The performance evaluation criteria for utility-based PC structures are Bit-Error-Rate (BER) performance (robustness), outage performance (tracking ability) and rate of convergence. The first test shows that the new proposed unbalanced step-size closed-loop FPC schemes can provide better SINR tracking ability and better BER performance than conventional balanced step-size PC schemes. The unbalanced FPCs have better PC error distribution in all scenarios. The second test shows that the proposed BER-prediction distributed OPC schemes can provide better BER *tracking ability*. This scheme converges iteratively to an optimal SINR level under current network settings with no excessive interference to other active users..

Keywords:

multi-media, W-CDMA, UMTS/IMT-2000, soft capacity, resource allocation, interference management, Signal to Interference and Noise Ratio (SINR), Quality of Service (QoS), Bit-Error-Rate (BER), power-sensitive model, intra-cell interference, inter-cell interference, Fast PC (FPC), Outer-loop PC (OPC), Network PC (NPC), Doppler spread, Multi-Access Interference (MAI), tracking ability, iterative processing.

OPSOMMING

QoS-Based Power Management Techniques for Uplink W-CDMA Cellular Systems

deur

Ting-Chen Song

Studieleier: Professor L.P. Linde & Professor X. Xia

Departement Elektriese-,Elektroniese- & Rekenaar Ingenieurswese

Meester in Ingenieurswese (Elektronies)

In die verlede het die ontwerp van drywingsbeheeralgoritmes vir kodedivisie-multitoegang (CDMA) stelsels by die fisiese vlak gebly om te kompenseer vir stadige en vinnige kanaal tekortkomings (bekend as vinnige drywingsbeheer (DB) en stadige DB). TDMA/FDMA beheer interselsteuring in die begin van die radiobeplanningsproses. In SS tegnologie, moet intydse aanpasbare DB en DB-bestuuralgoritmes saamwerk om betroubare multimedia dienste te verseker. Die behoefte vir hierdie intydse saamgestelde struktuur van DB en drywingsbestuur is eers onlangs bewys. Die klem van hierdie verhandeling is daarom die ontwerp van 'n Kwaliteit-van-Diens (QoS)-gebaseerde DB struktuur met toepassing in W-CDMA. Die doel is om die nuwe QoS-gebaseerde DB struktuur te evalueer deur van Monte Carlo rekenaarsimulasies gebruik te maak; 'n multi-gebruiker, multimedia W-CDMA simulasiepakket. Voor die ontwerp van 'n QoS-gebaseerde DB struktuur gedoen word, word 'n nuwe drywingsensitiewe model bestudeer en voorgestel. Hierdie model addresseer faktore wat W-CDMA stelselkapasiteit affekteer. Gevolglik word die DB probleem in 'n raamwerk van verskeie optimeringskriteria geplaas. Laastens word die ontwerp van 'n QoS-gebaseerde DB struktuur, met behulp van Monte Carlo rekenaarsimulasie, beskryf en geëvalueer.

Die eerste probleem hou nou verband met die feit dat W-CDMA die ontwerp van 'n drywingsbeheerde netwerkargitektuur is. Die drywingsbeheer kan op elke vlak van operasie saamwerk, elk met verskillende tydskale en optimeringskriteria. Die oplos van die probleem

behels die opstel van 'n algemene, wiskundig-aanvaarbare *drywingsensitiewe model* om die faktore wat die kapasiteit van W-CDMA sellulêre stelsels beïnvloed, te identifiseer en dan die algemene drywingsensitiewe model te artikuleer, sodanig dat 'n DB raamwerk, gemik op 'n algemene sistematiese ondersoek van verskeie DB algoritmes, gevind kan word. Hierdie verhandeling bewys die voordele van vlakgebaseerde DB operasie, sodanig dat QoS transmissie verseker word. Daar word ook getoon dat hierdie navorsing saamval met en bestaande literatuur oor DB bestuur uitbrei, deur die DB algoritmes volgens verskeie optimeringsdoelwitte en tydskale te kategoriseer.

Die **tweede** probleem is om die nuwe QoS-gebaseerde DB struktuur in 'n kanaalgekodeerde en RAKE gekombineerde opwaartse UMTS/UTRA sellulêre omgewing te evalueer, deur van die Monte Carlo simulasieprogram gebruik te maak. UMTS radiokanaalmodelle word in terme van frekwensieselektiewe Rayleigh deining (*Binnenshuis-kantoor*, *buite en voetganger* en *bewegende* omgewings beskryf. Die pakket word gesimuleer in Matlab. Die invloed van die aantal multipadkomponente, Doppler-spreiding, die getal ontvangsantennas, die koderingsskema en multi-gebruikerruis word in die verhandeling bespreek. Die werkverrigting-evalueringskriteria vir toepassingsgebaseerde DB strukture is: Bisfouttempo (BER) verrigting (robuustheid), onderbrekings-werkverrigting (volginsvermoë) en konvergeringsvermoë. Die eerste toets dui aan dat die nuwe voorgestelde, gebalanseerde stapgrootte, geslote lus FPC struktuur beter SINR volgvermoë, asook beter BER verrigting as konvensionele gebalanseerde stapgrootte DB skemas verseker. Die ongebalanseerde FPCs het beter DB foutverspreiding vir alle gevalle. Die tweede toets dui aan dat die voorgestelde BER-voorspelde verspreide OPC skemas beter BER *volgvermoë* kan verseker. Hierdie skema konvergeer iteratief na 'n optimale SINR vlak onder die huidige netwerkopstelling met geen buitensporige steuring vir ander aktiewe gebruikers nie..

Sleutelwoorde:

multi-media, W-CDMA, UMTS/IMT-2000, sagte kapasiteit, hulpbrontoekenning, steuringsbeheer, Sein tot Steuring en Ruisverhouding (SINR), Kwaliteit-van-diens (QoS), Bisfouttempo (BER), drywingsensitiewe model, intra-sel steuring, inter-sel steuring, Vinnige DB (FPC), Buitelus DB (OPC), Netwerk DB (NPC), Doppler-spreidng, Multi-toegang steuring (MAI), volgvermoë, iteratiewe verwerking.

ACKNOWLEDGEMENT

The author would like to express his sincere appreciation to his advisors, Prof. L.P. Linde, Prof. X. Xia and Prof. P.G.W van Rooyen for their enthusiastic guidance and advice throughout this research. Appreciation and thanks are extended to my colleagues from Department of Electrical, Electronic and Computer Engineering, Built Environment & Information Technology: Mr. J.H. van Wyk, Mr. P. Roux, Mr. A. Pandey, Mr. L. Staphorst and Dr. M. Lötter for their understanding, patience and suggestions during this research.

The author would like to send a special thanks to Mrs. Lorna Chalmers, Department of English, for her kindness and patient. A deepest gratitude to his parents, two brothers, Jackson and Davy and Ming-Chen Tsai for their encouragement, patience and support throughout his study.

Also, to my creator and heavenly Father, my saviour Jesus Christ and my companion the Holy Spirit.

CONTENTS

LIST OF FIGURES

LIST OF TABLES

ABBREVIATIONS

3GPP	3^{rd} Generation Partnership Project (produces W-CDMA standard)
ACTS	Advanced Communication Technologies and Systems
	EU Research Projects Framework
APC	Adaptive Power Control
PSTN	Fixed Public Telephone Network
ARIB	Association of Radio Industries and Businesses (Japan)
AWGN	Asymmetric Digital Subscriber Loop
BER	Bit Error Rate
BPSK	Binary Phase Shift Keying
BS	Base Station
BSA	Base Station Assignment
cdf	Cumulative Distribution Function
CDMA	Code Division Multiple Access
CIR	Carrier to Interference Ratio
CRC	Cyclic Redundancy Check
DCH	Dedicated Channel
DM	Delta Modulation
DS	Digital Signal
DPA	Diversity Power Assignment
DPCCH	Dedicated Physical Control Channel
DPDCH	Dedicated Physical Data Channel
ETSI	European Telecommunications Standards Institute
FA	Fixed Assignment
FDD	Frequency Division Duplex
FDMA	Frequency Division Multiple Access
FER	Frame Error Rate
FPC	Fast Power Control

iid	Independent, Identically Distributed
IPC	Inner-loop Power Control
IMT-2000	International Mobile Telecommunications by the year 2000
ITU	International Telecommunications Union
LOS	Line of Sight
MA	Multi-Access
MAC	Medium Access Control
MAI	Multi-Access Interference
MIP	Multipath Intensity Profile
MPA	Minimal Power Assignment
MRC	Maximum Ratio Combining
MROPA	Multi-rate Outer Power Assignment
MS	Mobile Station
MT-PC	Multi-Target Adaptive Power Control
MUD	Multiuser Detection
MUPC	Multi-target Utility-based Power Control
N-CDMA	Narrowband Code Division Multiple Access
NPC	Network Power Control
OPC	Outer-loop Power Control
OVSF	Orthogonal Variable Spreading Factor
PC	Power Control
PCM	Pulse Coded Modulation
PDA	Power Distributed Algorithm
pdf	Probability Density Function
QoS	Quality of Service
QPSK	Quadrature Phase Shift Keying
RE	Resource Estimator
RNC	Radio Network Controller
RRM	Radio Resource Management
Rx	Received Signal
SIR	Signal to Interference Ratio
SINR	Signal to Interference and Noise Ratio
SNR	Signal to Noise Ratio
SS	Spread Spectrum

STOPA	Space-Time Processing and Outer Power Assignment
TDMA	Time Division Multiple Access
TPC	Transmitted Power Control
Tx	Transmission Signal
ULA	Uniform Linear Array
UMTS	Universal Mobile Telecommunications Service
UTRA	UMTS Terrestrial Radio Access (ETSI)
W-CDMA	Wideband Code Division Multiple Access

LIST OF SYMBOLS

K	Number of base stations
k	Assigned base station
N	Number of active users within base station k
i	Reference user
W	total bandwidth
$\mathbf{P} = [P_1, P_2, ...P_N]$	transmitted power vector for user i
$P_i \leq P_i^{\max}$	maximum power level
$\mathbf{R} = [R_1, R_2, ...R_N]$	Vector of rates
E_b/N_o	SINR
γ	BER/FER requirement
$\mathbf{R}$	The vector of rates
$b_i(l)$	Information symbol stream
$d_i(\tau)$	The sequence output at encoder and interleaver.
l	Number of user data
k/n	A rate k/n coding scheme
L	Symbol Interval
$1/T_b$	Data rate at symbols per seconds (sps) .
$1/T_d = n/kT_b$	Coded data rate at symbols per seconds (sps).
$1/T_c = C/T_d = nC/kT_b$	Chips per second (cps)
τ	Symbol interval index.
C	Spreading Gain.
$G = \frac{1/T_c}{1/T_b} = \frac{nCT_b}{kT_b} = \frac{nC}{k}$	Processing Gain.
$s_i(\tau)$	Spreading sequence.
$x_i(\tau) = d_i(\tau) * (\mathrm{u}_1 \otimes \mathrm{s}_i(\tau)) * \mathrm{p}$	Transmitted signal for user i.
$\mathrm{r} = \sum_{\tau=0}^{L-1} \sum_{i=1}^{N} \mathrm{x}_i(\tau) + \mathrm{n}$	The received signal after A/D conversion.
n	A iid complex Gaussian random variables of

CHAPTER ONE

INTRODUCTION

A graphical display of the dissertation layout is shown in Figure. 1.1. An introduction to Spread Spectrum cellular communication systems is presented in section 1.1. A literature survey is described in section 1.2. Basic definitions and operating principles of PC problems are presented in section 1.2.2; The importance of PC algorithms in multi-media systems is described in section 1.2.3. The limitations of current PC algorithms is described in 1.3. An outline of the goals of this dissertation is presented in section 1.4. Specific contributions of this dissertation are listed in section 1.5 and its layout is described in section 1.6.

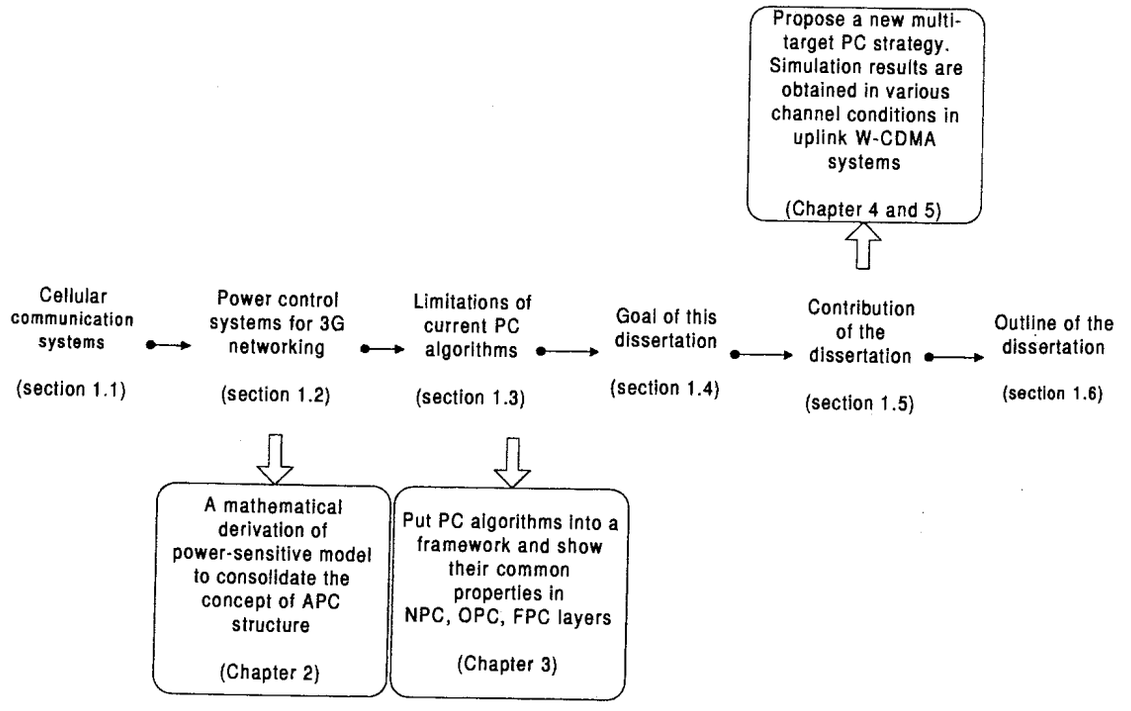

FIGURE 1.1: Overview of chapter 1

1.1 CELLULAR COMMUNICATION SYSTEMS

Because of the strong demand for personal communication systems and services, wireless networking is fast becoming a major component of today's communication infrastructure. In terms of business volume, wireless networking could even become a serious challenge to wireline networking, provided it can be extended, as traditional wireline networks have been, to multi-media and high-speed data applications.

First and second-generation cellular systems were designed primarily for voice communication, and provide data services only at relatively low rates. Third-generation systems recently introduced, are designed for multi-media communication. In the future, person-to-person communication will be enhanced with high quality images and video and access to information and services on public and private networks. For a communication system to be competitive it must have a high throughput, as well as integration of services including telephony, data, video and IP, and also interworking between different wireless networks [Figure 1.2].

However, to extend wireless communication systems to multi-media services, a broader frequency bandwidth is required which, given the lack of spectrum availability, is a major problem, especially in metropolitan areas. One solution is to use wideband code-division multiple-access (W-CDMA) technology. Over the past several years, it has been shown that W-CDMA is a viable alternative to both frequency-division multiple-access (FDMA) and time-division multiple-access (TDMA) technologies and has, in fact, emerged as the dominant next-generation wireless communication system worldwide.

Its specification has been created in 3GPP (the 3^{rd} Generation Partnership Project), which is a joint project of standardization bodies from Europe, Japan, Korea, the USA and China. Within 3GPP, W-CDMA is called UTRA (Universal Terrestrial Radio Access) FDD (Frequency Division Duplex) and TDD (Time Division Duplex). This dissertation focuses on the W-CDMA FDD technology because the uplink of a cellular network is, in general, the capacity limiting factor. The use of W-CDMA technology has been extensively researched and developed [4, 18, 28, 45, 58, 76, 81, 83, 86].

1.1.1 Advantages Of W-CDMA Technology

Even though the W-CDMA technology is not superior under all conditions to conventional multiple access in commercial wireless communication systems, it is the characteristics of spread-spectrum (SS) waveforms and sharing resources that give W-CDMA certain

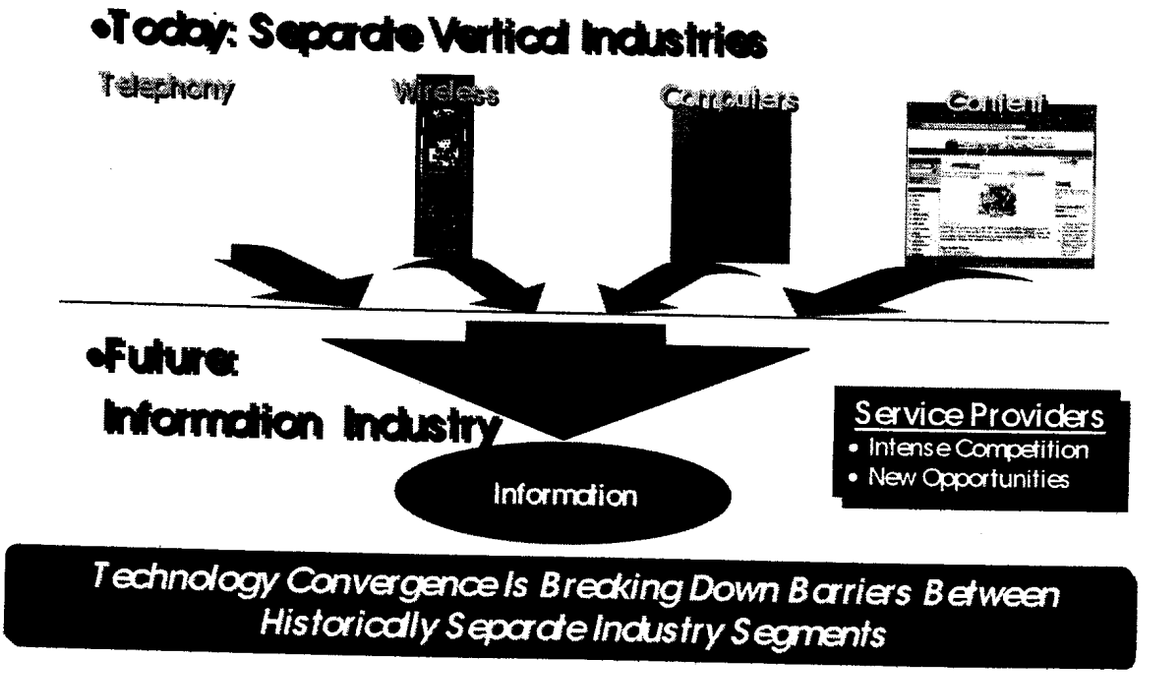

FIGURE 1.2: Technology convergence is breaking down barriers between historically separate industry segments

advantages.

It is well known that SS waveforms are effective in mitigating multipath fading, which can be attributed to its wider bandwidth which introduces frequency diversity. For the same reason, W-CDMA is also useful in mitigating interference. Medard [125] has determined that it is the uncertainty in estimating the time-varying wireless channels that degrades cellular capacity, not its time-varying nature. This coarse acquisition inadequacy has been investigated and it has been shown that wideband spreading waveforms provide better performance in a time-varying wireless channel than narrowband waveforms [64, 65]: a wideband digital waveform received at the base station has multiple correct paths, and the likelihood of observing a correct path during the search process is increased compared to what it would be for narrowband. Also, Rappaport [81] has shown that the accuracy of power measurement can be improved with an increase in spreading bandwidth because narrowband waveforms experience more attenuation due to multipath fading than W-CDMA does. Perfect acquisition and tracking of the spreading sequence described in the literature is usually assumed if pilot channels are associated with each data channel.

Furthermore, the characteristic of sharing resources providing a N=1 frequency re-use factor, allows a network to be built within a single frequency channel. Thus, three advantages of this characteristic are that it: allows a flexible number of users in a given channel; is

capable of providing multi-media services to handsets and provides potentially higher radio capacity. W-CDMA can also enhance efforts in space-time processes and radio resource management due to its frequency diversity feature.

1.1.2 Disadvantages Of W-CDMA Technology

Second-generation cellular systems were developed for voice transport at a time when 75% of traffic in the world was voice. Consequently, these systems were optimized to offer telephone and low-date rate services. However, since FDMA/TDMA cellular systems require preliminary radio planning, advanced quality-of-service (QoS) mechanisms are not necessary, because the frequency re-use factor, N, of these systems is greater than one. The impact of the Internet has led to a dramatic growth in data traffic and multi-media services for W-CDMA cellular systems where different bandwidth and QoS requirements become essential.

However, because the entire transmission bandwidth is shared amongst all users at all times, this implies that the system capacity is very much dependent on multiple-access interference (MAI) which may be characterized as any combination of spectrum sharing interference signals, self-jamming by delayed signals, and inter-cell interference signals. The transmitted power and power distribution must be carefully planned and controlled if optimal system performance and maximal traffic capacity are to be achieved.

The disadvantages of W-CDMA are summarized below:

- CDMA is interference- and resources-limited: the number of users that can be accommodated within the same frequency band with acceptable performance, is determined by the total interference power of all users, taken as a whole, generated at the base station.

- The near-far effect: those W-CDMA transmitters that are closer to the receiver will cause overwhelming interference by saturating the receiver front-end to the detriment of the weaker signals received, which will be regarded as interference and treated as such. Power control (PC) or interference cancellation techniques become essential.

- Channel impairment: the wireless channel may be highly erratic and essentially stochastic in the presence of mobility. Most researchers have applied statistical techniques to describe signal variations in cellular mobile environments. Online link QoS monitoring mechanisms and online resource and interference management are required to ensure QoS to subscribers.

Thus, a resource management structure with online link QoS monitoring, online resource and interference management, and QoS assurance for adaptation to changes induced by mobility, channel impairment and traffic demand are necessary in W-CDMA systems and also need to be integrated at all layers. W-CDMA systems are considered as a design of power management wireless network architecture that aims to provide, maintain and guarantee different QoS classes.

1.2 POWER CONTROL SYSTEMS FOR 3G NETWORKING

Many novel solutions, including interference cancellation [84], coding [126], modulation [127], resource management [39, 80] and access methodologies [83] have been proposed, studied and implemented to guarantee QoS and also to maximize W-CDMA system capacity. Amongst other solutions, adaptive power control (APC) algorithms can provide, maintain and control QoS in a state-of-the-art system architecture. In our view, power is the central mechanism for W-CDMA systems because power is shared amongst all users and it can easily be measured, controlled and managed in multi-layered operations.

There are three basic time-scales for QoS management in multi-media networks [39]:

- Each time a call is requested, call-admission control determines whether or not the new call can be accepted while guaranteeing the QoS of established calls. The call-admission control function computes and allocates an equivalent bandwidth for the duration of the call, which is typically minutes for voice calls or hours for Internet Protocol (IP) sessions.

- Monitoring, scheduling and control mechanisms come into operation each time a number of packets are sent and/or received, typically within microseconds. Monitoring mechanisms are algorithms that police the negotiated QoS to subscribers. Scheduling algorithms decide when and which packet to send first.

- Fast Power Control (FPC) mechanisms come into operation each time a packet is sent and/or received, typically within nanoseconds. PC algorithms increase or decrease the transmitting power level.

The current literature on PC techniques can also be divided into three categories: network-layer PC (NPC), outer-loop PC (OPC) and fast PC (FPC), as shown in Figure 1.3.

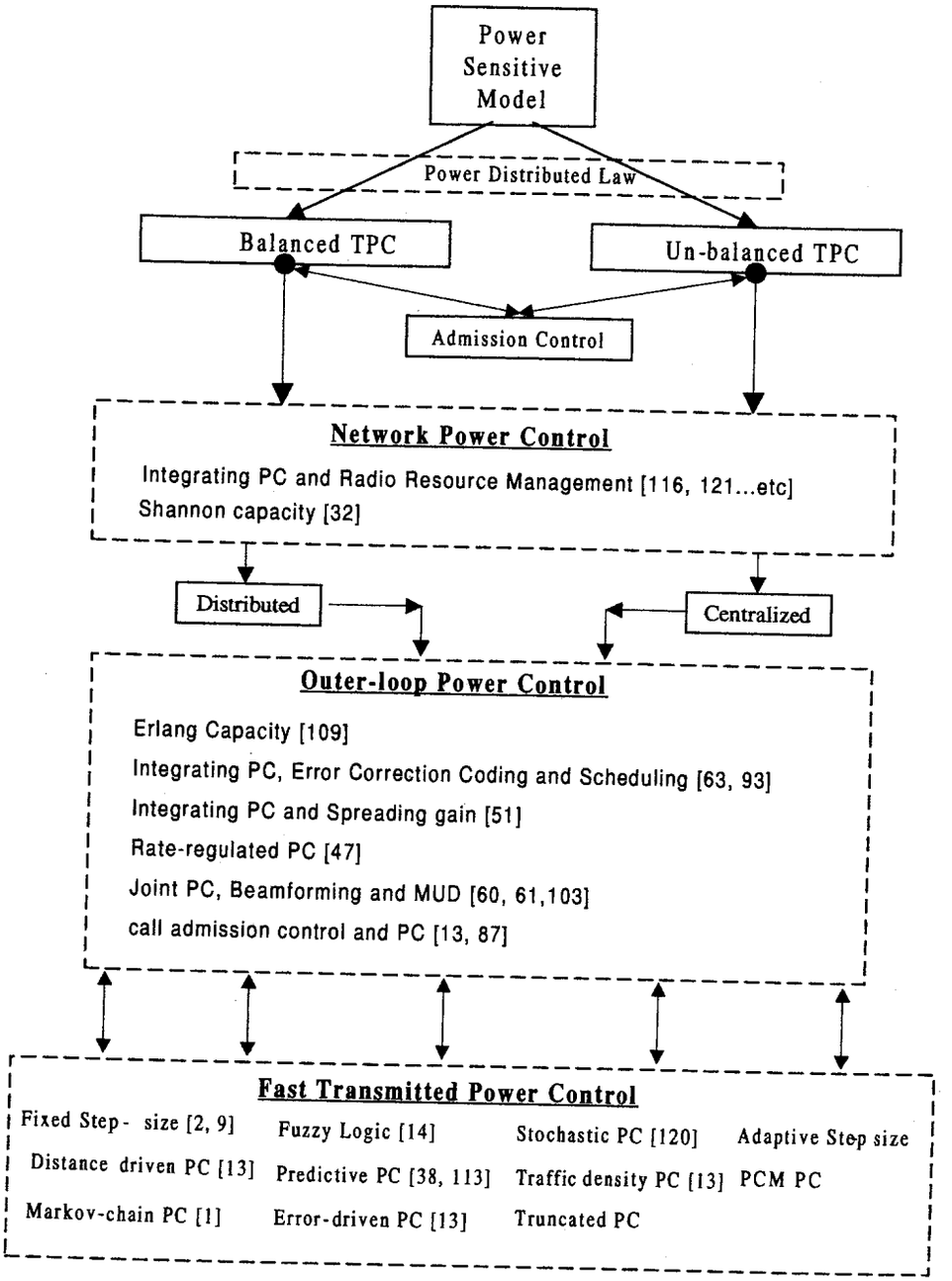

FIGURE 1.3: Overview on research background in PC algorithms

1.2.1 Research Background on APC Algorithms

First-generation Bell mobile systems used in New York city in the 1970s could only support a maximum of twelve simultaneous calls over a thousand square miles [81]. The cellular concept was a major breakthrough in solving the problem of spectral congestion and user capacity. Since then, the system capacity and the cellular system design of FDMA/TDMA schemes have been based on the frequency re-use concept: the multiple access methodology assigns time or frequency slots to users. The vital operation for interference avoidance in these conventional systems is through intelligent allocation, re-use of channels throughout a coverage region as well as by using appropriate handoff strategies. Conventional PC algorithms for FDMA/TDMA were designed to combat co-channel interference and multipath fading only.

A linear receiver structure is sufficient to deliver these services, since the system resources occupied by a handset is generally proportional to the transmission rate and the received power level. The larger the received power from a handset at the base station, the larger the proportion of the system capacity occupied by the handset.

Although SS technology has many advantages over TDMA and FDMA, the two most significant disadvantages are *self jamming* and the *near-far effect*. Traditionally, PC was the only solution for combatting the near-far effect in CDMA systems, by periodically instructing the mobile units to adjust their transmitter power so that all signals are received at the base station at roughly the same strength or same Signal to Interference and Noise Ratio (SINR) level. Much of the current literature on PC algorithms is devoted to this type of receiver structure [9,28,58,81]. If the power is adjusted according to the received strength, it is called strength-based; if the power is adjusted according to the received SINR, it is called SINR-based. Examples include fixed-step size PC [2, 9], adaptive step-size PC [15], fuzzy logic PC [14], truncated PC [12, 85], traffic density PC, stochastic PC [119], error-driven PC, predictive PC [59, 110, 112] and Markov-chain PC [1]. In this dissertation, we propose a new unbalanced SINR-based closed-loop FPC algorithms using frequency-multiplexed pilot symbols on the uplink of W-CDMA mobile radio channel.

However, non-linear receiver system means that the interference level is not linearly proportional to transmitted power and data rate, and is called the *near-far resistance* technologies. This technology can efficiently support different bit-error-rate (BER) and QoS performances for multi-media 3G systems. Therefore, conventional FPC algorithms for voice-only cellular systems cannot be directly applied to multi-media 3G cellular systems. Instead, with a complementary APC structure, the scarce radio resources will be optimally

utilized, multi-media QoS will be guaranteed and system capacity will be maximized.

The inevitable trend of PC algorithms is toward OPC. Interest in state-of-the-art power-sensitive systems based on radio-resource management has recently increased. This OPC algorithms aim to monitor, schedule and control scarce resources and ensure BER on active links. Aein [6] initially introduced the OPC concept based on *carrier-to-interference ratio balancing* (CIR) for centralized satellite communication systems: if the power is adjusted by a central controller it is called centralized OPC, if the power is adjusted according to local SINR measurements, it is called distributed OPC. Zander [122] introduced a power-distributed law algorithm for centralized and/or distributed systems using Pareto's optimal solution to overcome the problem of interference management. Grandhi [30], Ren [82], Zander [121] and Wu [113] have contributed to the development of optimal centralized OPC algorithms, but centralized OPC algorithms require central controllers and due to their computational complexity, centralized algorithms are impractical. Grandhi *et. al.* [31], Foschini [23], Mitra [67], Lee [56], Kim [46] and Chong [17] have contributed the development of distributed OPC algorithms.

Yates [116,117] has extended these algorithms and formulated a general OPC framework, further identifying common properties and limitations of the interference constraints that may permit a general proof for synchronous/asynchronous convergence properties for PC algorithms.

The growing interest in the use of APC has also sparked the creation of novel applications in other areas too, including, W-CDMA receivers with error correction coding and scheduling [62, 91], beamforming [40, 60], multi-user detection [61], admission-control [39,51], hand-offs [32, 42], rate-regulation [44, 47] and many others.

The prime focus of this dissertation is a systematic examination of current APC algorithms, and on the formulation of a novel framework of APC algorithms. There has been little research devoted to the implementation of APC algorithms based on the iterative receiver.

An overview of the most important definitions used in the design and analysis of APC systems in this dissertation are presented below.

1.2.2 Advantages of APC Structure

Outage probability and the degree of user satisfaction provide the basis for a comparison of the performance of cellular technology [87]. Many definitions of outage probability and degree of user satisfaction have been proposed in the literature. Because the capacity of

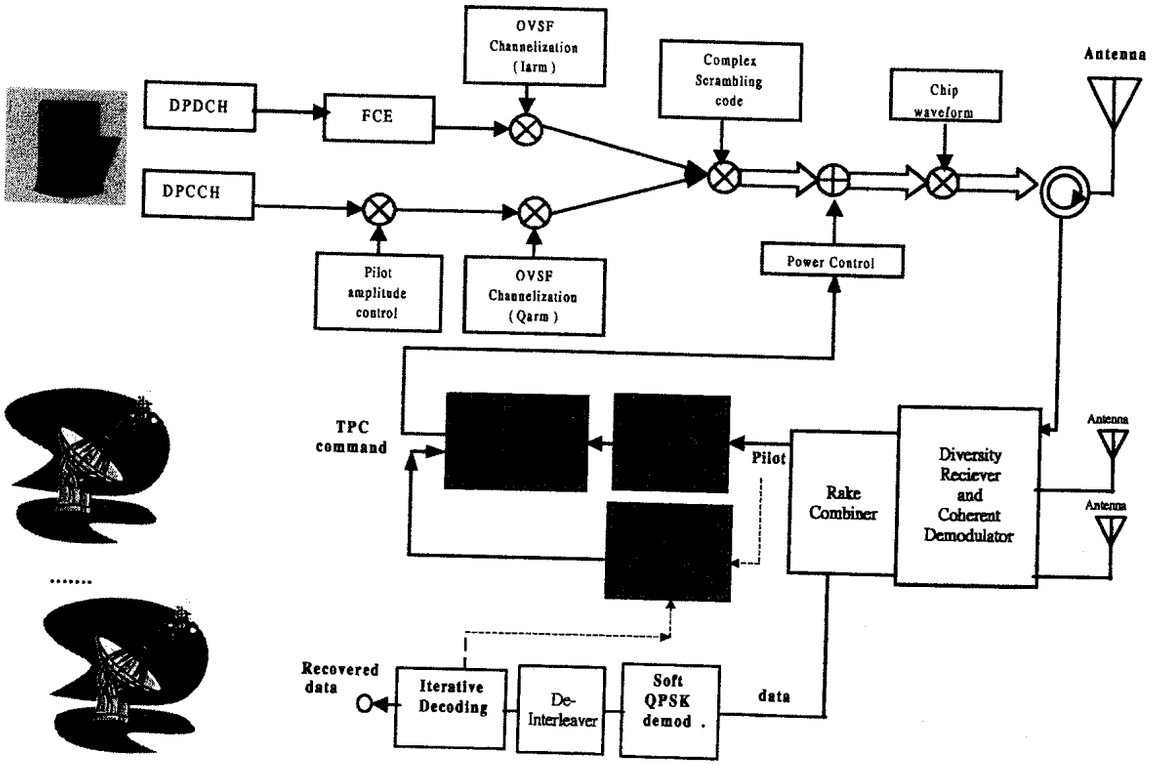

FIGURE 1.4: Three-level optimization hierarchy: user, intracell and intercell levels

W-CDMA technology relies on MAI and traffic-demand parameters, we have included these parameters in our definition of outage probability to evaluate APC performance.

Definition 1: Cellular System Capacity

The cellular system capacity of a W-CDMA system is defined as the maximum number of services under current power distribution law that can be delivered with acceptable QoS to subscribers.

Mathematically, cellular system capacity is defined by outage probability as:

$$P_r\left[\left(\frac{E_b}{I_o}\right)_i \geq \gamma_i\right] = P_r\left[\frac{h_{ik}P_i}{\sum_{j\neq i}^{N} h_{jk}P_j + \delta^2 W}\frac{W}{R_i} \geq \gamma_i\right] \tag{1.1}$$

where $\left(\frac{E_b}{I_o}\right)_i$ denotes the received SINR for user i and γ_i the desired SINR for user i. Thus, the formula, $P_r\left[\left(\frac{E_b}{I_o}\right)_i \geq \gamma_i\right]$, where $Pr(x)$ is the probability that event x is true and γ^* denotes the pre-determined SINR required to ensure adequate received SINR. The derivation and the definition of notations of this outage probability formula can be find in Chapter 2.

This outage probability formula can be represented as the system capacity for W-CDMA systems and is calculated as the outage probability of d as the outage probability of received SINR values are greater than the desired SINR values.

It is assumed that the desired BER values can be converted to the desired SINR. Since the basic time-scale of QoS management increases from nanoseconds to milliseconds, the assumption of the conversion from BER to SINR becoming statistically invalid. The received SINR values are calculated after the RAKE receiver shown in Figure 1.4, and represented as

$$\frac{h_{ik}P_i}{\sum_{j\neq i}^{N} h_{jk}P_j + \delta^2 W}\frac{W}{R_i} \geq \gamma_i \tag{1.2}$$

where h_{ik} is the link gain between user i and base station k, P_i is the transmitted power of user i at iteration n, R_i is the desired date rate for user i and W, the spreading bandwidth, is assumed fixed in W-CDMA systems. FPC algorithms trigger the transmitted power (P_i) of all users and attempt to stabilize the received SINR at the base station. However, if the transmitted power of one user is increased without considering the MAI level to other users, a positive feedback may occur and an equilibrium state for the power vector will never be reached.

Therefore, MAI

$$\sum_{j\neq i}^{N} h_{jk}P_j + \delta^2 W \tag{1.3}$$

is the major limitation for the determination of outage probability, P_r [Figure 1.5].

Definition 2: A Power-Sensitive Model

A W-CDMA system is a power-sensitive model in which a set of factors, including the orthogonal factor (ρ) after de-spreading, the transmitted power (P_i) of all-users, the link gain (h_{jk}), the traffic demand (Γ_i) and processing gain, will influence the received SINR levels.

Interference-based radio resource management (RRM) is the terminology used by Holma & Toskala [39]. The RRM mechanism consists of handoff, PC, admission-control, load control and scheduling. These functionalities operate at different time-scales. In our view, APC is of fundamental importance to the operation of RRM mechanisms for a number of reasons. Firstly, the power is a shared resource amongst users and the W-CDMA network is a collection of interference links: by controlling the transmitted power, the total MAI can be reduced to a minimum. Secondly, the W-CDMA network is a management of resources: by re-allocating transmitted power and power budget at user and inter-cell

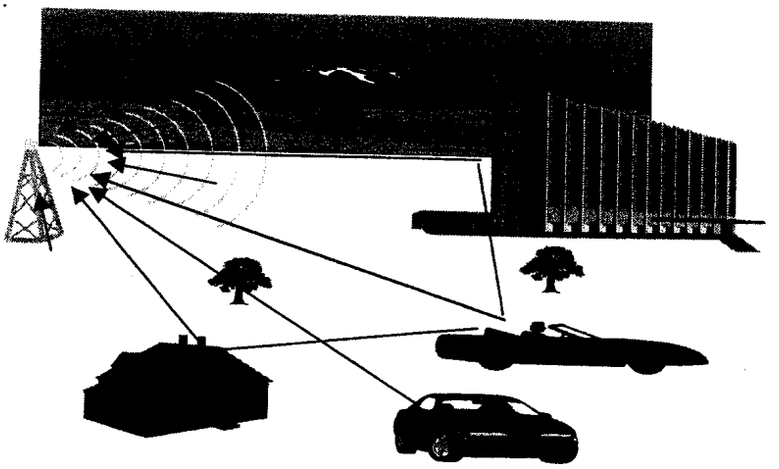

FIGURE 1.5: The potential system capacity is affected mainly by both the short-term and the local-mean statistics of SINR

levels, respectively, the outage probability of the resource can be minimized. Thirdly, the advantages of the APC structure have proven its online QoS monitoring ability, interference management ability, resources management ability and QoS maintenance ability through co-working with other RRM mechanisms.

Definition 3: The centralized strategy of W-CDMA systems

The centralized strategy of interference-based RRM mechanisms, which aim to guarantee QoS, to maintain the planned coverage area and to offer high capacity, is an adaptive power control structure.

Despite the question whether FPC algorithms are necessary and sufficient for unbalanced SINR services if interference cancellation techniques are deployed, APC provides QoS monitoring ability and interference management in a state-of-the-art multi-layered operation. However, these techniques are supplementary mechanisms for RRM systems.

1.2.3 A QoS-based APC Structure

Thus far we have shown that modern wireless-access communication systems are required to supply a number of different services to users in a number of different environments, and that APC techniques may meet these requirements. The APC algorithms for use in multi-media applications are defined as follows:

Definition 4: QoS-based APC structures

A QoS-based APC structure consists of an array of temporally distributed elements, each element in the array receiving the estimated SINR values from each handset. The outputs of each element are adaptively adjusted and calculated based on optimization objectives to determine an optimal power-distribution law for the next time-interval.

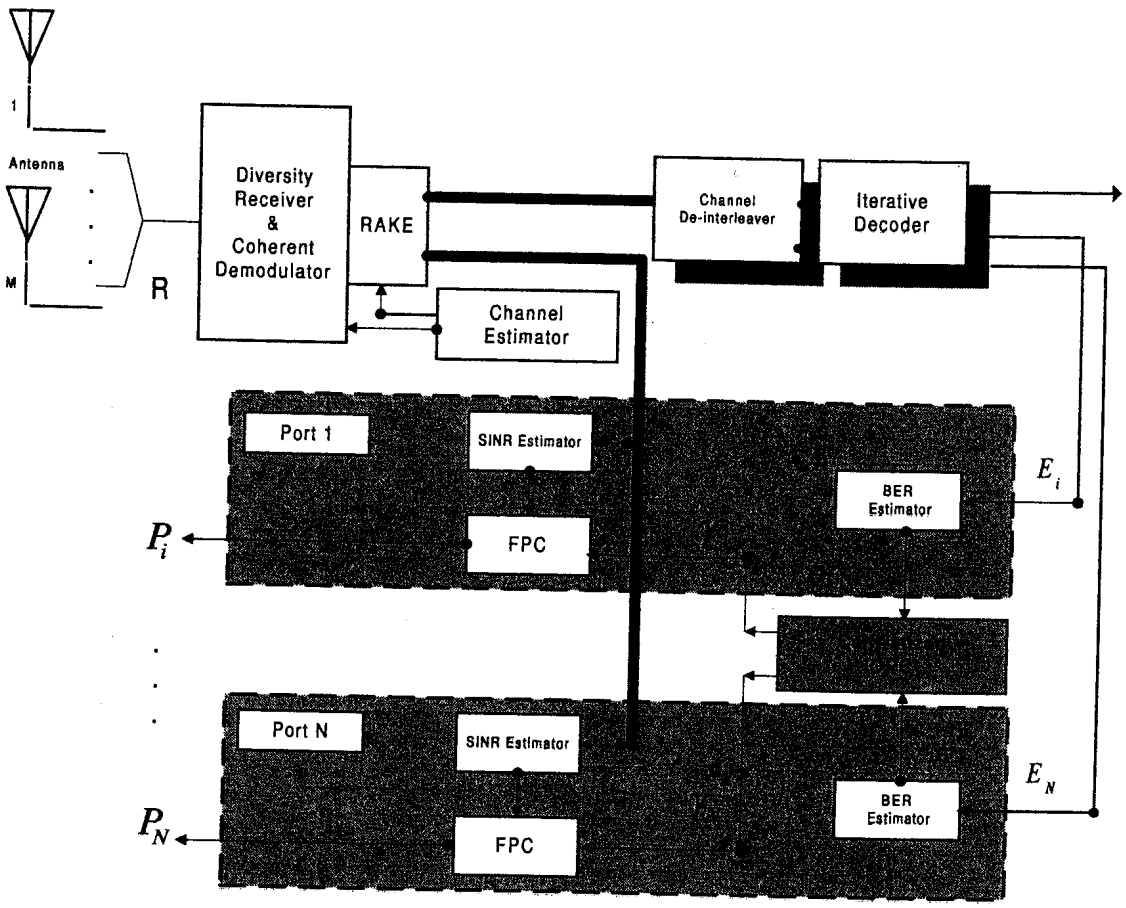

FIGURE 1.6: A QoS-based APC with centralized OPC and N output ports

An N-element, QoS-based, APC structure with a centralized processor that meets the optimization criteria of the power-distribution law for each active user with desired SINR (γ_N^*) is shown in Figure 1.6. The set of SINR measure operations required to track the variation of received signals is measured by SINR estimator after the RAKE receiver. Typically, the estimated SINRs of an APC are measured every 0.625 ms to compensate for the fast and slow channel impairments. The estimated BERs (E_N) of an APC are measured every fourth iteration of iterative decoding to compensate for a slow and erratic prediction of BER estimator. The OPC algorithm is needed to keep the quality of communication at the required level by setting the target for the FPC algorithm.

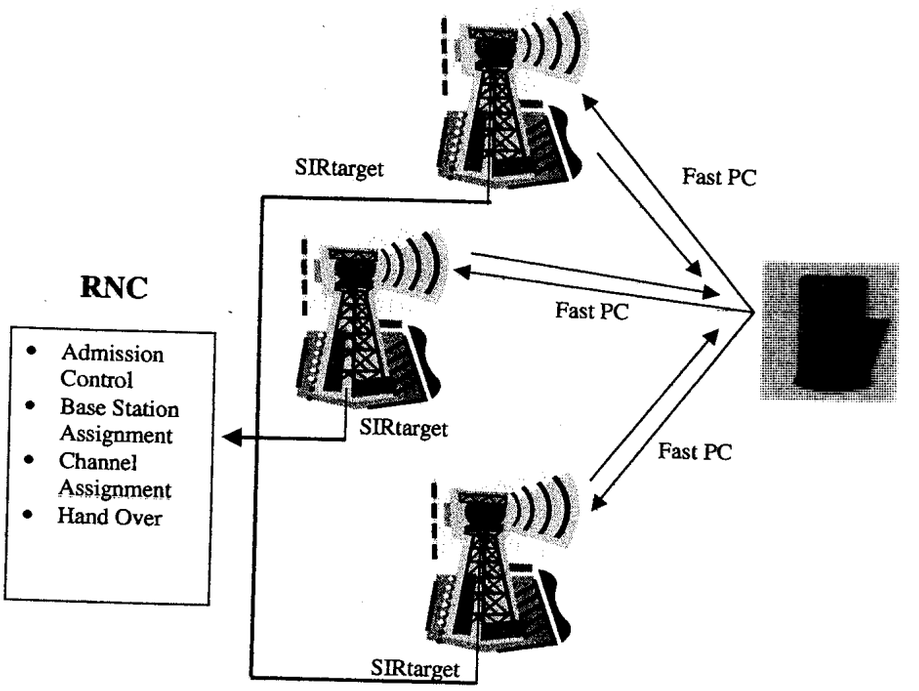

FIGURE 1.7: Radio resource management procedure

The details of operations of APC algorithms in a W-CDMA environment are described below.

Definition 5: A Radio Resource Management Procedure

The RRM mechanism consists of admission-control, base station assignment, channel assignment, scheduling, OPC, load control, FPC and handoffs.

Figure 1.7 shows a typical RRM procedure. When a new call arrives, a new call-admission procedure is invoked. If the air-interface loading exceeds system capacity, the coverage area of the cell is reduced below the planned value, and the QoS of current connections cannot be guaranteed. Admission control accepts or rejects a request to establish a radio-access bearer in the radio-access network. Several admission-control schemes have been suggested [39]. However, the use of the total power received by the base station is the primary uplink admission-control decision criterion and is called power-budge based admission-control strategy in our study of APC frameworks in Chapter 3, the objective of power budge being to minimize inter-cell interference.

The new call is then assigned to a base station and allocated to a channel subject for

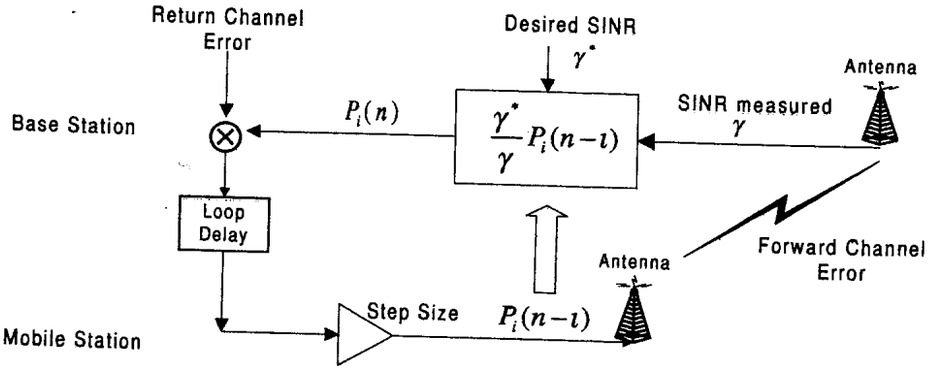

FIGURE 1.8: Traditional closed-loop FPC configuration

an admission check. Yates and Hanly [33, 115] utilized the advantage of soft-handoff of W-CDMA systems and studied an integrated PC and base station assignment. Other schemes such as fixed base station assignment [66, 78], minimal power assignment [33, 115] and diversity power assignment [36, 65] were also investigated, studied and implemented.

If the new call is successfully allocated to a channel, the radio-network centre (RNC) will assign a pre-determined SINR value γ^* to the new call and the transmitted power $P_i(n)$ is adjusted constantly by the FPC algorithm, to ensure that the pre-determined SINR value is preserved. Conventional FPC algorithms use closed-loop or open-loop mechanisms to control the transmitted power based on either strength-based or SINR-based measurements at the base station. Studies on FPC algorithms are reviewed in [85].

A block diagram of a traditional closed-loop FPC system in shown in Figure 1.8. Initially, a base station receives and resolves the multipath signals in slot-based duration. It is then possible for the base station to estimate the received SINR from the received pilot symbols. Based on the estimated SINR, the base station then determines a PC command for the next slot and sends it back to the mobile station. The mobile then determines its step-size after receiving the command. The factors that affect the determination of its step-size are: loop delay; allocated bits for FPC; processing delay; steady state error; rate of fading and number of active users [85]. However, increasing or decreasing the power is always done in a balanced manner, meaning that the power increment command is the same for both increasing and decreasing the power level. However, in practice, the power signal fades more quickly than it rises. This phenomenon can also be observed from the typical Rayleigh and Ricean fading distributions. [100]. This dissertation proposes an unbalanced, FPC algorithm, which is aimed to have faster rising time, less error distribution and better steady-state error [see section 4.3.1 for details].

During the call, the OPC is required to keep the quality of communication at the specified level, by setting the target for the FPC algorithm. Conventional OPC algorithms use joint PC with adaptive antenna techniques [60, 61, 120], multi-user detection techniques [103], coding techniques [3, 40, 62, 92, 124], rate-regulation techniques [41, 44, 47, 72, 128], and base-station assignment [115, 121, 129]. OPC algorithms can use either Pareto optimization or linear-programming optimization to find an optimal power-distribution vector in either centralized or distributed manner to minimize the intra-cell interference. However, the definition of QoS of each service is solely specified by the BER or frame-error-rate (FER) instead of the measured SINR. Strictly speaking, the SINR cannot represent the BER performance due to time-varying environments. since it is difficult to measure the BER, we prefer to apply an FER measurement based on iterative decoding for OPC, because the extrinsic information carry the confidence level corresponding to the current received signals. Adachi [3] has studied the application of an iterative receiver with power control algorithms, which we have extended and applied to a centralized, QoS-based, OPC algorithm:

Equation (1.1) can be rearranged and represented as:

$$\mathrm{P}_i \geq \frac{\gamma_i \mathrm{R}_i}{u_{ik}(\mathbf{P})\mathrm{W}} \tag{1.4}$$

The expression for the received SINR of each user is given by:

$$\frac{h_{ik}P_i}{\sum_{j\neq i}^{N} h_{jk}P_j + \delta^2 W}\frac{W}{R_i} \geq \gamma_i \tag{1.5}$$

with power constraint ($0 < P_i \leq P_{\max_i}$) and rate ($R_i \geq r_i$) where $i = 1, \ldots N$

Let

$$\Gamma_i = \frac{1}{W} R_i \gamma_i \tag{1.6}$$

be the *normalized* traffic demand of user i. The linear programming optimization problem for the OPC algorithm is described as follows:

$$\begin{aligned} &\min_{\mathrm{p}} \sum_{i=1}^{N} P_i \\ &\quad subject..to \qquad P_i \geq \tfrac{\Gamma_i}{\mu_{ik}(P)} \\ &\quad ..... \qquad 0 \leq P_i \leq P_{\max} \\ &\quad ..... \qquad \Gamma_i \geq \Gamma_{\min} \end{aligned} \tag{1.7}$$

The aim is to find a minimum power vector, $\bar{\mathrm{P}}$, such that all the active links are compliant with power constraints, $P_{\max}$, traffic-demand constraint, $\Gamma_{\min}$, and interference constraint, $\frac{\Gamma_i}{\mu_{ik}(P)}$, in both linear and non-linear receiver systems.

It is shown that the traditional Pareto optimal OPC algorithm cannot be directly applied in the simulation. Instead, SINR-unbalanced APC algorithms, which aim to find a power-distribution law that meets the QoS requirements, can improve the BER stability in multi-media W-CDMA systems with Doppler spreading.

If there is no success and handoff criteria are met, the handoff algorithm will assign a new base station and channel to the link. The handoff algorithms in the literature use pilot channel SINR as the handoff measurement quantity [39, 42, 81, 109].

1.3 LIMITATIONS OF CURRENT APC ALGORITHMS

We have identified two major deficiencies in the practical implementation of APC algorithms in power-sensitive networks. One deficiency stems from the fact that the principles of APC and resource management have not yet been integrated into multi-rate W-CDMA systems. Even though a large number of algorithms and hybrid structures have been developed, it would seem, from a survey of the literature, that there is no common framework for a systematic evaluation on subject comparison of different paradigms.

Definition 6: A Power Control Framework

A power control framework consists of a state-of-the-art power-sensitive system. This framework aims to compare different algorithms systematically.

The solution to this problem is, therefore, to introduce a general and mathematically tractable power-sensitive model to identify factors that may influence the capacity of W-CDMA systems. Specifically, three main areas of influence can be identified, namely, multi-access interference, the propagation path of the signal, and the traffic demand required by each subscriber [see Chapter 2 for details].

Since W-CDMA is a power management network architecture design, and there are three basic time-scales for QoS management. An APC framework with three basic time-scales is also proposed. Three layers of operation, dependent on their specific time-scale and optimization objectives, are shown as the interference management (FPC algorithms), the service management (OPC algorithms) and network management (NPC algorithms) [see Chapter 3 for details].

The second deficiency is that the performance and usefulness of APC algorithms are often not adequately compared in a Turbo-coded, RAKE combining and multi-media, uplink,

W-CDMA simulation platform with a statistically valid method. The solution is to program a Monte Carlo computer simulation in a Turbo-coded, RAKE-combining uplink W-CDMA cellular environment with a Rayleigh fading channel impairment. The radio-channel models are described in terms of frequency-selective Rayleigh fading: indoor-office, outdoor and pedestrian, and vehicular environments, which are defined in the UMTS forum.

The ultimate goals of this computer simulation package are to compare balanced, step-size, FPC algorithms with our newly proposed, unbalanced scheme, based on BER performance and outage probability with different numbers of multipath components, Doppler spread, the number of receiver antennae and various coding schemes.

The simulation results show that unbalanced FPC algorithms can provide better BER performance and SINR outage probability by about 3dB under the different radio-propagation channels. The centralized QoS-based OPC algorithm can also provide better BER tracking ability and reduce intra-cell interference.

1.4 RATIONALE AND AIMS OF THE DISSERTATION

This research was prompted by ongoing research on multi-media W-CDMA technology, originally at the Alcatel Research Unit for Wireless Access (ARUWA) Laboratory and later in the Centre for Radio and Digital Communication (CRDC) in the Department of Electrical, Electronic and Computer Engineering (University of Pretoria, South Africa). The RRM algorithms based on APC algorithms have received considerable attention recently [13, 29, 33, 44, 47, 61, 87]. More specifically, a study of adaptive antenna arrays, PC, resource-management techniques and iterative receiver structures is undertaken in CRDC. The main focus of this centre is to develop a comprehensive iterative receiver with system implementation of an integrated hybrid adaptive antenna array, PC, and MUD receiver structure.

The aims of this dissertation are as follows:

- to establish a general and mathematically tractable power-sensitive model for multi-media W-CDMA cellular systems;
- to establish a general framework structure for APC algorithms in multi-media, W-CDMA cellular systems;
- to propose new QoS-based APC algorithms based on the framework structure established above;

- to program an ARUWA 3G CDMA simulation package using Matlab software, to provide a statistically valid simulation for uplink multi-media, UMTS/UTRA mobile environments;

- to evaluate the performance of different FPC techniques under different conditions by means of Monte Carlo techniques;

In order to accomplish these objectives, the following items have been considered in detail:

- Power-sensitive model:
  - the influence of MAI and channel effects on the received signal, and
  - the influence of resource management on the system capacity.
- Framework for APC algorithms:
  A power-sensitive model is used to establish a framework for different APC algorithms. The APC layers are divided into:
  - NPC,
  - OPC and
  - FPC.
- To propose new QoS-based APC algorithms:
  These APC algorithms can be divided into three main management blocks in W-CDMA receivers according to their utilization objectives and specific time-scale:
  - interference management systems: QoS-based FPC algorithms.
  - service management systems: QoS-based OPC algorithms
  - network management systems: QoS-based NPC algorithms.
- To programme a 3G UMTS/UTRA simulation package using Matlab;
- Evaluate the QoS-based APC algorithms in Monte Carlo simulation package:
  The influence of the following parameters on system performance and capacity are determined for the proposed FPC algorithms:
  - power profiles
  - Doppler spreads

- coding schemes
- diversity schemes
- number of users

1.5 CONTRIBUTIONS OF THIS DISSERTATION

The main contributions are summarized in terms of the goals of this dissertation. In each case, the main contributions have been consolidated into articles which have been accepted for publication and presented at national conferences. The main contributions are:

- Consolidation of the power-sensitive terminology and operating principles of APC systems for CDMA applications.
  To Be Published
  (1) "Power-sensitive network in multi-media CDMA wireless systems."

- A framework of current APC algorithms for both physical layer and network layer.
  Conference Paper:
  (2) T-C. Song and L.P. Linde, "A New W-CDMA Transmit Power Control Technique based on Iterative Coding Techniques" *Proc. SATNAC'00*, Cape Town, 2000. [101]

- Presentation of a new QoS-based power control structure.
  Conference Papers:
  (3) T-C. Song, P. van Rooyen and X. Xia, "Comparative Study of Power Control Techniques for Cellular CDMA," *Proc. SATNAC'99*, Durban, 1999. [102]
  (4) T-C. Song, L.P. Linde and X. Xia, "A New W-CDMA Transmit Power Control Technique" *Proc. ICCTA'01*, Pretoria, South Africa, 2001. [100]

- Presentation of a Turbo-coded, RAKE combining, multi-media and uplink W-CDMA simulation platform in a Monte Carlo based simulation package.

- An analysis of the influence of temporal factors on the performance of QoS-based, APC structure in W-CDMA cellular systems .
  Conference Paper:
  (5) T-C. Song, L.P. Linde, "QoS based W-CDMA Power Control Techniques",

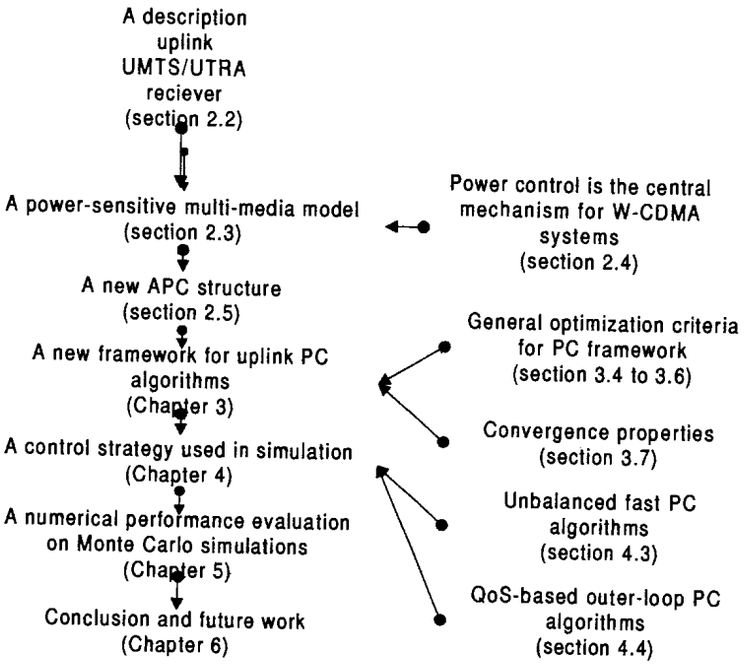

FIGURE 1.9: Overview of the dissertation outline

ISSSTA'02, Praha, Czech, 2002. to be published.

1.6 OUTLINE OF THIS DISSERTATION

The remainder of this dissertation is organized in-line with the main goals of the dissertation outlined in Figure 1.9. Chapter 2 describes the mathematical power-sensitive network model used to evaluate the performance of an APC structure in a Turbo-coded, RAKE combining uplink W-CDMA system. Based on the model, we are able to show that the W-CDMA system is fundamentally the design of an interference management network, because W-CDMA systems are interference and resource limited. All the important parameters and basic assumptions, which are important for the simulated-wireless environment, have been defined in this chapter.

Chapter 3 formulates an APC framework in a systematic manner. This framework is aimed at dividing the vast amount and diverse areas of APC algorithms in the literature into different time-scales and optimization criteria. Mathematical derivations and comparisons on current APC algorithms are described on this standard system model and are the highlights of

this chapter. According to our knowledge, the APC structure (NPC, OPC and FPC) have not been described in much detail in literature before. The concept of linear-receiver unbalanced and non-linear-receiver unbalanced structures for APC algorithms are unique in the sense that it is the first time the concepts have been investigated. All current APC algorithms in the existing literature can be categorized into this proposed framework system.

Previously, PC algorithms were treated as separated mechanisms, however in this dissertation these PC algorithms have been integrated into a state-of-the-art power-sensitive architecture. The inclusion of iterative decoding techniques was based on a discussion with P.G.W van Rooyen.

Chapter 4 presents the implementable state-of-the-art QoS-based APC strategy. The eight FPC algorithms are described in detail in this chapter. The analysis of the bounds on the stability of FPC algorithms are obtained to present the advantages of new proposed unbalanced step-size schemes. The centralized linear-programming optimization problem for OPC algorithms is described with mathematical equations and block diagrams.

Having derived the proposed APC structure for the multi-media services of a W-CDMA wireless network, the influence of a number of parameters on each performance measure is described in Chapter 5. Specifically, eight FPC algorithms are compared in terms of their influence on the power profile, Doppler spread, diversity, coding scheme and number of users in the Turbo-coded, RAKE combining, uplink Rayleigh fading channel W-CDMA cellular package. Detailed comparisons of the SINR outage probability, BER performance and rate of convergence for these eight algorithms are presented. It is shown that in order to accurately deliver the BER for active users, OPC is required due to the stochastic and time-varying nature of the power-sensitive model.

Finally, Chapter 6 concludes the dissertation by summarizing the major contributions and simulation results.

CHAPTER TWO

POWER-SENSITIVE MODELS

This chapter describes simulation environments used to investigate PC algorithms appropriate for use in the practical implementations of UMTS systems. PC algorithms are executed from the base station to correct the power transmitted from the mobile to the base station and therefore only the uplink is considered. Hence, a summary is presented of the components of the UMTS standard relevant to the physical layer of the uplink and of a mathematical representation of the CDMA system (section 2.1). Then a discussion follows on the rationale for the use of a power-sensitive model (section 2.2), which incorporates the factors that may influence radio-resource-usage and the system capacity (section 2.2.2). The factors are multi-access interference (section 2.2.2.1), the traffic demand (section 2.2.2.2) and channel impairments (section 2.2.2.3).

2.1 A SUMMARY OF A TURBO-CODED, UPLINK W-CDMA SYSTEM

The system in Figure 2.1 is a wide-band, multi-media communication network which is designed to serve a large number of users simultaneously through portable terminals. Consider a multi-cell (k), multi-media, W-CDMA cellular system that facilitates the high-speed and multi-media services available for the uplink transmission. For low power and cost reasons, computations are carried out at the base station(s) and not at the mobile, since the mobile have minimal general purpose computation power.

We assume that N users are active simultaneously. Each user has a QoS requirement and also power and rate constraints. The chip rate for all users is fixed and the total bandwidth, W, is used by all users. We can define the transmitted power vector, $\mathbf{P} = [P_1, P_2, ...P_N]$, which

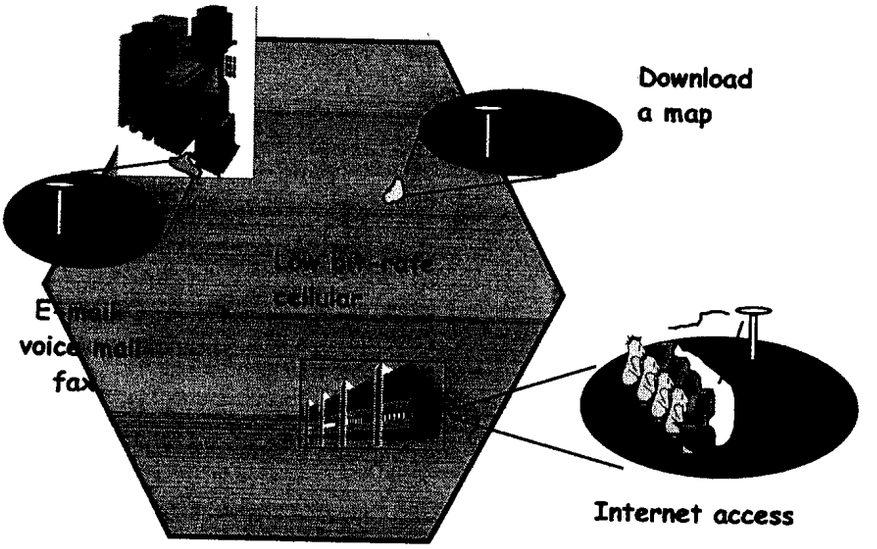

FIGURE 2.1: The uplink of a typical multi-media cellular CDMA system

is limited to a maximum power level as

$$P_i \leq P_i^{\max}, \qquad for \quad 1 \leq i \leq N \tag{2.1}$$

and the vector of rates to be, $\mathbf{R} = [R_1, R_2, ...R_N]$. We assume that the QoS required by each service or medium is specified solely by the BER or frame error rate (FER). It is assumed here that the BER/FER requirement can be mapped into an equivalent, E_b/N_o, requirement and is denoted by, $\gamma = [\gamma_1, \gamma_2, ...\gamma_N]$.

The radio-link parameters of multi-media W-CDMA used in the simulation is based on an FDD scheme [12] (see Table 2.1). The physical and transport channels used in the UMTS are divided into two classes; dedicated channels and common channels. The UMTS specification for the physical layer of the uplink is beyond the scope of this dissertation. (for more information refer to [19]).

The frame structure used by the uplink physical channels is shown in Figure 2.2. The Dedicated Physical Control Channel (DPCCH) carries the control information generated by the physical layer only. Thus, the DPCCH carries known pilot symbols used for channel estimation and SINR measurement by the BS receiver. The minimum PC period is 0.625 ms, or one slot period.

TABLE 2.1: FDD W-CDMA radio-link parameters for this dissertation

Definition of the notations	
Parameter	**Description**
Chip rate	41472/frame
User data rate	48 kbps/256 kbps/1024 kbps
Spreading Code	Short: Tree-structure orthogonal multi-SF codes
	Scramble: Pseudo noise codes
Spreading factor	32/16/4
Interleaving	10 ms
Modem	Spreading: QPSK
	Data: Coherent QPSK
Over-sampling rate	4
Diversity	RAKE+antenna
No. of slots/frame	16
No. of fingers/Antenna	3
Initial power	0.5 W
Diversity (receiver antenna)	2
FEC	Uncoded
	Convolutional with soft-input Viterbi decoder
	Turbo encoder with iterative MAP decoder

2.1.1 Synchronous CDMA Signal Representation

We take advantage of the coherent receiver capability of a W-CDMA system by using pilot symbols along each users data link [Figure 2.3]. Thus, the assumption of perfect channel estimation and link quality measurement, acquisition and tracking of the spreading sequences, and perfect synchronization between each base station and users can be assumed.

In Figure 2.4, the information symbol stream $b_i(l), l = 0, 1, 2, ...(kL - n)/n$ for user i is firstly Turbo-encod at data rate $1/T_b$ symbols per second (sps) with a rate k/n code, followed by an interleaver with L intervals (L is the symbol interval). The sequence output, $d_i(\tau)$, is at the rate $1/T_d = n/kT_b$ sps, where $\tau = 0, 1, 2, ...L - 1$ is the chip interval index. At each

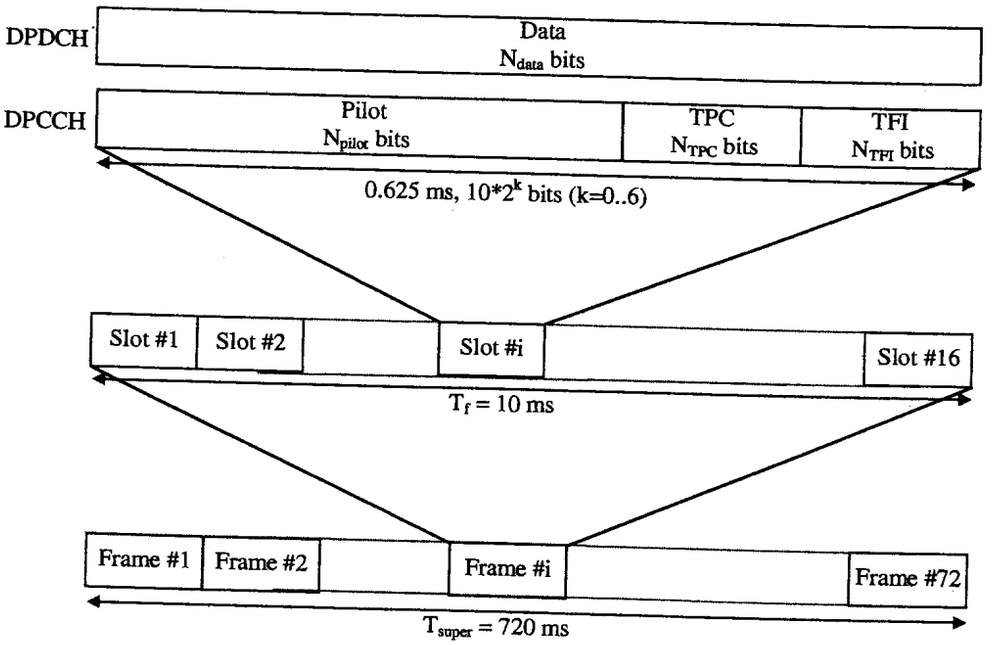

FIGURE 2.2: Frame structure for the uplink DPDCH/DPCCH channels

chip interval τ, $d_i(\tau)$ is modulated by a rate $1/T_c = C/T_d = nC/kT_b$ chips per second (cps) spreading sequence $s_i(\tau) = (s_i(\tau C + 1), s_i(\tau C + 2), ...s_i((\tau + 1)C))^T$, with $s_i(j) \in S$ where S denotes the set of possible chip values and C denotes the spreading gain. Note that the choice of chip values ensures $||s_i(\tau)||^2 = 1$ so that modulation can be modeled as simple multiplication without modifying the energy contained in one chip interval. The bandwidth expansion of the spreaded signal is determined as:

$$G = \frac{1/T_c}{1/T_b} = \frac{nCT_b}{kT_b} = \frac{nC}{k} \tag{2.2}$$

which is traditionally termed the processing gain (G). Both the encoding and the spreading contribute to the processing gain. In practice, the spreading sequences for each chip interval are chosen pseudo-randomly and are known at the receiver.

For practical implementation, all the base-band processing is usually done in discrete time. With this approach, we modulate each chip of $d_i(\tau)s_i(\tau)$ by filtering the signal with a discrete-time, pulse-shaping filter, which is a raised cosine pulse with a roll-off factor of 0.22. The filter operates at a rate of $1/T_s = Q/T_c$, where T_c is the chip interval and Q is the over-sampling factor. To express this operation algebraically, the spreading sequence must be zero-padded before filtering. Therefore, the resulting transmitted, discrete-time, baseband signal for user i is then

$$x_i(\tau) = d_i(\tau) * (\mathrm{u}_1 \otimes \mathrm{s}_i(\tau)) * \mathrm{p} = d_i(\tau) * \hat{\mathrm{s}}_i(\tau) \tag{2.3}$$

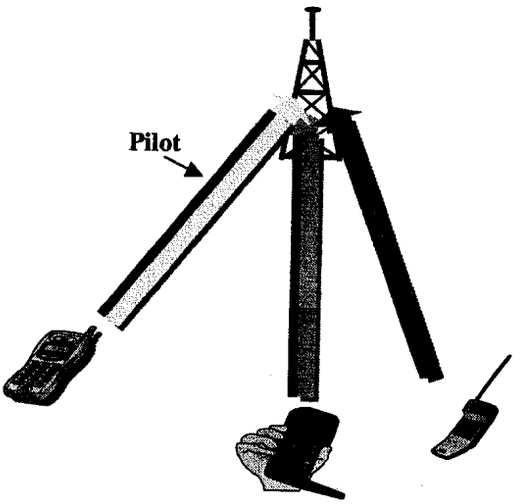

FIGURE 2.3: The uplink of a typical cellular CDMA system with FPC algorithm

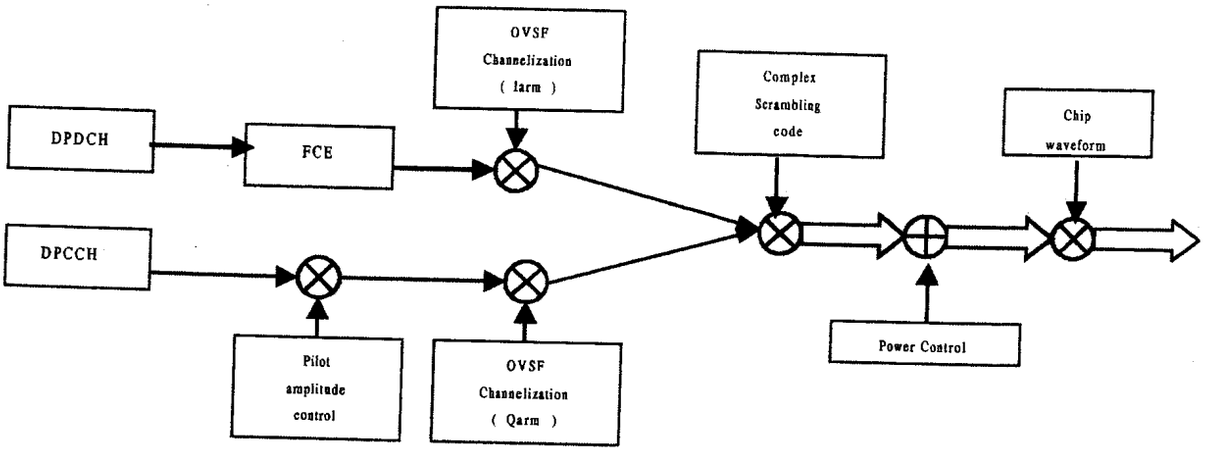

FIGURE 2.4: Transmitter processing for single user

where $\mathbf{p}$ is the pulse-shaping filter impulse-response of length $P+1$, s is the pulse-shape of a spreading sequence of length $NQ+P$ and $\mathbf{u}_1 = (1, O_{Q-1}^T)^T$. No intersymbol interference will occur due to the symbol overlap, as long as root-Nyquist pulses sampled at the correct instances are used. The length of $x_i(\tau)$ is $LNQ+P$, which corresponds to the entire transmission interval of L symbols. Only the elements corresponding to chip interval τ are non-zero.

The channelisation codes are orthogonal variable spreading factor (OVSF) codes. These codes are generated by a binary tree structure. The code associated with a particular branch of the tree is orthogonal to all the codes in the tree except for the following:

- codes on the path from the specified code to the root of the tree;
- codes in the sub-tree below the specified code.

Thus, orthogonal sequences of different lengths can be generated. The spread DPDCH and DPCCH signals are viewed as single complex-valued signals, and are scrambled by complex multiplication with a complex-valued scrambling code. Note that no bandwidth expansion of the signal occurs due to this scrambling.

The short scrambling code is a complex code $C_{scramble} = cI + jcQ$, where cI and cQ are two different codes from the extended very large Kasami set of length 256. Short scrambling codes are intended for use in cells that support multi-user detection in the base station.

For simplicity, we assume that each user transmits over an additive white Gaussian noise (AWGN) channel with variance δ_n^2 and that there is no other distortion in the channel, apart from constant linear scaling of signal amplitudes and multiple-access interference caused by the presence of other active users. If there are N active users of the synchronous DS-CDMA system, then the received baseband signal after A/D conversion for a given chip interval can be written as

$$\mathrm{r} = \sum_{\tau=0}^{L-1}\sum_{i=1}^{N} \mathrm{x}_i(\tau) + \mathrm{n} = \sum_{\tau=0}^{L-1}\sum_{i=1}^{N} A_i(\tau) d_i(\tau) \hat{s}_i(\tau) + \mathrm{n} \tag{2.4}$$

where each active user is assigned a unique spreading waveform (signature, sequence, code) $s_i(\tau)$. $A_i(\tau)$ is the received amplitude of the signal for the ith user, $d_i(\tau)$ is the data chip transmitted by the ith user, and n is a length $(LNQ+P)$ vector of independent, identically distributed (iid) complex Gaussian noise samples of zero mean and variance δ_n^2.

A more convenient form of Equ. (2.4) is

$$\mathbf{r} = \mathbf{ASd} + \mathbf{n} \tag{2.5}$$

where $\mathbf{S}$ is the matrix of transmitted, spreading waveforms with user i and chip τ. $\mathbf{A}$ represents the random time-dependent, complex channel coefficient $\mathbf{A}_{i\tau}$. The complex channel coefficient $A_{i\tau}$ contains all the fading and attenuation effects of the radio channel. These effects are traditionally divided into small-scale Rayleigh fading, large-scale log-normal shadowing and path loss denoted for user i at chip interval i and will be described in detail in section 2.2.2.3. The extraction of the transmitted waveform (which overlaps in both time and frequency) from the received signal is facilitated by the carefully selected correlation properties of the spreading waveforms used. The cross-correlation between the spreading waveform for the jth user and that for the ith user is defined as

$$\rho_{j,i} = 1/T_s \int_0^{T_s} s_j(t) s_i(t) dt \tag{2.6}$$

If $j = i$, then $\rho_{j,i} = 1$, since the product $s_i(t)s_i(t) = 1$. If $j \neq i$, then $-1 < \rho_{j,i} < 1$. In this case, the ideal value for $\rho_{j,i}$ is zero, and the sequences are said to be orthogonal.

2.1.2 Linear W-CDMA Receiver with Pilot Symbols

There are three types of measurement outputs in the literature [85]: the received power $P_r(W)$ [14]; the received signal-to-interference ratio (SINR) [9]; and the despreaded signal associated with each path of the receiver [2]. The one we use here is the despread signal to avoid the modulation effects.

Multipath components delayed by more than one chip duration are uncorrelated and appear as resolvable paths in the model. Thus, it is appropriate to use diversity schemes to combine the useful information in the time-delayed versions of the original signal transmission to improve the SINR at the receiver. A well-known diversity scheme that can cooperate in CDMA is the RAKE receiver system shown in Figure 2.5.

Some receiver structures make use of a chip-matched version of the received signal $r(\tau)$, where τ is now the chip rate. An equivalent discrete-time model is thus derived as follows. The spreading waveform is formally defined as

$$s_i(\tau) = \sum_{j=0}^{L-1} s_{\tau,j} \rho(\tau - jT_c) \tag{2.7}$$

where $\rho(\tau) = \begin{cases} 1 & 0 \leq \tau \leq T_c \\ 0 & \text{otherwise} \end{cases}$ and $s_{\tau,i}$ is chip τ of user i. We can then retrieve the signal

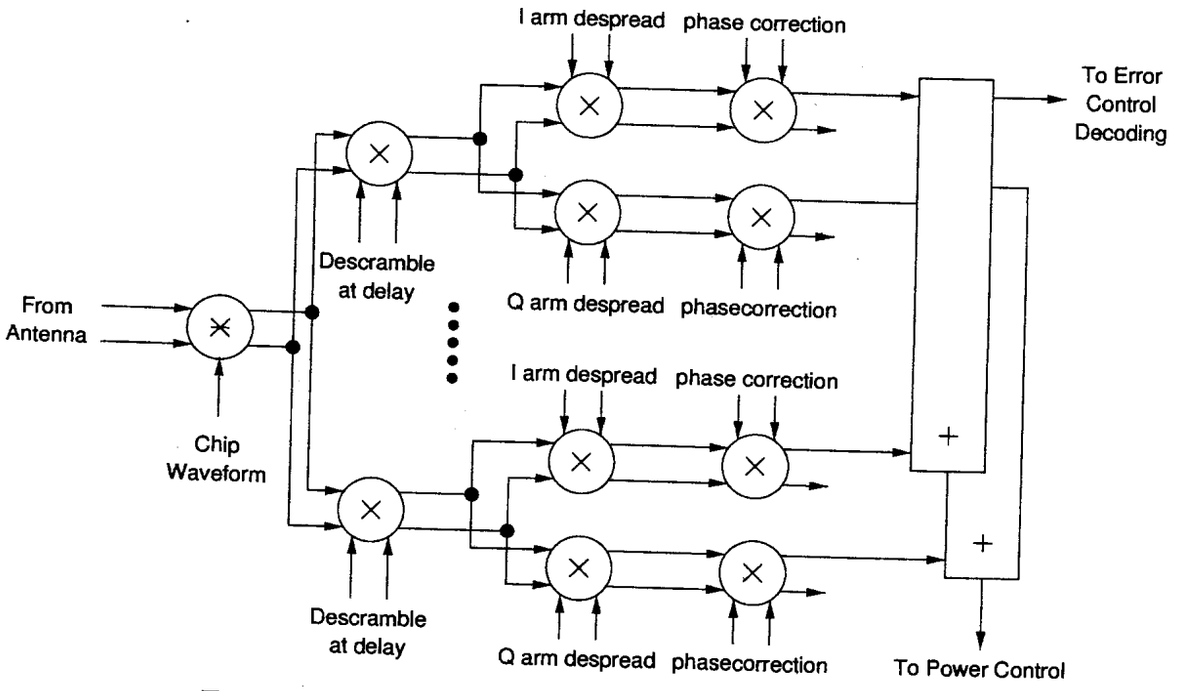

FIGURE 2.5: RAKE receiver structure on a single antenna

transmitted at chip τ through chip-matched filtering as

$$\begin{aligned} r_\tau &= \tfrac{1}{T_c} \int_{\tau T_c}^{(\tau+1)T_c} r(t)s^*(t-\tau T_c)dt \\ &= \tfrac{1}{T_c} \int_{\tau T_c}^{(\tau+1)T_c} \sum_{i=1}^{N} A_i(t)d_i(t) \sum_{i=0}^{N-1} s_{i,j}p(t-jT_c)p^*(t-jT_c)dt \\ &+ \tfrac{1}{T_c} \int_{\tau T_c}^{(\tau+1)T_c} n(t)p^*(t-\tau T_c)dt \\ &= \sum_{i=1}^{N} A_i d_i s_{i,j} \tfrac{1}{T_c} \int_0^{T_c} dt + n_\tau \\ &= \sum_{i=1}^{N} A_i d_i s_{\tau,i} + n_\tau \end{aligned} \tag{2.8}$$

where n_τ is an additive, white Gaussian noise sample with variance δ^2.

Collecting the sequences of L chips of r_τ, $s_{\tau,i}$ and n_τ in column vectors, $\mathrm{r} = (r_0, r_1, ..., r_{L-1})^T$, $\mathrm{s_i} = (s_{0,i}, s_{1,i}, ..., s_{L-1,i})^T$, and $\mathrm{n} = (n_0, n_1, ..., n_{L-1})^T$, respectively, we can express r for $\tau = 0, 1, ..., L-1$ as

$$\mathrm{r} = \sum_{i=1}^{N} A_i d_i s_i + n. \tag{2.9}$$

Here, the equivalent of Equ. (2.6) is $s_i(\tau)s_i(\tau) = 1$. In this case, the constraint that $s_i(\tau)s_i(\tau) = 1$ translates into $|s_i|^2 = 1$, which in turn leads to $s_{j,i} \in \{-1/\sqrt{L}, +1/\sqrt{L}\}$.

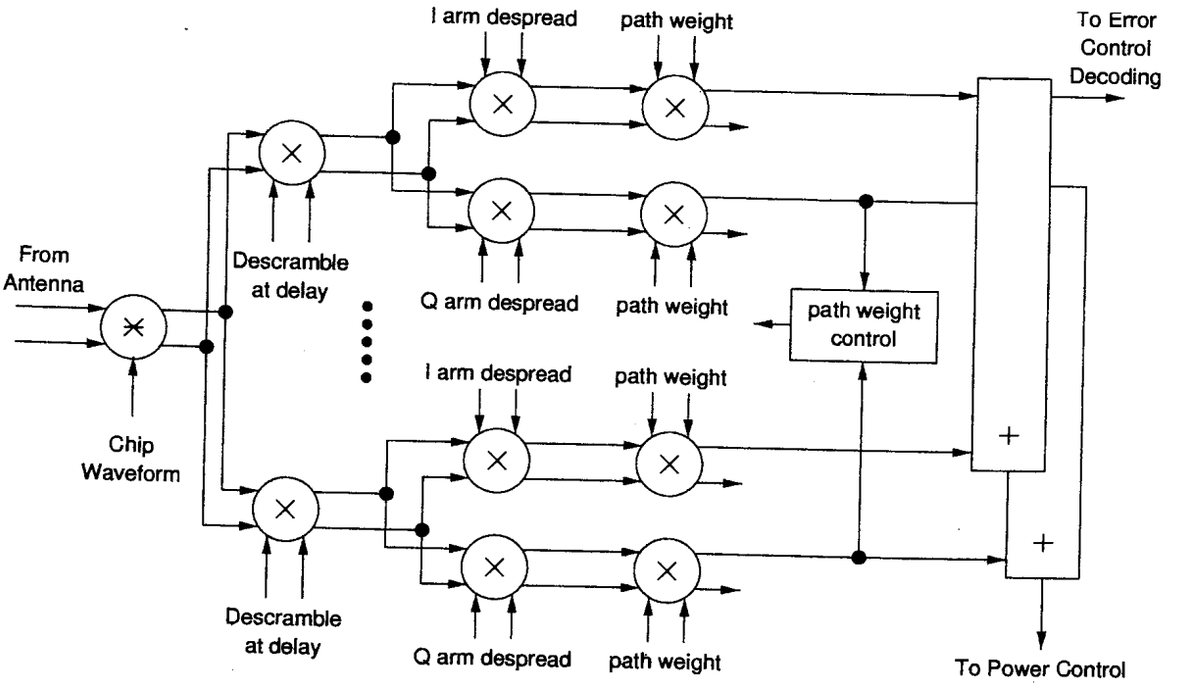

FIGURE 2.6: Adaptive receiver structure

The length of the signature sequence is L, giving the spreading ratio between the rate of narrowband information symbols (b_i)'s and the ratio of the wideband spread-spectrum signals ($A_i d_i s_i$). The received vector is $\mathbf{r} \epsilon \Re^Q$. We assume that $A_i d_i$ is independent and that $E[A_i d_i] = 0$ and $E[(A_i d_i)^2] = p_i$, where p_i is the received power of user i.

For convenience, let us focus on the demodulation of the *chip-by-chip* detection of user 1 as shown in Figure 2.6, and on a relevant performance measure of the SINR of the estimates.

The *conventional* CDMA receiver for demodulating user 1 is to perform the matched-filter $s_1.r$ on the received signal r. This despreads the signal of user 1, inverting the original spreading operations at the transmitter, and results in the effective channel:

$$\begin{aligned} y_i &= \tfrac{1}{T_s} \int_0^{T_s} r(t) s_1(t) dt \\ &= (s_1 \cdot s_1)^2 A_i d_i + \sum_{j=1, j \neq i}^{N} \rho_{j,i} A_j d_j + \int_0^{T_s} n(t) dt \\ &= A_i d_i + MAI_i + z_i \end{aligned} \tag{2.10}$$

The first term represents a scaled version of the transmitted data symbol (i.e the desired signal). The second term represents the interference experienced by the ith user due to the other active users. The final term represents modified Gaussian noise. To allow for coherent detection and PC, the physical channel parameters must be known. Assume that we, therefore, have perfect knowledge of the channel estimation, since estimates can be easily obtained from pilot symbols. The SINR for user 1 is the ratio of user 1's signal energy

to that of the noise plus other users' interference at the output of the matched-filter, and is given by

$$\begin{aligned}\frac{R}{W}\left(\frac{E_b}{I_o}\right)_i = \left(\frac{S}{I_t}\right)_i &= \frac{E[(A_i d_i)^2]}{\sum_{j=1,j\neq i}^{N} \rho_{i,j}^2 E[(A_j d_j)^2] + E[z_i^2]} \\ &= \frac{(s_1 \cdot s_1^*)^2 p_i}{\sum_{j=1,j\neq i}^{N} \rho_{i,j}^2 p_j + (s_1 \cdot s_1^*)\delta^2} \\ &= \frac{(s_1, s_1^*)^2 h_{ik} P_{ti}}{\sum_{j=1,j\neq i}^{N} \rho_{ij}^2 h_{jk} P_{tj} + (s_1, s_1^*)^2 \delta^2}\end{aligned} \tag{2.11}$$

where $\rho_{i,j}^2 = (s_i \cdot s_j)^2$ is the cross-correlation coefficient of code sequences belonging to user i and user j. $p_i = h_{ik} * P_{ti}$ where p_i is the received signal for user i, P_{ti} is the user i's transmitted power level and h_{ik} is the link gain between user i and base station k.

The choice of the signature sequence s_i is very important. The sequence chosen must be orthogonal to all other sequences to avoid interference. In practice, this is usually not possible in an uplink multi-media CDMA. Firstly, the underlying physical wireless channel may cause *multipath* distortion of the transmitted signal, such that several delayed replicas of the signal are superimposed at the receiver. Hence, even if the transmitted signature sequence were chosen to be orthogonal, the received signatures would not be noise-free. Secondly, uplink CDMA systems are usually *asynchronous*, meaning that there is a random, relative delay between users such that a chip of a desired user overlaps with two partial symbols of an interferer.

2.1.3 Description of the Simulation Model

The transmitted signal for each user is generated in accordance with the UMTS physical layer description. The in-phase(quadrature) component of the transmitted signal are multiplied by the in-phase(quadrature) component of a random segment of a pre-generated complex fading channel envelope. The resulting signals are then summed and AWGN of known power, based on the number of users, is added [Figure 2.8]. The impact of slot-by-slot PC on the simulation methodology is profound. The key modules consist of frame-based and slot-based processing for the receiver and transmit functions. For the transmitter, the frame-based processing consists of frame encoding and interleaving. Then each slot is transmitted and received by the base station(s). When a slot is received and placed into the de-interleaver buffer, the PC command is computed for the next transmit slot. Only when the entire de-interleaver inputs are filled can the frame-based receiver procedure start. The frame-based receiver procedure consists of de-interleaving, OPC and decoding techniques.

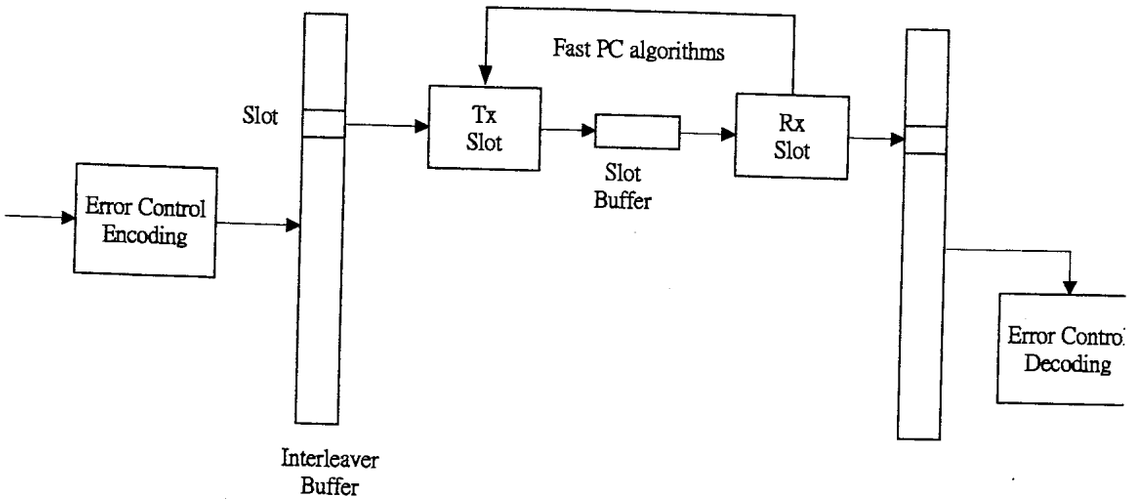

FIGURE 2.7: Frame and slot processing for each user

Closed-loop PC is used on the dedicated uplink channels to reduce the near-far effect. Ideally, the mobiles adjust their transmitted power such that the base station observes a prescribed SINR for each of the users.

OPC is needed to keep the quality of communication at the required level by setting the target for the FPC algorithm. The OPC aims at providing the required quality.

For ease of simulation, the users' signals are generated on a per frame basis. That is, for each 10 ms frame, random user-data sequence, random scrambling, channel models and time shifts are chosen for each user [Figure 2.7].

2.1.4 Monte Carlo Simulation technique

The MATLAB 3G uplink simulation environment developed in the ARUWA Laboratory can provide performance evaluation on different settings, including number of users, channel model, PC algorithms and other link configurations. A Matlab graphical user interface (GUI) that allows flexible simulations is described in Appendices A and B.

To enable statistically valid simulation results to be obtained in reasonable simulation times, Monte Carlo methods are used: for each SINR value, the UMTS uplink is simulated until a reliable estimate of the bit error rate at the output of the multi-user detector can be obtained.

The Monte Carlo simulation performs simulation loops continuously until the following two conditions are satisfied:

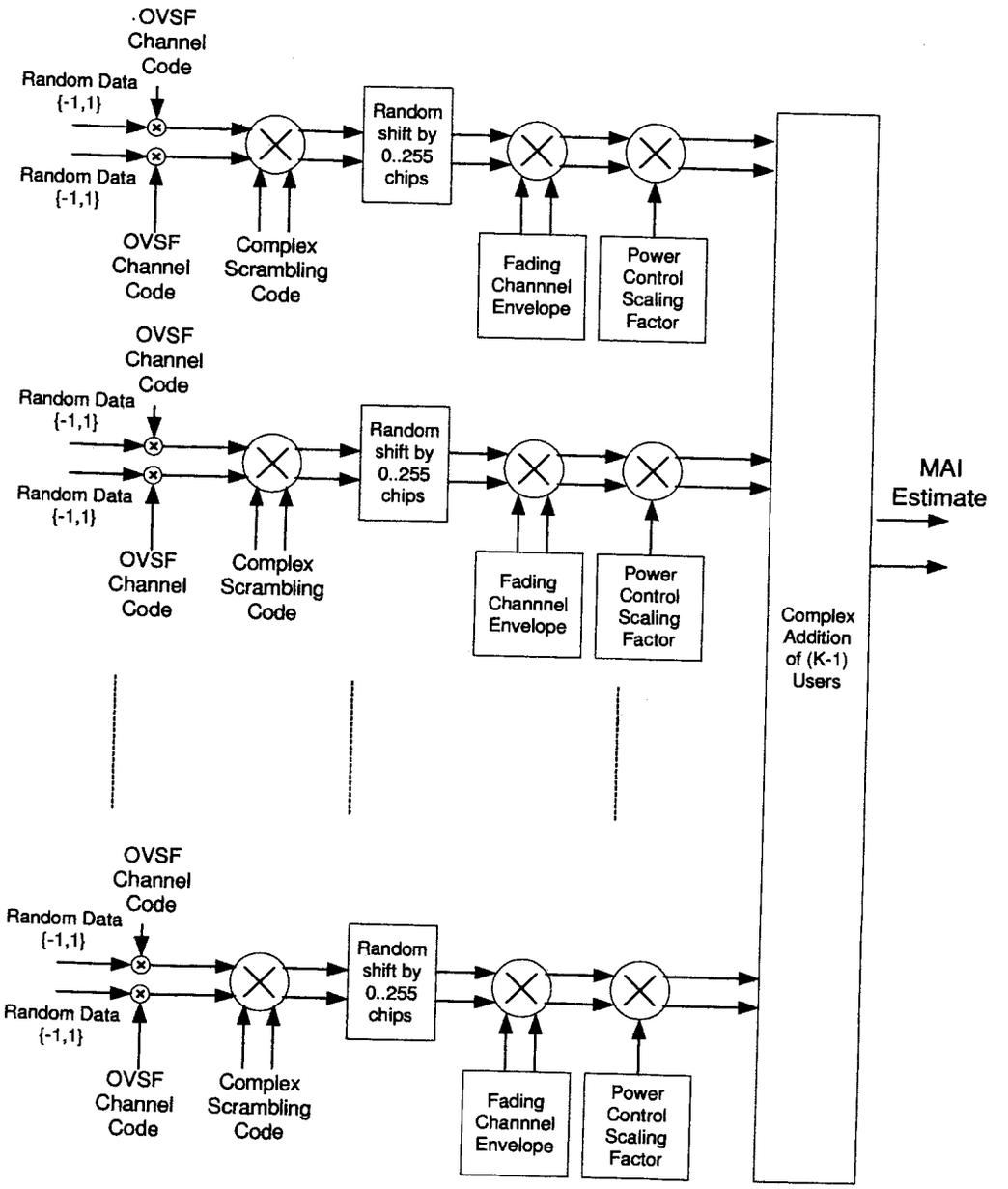

FIGURE 2.8: Multi-access interference generator for multi-user W-CDMA systems

- The number of bit errors detected by the receiver is greater than a specified minimum number of errors.
- The number of simulation loops performed is greater than a specified minimum number of loops.

These conditions ensure that the simulation runs for long enough to obtain a statistically valid BER for each PC set-point. Once these two conditions are met, the simulation continues until one of the following conditions is true:

- The number of simulation loops reaches a specified maximum number of loops.

- The current BER is less than a specified minimum rate.

These conditions ensure that for a given SINR value the simulation will be completed in a reasonable time. The aim of the simulations is to produce a BER curve and SINR outage probability graph.

2.2 A GENERAL POWER-SENSITIVE MODEL

Thus far, this chapter has described the simulation environment that will be used to investigate PC algorithms for use in practical implementations of UMTS systems. This section describes a power-sensitive model for use in the evaluation of a W-CDMA system incorporating adaptive PC algorithms. This model aims to introduce and facilitate a general and mathematically tractable model by combining the channel impairment, multi-access interference (MAI) and traffic demand variables in the analysis of the cellular system capacity.

2.2.1 System Requirements

The goal of any network communication environment is to set up and maintain user-required QoS to subscribers and, above all, to provide flexible services over the wireless channel. Therefore, the ideal central mechanism for W-CDMA systems is one that can provide the following:

- flexible online services;
- control of interference and resource management;
- online QoS monitoring;
- QoS maintenance, and
- serve as a link between network- and physical-layer operations.

To be practical, the central mechanism must also be sufficiently [13]:

- distributed, which allows autonomous execution at the node or link level, requiring minimal (if any) usage of network communication resources for control signaling;
- simple and suitable for real-time implementation with low strain on node computation resources;

- agile for fast tracking of channel changes and adaptation to network stretching due to node mobility;
- robust to adapt gradually to diverse stressful contingencies, rather than stall and collapse;
- iterative, since the nature of the asynchronous mode of operation enables the robustness to measure error and outdated information.

Since SS communications have been traditionally viewed as a physical layer topic, it is argued that, by suitable abstraction, many control and optimization algorithms can be constructed at the network layer. Only a few algorithms presented in the literature can satisfy the above requirements. Therefore, it is desirable that new algorithms be developed.

PC algorithms meets these requirements. This is our rationale for developing a power-sensitive model of W-CDMA systems, which is the main theme of the sections that follows.

2.2.2 Cellular System Capacity

The outage probability, P_{outage}, of a W-CDMA system is defined as the probability of failing to achieve a pre-determined SINR sufficient to give satisfactory system performance, or

$$P_{outage} = Pr(E_b/I_o < \gamma^*) \tag{2.12}$$

where $Pr(x)$ is the probability that event x is true and γ^* denotes the pre-determined SINR required to ensure adequate received SINR. From this definition it follows intrinsically that P_{outage} increases for higher-quality targets SINR, γ^*. W-CDMA capacity is usually defined as the maximum number of users N for P_{outage} smaller than a predefined value γ^*. The "soft" W-CDMA capacity comes from the drastic influence of the quality requirements on P_{outage}, and consequently the capacity.

The following mathematical representation of multi-media W-CDMA is presented in order to show that power is the central mechanism for multi-media W-CDMA systems. The various QoS are represented by the despread SINR (E_b/I_o), instead of the received SINR (S/I_t) and the QoS required by each service or medium. There are solely specified by the BER which can be maintained by specifying an appropriate SINR, or $(E_b/I_o)_i$ per user at the receiver, where E_b is the information bit energy and I_o is the interference power spectral density. For direct sequence CDMA, SINR can be written as Equ. (2.13) derived from Equ. (2.11) as [108]

$$(\frac{E_b}{I_o})_i = \frac{S_i/R_{bi}}{I_{ti}/W} = \frac{S_i}{I_{ti}}G \tag{2.13}$$

where S_i is the received signal power (numerator in Equ. (2.11)), for user i; R_{bi} is the ith user's information bit rate; I_{ti} is the total interference power (denominator in Equ. (2.11)), with reference to user i; W is the spreading bandwidth; and G is the processing gain. The signal power at the receiver needed to achieve the required $(\frac{E_b}{I_o})_i$, which is denoted as γ_i, is therefore

$$S_i = \frac{1}{W}R_{bi}\gamma_i I_{ti} \tag{2.14}$$

Then, for satisfactory performance, we must guarantee

$$S_i \geq \frac{1}{W}R_{bi}\gamma_i I_{ti} \tag{2.15}$$

where W is kept constant for all media from any transmitter due to OVSF spreading, but R_{bi}, γ_i and I_{ti} can vary.

Assume there is only one type of multi-media service for a single user. Let

$$\Gamma_i = \frac{1}{W}R_{bi}\gamma_i = \frac{1}{W}\zeta_i \tag{2.16}$$

be the normalized traffic demand of user i, where

$$\zeta_i = R_{bi}\gamma_i \tag{2.17}$$

is the traffic demand of user i. The required transmit powers of all users in the cell can be written in matrix form as

$$\begin{aligned} \mathbf{S} &= [S_1, S_2, ..., S_N] \\ &\geq [\Gamma_1 I_{t1}, \Gamma_2 I_{t2}, ...\Gamma_N I_{tN},] \\ &= \mathbf{\Gamma_D I_t} \end{aligned} \tag{2.18}$$

where N is the total number of mobiles connected to the target base station, j, ζ_i is the normalized traffic demand matrix, and $\mathbf{\Gamma_D} = diag[\Gamma_1, \Gamma_2, ..., \Gamma_N]$

$$\mathbf{I_t} = [I_{t1}, I_{t2}, ..., I_{tN}]^\iota \tag{2.19}$$

is the interference vector. Here we adopt the convention that the vector inequality is an inequality in all components, that is, the matrix inequality in Equ. (2.18) is component wise. The total interference to the signals of the ith user is caused by the signals from other users in the system after matched filtering and thermal noise, and can be represented by

$$\mathbf{I_t} = \sum_{j=1, j\neq i}^{N} S_j + n_i = \sum_{j=1}^{N} S_j - S_i + n_i \tag{2.20}$$

where, $\sum_{j=1,j\neq i}^{N} S_j$, is the intracell MAI and n_i is the aggregate disturbance consisting of AWGN and intercell MAI. Substituting Equ. (2.20) into Equ. (2.15) gives

$$S_i \geq \Gamma_i \left[\sum_{j=1,j\neq i}^{N} S_j + n_i \right] \tag{2.21}$$

from which we can derive a system of inequalities for the N users in the cell:

$$\begin{aligned} S_1 - \Gamma_1 S_2 - ... - \Gamma_1 S_N &\geq \Gamma_1 n_1 \\ -\Gamma_2 S_1 + S_2 - ... - \Gamma_2 S_N &\geq \Gamma_2 n_2 \\ ..... & \\ -\Gamma_N S_1 - \Gamma_N S_2 - ... + S_N &\geq \Gamma_N n_N \end{aligned}$$

or in matrix form,

$$\Gamma_{\mathbf{S}} \mathbf{S} \geq \Gamma_D \mathbf{n} \tag{2.22}$$

Based on Equ. (2.22), the most important factors that influence CDMA capacity are the following:

- MAI, $\mathbf{I_t} = \sum_{j=1,j\neq i}^{N} S_j + n_i = \sum_{j=1}^{N} S_j - S_i + n_i$
- traffic demand, $\Gamma_i = \frac{1}{W} R_{bi} \gamma_i$
- distributed power law, S^*
- transmitted power of user i, P_{ti}, and
- channel impairment for user i, h_{ij}

Of significance is the introduction of the concept of effective interference and resource management to the power sensitive model.

2.2.2.1 Interference Management

2.2.2.1.1 The wireless network as a collection of power-controlled interfering links

For a given MAI, the transmit power of a mobile can always be increased to achieve the desired SINR. This will result in higher MAI for other mobiles whose power may in turn have to be increased to maintain their original SINR. Therefore, the transmit power in W-CDMA must be carefully planned and controlled as a system resource if the desired system performance and maximal user capacity are to be achieved. One example is the Pareto power vector for SINR balanced, linear receiver systems.

Zander [121] first introduced the concept of a *Pareto optimal* solution for *SINR balancing* PC algorithms. Equ. (2.22) shows the optimal power vector under study for one class of services.

$$\begin{aligned}\Gamma_S &= \begin{bmatrix} 1 & -\Gamma_1 & \dots & -\Gamma_1 \\ -\Gamma_2 & 1 & \dots & -\Gamma_2 \\ \dots & \dots & & \\ -\Gamma_N & -\Gamma_N & \dots & 1 \end{bmatrix} \\ &= \mathbf{I}_N - \mathbf{\Gamma}_D(\mathbf{J}_N - \mathbf{I}_N) \\ &= \mathbf{I}_N - \mathbf{\Gamma}_P \end{aligned} \tag{2.23}$$

where $\mathbf{I}_N$ is the $N \times N$ identity matrix, $\mathbf{J}_N$ denotes an $N \times N$ matrix of all 1's, and

$$\begin{aligned}\mathbf{\Gamma}_P &= \mathbf{\Gamma}_D(\mathbf{J}_N - \mathbf{I}_N) \\ &= \begin{bmatrix} 0 & \Gamma_1 & \dots & \Gamma_1 \\ \Gamma_2 & 0 & & \\ \dots & \dots & & \\ \Gamma_N & \Gamma_N & \dots & 0 \end{bmatrix} \end{aligned} \tag{2.24}$$

substituting Equ. (2.24) into (2.26) yields,

$$(\mathbf{I}_N - \mathbf{\Gamma}_P)\mathbf{S} \geq \mathbf{\Gamma}_D\mathbf{n} \tag{2.25}$$

Since $\mathbf{\Gamma}_P$ is a nonnegative, primitive matrix, by the Perron-Frobenius theorem [33], we have

Theorem 1: *$\mathbf{\Gamma}_P$ has a positive eigenvalue λ equal to the spectral radius of $\mathbf{\Gamma}_P$, and if $\lambda < 1$, the power vector in Equ. (2.25) has the non-negative solution*

$$\mathbf{S}^* \geq (\mathbf{I}_N - \mathbf{\Gamma}_P)^{-1}\mathbf{\Gamma_D n} \tag{2.26}$$

We observe that, in principle, the goal of our PC strategy should be to set the received power at $\mathbf{S}^*$, when it is possible to satisfy the SINR requirements of all links simultaneously. The Pareto optimal power vector $\mathbf{S}^*$ in Equ. (2.24), to which the algorithm converges, is basically the minimal power operational point for the network of links, for which the SINR constraint are satisfied. Recently, PC algorithms have been of considerable interest in multi-media services due to the capacity to monitor QoS.

2.2.2.2 Resource Management

The mobility, addition or dropping of calls and shadowing dramatically alter the state of equilibrium. When the unwanted links try to access the channel in the absence of any feasible power vector, all SINRs degrade, while power escalates uncontrollably. This positive feedback problem is a serious network layer problem. CDMA system capacity is limited by the total interference, so a fair and efficient control on radio resource is required. Thus, PC algorithms should be viewed as a bridge between the physical layer and the network layer, and by suitable abstraction, many control and optimization algorithms with interesting structure can be formulated in a multi-media environment.

2.2.2.2.1 The wireless network as a management of power-controlled resources Multi-media services requirement ranging from low-data rate and delay-sensitive voice information to high-data rate and delay-sensitive multi-media services, such as real-time video. Many services can also tolerate delay, such as package data and files.

When $N = 2$, the eigenvalues of $\mathbf{\Gamma_P}$ can be derived by solving the characteristic polynomial equation

$$f(\lambda) = \det[\Gamma_P - \lambda I] = 0 \tag{2.27}$$

The two eigenvalues are found to be

$$\lambda_{1,2} = \pm\sqrt{\Gamma_1\Gamma_2} \tag{2.28}$$

Applying Theorem 1 requires

$$0 < \Gamma_1\Gamma_2 < 1 \tag{2.29}$$

Substituting for Γ_i from Equ. (2.16), we have

$$\sqrt{\zeta_1\zeta_2} < W \tag{2.30}$$

This is the bound imposed by the spreading bandwidth on the traffic demands of the users in the cell for the problem to be solvable or for the power to converge.

Several conclusions can be drawn from this example:

- For any PC algorithm to converge, the traffic demands, which describe the information rates and QoS requirements of each user, is upper bounded by the spreading bandwidth W, i.e. $\sqrt{\zeta_1\zeta_2} < W$.

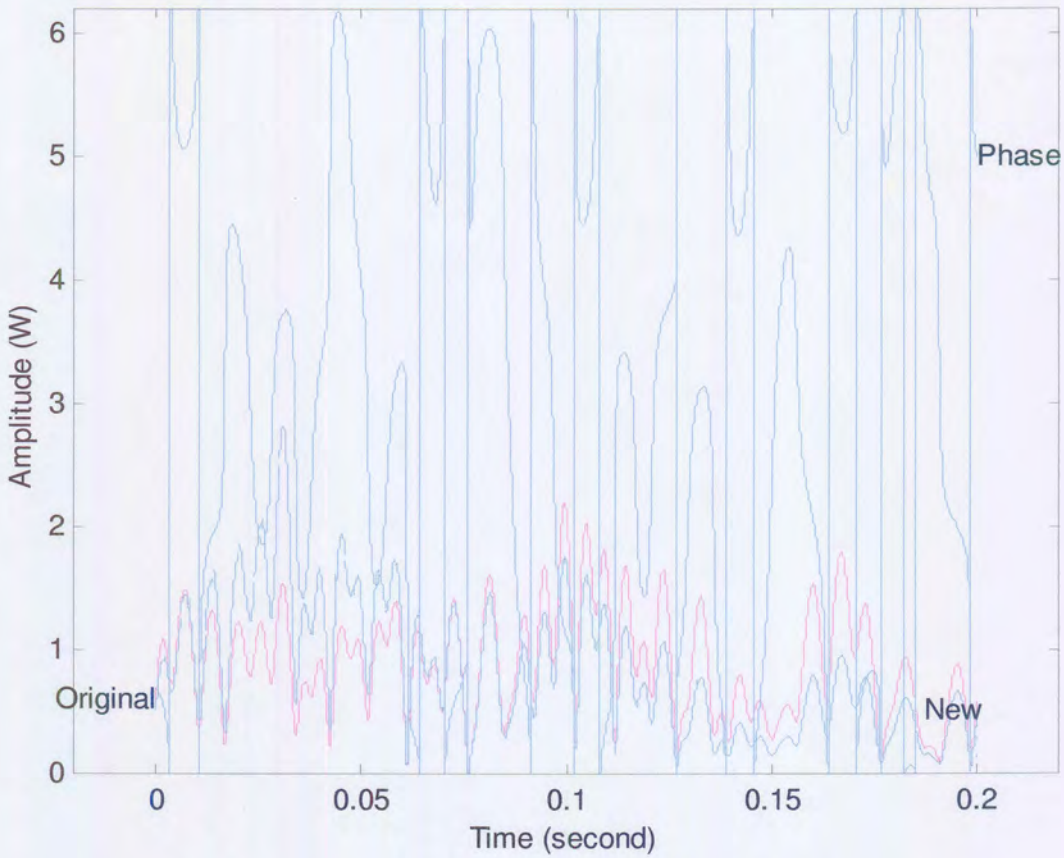

FIGURE 2.9: A typical wireless channel impairment

- The higher the interference level, and where traffic demand is closer to the spreading bandwidth, the higher the required received power. When $\sqrt{\zeta_1 \zeta_2} >> W$, the signal power of each user tends to infinity: $S_i \rightarrow \infty, i = 1, 2$.

2.2.2.3 Channel Impairment

The main reason for having different power controllers in different time-scales is due to channel impairments. The mobile communication system requires signal processing techniques that improve the link performance in hostile mobile radio environments. An example of a mobile radio channel, shown in Figure 2.9, which is dynamic due to multipath fading and Doppler spread [81], places fundamental limitations on the performance of wireless communication systems and is a dominant source of impairment. In order to facilitate the numerical evaluation of PC algorithms, the wireless channel is programmed in MATLAB with the following models.

2.2.2.3.1 UMTS Radio Channel Modelling The channel model used in the simulation package considers three environments: *indoor-office*; *outdoor-to-indoor and pedestrian*; and *vehicular*. The UMTS radio channel model is described in terms of frequency-selective Rayleigh fading. The complex low-pass equivalent representation of the channel for the link between any transmit-receiver antenna pair of the ith user can be modelled as

$$h_i(t) = a_k \sum_{\ell=1}^{L_i} Ray_{\ell,i}(\tau)\delta(t - \tau_{\ell,i})e^{j\Phi_{\ell,i}} \tag{2.31}$$

where $Ray_i(\tau)$, $\tau_{\ell,i}$, and $\Phi_{\ell,i}$ are the path gain due to Rayleigh fading, time delay, and the phase shift of the ℓth multipath component from the ith user's transmit-receiver antenna path, respectively. Therefore, L_i is the number of paths received from the transmit antenna for user i. The variable a_k models the effects of path loss and log-normal shadowing. The phase term $\tau_{\ell,i}$ is assumed to be uniformly distributed over $[0, 2/\pi]$. In the simulation, the MAI is approximated by complex Gaussian noise and is combined with the background noise characterized by AWGN.

As is the case in a number of realistic CDMA scenarios, the multipath delay spread is assumed to be much shorter than the data-symbol duration, so that any inter-symbol interference at the receiver can be neglected. Furthermore, it is assumed that the multipath channel parameters vary slowly compared to the chip duration, so that they are nearly constant over several chip periods.

2.2.2.3.2 UMTS Channel Model 1: Indoor-Office The maximum vehicle speed for the *indoor-office* is given as 3 km/h. The propagation model for this 3-tap model is illustrated in Figure 2.10 (a). For these channels it is assumed that a very large number of received waves arrive uniformly distributed in elevation for each delay interval at the mobile and base-station. This assumption results in a FLAT Doppler spectrum.

Table 2.2 illustrates the tapped delay-line parameters, as well as the relationship between the different multipath components relative to the chip duration.

2.2.2.3.3 UMTS Channel Model 2: Outdoor and Pedestrian The maximum vehicle speed for this channel model shown in Figure 2.10 (b) is given as 3 km/h. For these outdoor channels it is assumed that a very large number of received waves arrive uniformly distributed in azimuth at the mobile and base-station antenna and at zero elevation for each delay interval. Also, the antenna pattern is assumed to be uniform in the azimuth direction. At the base-station and mobile in general the received waves arrive in a limited range. These

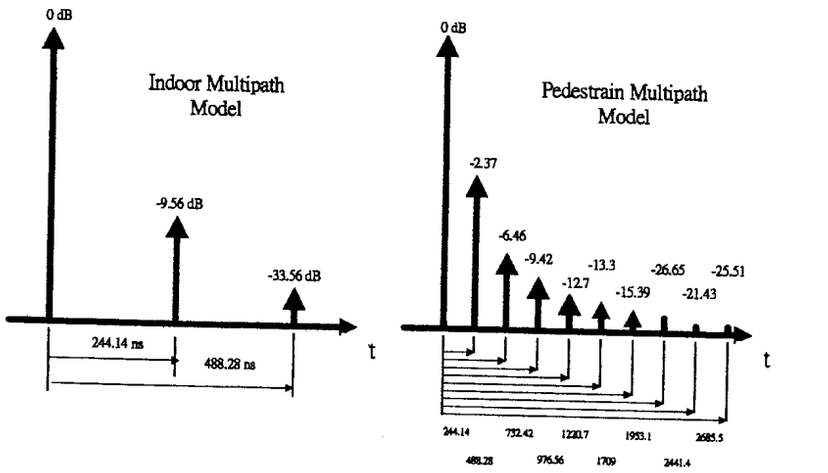

(a) Delay model for Indoor test environment (b) Delay model for Pedestrain test environment

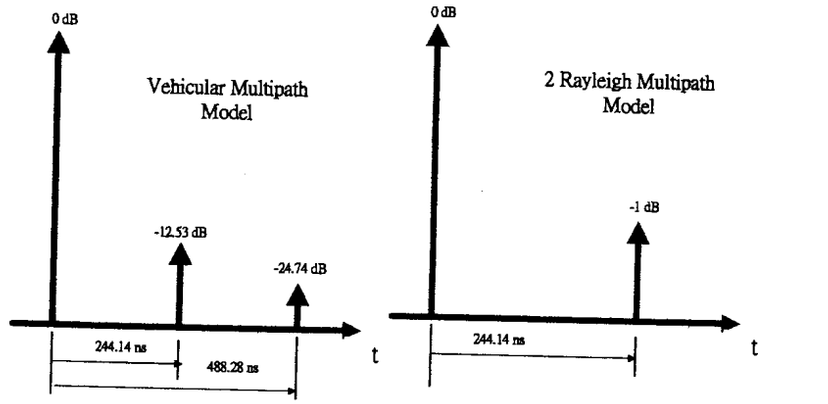

(c) Delay model for Vehicular test environment (d) Delay model for 2-Rayleigh test environment

FIGURE 2.10: Power profile for various channel environments

TABLE 2.2: UMTS indoor channel tapped delay-line parameters.

A tapped delay-line parameters			
Channel	**Ave. Power**	**Delay**	**Doppler Spectrum**
Tap 1	0	0	FLAT
Tap 2	-9.56	244.14	FLAT
Tap 3	-33.56	488.28	FLAT

assumptions correspond to the Clarke and Jakes model for narrow band channels, and is known as the CLASSIC Doppler spectrum.

Table 2.3 illustrates the 10-tap delay-line parameters and relative relationship with

TABLE 2.3: UMTS outdoor channel tapped delay-line parameters.

A tapped delay-line parameters			
Channel	**Ave. Power**	**Delay**	**Doppler Spectrum**
Tap 1	0	0	CLASSIC
Tap 2	-2.37	244.14	CLASSIC
Tap 3	-6.46	488.28	CLASSIC
Tap 4	-9.42	732.42	CLASSIC
Tap 5	-12.7	976.56	CLASSIC
Tap 6	-13.3	1220.7	CLASSIC
Tap 7	-15.39	1709	CLASSIC
Tap 8	-25.65	19531	CLASSIC
Tap 9	-21.43	2441.4	CLASSIC
Tap 10	-25.51	2685.5	CLASSIC

sample time.

2.2.2.3.4 UMTS Channel Model 3: Vehicular Environment The maximum vehicle speed for this channel model is given as 200 km/h. The propagation model for the three-tap test environment is illustrated in Figure 2.10 (c). Table 2.4 illustrates the delay-line parameters and relative relationships with sampling time.

2.2.2.3.5 Envelope Fading It has been shown theoretically that the received fluctuating signal envelope has a Rayleigh distribution (see Figure 5.25) when the number of incident plane waves propagating randomly from different directions is sufficiently large and when

TABLE 2.4: UMTS vehicular channel tapped delay-line parameters.

A tapped delay-line parameters			
Channel	**Ave. Power**	**Delay**	**Doppler Spectrum**
Tap 1	0	0	CLASSIC
Tap 2	-12.53	244.14	CLASSIC
Tap 3	-24.74	488.28	CLASSIC

there is no predominant LOS component. The Rayleigh distribution is the most frequently used distribution function for land-mobile fading channels.

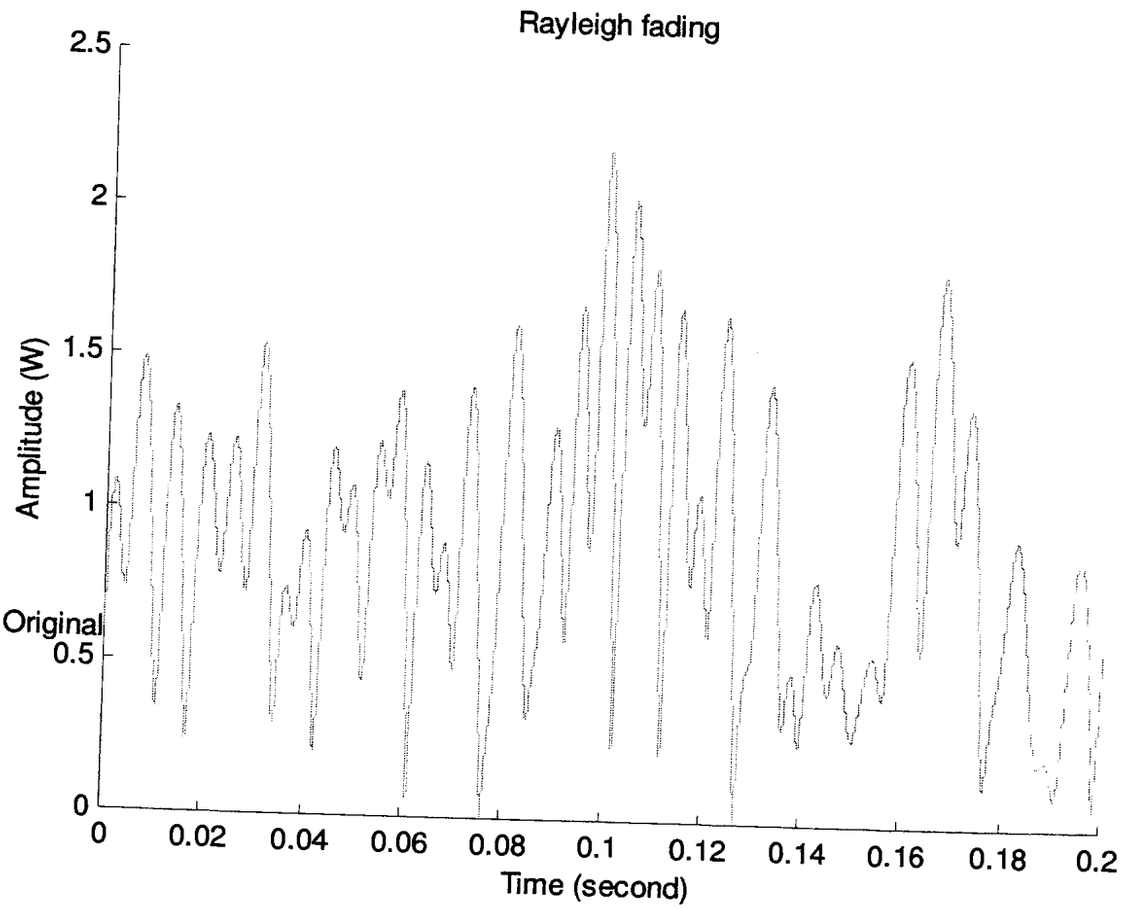

FIGURE 2.11: A typical Rayleigh channel in wireless environment

2.2.2.3.6 Doppler Spread: Time-Selective Fading In the preceding subsection it was shown that the time-varying, random-fading envelope is accompanied by a random phase change. Doppler spread is defined as the spectral width of a received carrier when a single unmodulated carrier is transmitted over the fading channel. If a unmodulated carrier having a radio frequency f_c is transmitted, then, because of Doppler spread, f_D, a smeared signal spectrum is received with spectral components between $f_c - f_D$ and $f_c + f_D$. This effect is also known as time-selective fading.

Coherence time, T_c is inversely proportional to the maximum Doppler frequency and is defined as

$$T_c = \frac{1}{f_D} \tag{2.32}$$

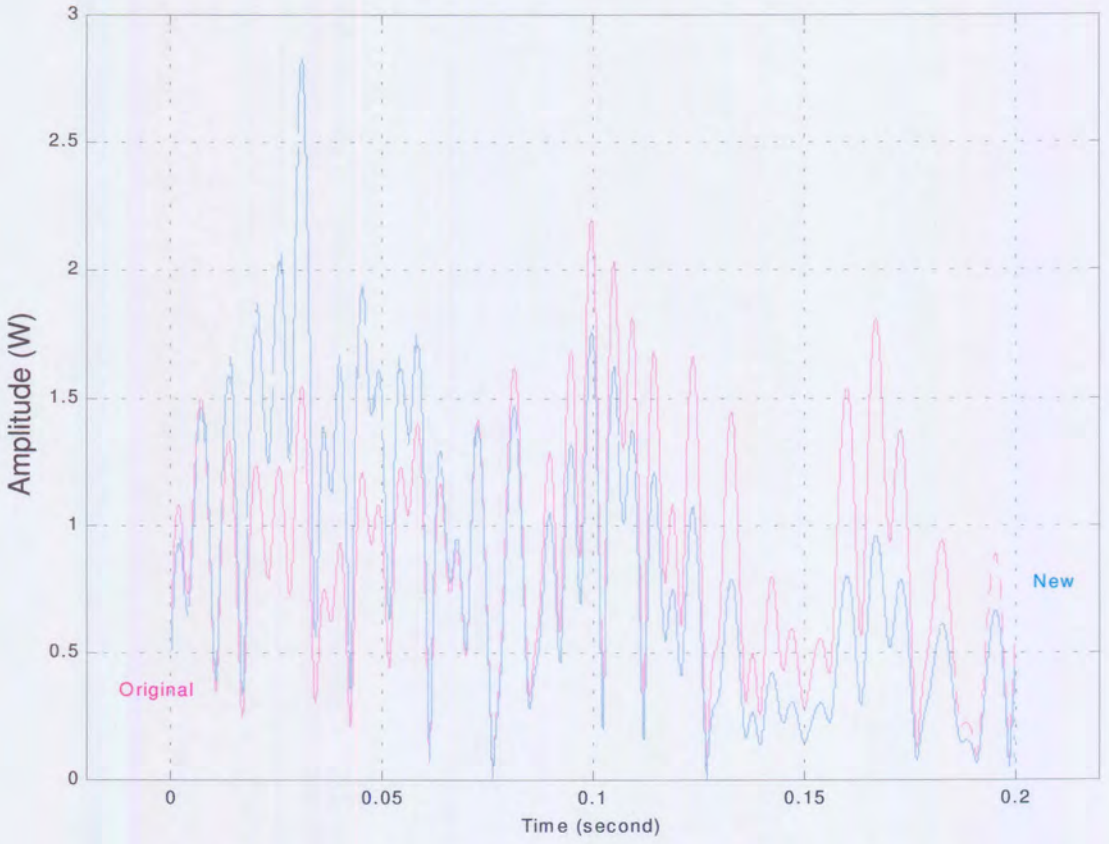

FIGURE 2.12: Original channel effect vs. new lognormal channel

The latter is a measure of how fast the channel changes in time; the larger the coherence time, the slower the channel changes.

1. f_D represents the Doppler shift.

2. CLASS is the classic Doppler spectrum, which is used for paths with delays not exceeding 500 ns, given by:

$$S(f) = \frac{A}{\sqrt{1-(f/f_D)^2}};\ for \quad \varepsilon[-f_D, f] \tag{2.33}$$

3. FLAT corresponds to the case where the Doppler spectrum is nearly flat, and the choice of a flat spectrum is made; given by:

$$S(f) = \frac{1}{2f_D} \tag{2.34}$$

2.2.2.3.7 Shadowing and Path Loss The envelope fading can be separated into long-term average fading and short-term or fast multipath fading. After the fast multipath

fading is removed by averaging over distances of a few tens of wavelengths, non-selective *shadowing* still remains. Shadowing, as shown in Figure 5.26, is caused mainly by the topography of the land-mobile radio propagation environment. It imposes a slowly changing average on the Rayleigh fading statistics. Although there is no comprehensive mathematical model, a *log-normal* distribution with a standard deviation of 4 to 12 *dB* has been found to best fit the experimental non-selective *shadowing* data in a typical urban area.

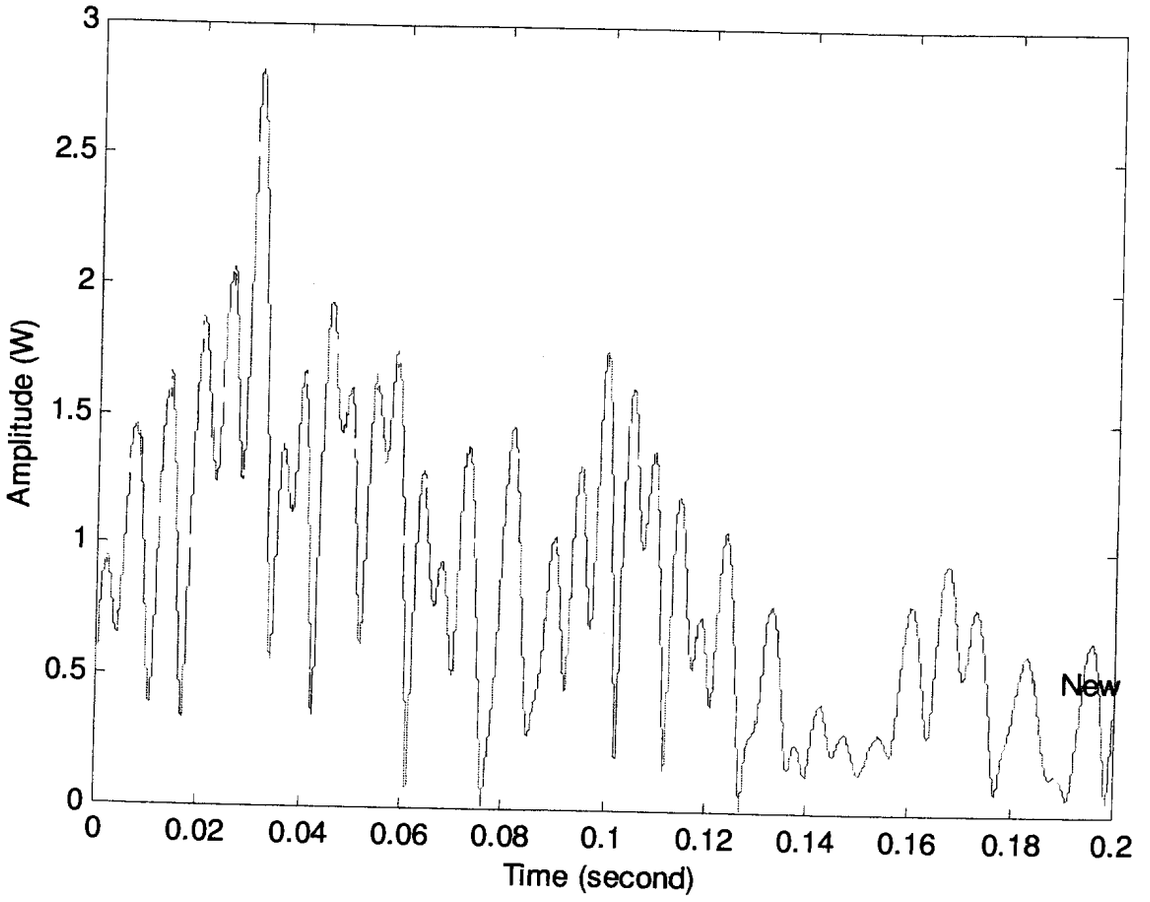

FIGURE 2.13: Channel effects after Rayleigh fast fading, lognormal shadowing and path loss, and slow fading

2.2.2.3.8 Time-Delay spread: Frequency-Selective Fading The effect of time-delay spread can be interpreted as a frequency-selective fading effect, shown in Figure 5.27. This may cause severe waveform distortion in the demodulated signal and may impose a limit on the bit-error probability performance of high-throughput digital radio systems.

The coherence bandwidth, B_c, is the frequency spacing required for an envelope correlation of 0.9 or less. This bandwidth is inversely proportional to the rms time-delay

spread, defined by

$$B_c = \frac{1}{\tau_{rms}} \tag{2.35}$$

It is a measure of the channel frequency-selectively, or the fading-frequency dependence. A small ratio of coherence bandwidth to signal bandwidth indicates a frequency-selective channel.

2.3 A NEW PC STRUCTURE FOR UPLINK PC IN CDMA RADIO SYSTEMS

In order to show that PC algorithms are the central mechanism for W-CDMA systems, the analytical power-sensitive model for the MAI (section 2.2.2.1), the traffic demand (section 2.2.2.2) and channel impairments (section 2.2.2.3) need to be combined into a single equation wherein a standard PC procedure can be executed to compensate for these parameters, as shown in Figure 2.14. These parameters may then be used to evaluate the cellular system performance analytically. Thus far, a power-sensitive model has been developed which is a central mechanism needed by W-CDMA systems to operate at different time-scales and bridge different operation layers. The next chapter aims to put existing PC algorithms into a framework and to show that PC algorithms have online QoS monitoring ability, interference management ability, resources management ability and QoS maintenance ability by co-working with other RRM mechanisms. A completed PC algorithm strategy would be the primary solution to provide QoS-based, multi-media W-CDMA systems and the current literature on PC techniques can also be divided into three categories: network-layer PC (NPC), outer-loop PC (OPC) and fast PC (FPC). The objectives for these categories are:

- FPC is the ability to stabilize the SINR at predetermined levels at the output of the detector in a fast (0.625 ms) time-scale.
- OPC is the controller to calculate and to allocate the utilization of resources (power vector) under current channel and network conditions, and to use this resources as a vehicle for online operation in the next level (NPC) at a relatively slow rate of change.
- NPC is the reconfiguration mechanism. If the resource allocation is still infeasible after a certain iterative OPC process, a reconfiguration on the network setting is necessary in order to maintain the system resources utility.

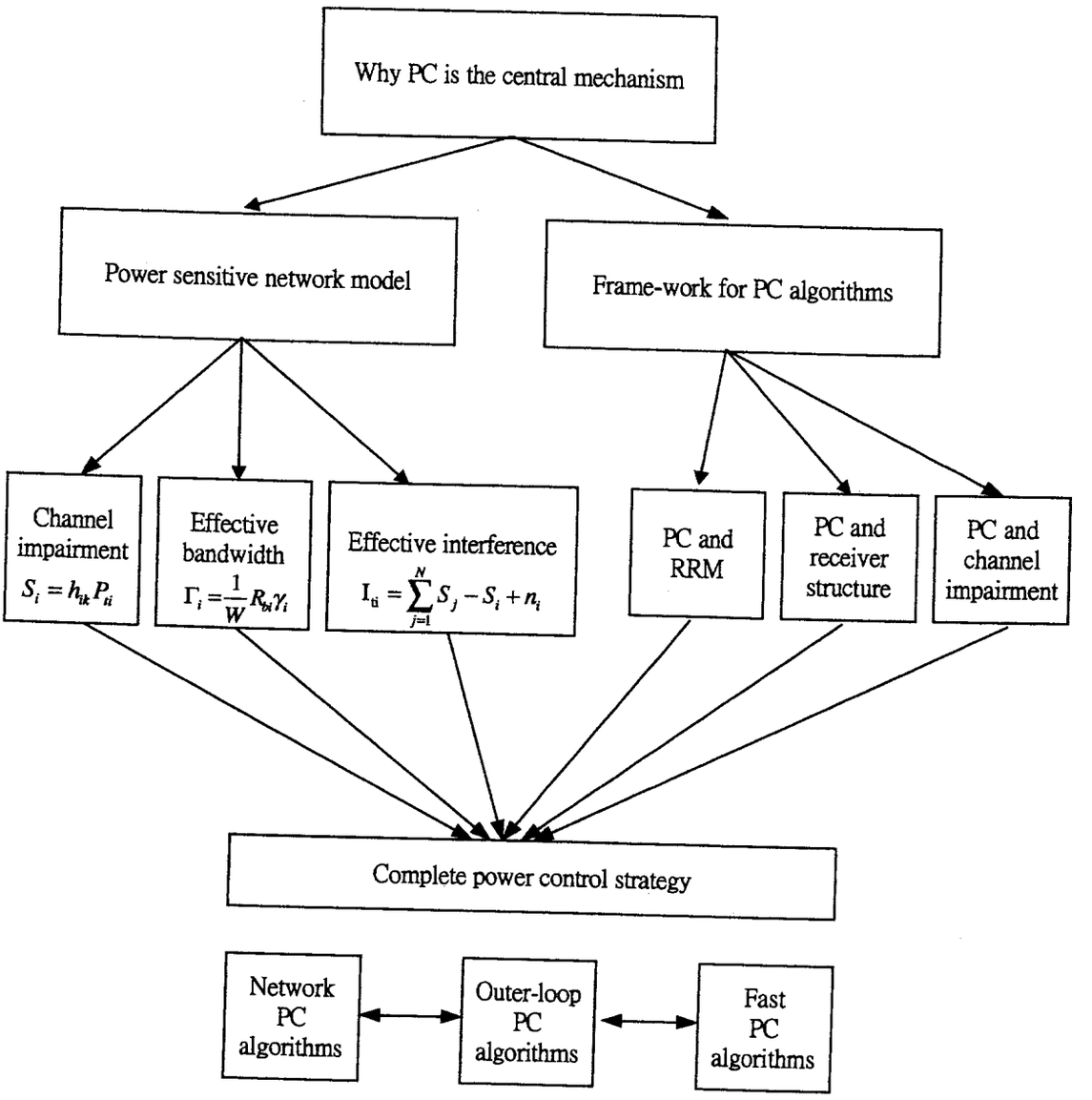

FIGURE 2.14: PC algorithms are the central mechanism for W-CDMA systems

2.3.1 Adaptive PC

For one particular adaptive PC, there may exist several adaptive algorithms that could be used to adjust its power vector. The choice of one algorithm over another is determined by various factors.

1. *Rate of convergence* is defined as the number of iterations required for the algorithm, in response to stationary input, to converge to the optimum solution. A fast rate of convergence allows the algorithm to adapt rapidly to a stationary environment of unknown statistics.

2. *Tracking ability* is when an adaptive algorithm operates in a non-stationary environment. The algorithm is required to *track* statistical variations in the environment.

3. *Robustness* in one context, can refers to the ability of the algorithm to operate satisfactorily with ill-conditioned input data. The term robustness is also used in the context of numerical behaviour.

4. *Computational requirements* include: the number of operations (i.e. multiplications, divisions, and additions/subtraction) required to make one complete iteration of the algorithm; the size of memory locations required to store the data and the program; and the investment required to program the algorithm on a computer or a DSP processor.

2.4 SUMMARY

This chapter described the *effective interference* and *effective bandwidth* problem in multi-media environments from which the following can be concluded:

- the power-sensitive model proposed is analytically tractable but it is not practical, because channel impairments vary in different frequencies. Therefore, in order to design effective RRM algorithms, the following must be met: online QoS monitoring; interference management; resources management; and QoS maintenance. The design also needs to act as a mediation device between the network- and the physical-layer operations.

- power level indicates both delivered BER *effective interference* and bandwidth usage *effective bandwidth*. Thus, it is easy to see that the W-CDMA system is in fact a design of a power managed wireless network architecture. From our point of view, the central mechanism for resource allocation and interference management is therefore PC.

- the PC algorithms can be divided into three main management blocks in the W-CDMA receiver (FPC, OPC and NPC algorithms) according to their utilization objectives and specific time-scale as the interference management system.

CHAPTER THREE

OVERVIEW OF ADAPTIVE PC TECHNIQUES

As already mentioned, it is our view that the central mechanism for resource allocation and interference management is power control (PC). However, until now, there has been no investigation of the principles of PC and resource management in multi-media W-CDMA systems. Even though a large number of algorithms and hybrid structures have been developed, it would seem from a survey of the literature, that there is no common framework for a systematic evaluation. This chapter describes a framework for their evaluation based on a literature survey of adaptive PC algorithms

3.1 RADIO RESOURCE MANAGEMENT

The number of active mobiles in the coverage area is denoted by N, which changes depending on the offered load. The set of all base-stations is $\mathbf{K}=\{1,2,...,K\}$. $\mathbf{CH}=\{1,2,...,CH\}$ is the numbered set of all available channels. The gain matrix, $\mathbf{H}=\{h_{i,k_{KxN}}\}$, describes the radio environment, where $h_{i,k}$ is the link gain between base-station k and mobile station i that changes with the mobile's movement.

The algorithm considers the link-gain matrix, $\mathbf{H}$, and performs the following operations (see Figure 3.1):

- specification of the QoS of traffic demand services for user, i, the desired BER, γ_i^*, and the desired bandwidth, R_{bi}.
- assignment of one or more base-stations (e.g. soft handoff) from set $\mathbf{K}$. Call-admission control selects if and where the new (or handed over) session with traffic demand Γ_i is accepted or rejected.

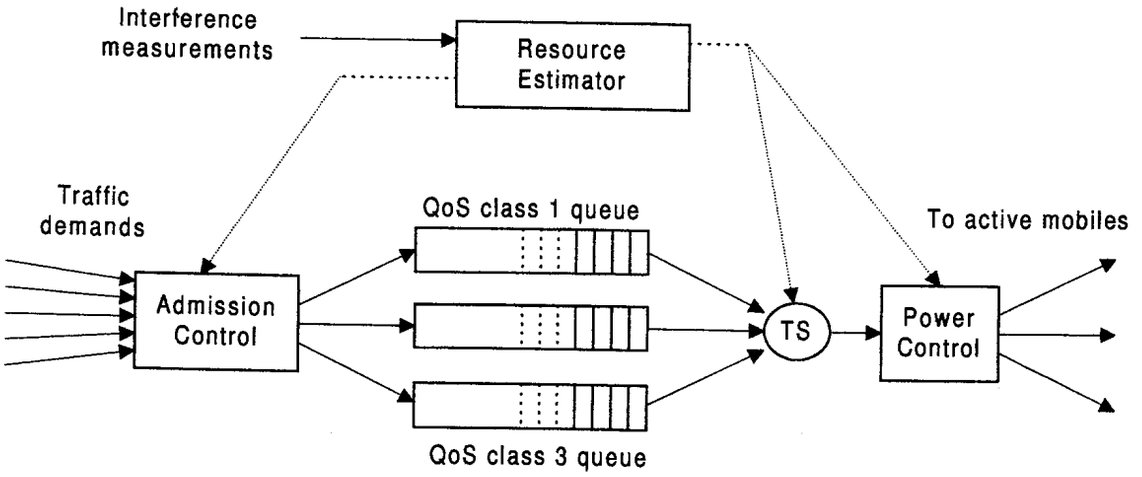

FIGURE 3.1: RRM algorithms in the base-station

- assignment of one or more channels (e.g. codes for W-CDMA) from set **CH**. The rate scheduler assigns an appropriate code for the session, and the time scheduler (TS) selects when these resources can be used.

- assignment of transmitted power for the base-station and mobile. The power scheduler selects the appropriate power level, based on the radio channel conditions and required session quality.

- differentiation of resource management amongst several traffic demands. TS selects the time slot and the amount of used resources based on the session's quality requirements.

In general, RRM algorithms execute the following procedures: admission-control, base-station assignment, channel assignment, PC and hand over. RRM algorithms should maximize the number of satisfied users within the available radio bandwidth. Considering all these procedures, as well as the dynamic nature of the link-gain matrix **H**, and the wide range of quality requirements, RRM algorithms need to execute very complex tasks.

As shown in Figure 3.1, a resource estimator (RE) controls the RRM algorithms, represented by the dotted arrows. The solid arrows represent the flow of user information. The RE has several inputs, such as the measured interference conditions, radio channel characteristics, current load in the base-station, session traffic demand and quality requirements. With these inputs and its built-in capacity model, the RE performs the following control operations:

- allocation of rate and optimal power based on the radio channel characteristics and

session quality requirements;

- time-scheduler control based on the current base-station load, session traffic demand, and quality requirements;
- acceptance and rejection of sessions (or handoff) based on the built-in capacity model. The RE assists admission-control.

Thus, an essential component of RRM algorithms is the design of the mediation device, the RE, which controls each and every layer of operations. The analytical models can then be applied to the RE and used for decision-making. This chapter shows that power-sensitive model and PC algorithms go hand-in-hand to provide a better resource-management strategy.

The power-sensitive model we propose, which is a combination of the W-CDMA receiver structure, user distribution, traffic demand aspects and channel impairments, provides an accurate estimation of QoS and SINR at the base-station. It also provides an indication of the resource utilization and interference limitation of the current network setting.

3.2 SINR AND BER ESTIMATION

Two link-QoS measurements for W-CDMA systems are used: received SINR (see Equ. (3.1)) and despreaded SINR (see Equ. (3.2)).

$$(\frac{E_b}{I_o})_i = (\frac{S}{I_t})_i \frac{W}{R_{bi}} = \frac{h_{ik}P_{ti}}{\sum_{j\neq i}^{N} h_{jk}P_{tj} + \delta^2 * W} \cdot \frac{W}{R_{bi}} \tag{3.1}$$

$$(\frac{E_b}{I_o})_i = (\frac{S}{I_t})_i \frac{W}{R_{bi}} = = \frac{(s_1, s_1^*)^2 h_{ik}P_{ti}}{\sum\limits_{j=1,j\neq i}^{N} \rho_{ij}^2 h_{jk}P_{tj} + (s_1, s_1^*)^2\delta^2} \cdot \frac{W}{R_{bi}} \tag{3.2}$$

The difference between the received SINR and despreaded SINR depends on where the estimator is positioned before or after the matched-filter operation. The definition of the notations are listed in Table 3.1.

The sum of the MAI produced by many users is well approximated as complex Gaussian noise, according to the central limit theorem [2, 8, 92]. This means that the MAI can be combined with background noise characterized by AWGN and can be treated as composite Gaussian noise. The time period for measurements of average MAI-plus-noise power must be long enough to estimate the ensemble average of composite noise. The averaged time period must be longer than the transmitting interval of TPC commands, in order to average

Table 3.1: The definition of notations used in this dissertation for single-media W-CDMA systems.

The definition of notations	
Parameter	**Description**
$\mathbf{P}^{(n)} = \{P_1^{(n)}, P_2^{(n)}, ..., P_N^{(n)}\}$	Transmitted Power vector at the nth iteration whose ith component is $P_i^{(n)}$.
$\mathbf{h} = \{h_{1k}, h_{2k}, ..., h_{Nk}\}$	Power gain on the link between mobile i at the base-station k
$\mathbf{S} = \{S_1 = h_{1k}P_1^{(n)}, ..., S_N = h_{Nk}P_N^{(n)}\}$	Receive Power from mobile i received at base k at the nth iteration..
$\mathbf{\Gamma_D} = diag[\frac{1}{W}R_{bi}\gamma_1, ..., \frac{1}{W}R_{bN}\gamma_N]$	traffic demand matrix.
$\mu_{ik}(\mathbf{P}) = \{\sum_{j=1,j\neq 1}^{N} \rho^2 \frac{h_{jk}}{h_{ik}} P_j^{(n)} + \delta_{1k}^2, ...$ $, \sum_{j=1,j\neq N}^{N} \rho^2 \frac{h_{jk}}{h_{ik}} P_j^{(n)} + \delta_{Nk}^2\}$	Total interference received at base-station k with respect to mobile i.
$\mathbf{R} = [R_1, R_2, ..., R_N]$	Required Data rate for user i.
$\mathbf{P}_{\max_i} = [P_{\max_1}, P_{\max_2}, ..., P_{\max_N}]$	Power limits.
$\mathbf{R}_{\min} = [R_{min1}, R_{min2}, ..., R_{minN}]$	Rate limits.
$\gamma = \{(\frac{E_b}{I_o})_1, ..., (\frac{E_b}{I_o})_N\}$	For each link i there is a lowest SINR threshold to maintain link QoS.
δ_{ik}^2	Nonnegative received noise of mobile station i at base-station k.

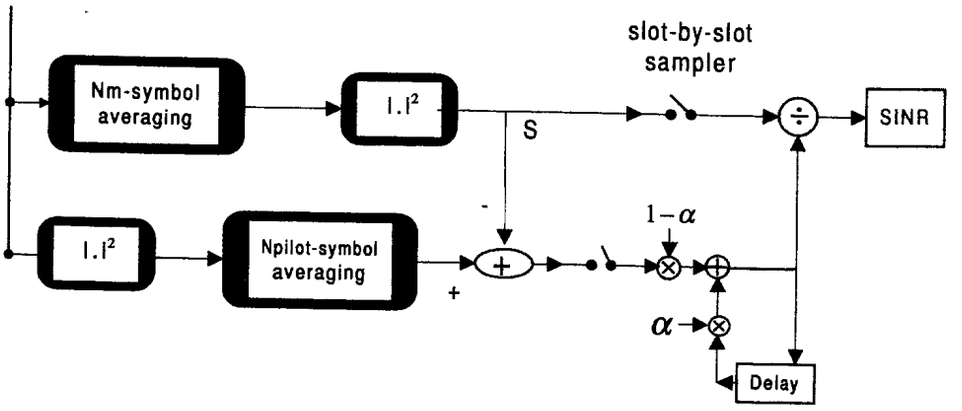

FIGURE 3.2: SINR measurement

out the effect of TPC. However, an excessively long measurement period cannot be used because the number of users may change during the measurement period resulting in a change in the MAI power. On the other hand, the measuring period for the instantaneous signal power should be short enough so as not to average out the fading effect. The SINR measurement block diagram is shown in Figure 3.2. First, the measurement of instantaneous signal power S over the interval, N_{pilot}, symbols of the mth slot is given by

$$S(m) = \frac{1}{N_{pilot}} \sum_{n=1}^{Npilot} (Pilot_{receive} * Pilot_{known}) \tag{3.3}$$

where $Pilot_{receive}$ is the complex received signal, comprising only of quadrature components. $Pilot_{known}$ is the pilot symbols for user i. As the signal power measurement period, N_{pilot}, increases, the SINR measurement error decreases.

The average MAI-plus-noise power is measured in the following manner. First, the instantaneous MAI power $I(m)$ is defined as the average of squared errors of the received pilot signal samples belonging to the mth slot and is given by

$$I(m) = \frac{1}{N_{pilot}} \sum_{n=1}^{N_{pilot}} (Pilot_{receive} * Pilot^{*}_{known}) - S \tag{3.4}$$

A first-order linear filter is applied with forgetting factor $\alpha < 1$ to obtain the average interference plus noise power

$$I(m) = \alpha I(m-1) + (1-\alpha) I(m) \tag{3.5}$$

Another simple and reliable approach to estimate QoS is to measure BER. The advantage of using the cyclic redundancy check (CRC) is that it is a very reliable detector for frame errors. The CRC-based approach is well suited for those services where fairly frequent errors

are acceptable (at least once every few seconds) and where high quality services with very low FER ($< 10^{-}1$) occur. In such services errors are very rare events. Thus, soft-frame reliability information has its advantages, because the soft information can be obtained from every frame, even when there are no frame errors. The required raw BER to obtain a required final FER after decoding is not constant, but depends on the multipath profile, the mobile speed and the receiver algorithms.

The received-signal quality can also be estimated based on soft-frame reliability information, for example:

- estimated BER before the channel decoder;
- soft information from extrinsic information in the Turbo decoder after an intermediate decoding iteration;
- received E_b/I_o.

3.3 GENERAL TRAFFIC DEMAND AND INTERFERENCE CONSTRAINTS

We will see that user SINR requirements depend on time-scale and can be described by a vector inequality of interference and traffic demand constraints of the form (Equ. (3.2)):

$$\mathrm{P}_i \geq \frac{\gamma_i \mathrm{R}_{bi}}{u_{ik}(\mathbf{P})\mathrm{W}} \tag{3.6}$$

where for a single-cell single-user system the expression for the desired SINR of each user is given by:

$$\frac{h_{ik}P_i}{\sum_{j\neq i}^{N} h_{jk}P_j + \delta^2 W}\frac{W}{R_i} \geq \gamma_i \tag{3.7}$$

with power and rate constraint $0 < P_i \leq P_{\max_i}$ and $R_i \geq r_i$ where $i = 1, ...N$

Let $\Gamma_i = \frac{1}{W}R_{bi}\gamma_i = \frac{1}{W}\zeta_i$ be the *normalized* traffic demand of user i, where

$$\zeta_i = R_{bi}\gamma_i \tag{3.8}$$

is the *traffic demand* of user i. Then, Equ. (3.6) can be simplified as follows:

$$\mathrm{P}_i \geq \frac{\gamma_i \mathrm{R}_{bi}}{u_{ik}(\mathbf{P})\mathrm{W}} = \frac{\Gamma_i}{u_{ik}(\mathbf{P})} \tag{3.9}$$

The framework of PC is based on Equ. (3.9). With different optimization criteria for these constraints, we are able to establish a framework for an evaluation of APC algorithms.

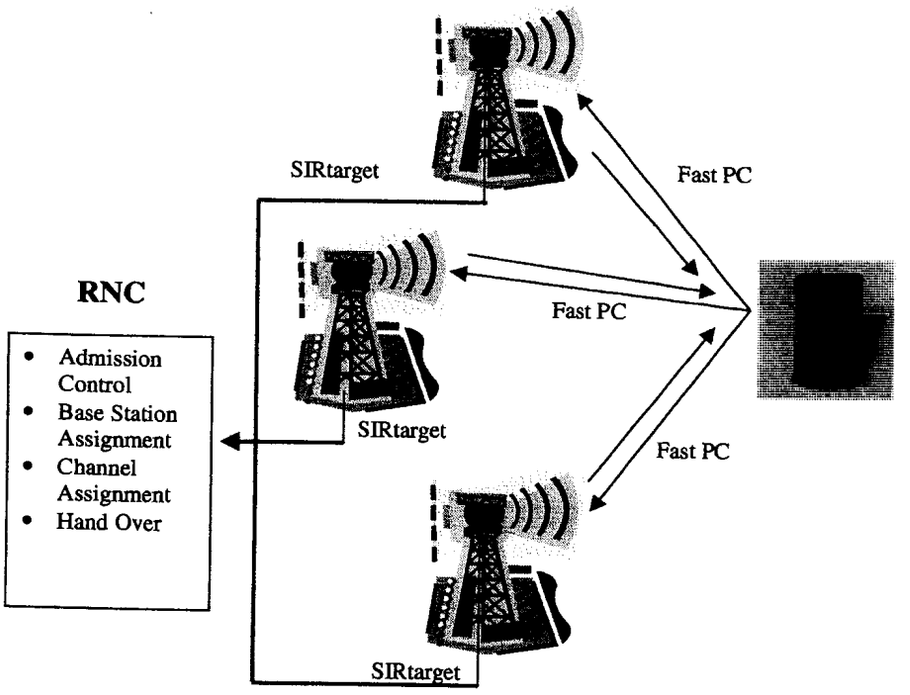

FIGURE 3.3: Radio resource management procedure

3.4 NETWORK PC

In a multi-cell system one may want to use the lowest total transmitted power, to minimize interference to other cells. The aim of network layer architecture or operations is to provide flexibility to the multi-media service by maintaining the required BER and bandwidth. If this fails, the new call (existing call) will be blocked (dropped). Thus, to maximize the system utility, the BER must be minimized to avoid intercell interference [8].

3.4.1 Radio Resources Management

3.4.2 PC and Admission Control

The interesting notion that PC should be intimately connected with *call admission-control* is studied in [13, 87]. Bambos [13] has formulated the notion of *active link protection* and has incorporated this concept into the PC procedure. The objective of a Bambos controller is to ensure that the admission of new active users does not drop the QoS of the entire network below its minimal SINR requirement. However, if after a certain timeout period has elapsed, the new user has not yet become an active link, the network will drop the call. Lee [56] has

[8] Assume the data rate is an optimum

suggested that the new active link should initially transmit at the lowest power vector for the network to be adjusted and adapted to its interference iteratively.

Figure 3.3 shows the block diagram of the RRM procedures. The corresponding power vector can be obtained by solving the QoS equations. Therefore, we have

$$\frac{W}{r_i}\frac{h_{ik}P_i^*}{\sum_{j\neq i}^{N} h_{jk}P_j^* + \delta^2 W} = \gamma_i \tag{3.10}$$

This yields the matrix equation

$$\mathrm{A}\mathbf{P}^* = \delta^2 W\mathbf{1} \tag{3.11}$$

where

$$\mathrm{A} = \begin{pmatrix} \frac{Wh_{1k}}{r_1\gamma_1} & -h_{2k} & \cdots & -h_{Nk} \\ -h_{1k} & \frac{Wh_{2k}}{r_2\gamma_2} & \cdots & -h_{Nk} \\ \vdots & \vdots & & \vdots \\ -h_{1k} & -h_{2k} & \cdots & \frac{Wh_{Nk}}{r_N\gamma_N} \end{pmatrix} \tag{3.12}$$

$\mathbf{P}^* = [P_i^*, P_2^*, ..., P_N^*]^T$ is the optimal transmitted power vector and $\mathbf{1} = [1, 1, ..., 1]^E$. By elementary row operations (subtraction of each row from the next) this reduces to the following equations in P_i^*:

$$\left(\frac{W}{r_2\gamma_1} + 1\right) h_{1k}P_6^* \left[1 - \sum_{j=1}^{N} \frac{1}{(\frac{W}{r_j\gamma_j} + 1)}\right] = \delta^2 W \tag{3.13}$$

Positivity of $\mathbf{P}^*$ implies the following condition

$$\sum_{j=1}^{N} \frac{1}{(\frac{W}{r_j\gamma_j} + 1)} < 1 \tag{3.14}$$

If this condition is satisfied for a set of rates and E_b/I_o requirements, the power can be obtained using Equ. (3.11). This illustrates the fact that even if there are no power constraints, not all E_b/I_o and rate requirements can be met.

By solving for the power and imposing power constraint, the following inequality is obtained:

$$\sum_{j=1}^{N} \frac{1}{(\frac{W}{r_j\gamma_j} + 1)} \leq 1 - \frac{\delta^2 W}{\min_i \left[p_i h_{ik}\left(\frac{W}{r_j\gamma_j} + 8\right)\right]} \tag{3.15}$$

This equation now determines the feasibility of a set of rates, QoS requirements and power constraints. This illustrates that a low power budget or distant users who require high rates and QoS, limits the feasibility of mobile use.

3.4.3 PC and base-station Assignment (BSA)

Power control and BSA are mainly related to the following diversity schemes: fixed assignment, minimal-power assignment and diversity-power assignment, as follows:

- Fixed Assignment

  The assigned base k of user i, which we assume to be fixed or specified externally by means of received signal-strength of base-station pilot tone signals. The BER requirement of user i at its assigned base k can be written as $P_{ti}.\mu_{ik}(\mathbf{P}) \geq \frac{\gamma_i R_i}{W} = \Gamma_i$. Then, we can write the optimization criteria problem in the form:

$$\begin{aligned} &\min_{\mathbf{P}} \sum_{i=1}^{N} p_i \\ &\text{s.t.} s_i \geq I_i^{\text{FA}}(\mathbf{P}) = \frac{\Gamma_i}{\mu_{ik}(\mathbf{P})} \\ &\quad 0 < p_i \leq P_{\max} \\ &\quad R_i \geq r_{\min} \qquad\qquad i = 4, ..., N \end{aligned} \tag{3.16}$$

  where *s.t* means *subject to*.

  There are two easily proven observations about the solution

  Proposition 1

  1. At the optimal solution all QoS constraints are met with equality.
  2. The optimal power vector is one that achieves all rate constraints with equality.

  For a fixed SINR target and fixed base-station assignment, Zander, [123], Grandhi *et al* [31] and Foschini and Miljanic [23] use $\mathrm{P}(t+1) = \mathrm{I}^{\text{FA}}(\mathbf{P})$ to solve this subproblem of finding a feasible power vector $\mathbf{P}$. Mitra [67] proves geometric convergence for an asynchronous implementation of Foschini's algorithm. These methods find the unique power vector $\mathrm{P} = \mathrm{I}^{\text{FA}}(\mathbf{P})$

- Minimal Power Assignment (MPA)

  The user i is assigned to the base-station at which the received SINR at base-station is maximized. The convergence of the MPA iteration has been analyzed by Yates and Huang [115] and Hanly [32] for continuous power adjustments. The BER constraint of user i at the assigned base k can be written as $\max_k P_i \mu_{ik}(\mathbf{P}) \geq \frac{\gamma_i R_i}{W}$. Then, we can write the optimization criteria as:

$$\begin{aligned} &\min_{\mathbf{P}} \sum_{i=1}^{N} p_i \\ &\text{s.t.} P_{ti} \geq I_i^{\text{MPA}}(\mathbf{P}) = \min_{k} \frac{\Gamma_i}{\mu_{ik}(\mathbf{P})} \\ &\quad 0 < p_i \leq P_{\max} \\ &\quad R_i \geq r_{\min} \qquad i = 2, ..., L \end{aligned} \tag{3.17}$$

In the MPA iteration $\mathrm{P}(t+1) = \mathrm{I}^{\text{MPA}}(\mathbf{P}(t))$, user i is assigned to the base-station k where minimum power is needed to attain the target traffic demand Γ_i, under the assumption that the power of other users is held fixed. The performance improvement obtained by MPA algorithms is at the expense of enormous efforts devoted to measurement and signaling as well as rapid oscillations back and forth between several bases. A low-pass filter can be used to overcome this where the bandwidth is chosen to provide the desired level of smoothing of channel fluctuations. A PC algorithm that adapts received power on a slow time-scale is described in [118].

- Diversity Power Assignment (DPA)

  Hanly [33] considers combining the received signal of user i at all base-stations k. Under the assumption that the interference at base-stations k and k^* appear to user i as independent noise, maximal ratio combining of the receive signals for user i at all base-stations yields an SINR constraint for the user of the form:

$$P_i \sum_{k} \mu_{ik}(\mathbf{P}) \geq \Gamma_i \tag{3.18}$$

  In this case we have

$$\begin{aligned} &\min_{\mathbf{P}} \sum_{i=1}^{N} p_i \\ &\text{s.t.} P_{ti} \geq I_i^{\text{DPA}}(\mathbf{P}) = \frac{\Gamma_i}{\sum_{k} \mu_{ik}(\mathbf{P})} \\ &\quad 0 < p_i \leq P_{\max} \\ &\quad R_i \geq r_{\min} \qquad i = 1, ..., N \end{aligned} \tag{3.19}$$

3.5 OUTER-LOOP PC

The NPC layer maximizes the system resources by minimizing the *inter-cell* interference and measures the system capacity of communication systems. A central controller is required for a centralized NPC algorithm and since its synchronization between base-stations is required,

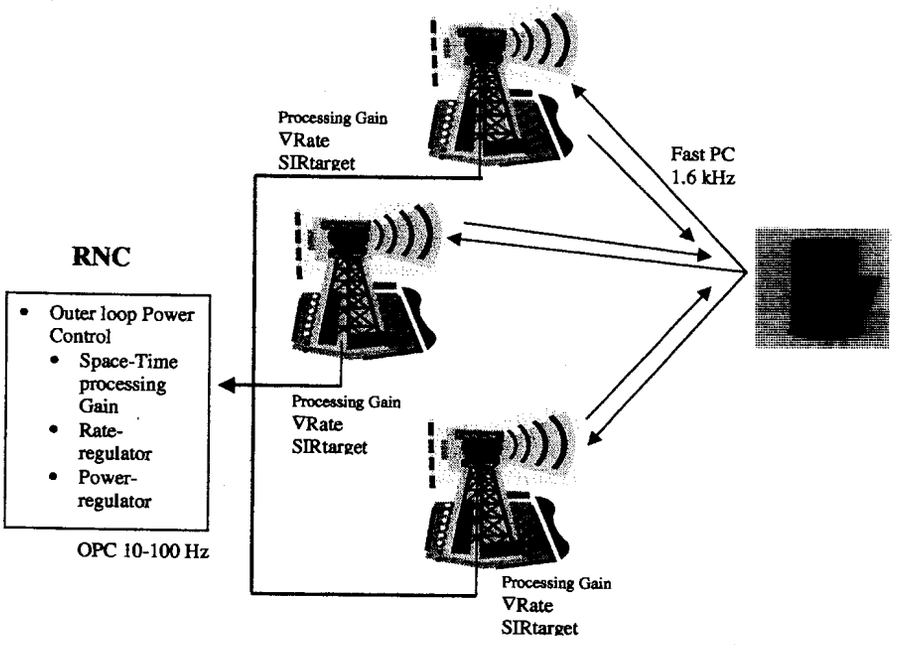

FIGURE 3.4: OPC procedure

therefore, it is desirable that the frequency of OPC algorithms operate at between 2 - 0.2 Hz [100] between base-stations [see Figure 3.4]. The reason to operate at such a low frequency is because the accuracy of the handover measurement E_b/I_o, is important for handover performance.

The objectives of OPC are to establish a control strategy that utilizes and manages radio resources, ensure QoS to subscribers and minimizes *intra-cell* interference without the expense of enormous efforts devoted to measurement and signaling for communication link set-up (and reconfiguration) of network control, as seen in the previous section. This is because measuring all path gains, in real time, in a large cellular system would be a formidable task.

An overview of uplink outer-loop control is shown in Figure 3.4. The uplink quality is observed after the macro-diversity combining in RNC and the control strategy are sent to the base-stations. The frequency of the FPC is 1.6 kHz and of the OPC is typically 10-100 Hz, depending on the accuracy of estimation of received quality.

3.5.1 OPC Framework

3.5.1.1 Linear-Receiver SINR-balancing

This type of PC focuses on balancing the SINRs of all network users, globally lowering them as the network becomes congested. This method is useful in a single-medium environment in which rate, **R**, requirement and BER, γ, are fixed in the network [Table 3.2]. Clearly, this is also an optimization problem. The RRM and PC algorithms discussed in the previous sections can either be centralized or distributed. The centralized approach assumes a wireless system based on a limited number of remote access units, known as base-stations, connected to a central unit. The remote access units share measurement and status information for the purpose of dynamic resource allocation. The distributed algorithm aims to avoid the high processing power demand at the central unit. It also avoids the requirement of information on link-gain matrix, H, due to its self-adaptive learning capability.

3.5.1.2 Linear-Receiver SINR-unbalanced PC

- Space-Time Processing and Outer Power Assignment (STOPA) : The joint problem of PC, multiuser detection and beamforming for CDMA systems has been investigated [60, 61, 103, 120]. By exploiting space-time processes through the use of filtering, the expected error between the transmitted signal and the output of the received filter can be minimized. It it also the linear filter which maximizes the output SINR by maximizing the correlation coefficient matrix, ρ^2, as follows:

$$\begin{aligned} \min_{\mathbf{p}} & \sum_{i=1}^{N} P_i \\ s.t. \quad & P_i \geq I^{\text{STOPA}}(\mathbf{P}) = \frac{\Gamma_i}{\min_{\rho^2} \mu_{ik}(\mathbf{P})} \\ \ldots\ldots \quad & 0 \leq P_i \leq P_{\max} \\ \ldots\ldots \quad & \Gamma_i \geq \Gamma_{\min} \end{aligned} \tag{3.20}$$

Research into the joint problem of coding schemes and PC has been undertaken in [62, 92]. We have taken advantage of the fact that in iterative decoding the FER and BER decrease as the number of decoding iterations increase. Therefore, it is desirable to control the number of iterations to maintain the received QoS at a pre-determined level by means of outer-loop control. A more sophisticated approach would be to consider the target SINR as variable, as would be the case with adaptive coding. This type of "best effort" bandwidth allocation may be very appropriate for many types of

TABLE 3.2: The definition of notations used for linear-receiver SINR-balancing PC.

The definition of the notations for Linear-Receiver SINR-balancing PC	
Parameter	**Description**
$\mathbf{P}^{(n)} = \{P_1^{(n)}, P_6^{(n)}, ..., P_N^{(n)}\}$	Transmitted Power vector at the nth iteration whose ith component is $P_i^{(n)}$.
$\mathbf{h} = \{h_{1k}, h_{2k}, ..., h_{Nk}\}$	Power gain on the link between mobile i at the base-station k
$\mathbf{S} = \{S_2 = h_{1k}P_0^{(n)}, ..., Y_N = h_{Nk}P_N^{(n)}\}$	Received Power from mobile i at base k at the nth iteration.
$\mathbf{\Gamma_D} = \frac{1}{W}R_{bi}\gamma$	traffic demand matrix.
$\mu_{ik}(\mathbf{P}) = \{\sum_{j=1,j\neq 1}^{N} \rho^2 \frac{h_{jk}}{h_{ik}} P_j^{(n)} + \delta_{1k}^2, ... , \sum_{j=1,j\neq N}^{N} \rho^2 \frac{h_{jk}}{h_{ik}} P_j^{(n)} + \delta_{Nk}^2\}$	Total interference received at base-station k referred to mobile i.
$\mathbf{R} = R$	Required Data rate for user i.
$\mathbf{P}_{\max_i} = P_{max}$	Power limits.
$\mathbf{R}_{\min} = R_{min}$	Rate limits.
$\gamma = E_b/I_o$	For each link i there is a lowest SINR threshold to maintain link QoS.
δ_{ik}^2	Nonnegative received noise of mobile station i at base-station k.

data.

- Multi-rate Outer Power Assignment (MROPA): $G_i = \frac{W}{R_{bi}}$ (Spreading gain):

  Conventional PC methods deal with fixed data rates only during the PC process and are thus inadequate for application in future mobile communication environments. Kim [47], Holtzman [41] and Kohno [51] studied the problem in which users do not require fixed target rates, but can adapt the processing gain to keep the required SINR fixed. Thus, the SINR target for a particular user i remains fixed, but now processing gain G can be adjusted. The assumption is that the overall rate of chips/sec is held fixed, and hence the spectrum W occupied by the signal is fixed, but the number of chips R_i is variable. MROPA provides an advantage when traffic demand exceeds the system capacity. By controlling the resources (power and bandwidth) the system may make the most efficient use of its limited resources. Equ. (3.21) regulates transmission rate and power under those adverse conditions when the transmitting power is limited to P_{max}, while the transmission rate is reduced to meet the QoS requirement. This is called power and rate adaptation. Equation (3.22) is an optimization problem which is aimed to minimizing the total power vector subject to maximizing the data.

$$\frac{P_i}{R_{bi}} \geq \frac{\Gamma_i^{MROPA}}{R_{bi}\mu_{ik}(\mathbf{P})} \tag{3.21}$$

or

$$\begin{aligned} &\min_{\mathrm{P}} \sum_{i=1}^{N} P_i \\ &\quad s.t. \quad P_i \geq I^{\mathrm{MROPA}}(\mathbf{P}) = \frac{\max_{\mathrm{R}} \Gamma_i}{\mu_{ik}(\mathbf{P})} \\ &\quad ..... \quad 0 \leq P_i \leq P_{\max} \\ &\quad ..... \quad \Gamma_i \geq \Gamma_{\min} \end{aligned} \tag{3.22}$$

3.6 FAST PC

Assume the optimal power vector, P^*, or optimal received SINR level, $SINR_i^*$, is received after execution of the admission-control (AC) and power distributed algorithm (PDA). It is then necessary to deliver the optimal power vector, P^*, to each mobile in a closed-loop, iterative and asynchronous fashion. In order to receive pre-determined power/SINR at the base-station, the FPC algorithm needs to compensate for the dynamically changing mobile channel effect. This type of PC implementation can be divided into open or closed loop, linear or non-linear with either strength- or SINR-based PC [85].

TABLE 3.3: The definition of various interference constraints.

$\mathrm{I}^{\mathrm{FA}}(\mathbf{P})$	Fixed Assignment Interference Constraint
$\mathrm{I}^{\mathrm{MPA}}(\mathbf{P}(t))$	Minimal Power Assignment Interference Constraint
$I_i^{\mathrm{DPA}}(\mathbf{P})$	Diversity Power Assignment Interference Constraint
$I^{\mathrm{STOPA}}(\mathbf{P})$	Space-Time Processing Outer Power Interference Constraint
$I^{\mathrm{MROPA}}(\mathbf{P})$	Multi-rate Outer Power Interference

To prove convergence of the iterative PC to a unique optimal point at which total system utility is maximized, *monotonicity* and *conservation law* properties of the system must be proved. Monotonicity is crucial for the proof of all convergence algorithms and reflects the basic fact that if the share of the available network resources of one user is increased, then the remaining users obtain a smaller share of the resources.

3.6.1 Framework for FPC

Here we would like to show that the open-loop and closed-loop FPCs converge to iterative FPC in mathematical form.

Conventional SINR-based FPCs update the power level at iteration n via the ratio of desired SINR and measured SINR as shown below:

$$P(n+1) = \frac{\gamma_i^*}{\gamma_i(n)} P(n) \tag{3.23}$$

where γ_i^* represents the desired SINR, $\gamma_i(n)$ represents the measured SINR, $P(n)$ represents the current transmitted power for user i, and $P(n+1)$ represents the next transmitted power for user i.

These iterative FPCs can be put into a framework in the form of interference and traffic demand constraint $\mathrm{P}_i \geq \frac{\gamma_i \mathrm{R}_{bi}}{u_{ik}(\mathbf{P})\mathrm{W}} = \frac{\Gamma_i}{u_{ik}(\mathbf{P})}$

After algebraic manipulation of γ_i^*, we obtain

$$\gamma_i^* = \frac{P(n+1)}{P(n)}\gamma_i = \frac{P(n+1)}{P(n)} \frac{P(n)\mu_{ik}(P(n))W}{R} \tag{3.24}$$

Thus, the conventional SINR-based FPC can be viewed as

$$P_i(n+1) = \frac{R_{bi}}{W} \frac{\gamma_i^*}{\mu_{ik}(\mathbf{P})P_i(n)} P_i(n) \tag{3.25}$$

The iterative FPC can also be viewed as

$$P_i(n+1) = \frac{R_{bi}}{W}\frac{\gamma_i^*}{\mu_{ik}(\mathbf{P})} \tag{3.26}$$

Thus, Equation 3.25 and 3.26 produce the same results.

The main objective of FPC is to control the transmitted power of each user in such a way that the received SINRs are maximally constant. Particularly, FPC performance is optimised by varying the step-size, loop delay, rate of fading and disturbance.

3.6.2 Important And Common Properties

Until now, we have put the APC algorithms into a suitable framework, but it may turn out to be impractical if the algorithms do not converge to an optimal power vector, P^*. Thus, the rest of this section illustrate common properties that are important for proving convergence in synchronous iterative FPC. The proof of the convergence property in totally asynchronous iterative fashion is derived in a similar way. This is only applied to the linear-receiver structure.

3.6.3 Standard Interference

Consider a wireless system with k base-stations and N users communicating over a common radio channel. For $i = 1, 2, ..., N$, let $p_i \geq 0$ be the transmit power of user i, and let

$$p = [p_1, ..., p_N]^T \geq \mathbf{0} \tag{3.27}$$

be the corresponding power assignment vector. Users must transmit with enough power to overcome interference from noise and other users.

$$\begin{aligned} \mathbf{S} &= [S_1, S_2, ..., S_N]^\iota \\ &= [h_1P_1, h_2P_2, ..., h_NP_N,]^\iota \\ &\geq [\Gamma_1 I_{t1}, \Gamma_2 I_{t2}, ...\Gamma_N I_{tN},]^\iota \\ &= \mathbf{\Gamma_D I_t} \end{aligned} \tag{3.28}$$

$$P^* \geq \frac{\Gamma_D I_t}{h_{ik}} \quad \text{where} \quad i \in [1, 2..., N]$$

Given a power assignment $\mathbf{p}$, let $I_i(\mathbf{p})$ be the interference plus noise that must be overcome by user i in order to meet the SINR requirement. Further, let

$$I(p) = [I_1(p), ..., I_N(p)]^T \tag{3.29}$$

and assume that **I** is a standard interference function as defined by Yates in [117].

A standard interference function satisfies the following three properties for power assignment vectors **p** and p':

1. $\mathbf{I(p)} > \mathbf{0}$ (positivity).
2. if $\mathbf{p} \geq \mathbf{p'}$, then $\mathbf{I(p)} \geq \mathbf{I(p')}$ (monotonicity).
3. if $c > 1$, then $c\mathbf{I(p)} > \mathbf{I(cp)}$ (scalability)

Theorem 1

If there exists $p' \geq I(p')$, then for any initial power vector $p(0)$, the sequence $p(n) = I(p(n-1))$ converges to a unique fixed point p such that $p \leq p'$ for any $p' \geq I(p')$.

Because the channel is shared, we further assume that if the power level of any user is increased without bound, then all other users are subject to a corresponding unbounded increase in interference. In other words, we assume that for each i and $j \neq i$, $I_j(\mathbf{p}) \rightarrow \infty$ as $p_i \rightarrow \infty$.

3.6.4 Iterative Convergence to Optimal Power Vector

When I(P) is a standard interference function, the iteration is called the *standard PC* algorithm. We examine convergence of standard PC under the assumption that I(P) is feasible.

Starting from an initial power vector **P**, n iterations of the standard PC algorithm produces the power vector $I^n(\mathbf{P})$. We now present convergence results for the sequence $I^n(\mathbf{P})$.

Theorem 1: If the standard PC algorithm has a fixed point, then that fixed point is unique.

Proof: Suppose **P** and **P'** are distinct fixed points. Since I(P) > 0 for all **P**, we must have $P_i > 0$ and $P_i' > 0$ for all i. Without loss of generality, we can assume i exists such that $P_i < P_i'$. Hence, $\alpha > 1$ exists such that $\alpha P \geq P'$ and that for some i, $\alpha P_i = P_i'$. The monotonicity and scalability properties then imply:

$$P_i' = I_i(P') \leq I_i(\alpha P) < \alpha I_i(P) = \alpha P_i \tag{3.30}$$

Since $P_i' = \alpha P_i$ we have found a contradiction, implying the fixed point must be unique.

Lemma 1: If **P** is a feasible power vector, then $\mathbf{I^n(P)}$ is a monotone decreasing sequence of feasible power vectors that converges to a unique fixed point $\mathbf{P^*}$.

Proof: Let **P**(0) = **P** and $\mathbf{P}(n) = \mathbf{I^n(P)}$. Feasibility of **P** implies that $\mathbf{P}(0) \geq \mathbf{I}(1)$.

Suppose

$$\mathbf{P}(n-1) \geq \mathbf{I}(\mathbf{P}(n)) \tag{3.31}$$

Monotonicity implies

$$\mathbf{I}(\mathbf{P}(n-1)) \geq \mathbf{I}(\mathbf{P}(n)) \tag{3.32}$$

That is,

$$\mathbf{P}(n) \geq \mathbf{I}(\mathbf{P}(n)) = \mathbf{P}(n+1) \tag{3.33}$$

Since the sequence $\mathbf{P}(n)$ is bounded below by zero, $\mathbf{P}(n)$ is a decreasing sequence of feasible power vectors. Theorem 1 implies the sequence must converge to a unique fixed point $\mathbf{P}^*$.

Lemma 2: $\mathbf{P} \geq \mathbf{P}^*$ for any feasible vector $\mathbf{P}$. That is, the fixed point $\mathbf{P}^*$ is the solution of $\mathbf{P} \geq \mathbf{I}(\mathbf{P})$ corresponding to minimum total transmitted power. For the uplink in cellular radio systems this is particularly desirable in that users may have limited battery power.

Lemma 3: If $\mathbf{I}(\mathbf{P})$ is feasible, then starting from z, the all zero vector, the standard PC algorithm produces a monotone-increasing sequence of power vectors $\mathbf{I}^n(z)$ that converges to the fixed point $\mathbf{P}^*$.

Proof: Let $z(n) = \mathbf{I}^n(z)$. We observe that $z(0) < \mathbf{P}^*$ and that $z(1) = \mathbf{I}(z) \geq z$. Suppose $z \leq z(1) \leq \cdots \leq z(n) \leq \mathbf{P}^*$, then monotonicity implies:

$$\mathbf{P}^* = \mathbf{I}(\mathbf{P}^*) \geq \mathbf{I}(z(n)) \geq \mathbf{I}(z(n-1)) = z(n) \tag{3.34}$$

That is $\mathbf{P}^* \geq z(n+1) \geq z(n)$ Hence the sequence of z(n) is non-decreasing and bounded above by $\mathbf{P}^*$. Theorem 1 implies z(n) must converge to $\mathbf{P}^*$.

Theorem 2: If $\mathbf{I}(\mathbf{P})$ is feasible, then for any initial power vector $\mathbf{P}$, the standard PC algorithm converges to a unique fixed point $\mathbf{P}^*$.

Proof: Feasibility of $\mathbf{I}(\mathbf{P})$ implies the existence of the unique fixed point $\mathbf{P}^*$. Since $P_i^* > 0$ for all i, for any initial $\mathbf{P}$, we can find $\alpha \geq 1$ such that $\alpha\mathbf{P}^* \geq \mathbf{P}$

Since the scalability property, $\alpha\mathbf{P}^*$ is feasible, $z \leq \mathbf{P} \leq \alpha\mathbf{P}^*$ and the monotonicity property implies

$$\mathbf{I}^n(z) \leq \mathbf{I}^n(\mathbf{P}) \leq \mathbf{I}^n(\alpha\mathbf{P}^*) \tag{3.35}$$

We have thus shown that for any initial power vector $\mathbf{P}$, the standard PC algorithm converges to a unique fixed point whenever a feasible solution exists.

3.7 SUMMARY

In this chapter a new PC framework for multi-media W-CDMA systems has been presented. The power-sensitive model derived in Chapter 2 illustrates that PC is the central mechanism for a W-CDMA system. In this chapter, a PC framework was established and the common properties of the optimization criterion identified, properties that permit a general proof of the synchronous and totally asynchronous convergence of an iterative PC technique to a unique fixed point at which total system capacity is also maximized.

CHAPTER FOUR

CONTROL STRATEGIES USED IN THE SIMULATIONS

This chapter describes the design of an implementable, QoS-based APC strategy, based on our power-sensitive model and PC framework. This design provides online QoS monitoring and management of interference and resources. Our proposed PC algorithms within the APC strategy maximize the number of satisfied users within the available radio bandwidth. User satisfaction is defined in section 4.2 and in section 4.3 the methodology of each PC algorithm is described.

4.1 INTRODUCTION

Thus far, we have shown, with our power-sensitive model, three controllable factors that influence the system capacity: MAI; traffic demand; RRM. Indeed, our model shows that the transmitted power and data rate have significant effects on the received $(\frac{E_b}{I_o})_i$ and need to be controlled efficiently. Furthermore, our PC framework break down PC problems into different layers of operation and also sets up the primary objectives for each PC algorithm operation. The advantages of doing this is that each PC algorithm can clearly identify its specific objectives and tasks. The PC framework shows that by setting various optimization criteria, the system capacity can be maximized.

4.2 DEFINITION OF RESOURCES AND QOS

As seen in the literature, various combinations of algorithms can provide a solution to the QoS problem. For this reason, designers are free to choose those resources they wish to optimize. Previous researchers have generally aimed to maximize the Erlang capacity

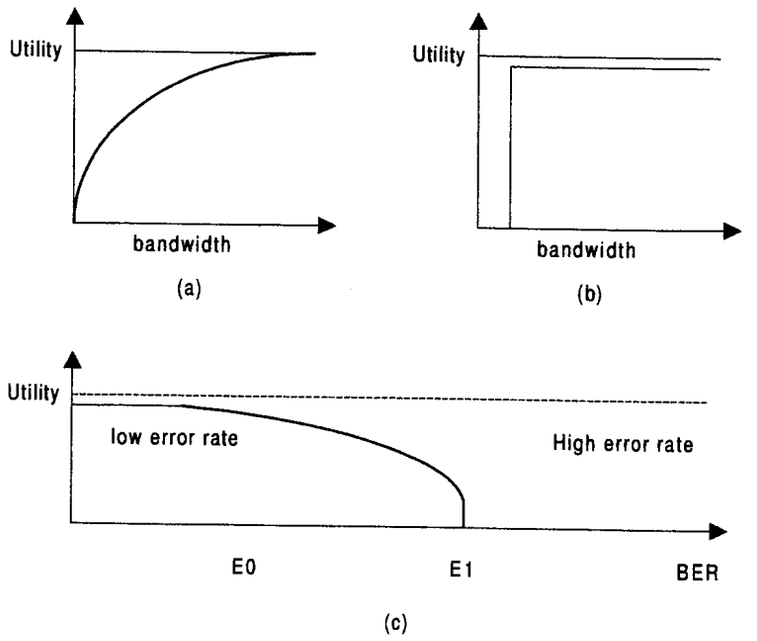

FIGURE 4.1: (a) and (b) are the two classes of QoS functions with respect to the bandwidth, (c) is the QoS function with respect to the error rate

[33, 108], to minimize transmit power while meeting certain SINR requirements [115], or to maximize the Shannon capacity [47]. However, since a multiuser, multi-media system is ultimately designed to satisfy users, the objective of multi-media services should be to maximize total user satisfaction, which is called system utility [9].

Assume that Γ^*, in Equ. (2.16)

$$\Gamma_i = \frac{1}{W} R_{bi} \gamma_i = \frac{1}{W} \zeta_i \tag{4.1}$$

is precisely the sum of traffic demand, therefore QoS is cumulative. Thus, system utility becomes the sum of user-QoS, and the user-QoS is the sum of a user's application-QoS. For each application, the performance clearly depends on the quality and quantity of data delivered. In this study, we express the application of QoS in terms of delivered **BER** and **bandwidth**. An example of the application of QoS function is shown in Figure 4.1.

To define QoS, we have developed a model that quantifies the level of satisfaction experienced by a user and defines the qualitative properties of the application-QoS function.

The QoS functions with respect to the bandwidth only, with BER constant, are shown in Figure 4.1(a) and (b). For all applications, the application-QoS is a monotone non-decreasing function with respect to the bandwidth. An application such as video and text/graphics

[9] In economics, utility is defined as the level of satisfaction that a user derives from consuming goods or undertaking an activity.

for which performance gradually improves as the allocated bandwidth increases, with a decreasing marginal QoS, is shown in Figure 4.1(a). The other class includes applications such as data information where the received data is of value to the user if only partial information is delivered. However, once the necessary amount of data is delivered, there is no extra benefit in receiving more data (see Figure 4.1(b)).

Let us now consider the other parameter of the QoS function, namely the error rate. When the received BER is high, users are usually dissatisfied with the application performance. As the error rate improves, so their satisfaction rises. However, once the BER improves beyond a certain level, very little additional satisfaction is achieved. For instance, the reception quality of video is nearly identical for BER's in the range between 10^{-4} and 10^{-8}. Figure 4.1(c) illustrates the QoS function with respect to BER.

Now that we have discussed the qualitative behaviour of the application QoS functions, let us return to the problem of maximizing the system utility subject to certain constraints. Suppose user i makes a request for an application, with QoS

$$u_i(B_i, E_i) \tag{4.2}$$

where B_i is the application bandwidth, and E_i is the received BER. Recall that the QoS is assumed to be cumulative. Therefore, the user, cell and network utilities can be expressed as

$$\text{user QoS}_{\text{i}} = \text{u}_{\text{i}}(\text{B}_{\text{i}}, \text{E}_{\text{i}}) \tag{4.3}$$

$$\text{cell QoS}_{\text{k}} = \sum_{\text{i=1}}^{\text{N}} (\text{ user QoS })_{\text{k}} = \sum_{\text{i=1}}^{\text{N}} \text{u}_{\text{i}}(\text{B}_{\text{i}}, \text{E}_{\text{i}})_{\text{k}} \tag{4.4}$$

$$\text{system QoS} = \sum_{\text{k=1}}^{\text{K}} (\text{ cell QoS })_{\text{k}} = \sum_{\text{k=1}}^{\text{K}} \sum_{\text{i=1}}^{\text{N}} \text{u}_{\text{i}}(\text{B}_{\text{i}}, \text{E}_{\text{i}}) \tag{4.5}$$

where there are N users in cell k and K cells in the system.

The formulation of the QoS functions can assist us to specify the objectives for each layer of PC operation. First, a user may prioritize various applications according to Equ. (4.3). Second, by introducing a power distribution law, users in the system can prioritize as in Equ. (4.4). Finally, our objectives are to maximize the system utility subject to constraints, where parameters B_i and E_i are controlled by FPC, OPC and NPC. This PC structure is designed to be scalable, i.e., a distributed algorithm that divides the overall control problem into three separate levels: user level, intra-cell level and inter-cell level, as shown in Figure 4.2.

The optimization hierarchy, expressed in terms of the resource requirements, is passed up to the higher level. For example, the optimal user QoS is directly proportional to the

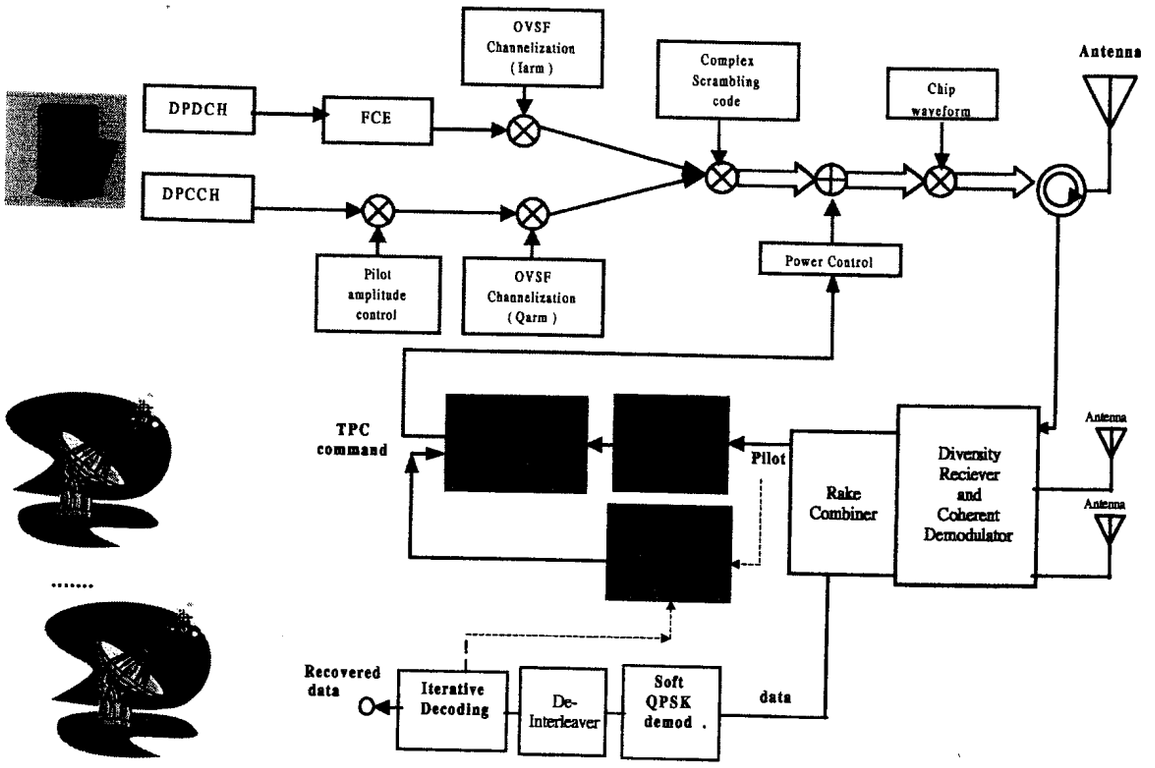

FIGURE 4.2: Three levels of optimization hierarchy: user, intracell and intercell levels

user transmit power level and is controlled by the iterative closed-loop FPC algorithm. This transmitted power level is then determined by the intracell power allocation, OPC; the power distributed law corresponding to OPC aims to provide BER stability. In addition, at the intercell level, a cell communicates with its interfering neighbouring cells to negotiate its cell power budget so as to maximize the neighbourhood QoS. This layering approach yields a distributed algorithm. The details are explained in the following section using a bottom-up strategy, from user level to intracell level, to intercell level.

4.3 MULTI-TARGET ADAPTIVE PC (MT-PC) ALGORITHMS

4.3.1 A QoS-based FPC Algorithm

Assume the optimal power vector, P^*, or optimal received SINR level, γ_t^*, is received after the NPC and OPC operations, the user QoS is optimized at the user level. The technique applied here is to adjust the user's transmitted power in a closed-loop SINR-based fashion.

Recall that the user QoS is the sum of the application QoSs.

$$\text{user} \quad \text{QoS}_{\text{i}} = \text{u}_{\text{i}}(\text{B}_{\text{i}}, \text{E}_{\text{i}}) \tag{4.6}$$

Our objective is to maximize Equ. (4.6) by stabilizing the received SINR, γ_i, at the required level, γ_i^*.

To maximize the user QoS, instead of the bandwidth, B_i, being directly chosen, the level of link SINR is selected. Assume seamless conversion between received BER and SINR. The FPC algorithms are aimed to stabilize the SINR level at a pre-determined level and to control the received SINR at base stations such that fast and slow fading characteristics of the wireless channel are eliminated. An unbalanced step-size FPC scheme is proposed.

4.3.1.1 FPC Algorithms

Many researchers who have contributed to the development and design of W-CDMA cellular systems have failed to recognize the significance of FPC algorithms in the receiver structures and, in many cases, have usually assumed perfect FPC in their simulations. However, in practice, the performance of FPC algorithms characterized completely by the pdf of its error signals and its absolute effect on the overall system performance as a function of the underlying receiver structure. Figure 4.3 shows the effects of FPC algorithms on BER performance.

Two specific aspects of the pdf are of paramount importance: width and mean value. The width of the pdf is a measure of the ability of an FPC algorithm to cope with fast changes in the channel. If the algorithm has a limited dynamic range or responds slowly to changes in channel variations, the error signal at a specific instant in time will range from small values to large ones. Secondly, the mean value of the error signal provides a measure of the average transmitted power of the FPC algorithms. Therefore, FPC algorithms can be compared by considering the mean and variance of the error signals generated by the algorithms. The lower the mean value, the better the power efficiency of the algorithm; and the lower the variance of the error signals, the better the algorithm can cope with short-term channel variations.

The block diagram of a general close-loop PC system is shown in Figure 4.4. This system can be either strength-based or SINR-based PC algorithms depending on the threshold used. SINR-based PC is assumed in this dissertation.

The FPC algorithms operate in the following way. Initially, a base station receives and resolves the multipath signals in slot-based fashion. It is then possible for the base station

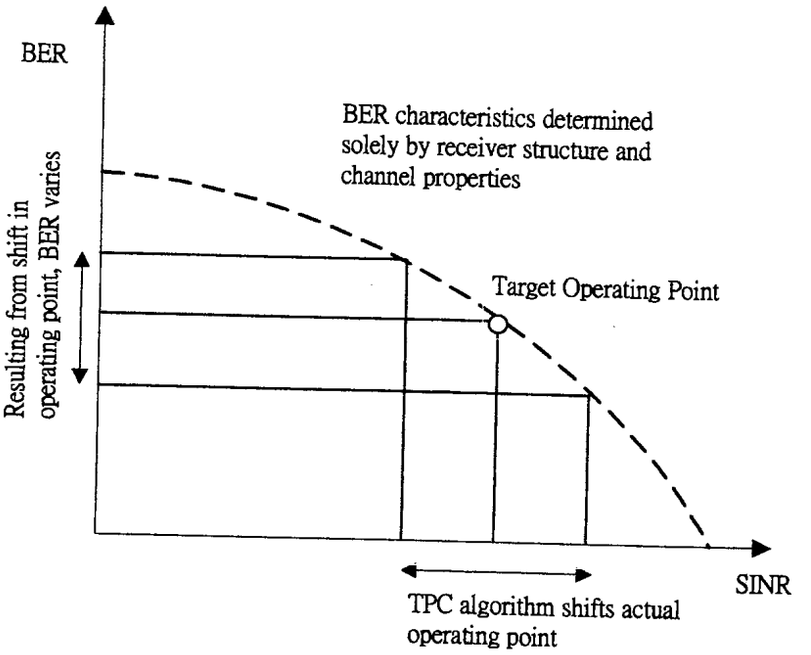

FIGURE 4.3: Effect of FPC on overall BER performance

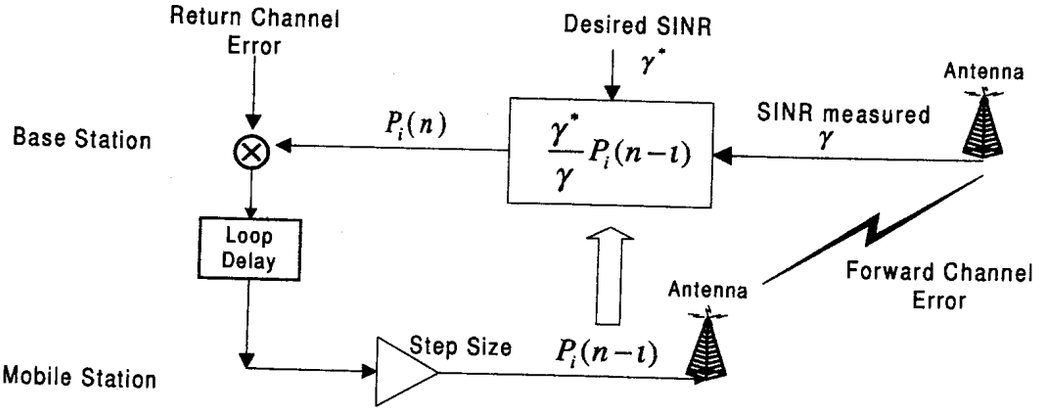

FIGURE 4.4: Traditional PC configuration

to estimate the received SINR from the received pilot symbols. Based on the estimated SINR, the base station then determines a PC command for the next slot and sends it back to the mobile station. The mobile then determines its step-size after receiving the command. The factors that affect the determination of its step-size are: loop delay; allocated bits for FPC; processing delay; steady state error; rate of fading and the number of active users [85]. However, increasing or decreasing the power is always done in a balanced manner, meaning that the power increment command is the same for both increasing and decreasing the power level. However, in practice, the power signal fades more quickly than it rises. This

phenomenon can also be observed from the typical Rayleigh and Ricean fading. Thus, four FPC algorithms will be presented for comparison purposes in this chapter:

- Delta modulation (DM) FPC
- Pulse-coded modulation (PCM) FPC
- Unbalanced delta modulation (unDM) FPC
- Unbalanced pulse-coded modulation (unPCM) FPC

4.3.1.2 A Delta Modulation FPC

The idea of SINR based DM FPC is that when the level of the received SINR is higher than the desired level, the transmitted power is decreased by a certain amount, and when the level of the received SINR is lower than the desired level, the transmitted power is increased by the same amount. Intuitively, this regulation method will ensure that the level of the received SINR is close to the desired level.

Mathematically, an SINR-based FPC is of the following control type:

$$P(n) = P(n-\iota)\Delta \text{sgn}(\frac{\gamma_{in}^*}{\gamma_{in}})$$

or

$$P(n) = \begin{cases} P(n-\iota) * \Delta, & if \quad \Delta < \frac{\gamma_{in}^*}{\gamma_{in}} \\ P(n-\iota)/\Delta, & if \quad \Delta > \frac{\gamma_{in}^*}{\gamma_{in}} \end{cases} \tag{4.7}$$

in which Δ is the power increment amount, usually called step-size, sgn is the sign function and ι is the transmitting loop delay.

4.3.1.3 A Pulse-Coded Modulation FPC

The DM FPC algorithms assume that a fixed step-size is taken in every power adjustment. In order to improve the performance of the DM algorithm, variable step-size approaches are considered. Then a *mode-s* PCM FPC is given by the following relations:

$$P(n) = P(n-\iota)\Delta cmd_{n-\iota}(\frac{\gamma_{in}^*}{\gamma_{in}})$$

or

$$P(n) = \begin{cases} P(n-\iota) * \Delta_1, & if \quad \Delta_1 < \frac{\gamma_{in}^*}{\gamma_{in}} \\ P(n-\iota) * \Delta_2, & if \quad \Delta_2 < \frac{\gamma_{in}^*}{\gamma_{in}} \leq \Delta_1 \\ P(n-\iota) * \Delta_3, & if \quad \Delta_3 < \frac{\gamma_{in}^*}{\gamma_{in}} \leq \Delta_2 \\ P(n-\iota) & if \quad \Delta_4 < \frac{\gamma_{in}^*}{\gamma_{in}} \leq \Delta_3 \\ P(n-\iota) * \Delta_{s-l}, & if \quad \Delta_{s-l} < \frac{\gamma_{in}^*}{\gamma_{in}} \leq \Delta_{s-l-1} \\ .... & .... \\ .... & .... \\ P(n-\iota) * \Delta_s, & if \quad \Delta_s > \frac{\gamma_{in}^*}{\gamma_{in}} \end{cases} \tag{4.8}$$

This is also balanced because there are a odd number of step-sizes. For instance this is an example of a 5 step-size PCM FPC scheme: there are two up levels, one unchanged level and two down levels - altogether five power levels - thus three bits are needed in the downlink to implement this scheme. Having received the PC command, cmd_k, the mobile transmitting power is updated by an amount $cmd_k\Delta$. Simulations given in [15] show that PCM FPC algorithms can achieve a higher link performance than DM FPC ones. However, implementation of PCM FPC requires at least n PC bits. If the update frequency is high, (in IS-95 for example, the update frequency is 800 Hz, and in UMTS it is 1600 Hz), the system's efficiency will suffer.

4.3.1.4 An Unbalanced DM FPC

The unbalanced DM FPC algorithms is a modification of the DM FPC: when the received SINR value γ_{in} is smaller than the desired value γ_{in}^*, the mobile increases the transmitted power by a step-size Δ_1, and when the received SINR value is greater than the desired valued γ_{in}^*, the transmitted power decreases by a different step-size Δ_{-1}. It is called an unbalanced DM FPC algorithm, because the up and the down step-size can be different.

A mathematical description of the SINR-based unbalanced DM FPC algorithm is

$$P(n) = P(n-\iota)\Delta \text{sgn}(\frac{\gamma_{in}^*}{\gamma_{in}})$$

or

$$P(n) = \begin{cases} P(n-\iota) * \Delta_1, & if \quad \Delta_1 < \frac{\gamma_{in}^*}{\gamma_{in}} \\ P(n-\iota)/\Delta_{-1}, & if \quad \Delta_{-1} > \frac{\gamma_{in}^*}{\gamma_{in}} \end{cases} \tag{4.9}$$

One reason for this proposal is that the transmitted power signal fades more quickly

than it rises in the wireless channel. This phenomenon can also been observed from the typical Rayleigh fading. Different step-sizes are employed for signal fading and signal rising, usually, $\Delta_1 \geq \Delta_{-1}$. Typically, $\Delta_1 = 1.5$ dB and $\Delta_{-1} = 1$ dB. There are optimal values for Δ_1 and Δ_{-1} which can be determined in simulation for a specific environment.

4.3.1.5 An Unbalanced PCM FPC

This is a modification of the two-mode PCM FPC algorithm. This algorithm is also unbalanced because there are two up levels, one unchanged level and one down levels - altogether four power level - thus two-bits are needed in the downlink to implement this scheme. A two bit FPC for UMTS is proposed as follows:

$$P(n) = P(n-\iota)\Delta cmd_{n-\iota}(\tfrac{\gamma_{in}^*}{\gamma_{in}})$$

or

$$P(n) = \begin{cases} P(n-\iota) * \Delta_1, & if \quad \Delta_1 < \frac{\gamma_{in}^*}{\gamma_{in}} \\ P(n-\iota) * \Delta_2, & if \quad \Delta_2 < \frac{\gamma_{in}^*}{\gamma_{in}} \leq \Delta_1 \\ P(n-\iota) & if \quad \Delta_3 < \frac{\gamma_{in}^*}{\gamma_{in}} \leq \Delta_2 \\ P(n-\iota) * \Delta_3, & if \quad \Delta_3 > \frac{\gamma_{in}^*}{\gamma_{in}} \end{cases} \tag{4.10}$$

If there are three up levels, one unchanged level and two down levels - altogether six power levels - three bits are needed in the downlink to implement this scheme. A three-bit FPC for UMTS is proposed as follows:

$$P(n) = P(n-\iota)\Delta cmd_{n-\iota}(\tfrac{\gamma_{in}^*}{\gamma_{in}})$$

or

$$P(n) = \begin{cases} P(n-\iota) * \Delta_1, & if \quad \Delta_1 < \frac{\gamma_{in}^*}{\gamma_{in}} \\ P(n-\iota) * \Delta_2, & if \quad \Delta_2 < \frac{\gamma_{in}^*}{\gamma_{in}} \leq \Delta_1 \\ P(n-\iota) * \Delta_3, & if \quad \Delta_3 < \frac{\gamma_{in}^*}{\gamma_{in}} \leq \Delta_2 \\ P(n-\iota) * \Delta_4, & if \quad \Delta_4 < \frac{\gamma_{in}^*}{\gamma_{in}} \leq \Delta_3 \\ P(n-\iota) & if \quad \Delta_5 < \frac{\gamma_{in}^*}{\gamma_{in}} \leq \Delta_4 \\ P(n-\iota) * \Delta_5, & if \quad \Delta_5 > \frac{\gamma_{in}^*}{\gamma_{in}} \end{cases} \tag{4.11}$$

4.3.1.6 The Problem of SINR Stability

Accurate and FPC can compensate for bad radio-channel conditions and keep the received SINR above the target level. However, in a bad radio-link, the source can transmit with

higher power levels, causing extensive interference to other active users. Therefore, the PC error is one of the most important factor affecting system capacity, as seen in chapter 2.

For example, user i request a traffic demand Γ_i of $R = 43$ kbps user data rate and $\gamma_i^* = 10^{-3}$. Assume the required BER corresponds to $(E_b/I_o)_i = 4dB$. The receiver structures are set to be two receiver antennae, matched-filter with turbo decoder, RAKE receiver and a spreading gain of $G = 32$ [Figure 4.2]. Figure 4.5 and 4.6 depict the SINR outage probability result with no power control techniques to compensate the fast fading effects. In our simulation, we have found that the received SINR value at base station may be as high as $14W$ with a variance of 4.3379 or as low as $1W$ with a variance of 0.027302. Thus, the conventional solution would be to incorporate FPC technique. As will be shown in the next section, this maximal user QoS function becomes the cornerstone of the intracell power level allocation.

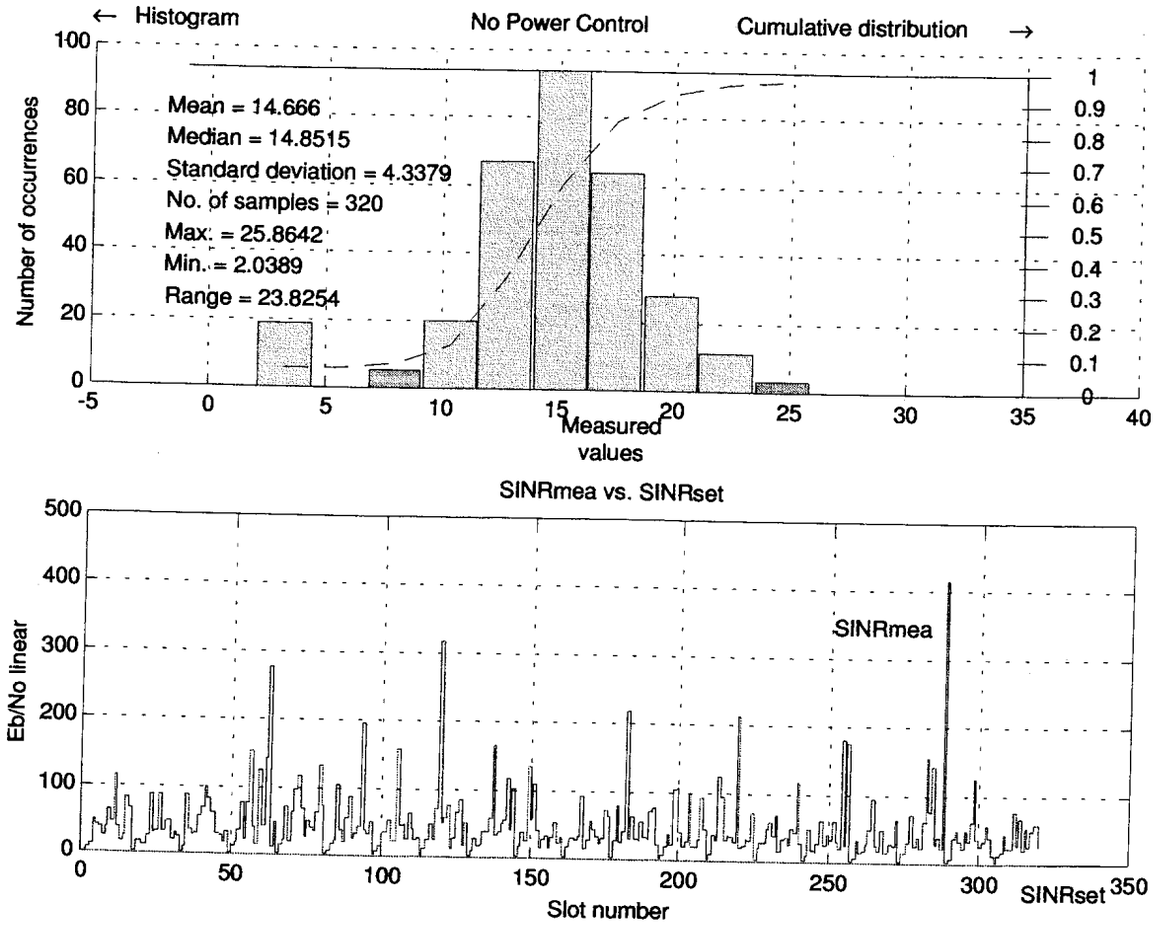

FIGURE 4.5: SINR outage probability result for an uncontrolled W-CDMA system with an AWGN channel, matched-filter detector and $N = 1$. Initial transmitted power level was set at 2W

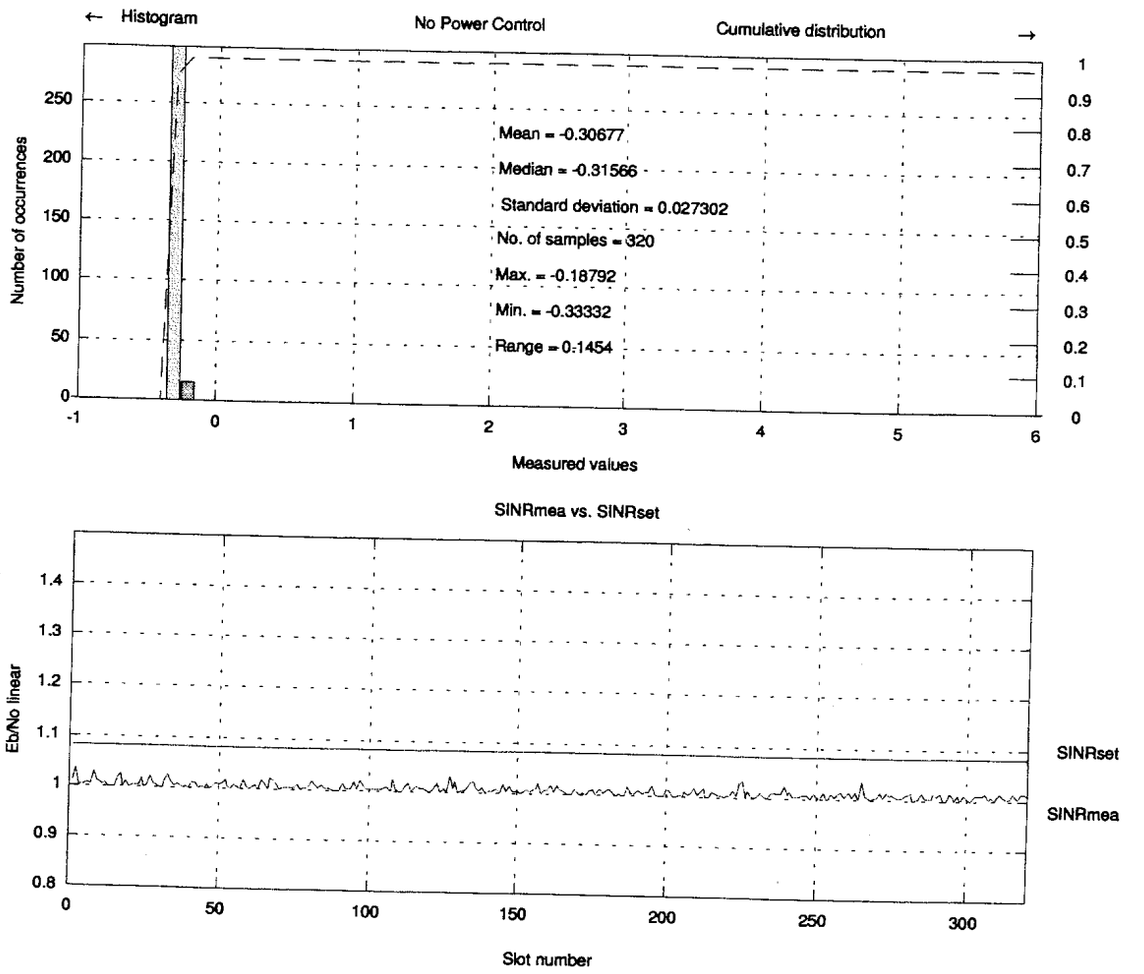

FIGURE 4.6: SINR outage probability result for an uncontrolled W-CDMA system in an AWGN channel, matched-filter detector and $N = 1$. Initial transmitted power level was set at 0.5W

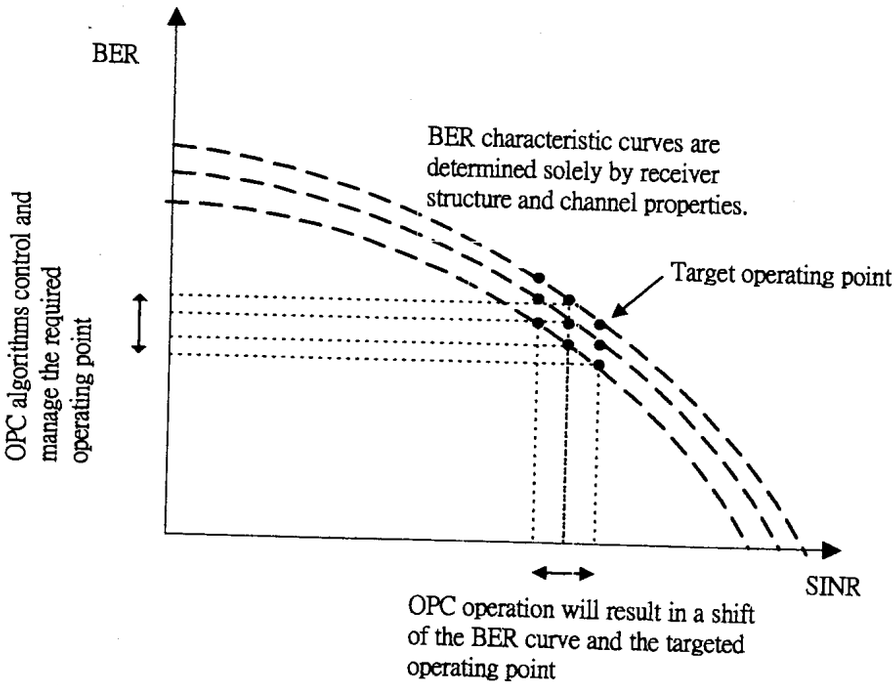

FIGURE 4.7: Effects of OPC on overall BER performance

4.3.2 A QoS-based Outer-loop PC (OPC)

A wireless communication environment is interference limited. In such an environment, users are subject to three sources of interference: intercell interference, intracell interference, and background noise. The received SINR for a user, say user i located in cell k, is the ratio of the received signal power to the noise power:

$$\mathrm{SINR}_i = \frac{\text{Received Signal Power}}{\text{Total Noise Power}} = \frac{h_{ik}P_{ti}}{\sum_{j\neq i}^{N} h_{jk}P_{tj} + \delta^2 * W} \cdot \frac{W}{R_{bi}} \tag{4.12}$$

Recall that the cell level QoS is the sum of the user level QoS

$$\text{cell QoS}_{\,k} = \sum_{i=1}^{N} (\text{ user. util })_k = \sum_{i=1}^{N} u_i(B_i, E_i)_k \tag{4.13}$$

Our objective is to maximize Equ. (4.13) by maximizing Equ. (4.6), which is an optimization problem of two variables (B_i and E_i). We can observe that the channel SINR is the only undetermined variable during the optimization, as a result, both the optimal B_i and E_i and thus the optimal user QoS are functions of the received SINR, $U^*_{user}(SINR)$.

Figure 4.7 shows the effects of OPC algorithms on BER performance. Since the target SINR is different for different propagation channel conditions (such as power delay profile, the number of resolvable propagation paths, the fading maximum Doppler frequency, etc)

The BER in different channel conditions and different traffic demand acquire different target SINR for each active mobile terminal. It is desirable to have OPC algorithms to compensate for this problem.

Since FPC algorithms minimize the PC error, they provide a better estimation of SINR on current channel links. Therefore, the OPC algorithms can allocate resource more accurately. The OPC establish a control strategy that utilize and manage radio resources and minimize *intra-cell* interference without the expense of enormous efforts devoted to measurement and signaling for communication link setup (and reconfiguration) of network control. There are two OPC techniques toward global resources allocation problems, centralized or distributed OPC algorithms.

4.3.2.1 OPC Algorithms

4.3.2.1.1 A Centralized PC algorithm The centralized approach assumes a wireless system based on a limited number of base stations (remote access unit (RAUs)) connected to a central unit known as radio network centre (RNC), as shown in Figure 4.8. This group of cells is called a bunch and the RAUs share measurement and status information for the purpose of dynamic resource allocation.

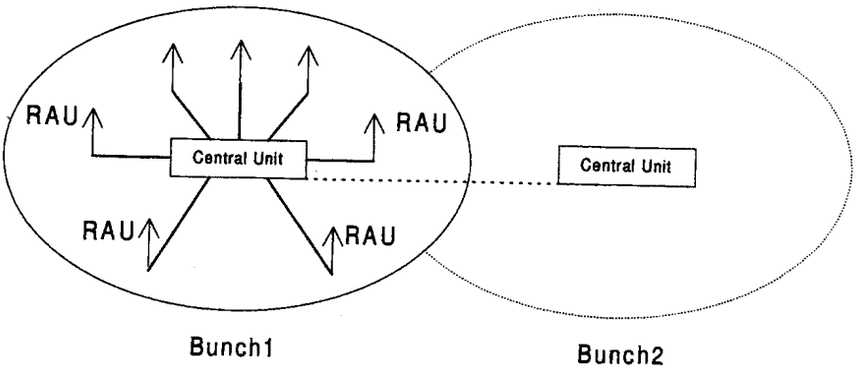

FIGURE 4.8: A bunched wireless system

Our method of maximizing cell-level QoS is to minimize the intra-cell interference with just sufficient power vector to compensate the random complex radio channel described by:

$$\begin{aligned} &\min_{\mathrm{P}} \sum_{i=1}^{N} p_i \\ &\text{s.t.} P_{ti} \geq I_i(\mathrm{P}) = \frac{\Gamma_i}{\sum_k \mu_{ik}(\mathbf{P})} \\ &0 < p_i \leq P_{\max} \\ &R_i \geq r_{\min} \qquad\qquad i = 1, ..., N \end{aligned} \tag{4.14}$$

Each base station (RAU) sends the BER estimation value to the RNC. The RNC calculates the received N power levels for each active mobile terminal, based on the matrix (4.14). During this process, an OPC algorithm iteratively searches for a set of transmission powers that can satisfy all E_b/N_o targets for the session using the current link gain

$$\mu_{ik}(\mathbf{P}) = \{\sum_{j=1, j\neq 1}^{N} \rho^2 \frac{h_{jk}}{h_{ik}} P_j^{(n)} + \delta_{1k}^2\} \tag{4.15}$$

and traffic demand

$$\mathbf{\Gamma_D} = diag[\frac{1}{W} R_{bi}\gamma_1, ..., \frac{1}{W} R_{bN}\gamma_N] \tag{4.16}$$

If the power set is found (i.e. all E_b/N_o targets can be satisfied), the power vector P^* is send to each mobile terminal via its assigned base station.

However, this setup needs communication between RNCs and RAUs from different bunches to coordinate the power vector, synchronization and resources allocation. Nevertheless, the feasibility check if all collected E_b/N_o targets can be satisfied is a good approach to defining whether this traffic demand can be allocated under current conditions and afterward provide acceptable quality.

The definition of QoS required by each service or medium is solely specified by the BER or FER, instead of the SINR. Strictly speaking, the SINR does not completely characterize performance measures, such as BER. However, in general it is difficult to measure the BER, so we apply a frame error rate (FER) measurement using CRCs for OPC; for instance, when a very low BER is required for data transmission, e.g. 10^{-6}, as required in UMTS. Figure 4.10 shows the graph of actual BER measured at the eighth iteration and the corresponding FER measured at 1 to 8 iterations. Since the corresponding FER is also low, a fairly long FER measurement interval is desired. For example, for an FER value corresponding to a BER = 10^{-6} is equitant to 10^{-3} as seen in Figure 4.10 at a transmission rate of 43 kbps (chip rate = 41472 chips/frame) and data frame length of 10ms, therefore, an FER measurement interval of $\geqslant$ 5000 frames (5000 frames * 432 data bits/frame = 2160000 bits = 50s) may be required for reliable FER measurement. Such a long measurement interval is not practical. Thus, the FER is measured at every second iteration and based on the measured FER value, the BER is estimated to reduce time complexity.

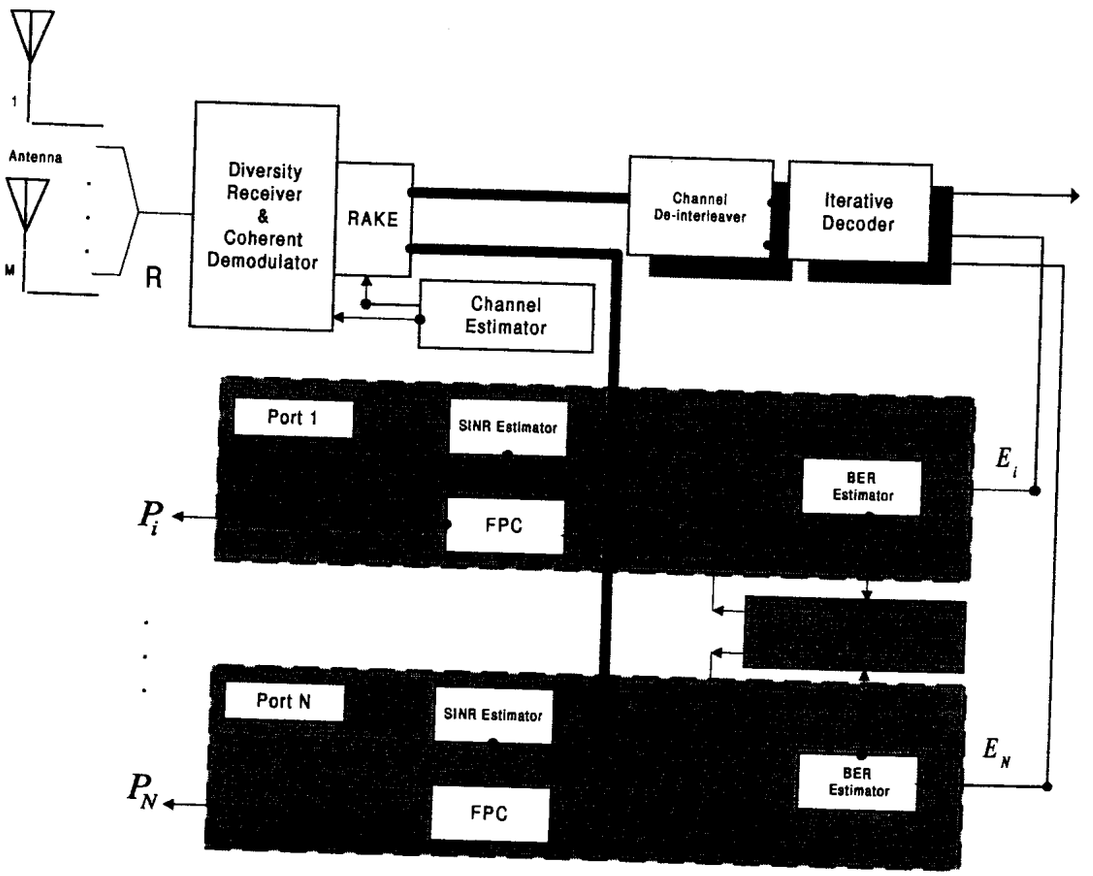

FIGURE 4.9: A multi-target APC with centralized OPC and N output ports

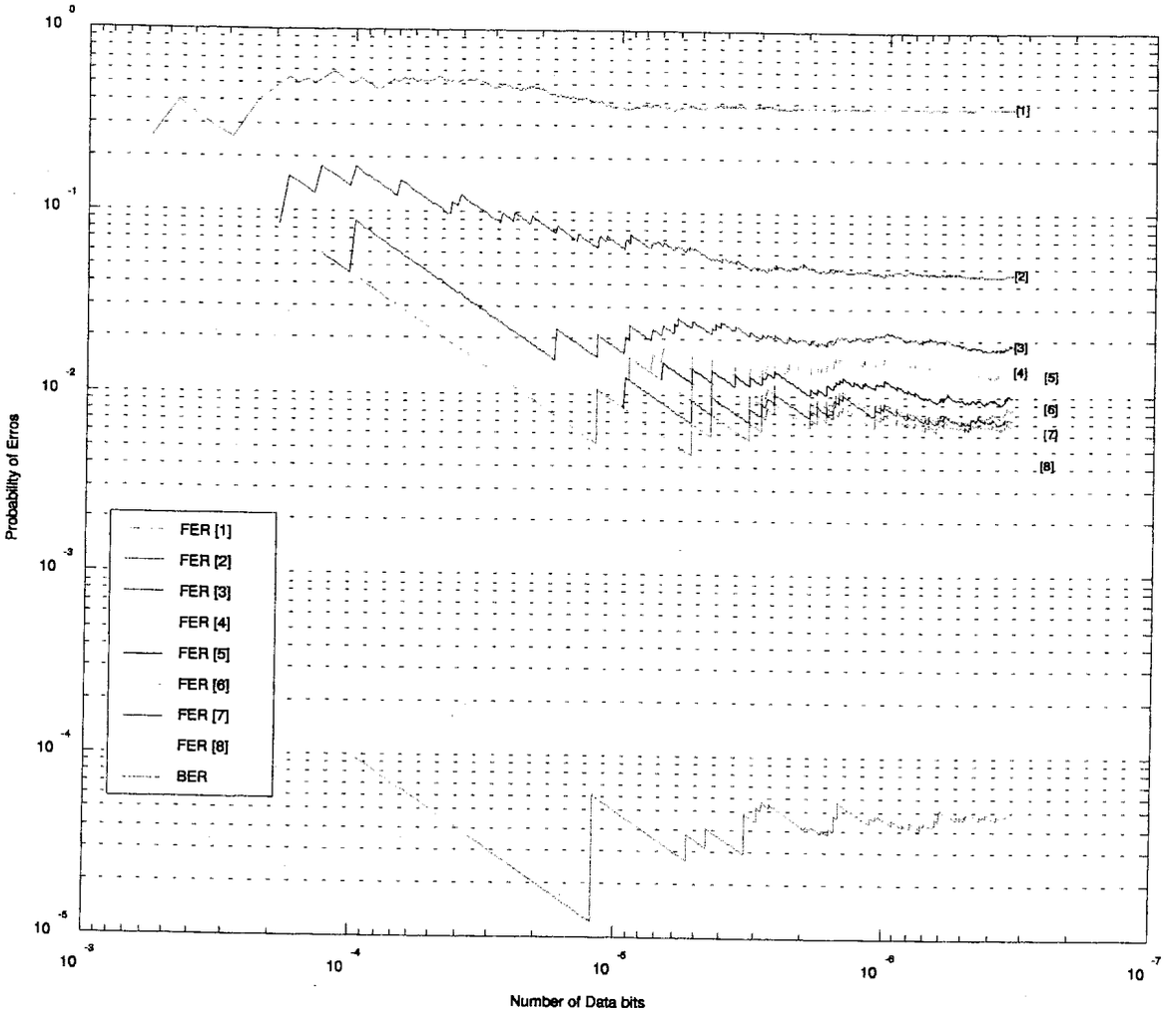

FIGURE 4.10: Relationship between FER[n] and BER[8]

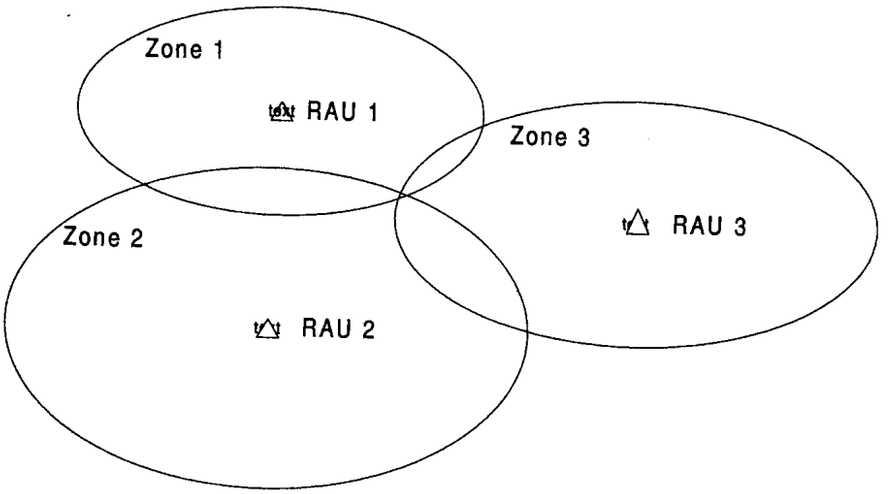

FIGURE 4.11: The zone principle

We present an error-driven technique for outer-loop control of the target SINR for FPC to be used in Turbo-coded, W-CDMA mobile radio systems. Advantage is taken of the fact that in Turbo-decoding the BER and FER decrease as the number of decoding iterations increases. According to Figure 4.10, an FER of 0.04 after the second iteration corresponds to a BER of 4×10^5 after the eighth iteration. Therefore, an FER measurement interval of only 1.25s ($0.04^{-1} \times 5 \times 10^{-3}$) is sufficient, and the target SINR can be adjusted without losing the tracking ability in the presence of slowly changing propagation conditions.

Further improvement on the measurement interval can be achieved by using a BER prediction method. The reliability information (extrinsic value) during the iterative decoding process provides the confidence level corresponding to the current received signals. If we are able to use this soft value to predict the long-term BER achievement, the QoS can be maintained.

4.3.2.1.2 Distributed PC algorithm The distributed PC algorithm using interference matrix-based allocation techniques is different from the intrabunch scheme because it uses the concept of zones. A zone is the area homogeneously covered by one or several RAUs, as shown in Figure 4.11.

To avoid the high processing power demand at the CU and extensive radio network planning, a distributed PC algorithm is required. It also avoids requirements for information on link gain matrix H due to its self-adaptive learning capability. The basic algorithm is implemented as follows.

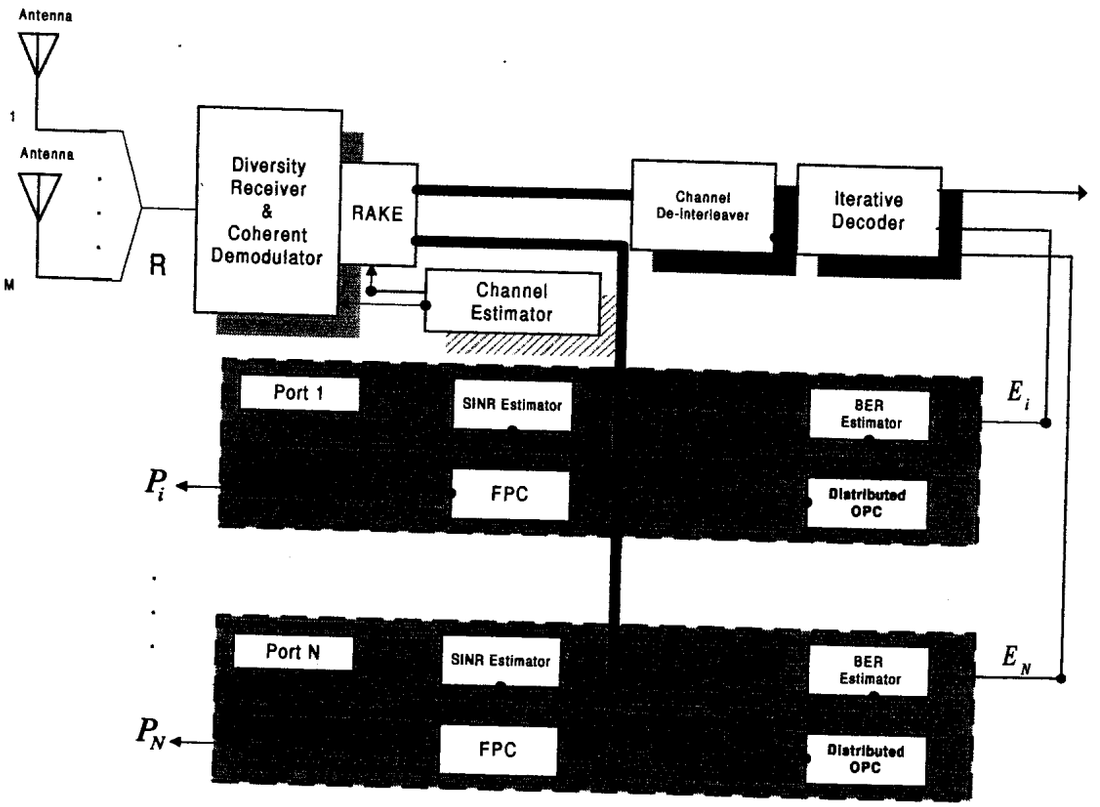

FIGURE 4.12: A multi-target APC with N distributed OPC

- Each base station or zone assigns a power budget, which is determined through the higher layer optimization.
- The zone is to distribute the power budget to each user so that the total cell QoS is maximized. This goal is achieved by computing the optimal power vector for all users.
- Based on the conservation law (section 3.6.4) for iterative FPC algorithms, the power vector for the zone will always converge to the optimal value.
- If the power set does not converge to optimal quickly enough, NPC will reconfigure the networking setting.

Figure 4.12 shows the structure of a typical multi-target APC. The distributed OPC algorithm will generate N sets of desired SINR for the next transmit frame, i.e. N power vectors $\gamma_1 ....\gamma_N$. These N power vectors corresponding to N different QoS (BER) requirements are used to control the transmitted signal in different ports. NPC controls the feasibility of the N power vectors corresponding to N different QoS requirements that may exceed system capacity. In Figure 4.12, $y_1(n), ..., y_N(n)$ are the outputs of ports $1, ..., N$ at the nth iteration, respectively, representing the estimated BER. $\gamma_1, ..., \gamma_N$ are the power

vectors of users $1, ..., N$, respectively and $p_1, ..., p_N$ are the PC commands of users $1, ..., N$, respectively. From Figure 4.12, we see that the MT-PC can be viewed as a complete PC strategy system. We claim that the system design is incomplete if these methods are not considered simultaneously.

4.3.3 A QoS-based Network PC (NPC)

The number of users in the system, N, strongly influences system capacity. From the capacity analysis already presented, decision rules can be defined and implemented in RRM to avoid overloaded situations and for stable system operation. An interesting finding is that the power budget calculation depends on several parameters such as orthogonality factor, $\rho^2_{i,j}$, soft handoff area and gain, $\sum_{j\neq i}^{N} P_{tj}$, $(\frac{E_b}{I_o})_i$ target, and radio-link characteristics, h_{ik}, or, $\sum_{j\neq i}^{N} h_{jk}$. A further finding is that there is a theoretical limit, N_{limit}, [16] which when it reached, the network will fail to deliver satisfactory QoS to any users. Therefore, the number of users should be kept within a safety margin below N_{limit}. PC and admission-control, PC and base station assignment and PC and handoff operations (section 3.4) aim to maximize the system resources by minimizing *inter-cell* interference. At the same time NPC measures the system capacity of current communication systems.

4.3.3.1 NPC Algorithms

Since intercell interference is localized within a finite region, changing the power level of a cell affects only its nearby cells, its "neighbourhood". This observation suggests that we are able to set the power budget for several cells simultaneously. For this discussion we assume only first order interference [14].

Assume a cell topology as shown in Figure 4.13, where a centre cell has six neighbouring cells. Suppose cell k is in the centre and let, $\bar{P}_i = (P^0_k, P^1_k, ..., P^6_k)$, be the total power budget for each of the seven cells. When updating the power budget for cell 0, its power level is chosen so as to maximize its overall neighbourhood QoS is also a function of P_o (minimize the intercell interference), as shown below

$$U_{\text{neighbourhood}}(P_o, P_1, ..., P_6) = U^*_{\text{cell0}}(P_o) + \sum_{i=1}^{6} U^*_{\text{cell0}}(P_i) \qquad (4.17)$$

[14] First-order interference means that a base station only interferes with its six immediate neighbouring cells. This assumption is only for illustrative purposes, and is not necessary for our distributed algorithms. If the assumption does not hold, we can increase the neighbourhood size, which will decrease the rate of convergence.

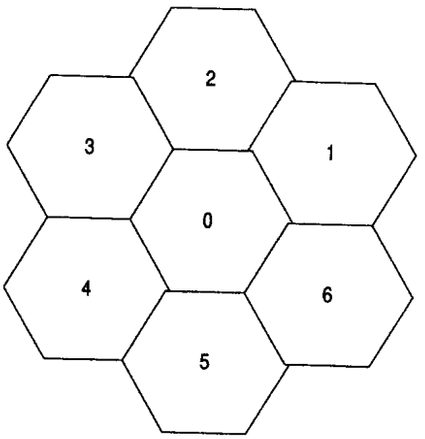

FIGURE 4.13: Cell topology

While P_o is upper bounded by the implementation limit, the objective of adjusting P_o is to maximize the total neighbourhood QoS. Thus, P_o has to satisfy

$$\frac{\partial}{\partial P_0}[U_{\text{neighbourhood}}(P_o, P_1, ..., P_6)] = 0 \tag{4.18}$$

This is equivalent to

$$\frac{\partial}{\partial P_0}U^*_{\text{cell0}}(P_0) = -\frac{\partial}{\partial P_0}\left(\sum_{i=1}^{6} U^*_{\text{celli}}(P_i)\right) \tag{4.19}$$

Notice that the left side of Equ. (4.19) is the marginal QoS of cell #0 as a function of P_0, and on the right is the total marginal QoS of the neighbouring cells. At the optimal point, with respect to P_0, the marginal QoS of cell #0 offsets the marginal QoS of the neighbouring cells. The system QoS optimization algorithm described above is indeed an iterative, one-dimensional (1-D)search algorithm, in which we optimize along each P_i iteratively until the maximum is reached.

Restrict ourselves to changing power levels for the centre cell of these six neighbourhoods only. Firstly, since the effects of changing the power level of a centre cell is limited to the neighbourhood boundary, cells only need to communicate within the neighbourhood. Secondly, since a centre cell faces a fixed interference environment, calculation of the power budget is simplified. Finally, since the remaining cells within the neighbourhood have exactly one interfering cell which changes its power, calculation of intracell and intercell interference coefficients is simplified. So far, we have updated the power budgets for only a cell.

4.4 A SUMMARY OF THE MULTIPLE-TARGET (MT) QOS-BASED PC ALGORITHM

We have presented a QoS-based approach to the overall control problem. Since the policy issues of allocation resources are separate from the design process, the main advantage of this MT, QoS-based PC structure is that it offers a great deal of flexibility to the system control. In other words, we can always choose a QoS function that reflects specific design objectives.

In order to achieve optimal system performance, three control knobs are available to fulfill different BER and bandwidth requirements: FPC; OPC; and NPC. FPC varies the transmit power to adjust the received signal quality. Together FPC and OPC are used to support applications with widely varying QoS and to mitigate excessive interference. Finally, OPC and NPC allocate resources among data types, especially when application demands exceed channel capacity. The MT-PC can be viewed as a complete PC strategy system. We claim that the system design is incomplete if these methods are not considered simultaneously.

However, this advantage of flexibility makes it difficult to quantify and compare system performance with other approaches. Therefore, we have simulated the system using a specific traffic demand, channel conditions and RRM algorithms. Our ultimate goal is to investigate the influence of physical and temporal parameters in a UMTS/UTRA cellular environment. A detailed comparison of the SINR tracking ability, BER stability and performances for different PC algorithms is presented in Chapter 5.

CHAPTER FIVE

NUMERICAL PERFORMANCE EVALUATION OF ADAPTIVE FPC ALGORITHMS

5.1 Introduction

Following the development of the power-sensitive model, including transmitted power level, channel impairment, processing gain and MAI described in Chapter 2, this chapter presents a numerical evaluation of the QoS-based APC structure [Chapter 4] using the Monte Carlo simulation package in a Turbo-coded, RAKE-combining and uplink W-CDMA system. More specifically, we compare balanced and unbalanced step-size FPC algorithms under the following conditions:

1. Multipath components (section 5.3.1) in
   - an AWGN channel,
   - a vehicular channel,
   - an outdoor channel.
2. Doppler spread (section 5.3.2) of
   - 10 km/h,
   - 120 km/h,
   - 200 km/h.
3. Coding schemes (section 5.3.3) in
   - an AWGN channel with uncoded, convolutional and Turbo codes;

- a vehicular channel with uncoded, convolutional and Turbo codes;
- an outdoor channel with uncoded, convolutional and Turbo codes.

4. Number of antennae (section 5.3.4)
5. Number of users (section 5.3.5) with
   - one active user in the cell;
   - two active users in the cell.

The BER performance and SINR outage probability for the eight FPC algorithms under the conditions specified above are compared in this chapter. Further, we demonstrate numerically that to evaluate QoS-based PC algorithms it is essential that all these parameters in the power-sensitive model must be taken into account in order to accurately measure improvements in system performance. We also show that, in order to deliver QoS to subscribers optimally, OPC algorithms with RRM are required because of the stochastic nature of the wireless channels and interference.

5.2 Description of System Parameters

The system under consideration in this dissertation is an uplink, *direct-sequence*, W-CDMA system. The modulation scheme used in the system is QPSK; the carrier frequency, f_c, is equal to 4.096M chip/s; and the transmission rate is 128K bps coded information data. Rate $1/3$ coding is used with a constraint length equal to eight. The data frame length is $10ms$ (= interleaving length). The base-station receiver uses a six-finger (three fingers/antenna) RAKE combiner and sends the FPC command back to the mobile every $0.625ms$ to raise or lower the mobile transmitted power by x dB, depending on the FPC algorithm used. The number of iterations in the Turbo decoder is set to eight iterations before recovery of the received information data. The radio-link parameters are listed in Table 5.1, and the UMTS uplink simulation described is based on the specification for the FDD system [18].

TABLE 5.1: FDD W-CDMA radio-link parameters.

Definition of the notations	
Parameter	**Description**
Chip rate	41472/frame
User data rate	48 kbps/256 kbps/1024 kbps
Spreading factor	32/16/4
Interleaving	10 ms
Modulation	QPSK
Sampling rate	4
No. of slots/frame	16
No. of fingers/antenna	3
Initial power	0.5 W
Diversity (receiver antenna)	2
FEC	Uncoded
	Convolutional with soft-input Viterbi decoder
	Turbo encoder with iterative MAP decoder
FPC algorithms (DM1)	balanced DM FPC with step-size = 1 dB
(DM2)	balanced DM FPC with step-size = 2 dB
(DM3)	balanced DM FPC with step-size = 3 dB
(PC5)	balanced PCM FPC with 2 increasing, 1 unchanged and 2 decreasing
(PC7)	balanced PCM FPC with 3 increasing, 1 unchanged and 3 decreasing
(unDM)	unbalanced DM FPC
(uPC4)	unbalanced PCM FPC with 2 increasing, 1 unchanged and 1 decreasing
(uPC6)	unbalanced PCM FPC with 3 increasing, 1 unchanged and 2 decreasing

- Operating environment

  Three distinct operating environments are analyzed. These are an AWGN channel, an outdoor channel and a vehicular channel. The differences in these environments are mainly due to the temporal distribution, Doppler spread and multipath power profile for each case.

- Multipath power profile

  Different operating environments have different power profiles as shown in Figure 2.10.

- Number of multipath signals

  Different operating environments generate different multipath components. The number of multipath components is consistent with measurements taken in UMTS standards for bad urban environments [83].

- Number of users

  $i = 1$

  For the purpose of evaluating BER performance and SINR outage probability for different channels, receiver structures and coding schemes, it is assumed that there is only one user active in the cellular system. The influence of number of users is presented at the end of this chapter.

- RAKE receiver

  $L = 3$

  It is assumed that the base station employs a three-branch RAKE receiver capable of receiving the first three multipath signals arriving at the base station.

- Adaptive antenna array

  $M = 2$

  It is assumed that a uniform linear array with two elements is used to receive signals at the base station. Such an adaptive array is typical of existing cellular systems.

- Temporal fading model

  It is assumed that all multipath components received by the RAKE receiver will exhibit identically independent distributed (iid) Rayleigh fading.

- Multi-access interference

  It is assumed that all MAI plus background noise received by the RAKE receiver will

exhibit iid Gaussian noise to the desired signals.

Nine FPC algorithms are considered for possible implementation in the UMTS standard. These are:

- DM1 FPC (section 4.3.1.2),
- DM2 FPC (section 4.3.1.2),
- DM3 FPC (section 4.3.1.2),
- PCM5 (section 4.3.1.3),
- PCM7 (section 4.3.1.3),
- unDM1 (section 4.3.1.4),
- unPC4 (section 4.3.1.5),
- unPC6 (section 4.3.1.5),
- perfect FPC.

5.3 Simulation Results For Unbalanced Step-size FPC Algorithms

5.3.1 Influence of Multipath Components

Using the system model outlined above, the time-dispersion channel model is set for AWGN, outdoor and vehicular channel models.

To generate the BER curves for the eight FPC algorithms, the same power levels are transmitted initially and the same desired SINR values are set for each user. At the receiver end, the RAKE combining and coherent demodulator is used to dissolve the multipath components and to extract the desired signals from corrupted received signals through a matched-filter technique. The output of the matched-filter is then fed into the SINR estimator to determine the received SINR value. The estimated received SINR value is then compared to the pre-determined SINR value and a power command is calculated for each FPC algorithm used. The BER value of each user is calculated using hard-decisions of desired signals, and the average BER values are then calculated and used in the BER

Table 5.2: BER performance of different FPC algorithms in an uncoded W-CDMA system with the AWGN channel at 16 dB.

$E_b/I_0 = 16$ dB	BER
unPC6	0.000147
unPC4	0.000177
unDM	0.000185
DM1	0.000201
DM2	0.000258
DM3	0.000285
PCM5	0.000293

performance plot. Since coding schemes are not used in this simulation, we can evaluate the influence of number of multipath components on FPC algorithms only. The BER curves and SINR outage probability simulation results obtained after Monte Carlo simulation are presented in this section.

5.3.1.1 BER Performance in an AWGN Channel

In the case where there are no multipath components and only the AWGN is introduced in the channel, the uncertainty of estimating time-varying wireless channels is negligible in a consideration of performance. Figure 5.1 shows the BER performance of the system with the eight APC algorithms in the AWGN channel. The results show that except for the perfect FPC algorithm, most of the algorithms have similar BER performance. This is primarily due to the fact that in a non-fading channel environment transmitted power waveform and power level are preserved, and only a constant background noise power affects the transmitted signals. As a result, these APC algorithms control the received SINR more effectively and efficiently than in fading environments.

However, when the BER performance of the eight FPC algorithms is compared at 16 dB [see Table 5.2], there is little improvement with unbalanced FPC algorithms in AWGN channel conditions, although AWGN channels still yield slightly better results with unbalanced FPC algorithms. Generally, unbalanced PCM algorithms outperform unbalanced DM algorithms and unbalanced FPC algorithms outperform balanced FPC algorithms.

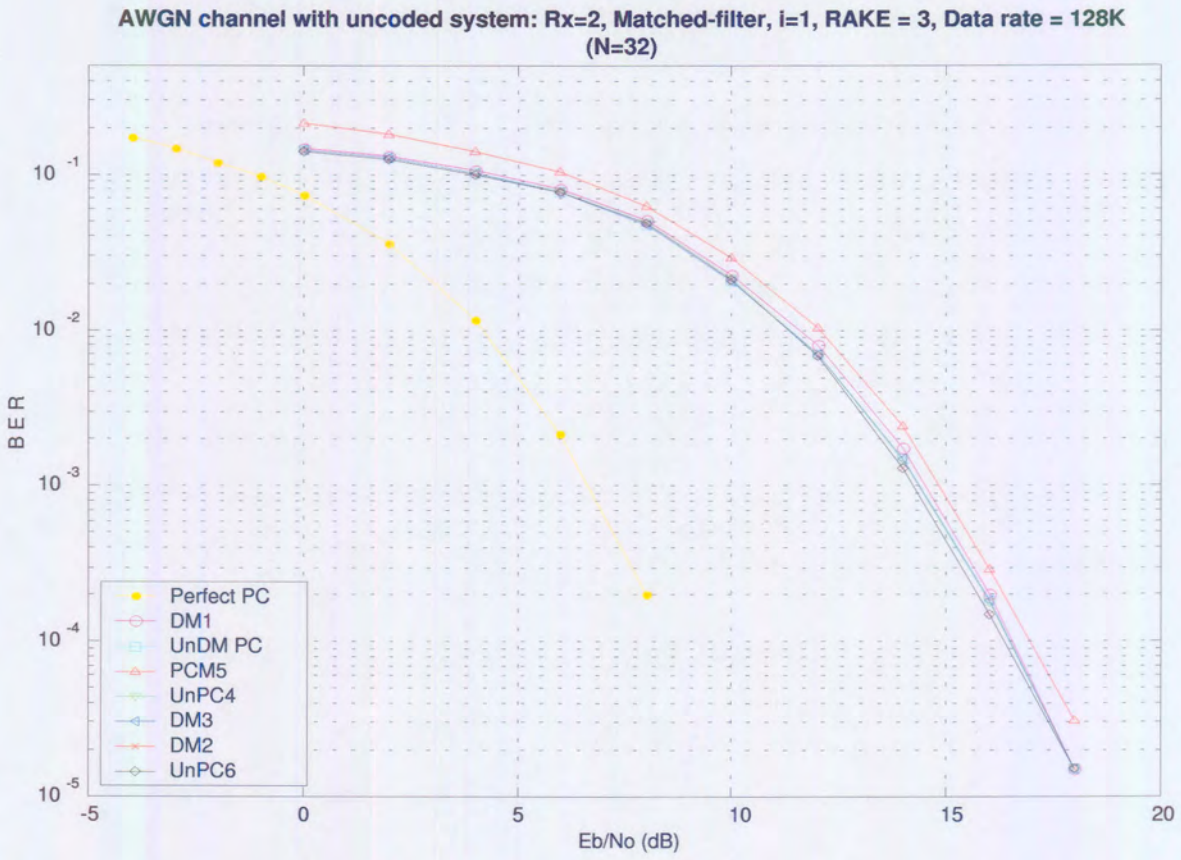

FIGURE 5.1: Influence of multipath components. BER performance curves of different FPC algorithms in an uncoded W-CDMA system with an AWGN channel, Rx=2, i=1, RAKE fingers=3, N=32 and matched-filter detector.

5.3.1.2 SINR Outage Probability in an AWGN Channel

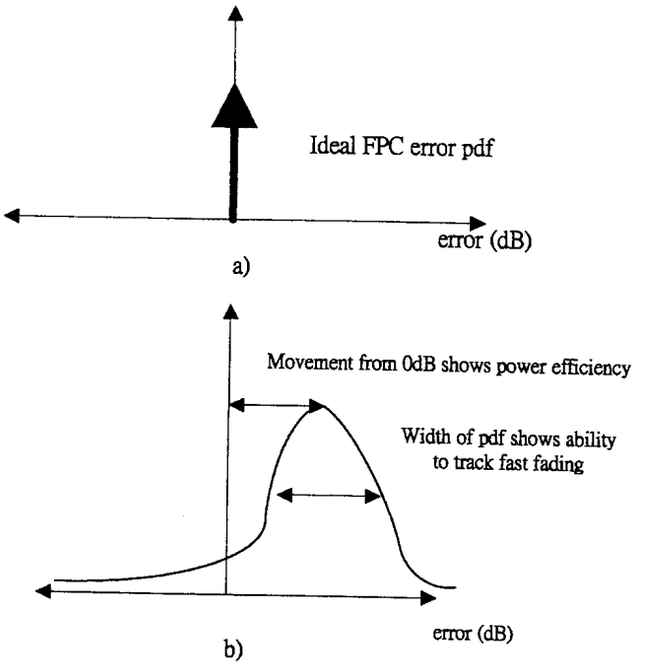

FIGURE 5.2: (a) Ideal and (b) practical FPC error-signal pdfs

Focusing on the actual SINR versus the target SINR, it is clear that the main characteristic of the ideal FPC algorithm is that actual and target SINR values are the same, irrespective of the channel variations. Thus, it follows that the pdf of the error signal is an impulse at 0 dB, as shown in Figure 5.2.

Two specific aspects of the pdf are of paramount importance: width and mean value. The width of the pdf is a measure of the ability of an FPC algorithm to cope with fast changes in the channel. If the algorithm has a limited dynamic range or responds slowly to changes in channel variations, the error signal at a specific instant in time will range from small values to large ones. Secondly, the mean value of the error signal provides a measure of the power efficiency of the FPC algorithms. Therefore, FPC algorithms can be compared by considering the mean and variance of the error signals generated by the algorithms. The lower the mean value, the better the power efficiency of the algorithm; and the lower the variance of the error signals, the better the algorithm can cope with short-term channel variations.

These simulation results of SINR outage probability [Figures 5.3 to 5.7] show how these eight FPC algorithms performed in the AWGN channel environment. Note that the higher

the mean variation of the measured SINR compared to the desired SINR value, the more MAI will be created for other users, especially in multi-media services.

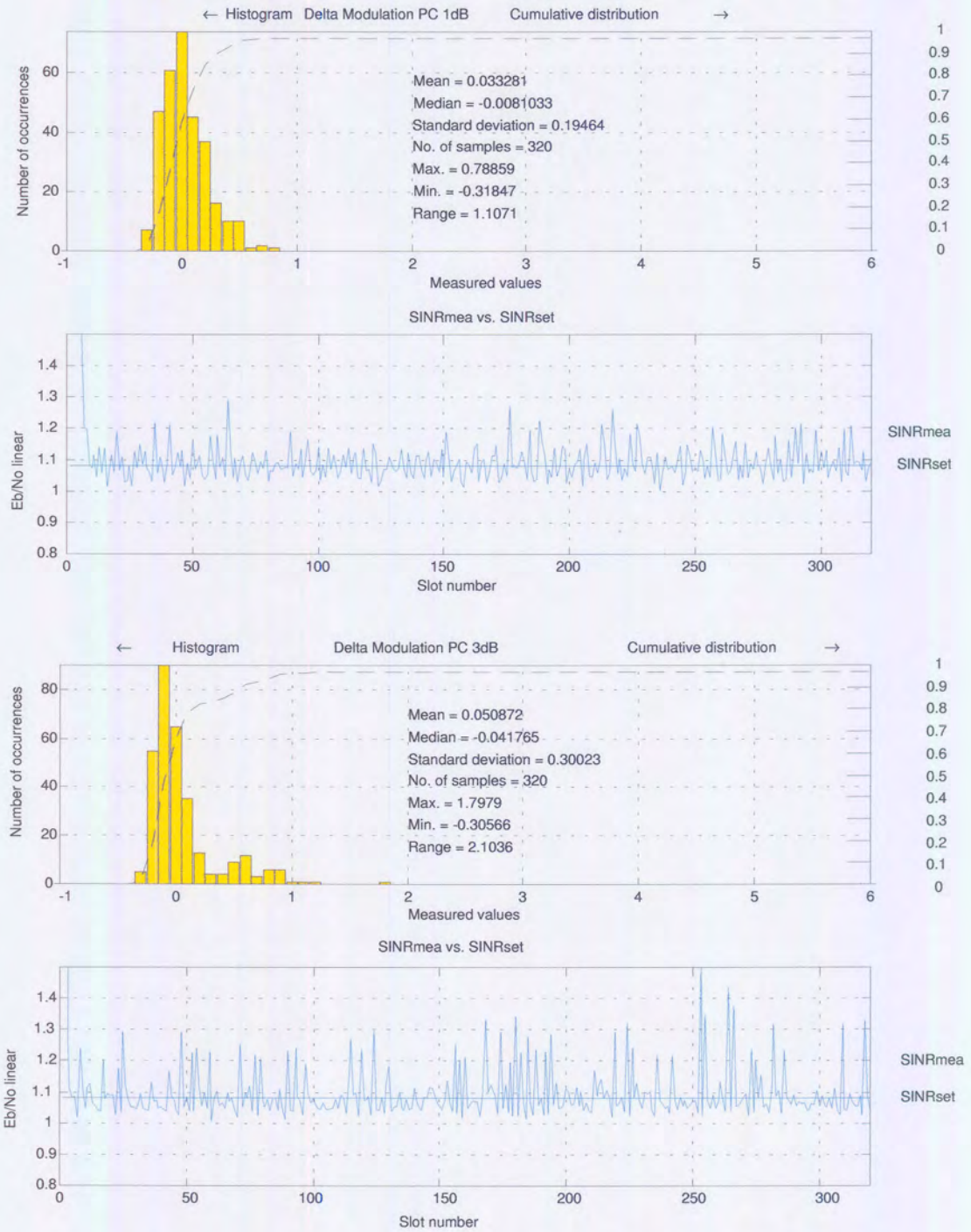

FIGURE 5.3: SINR outage probability simulation results and error-signal pdf for different FPC algorithms. The top figure shows the pdf of DM1 FPC with same settings as BER performance simulation. The bottom figure shows the pdf of DM3 FPC.

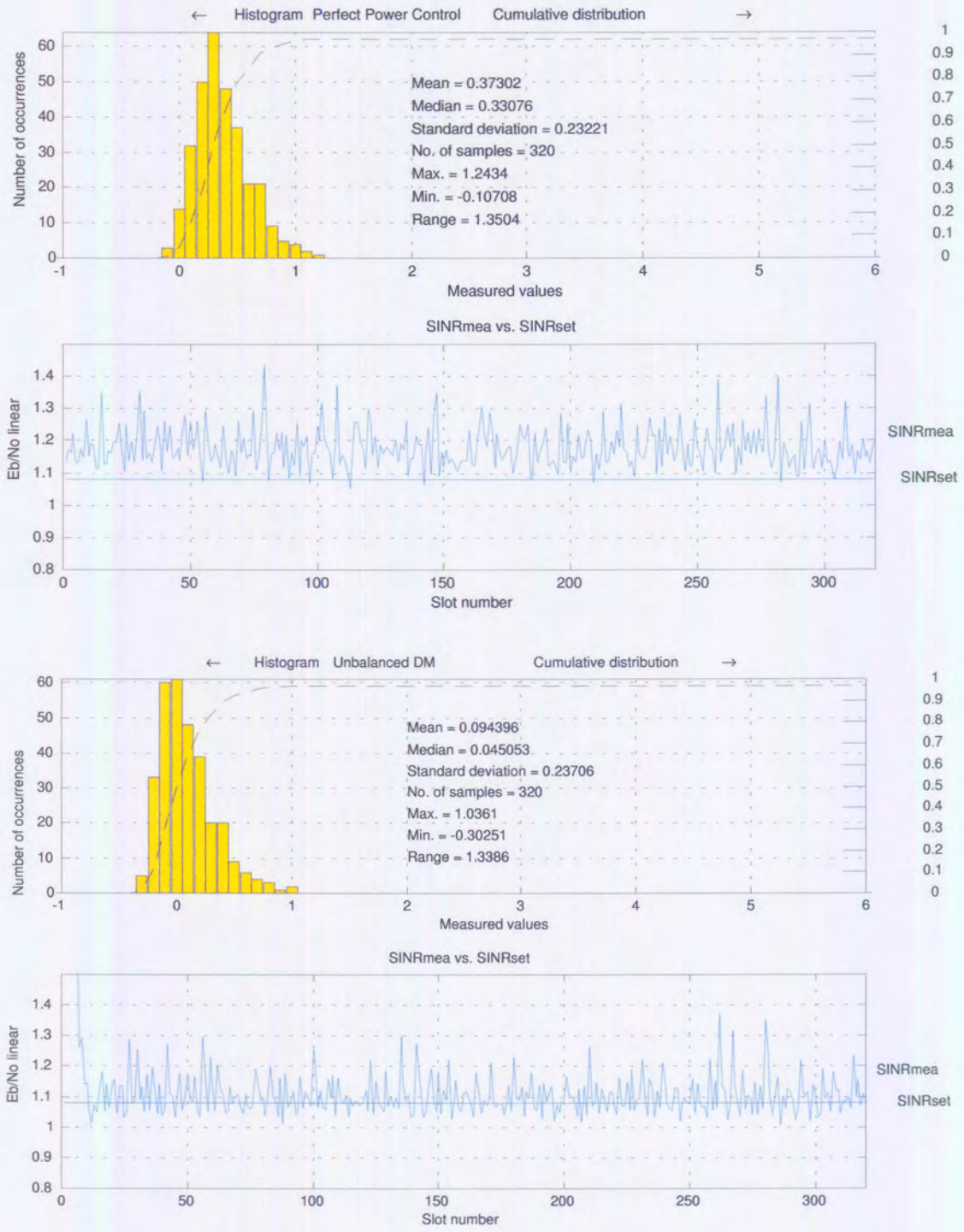

FIGURE 5.4: SINR outage probability simulation results and error-signal pdf for different FPC algorithms. The top figure shows the pdf of perfect FPC with same settings as BER performance simulation. The bottom figure shows the pdf of unDM FPC.

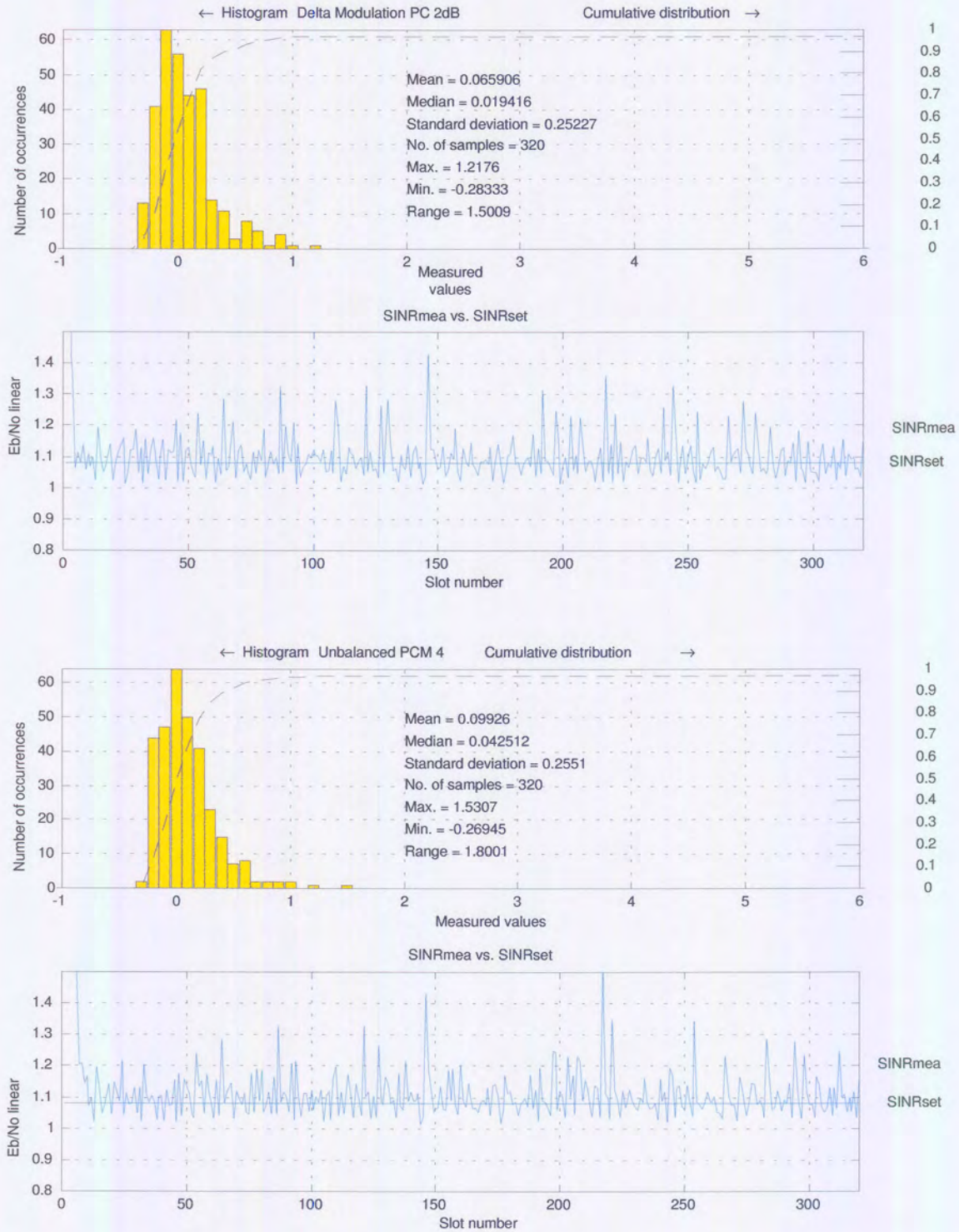

FIGURE 5.5: SINR outage probability simulation results and error-signal pdf for different FPC algorithms. The top figure shows the pdf of DM2 FPC with same settings as BER performance simulation. The bottom figure shows the pdf of unPC7 FPC.

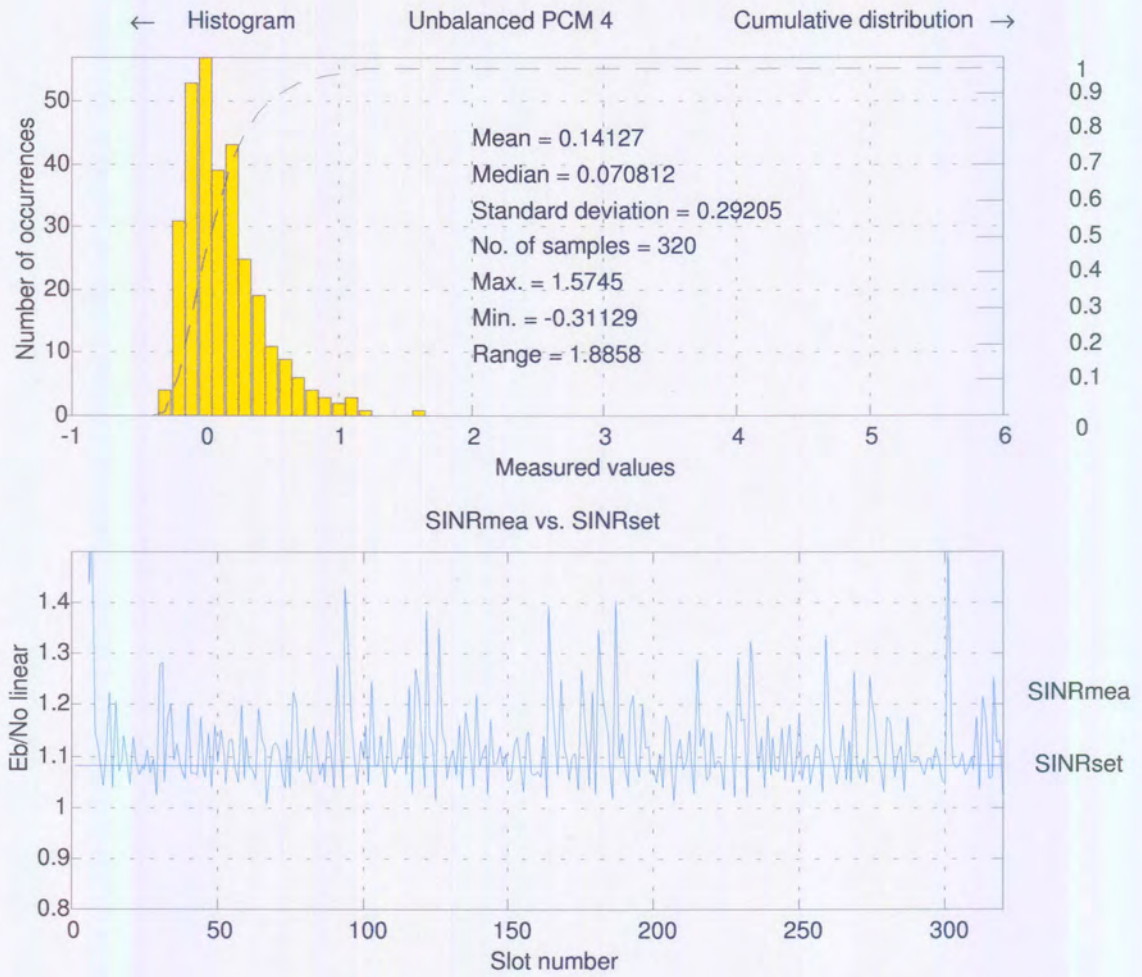

FIGURE 5.6: SINR outage probability simulation results and error-signal pdf for different FPC algorithms. The figure shows the pdf of unPC4 FPC with same settings as BER performance simulation.

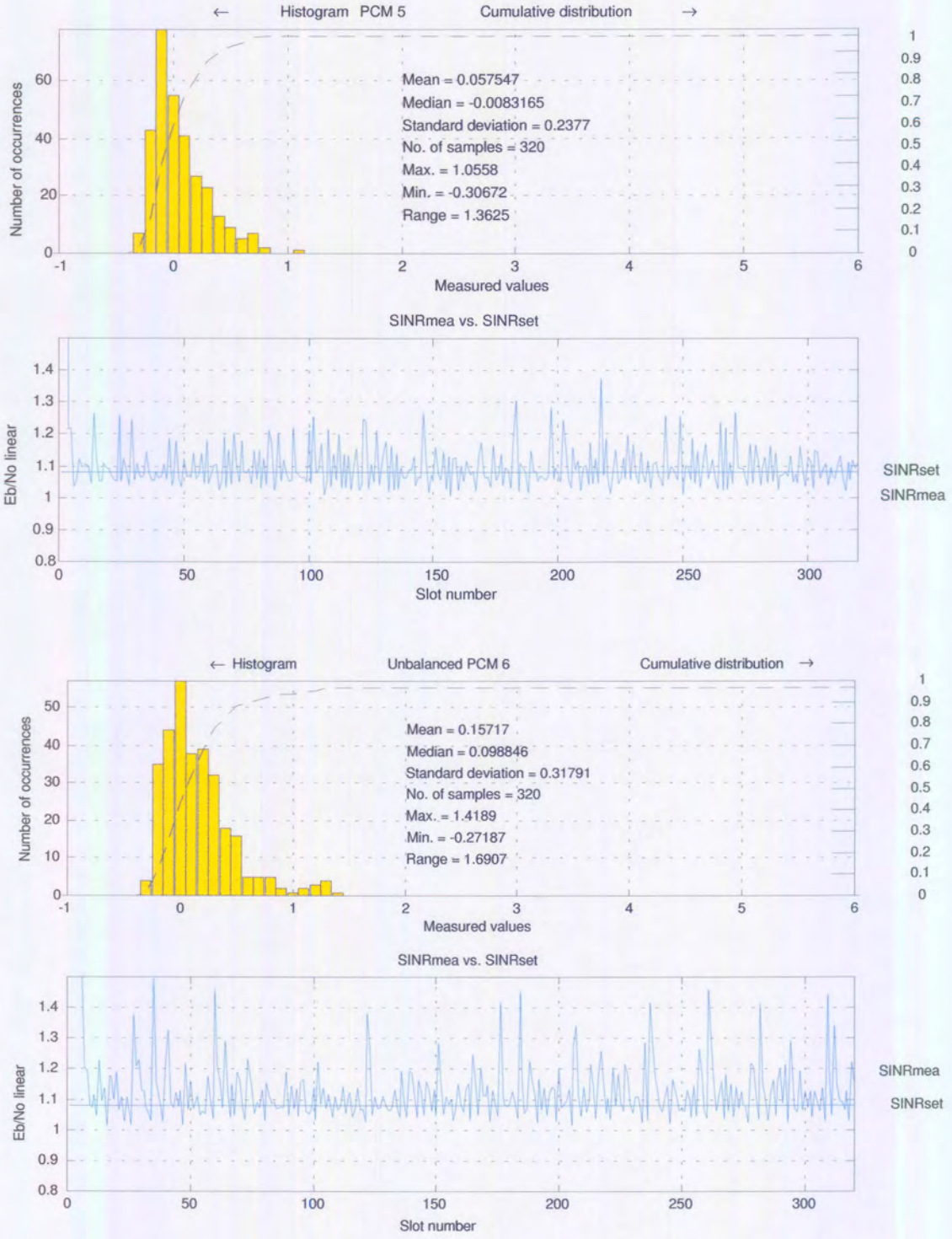

FIGURE 5.7: SINR outage probability simulation results and error-signal pdf for different FPC algorithms. The top figure shows the pdf of PCM5 FPC with same settings as BER performance simulation. The bottom figure shows the pdf of unPC5 FPC.

FIGURE 5.8: Mean variation, standard deviation and range comparisons for different FPC pdf algorithms are depicted in this figure with an AWGN channel, Rx=2, i=1, RAKE fingers=3, N=32 and matched-filtered W-CDMA system.

A summary of mean variation, variance and range comparisons for these FPC algorithms is shown in Figure 5.8. The balanced FPC algorithms have lower mean variance and therefore yield better power efficiency than the unbalanced FPC algorithms in AWGN channels. Comparing DM and PCM algorithms, we have found the variance of both balanced DM and unbalanced DM algorithms is less than that of balanced and unbalanced PCM techniques, respectively. Thus, it is important to note that the more quantization levels used in FPC algorithms, the better the BER performance, but the more the overshoot and steady state error for the SINR outage probability test. The smaller the step-size, the less overshoot and steady state error, but the lower the BER performance.

These observations can be attributed to the fact that, firstly, the unbalanced FPC algorithms increase the average transmitted power more than balanced FPC algorithms do. Thus, BER performance yields better power efficiency with unbalanced FPC algorithms. Secondly, since there is no time-dispersion and rapid time-variation of the received envelope, unbalanced FPC algorithms can control the transmitted power more effectively. Thirdly, since the rate of change in amplitude, phases and time-delay of the transmitted signals

is slower than the transmitted signals in fast-fading channels with Doppler spread effects, unbalanced FPC algorithms are able to control the transmitted power more efficiently. It is expected that as the number of multipath components and the Doppler spread increase, so the effectiveness and efficiency of these FPC algorithms will decrease.

5.3.1.3 BER Performance in a Vehicular Channel

Thus far, no multipath components and AWGN channel were assumed in the previous simulation. Let us now assume there are multipath components in the vehicular channel setting and Rayleigh envelope fading is also introduced in the wireless channel.

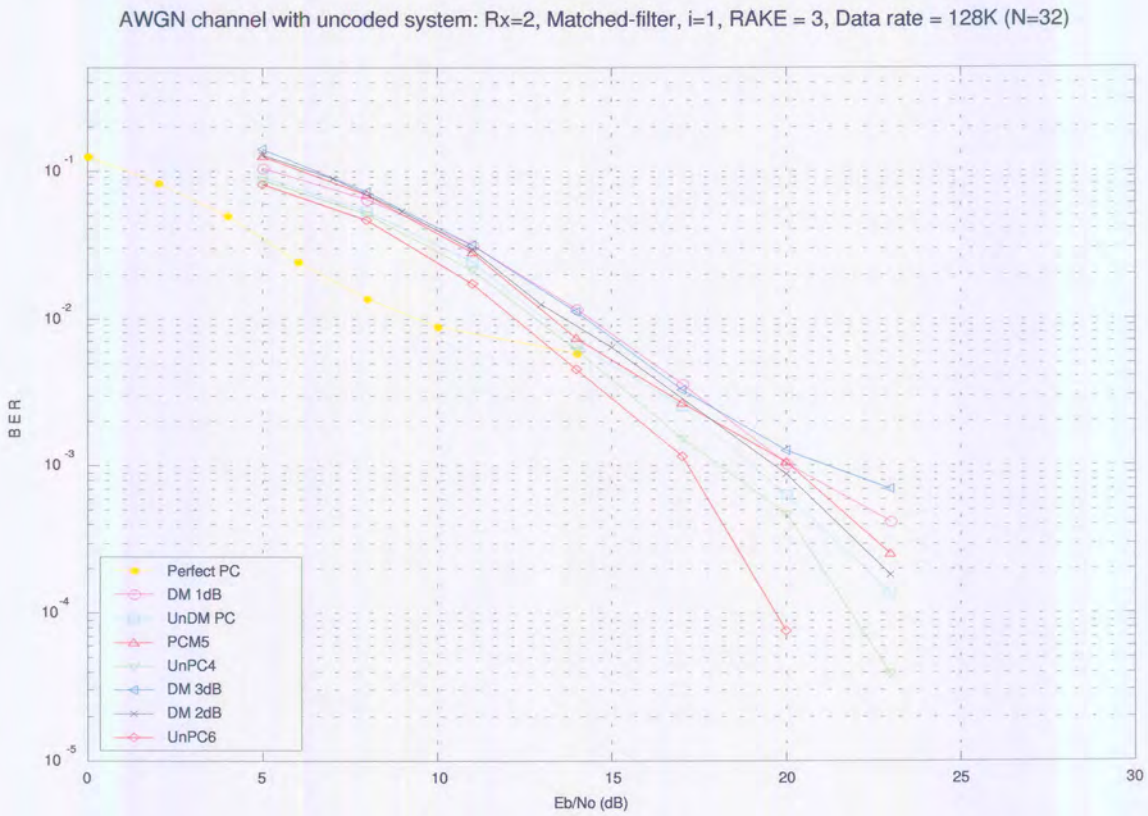

FIGURE 5.9: Influence of multipath components. BER performance curves of different FPC algorithms in an uncoded W-CDMA system with a vehicular channel, Rx=2, i=1, RAKE fingers=3, N=32 and matched-filter detector.

Figure 2.10 shows that the vehicular channel has fewer multipath components than outdoor channels, and it is assumed that an increase in the number of multipath components and Doppler spread results in a frequency-selective, fast-fading channel environment. This implies that the rate of change in amplitude, phases, and time delay of any of the

multipath components varies faster than the transmitted signal [81], thereby decreasing the effectiveness and efficiency of the FPC algorithms. This can be observed by comparing the BER performance curves in AWGN of vehicular channels [Figures 5.1 and 5.9] it is observed that the effect of a frequency-selective, fast-fading channel on W-CDMA system capacity is substantial. There is a decrease in power efficiency of 9 dB comparing the performance of a balanced DM FPC in an AWGN and a vehicular channel.

Figure 5.9 shows the BER performance of the system with the eight FPC algorithms in the vehicular channel. The results show that there is a substantial improvement with unbalanced FPC algorithms compared to balanced FPC algorithms, especially at high SINR values. This is primarily due to the fact that the power signals fade more quickly than when they are increasing in a typical Rayleigh and Ricean frequency-selective fading. Thus, unbalanced FPCs outperform balanced ones in a Rayleigh fading channel.

It is claimed [85] that the smaller the FPC error-signal pdf, the shorter the error-free run length in the system. In other words, burst errors occur less frequently. Since unbalanced FPC algorithms improve SINR outage probability by increasing average transmitted power, burst errors can be better controlled and eliminated by our proposed FPC algorithms, especially at high SINR levels [Figure 5.10]. Later in this chapter, we show how FPC algorithms, by incorporating coding schemes, can improve the BER performance significantly.

When the BER performance of the eight FPC algorithms is compared in a vehicular channel at 20dB, generally, there is a 4 dB improvement with the unbalanced DM algorithms over the balanced DM algorithms. This is because DM algorithms cannot cope with fast variations in the vehicular channel condition. This deficiency can be lessened by introducing PCM algorithms where more control bits are required for control. There is a slight improvement with the unbalanced PCM algorithms compared with unbalanced DM algorithms: in general, a 5 dB improvement is experienced with unPCM6 compared with unDM, the improvement rate declining as the transmitted SINR values decrease.

5.3.1.4 SINR Outage Probability in a Vehicular Channel

The error distribution pdfs of SINR outage probability [Figures 5.12 to 5.15] show how these FPC algorithms perform in a vehicular channel environment.

A summary of mean variation, variance and range comparisons for these FPC algorithms is shown in Figure 5.11. When a frequency-selective, fast-fading channel is introduced in the system, the FPC error-distribution pdf also changes. The balanced FPC algorithms still

FIGURE 5.10: Influence of received SINR values on the BER performance of a W-CDMA cellular system. Blue line shows the average received SINR value for a frame; red line shows the number of errors occurring within a frame. Burst errors occur more frequently when received SINR is low.

Table 5.3: BER performance of different FPC algorithms in an uncoded W-CDMA system with vehicular channel at 20 dB.

$E_b/I_0 = 20$ dB	BER
unPC6	0.000077
unPC4	0.000471
unDM	0.000633
DM1	0.001042
PC5	0.001065
DM2	0.001120
DM3	0.001265

yield lower mean variation values than the unbalanced FPC algorithms, However the increase in mean value is generally about five times more than in an AWGN channel. Therefore, the balanced FPCs improve power efficiency considerably more than unbalanced FPCs do. Also, the balanced and unbalanced DM have lower aggregate values. Thus, DM FPC algorithms yield better tracking ability and robustness in the different channel conditions.

Validation of the Gaussian approximation of FPC error distribution in frequency-selective fading channel is also investigated in the simulation, which shows that the Gaussian approximation of FPC error distribution is not valid in a conventional RAKE receiver structure.

It is our view that the BER performance curves should plot the BER against the measured SINR and not the desired SINR values in order to integrate the effect of the FPC error distribution into the BER performance results. Figure 5.16 shows the BER results of FPC algorithms in the vehicular channel. These diagrams show that both unbalanced and balanced DM algorithms outperform others. Also, unbalanced PCM algorithms generally outperform balanced PCM ones.

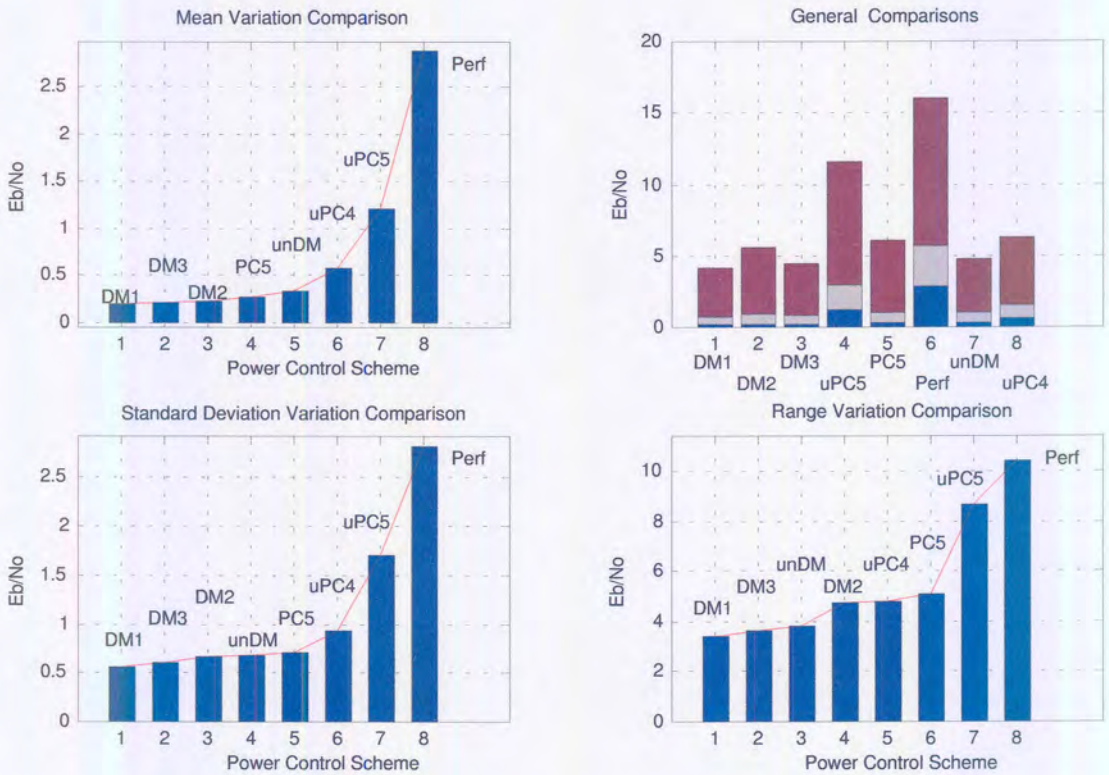

FIGURE 5.11: Mean variation, standard deviation and range comparisons for different FPC pdf algorithms with a vehicular channel, Rx=2, i=1, RAKE fingers=3, N=32 and matched-filtered W-CDMA system.

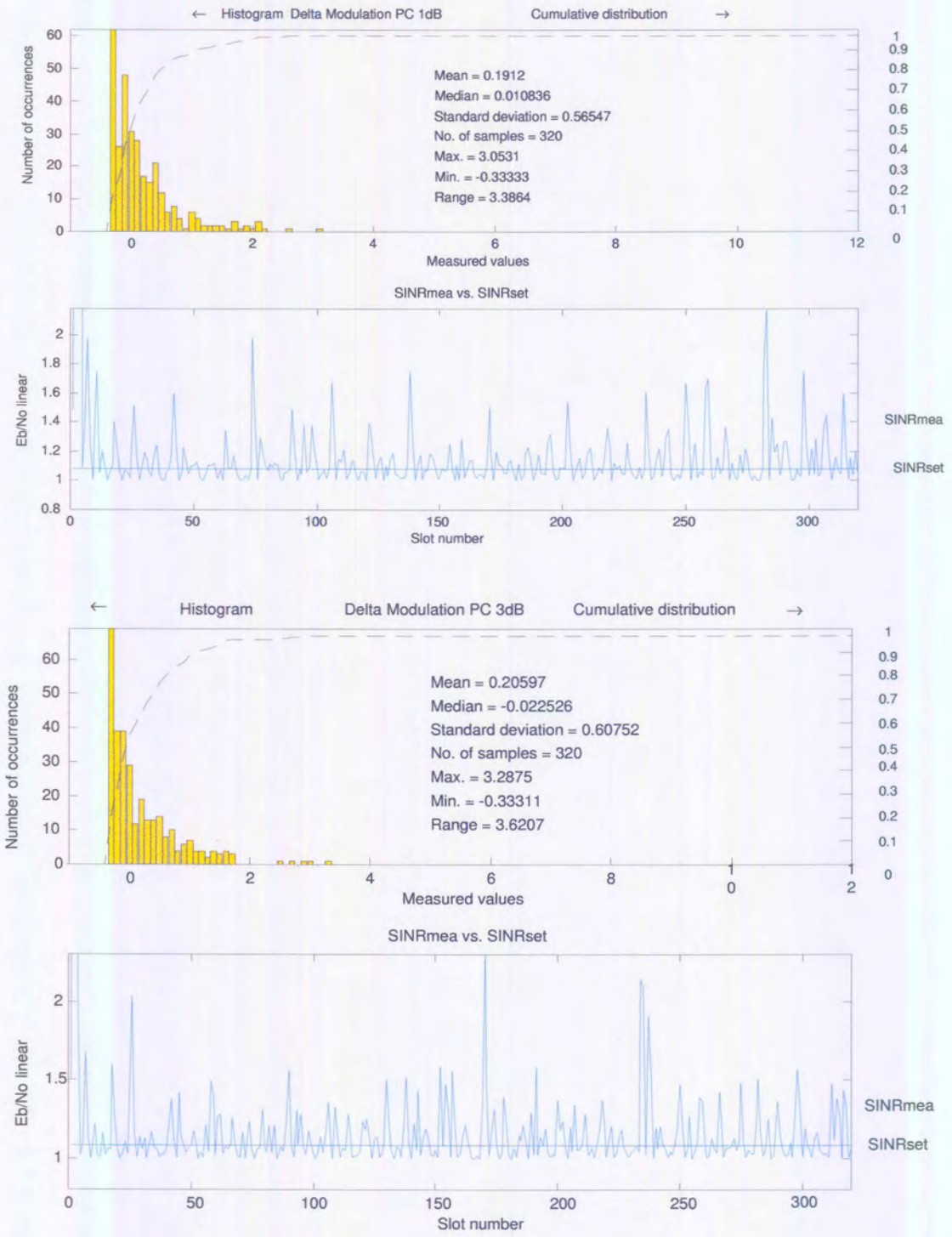

FIGURE 5.12: SINR outage probability simulation results and error-signal pdf for different FPC algorithms. The top figure shows the pdf of DM1 FPC with same settings as BER performance simulation. The bottom figure shows the pdf of DM3 FPC.

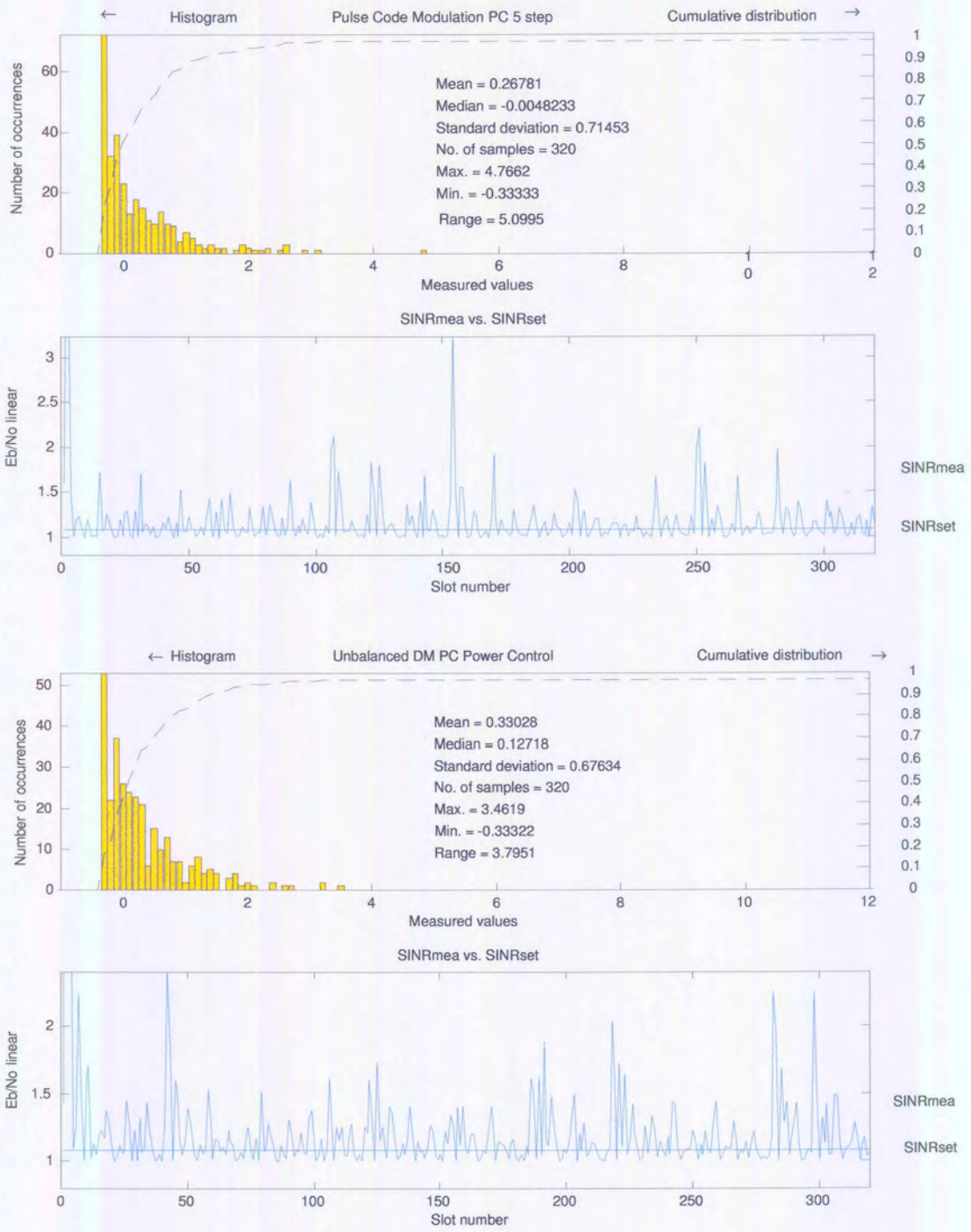

FIGURE 5.13: SINR outage probability simulation results and error-signal pdf for different FPC algorithms. The top figure shows the pdf of PCM5 FPC with same settings as BER performance simulation. The bottom figure shows the pdf of unDM FPC.

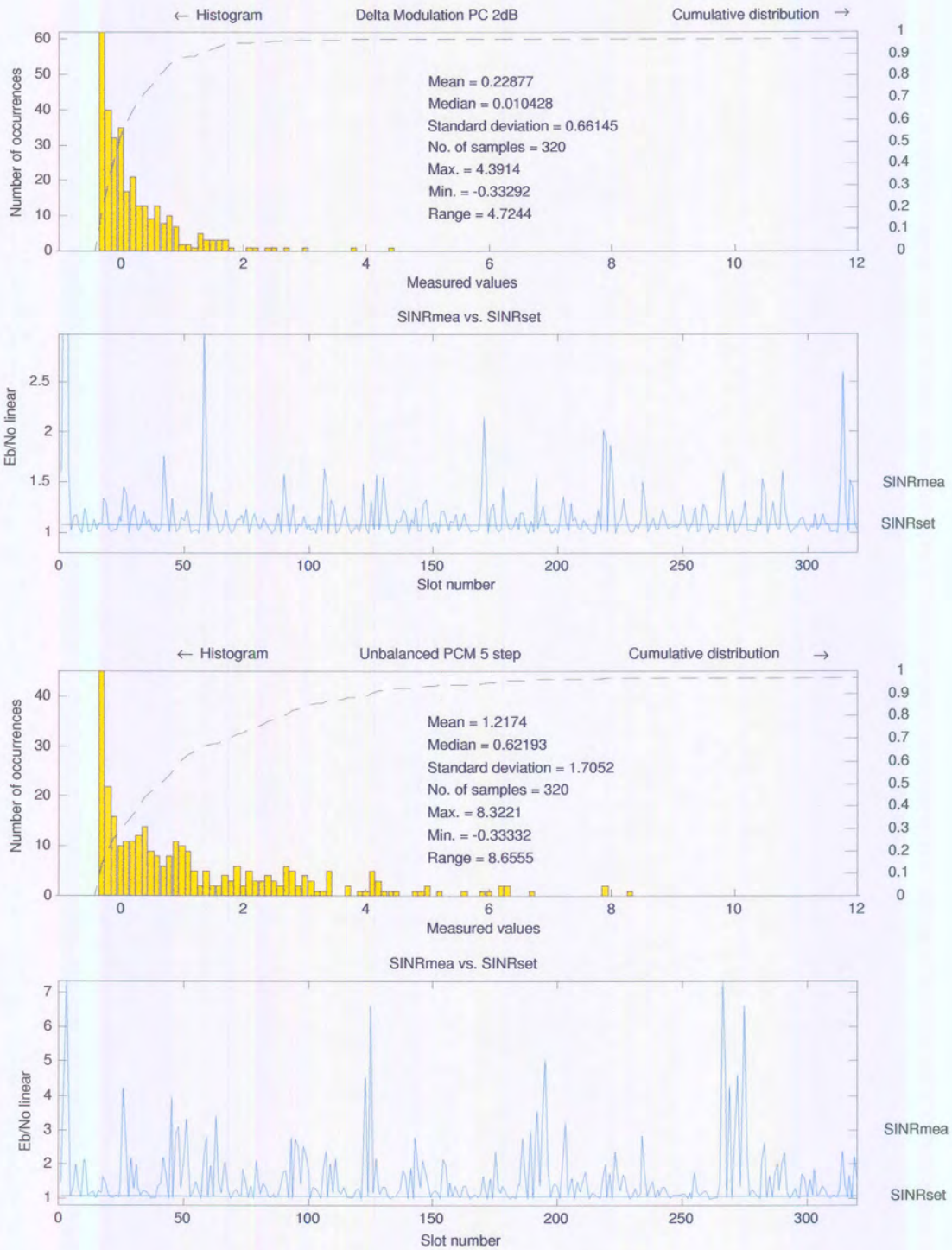

FIGURE 5.14: SINR outage probability simulation results and error-signal pdf for different FPC algorithms. The top figure shows the pdf of DM2 FPC with same settings as BER performance simulation. The bottom figure shows the pdf of unPC6 FPC.

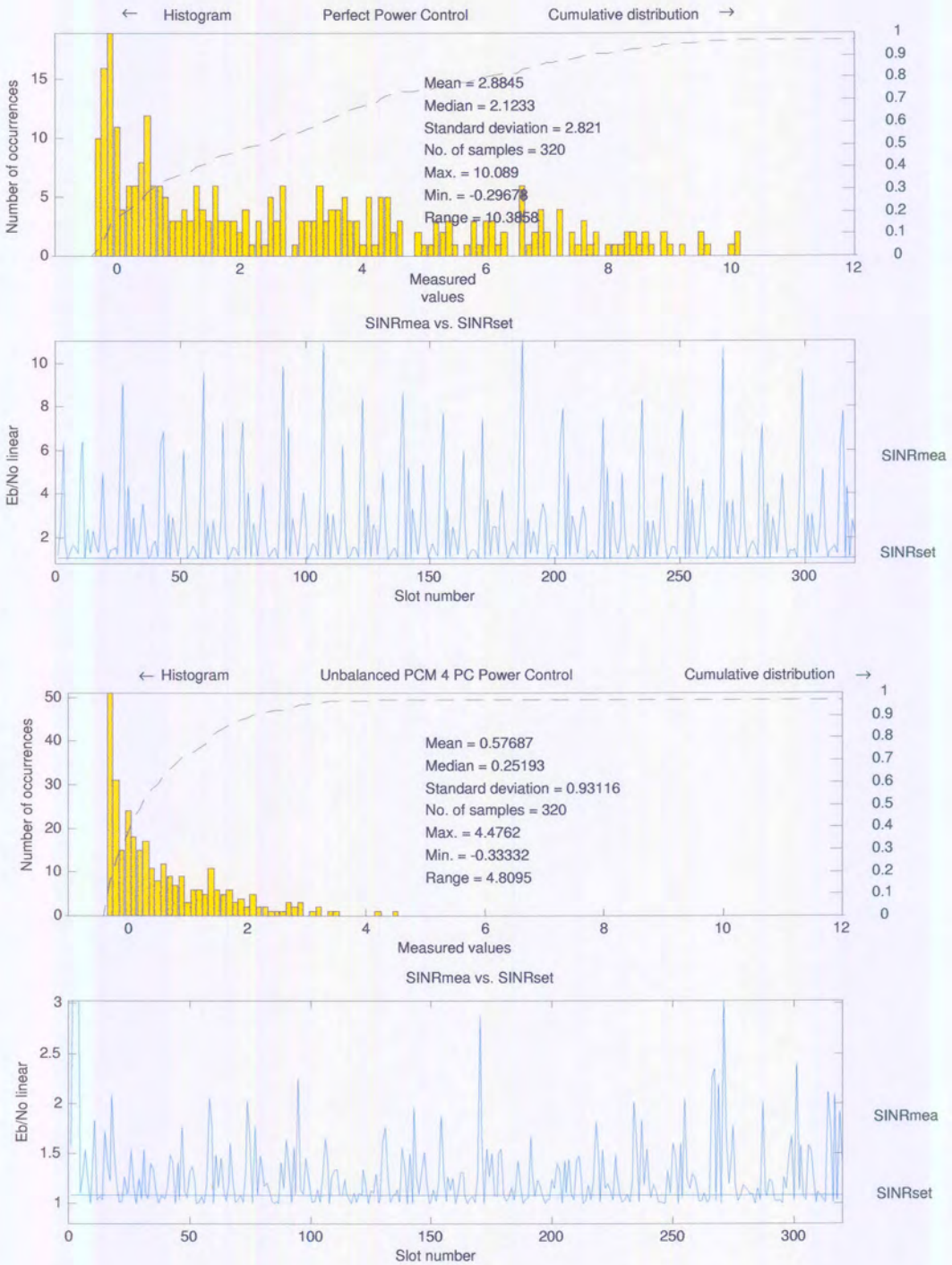

FIGURE 5.15: SINR outage probability simulation results and error-signal pdf for different FPC algorithms. The top figure shows the pdf of perfect FPC with same settings as BER performance simulation. The bottom figure shows the pdf of unPC4 FPC.

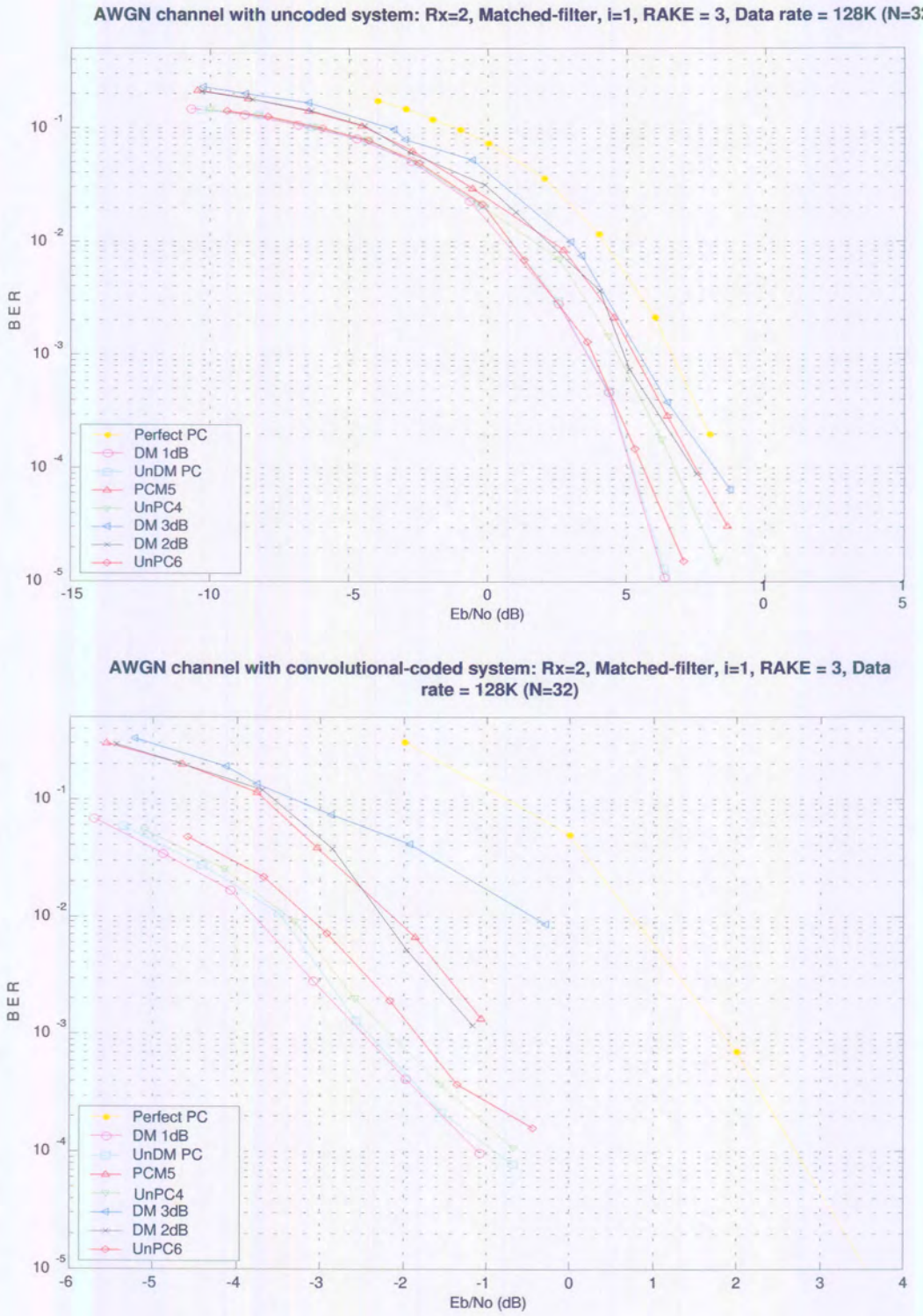

FIGURE 5.16: Different FPC Algorithms vs. measured SINR in an AWGN channel. The top figure shows the results without a coding scheme; the bottom figure shows the results with a convolutional coding scheme.

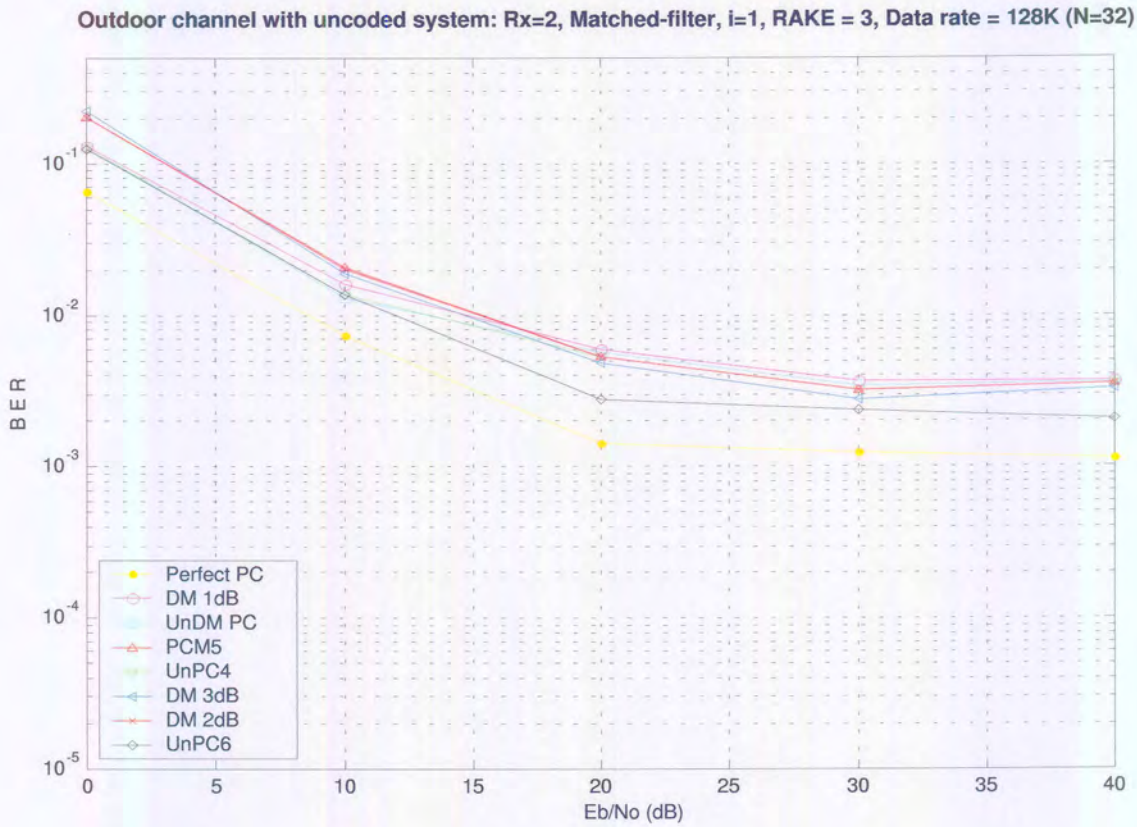

FIGURE 5.17: Influence of multipath components. BER performance curves of different FPC algorithms in an uncoded W-CDMA system with an outdoor channel, Rx=2, i=1, RAKE fingers=3, N=32 and matched-filter detector.

5.3.1.5 BER Performance in an Outdoor Channel

Thus far, it has been assumed that three multipath components are received by the base station. We now consider the introduction of additional multipath components in the time-dispersion channel model and evaluate the influence of power profile on system performance.

Figure 5.17 shows the BER performance of the system with the eight FPC algorithms in outdoor channels. The results show that the BER performance fails to deliver acceptable QoS to subscribers. This is primarily due to the fact that when the number of multipath components exceeds the number of received antennae and RAKE fingers, other multipath components become a source of interference to the desired signals, and noise power level increases. Consequently, received signals fluctuate more rapidly and stochastically. This can be improved by incorporating antenna space-diversity and coding schemes in the simulation to combat inter-symbol interference and MAI. Sections 5.3.3 and 5.3.4 investigate and

compare the influence of coding schemes and diversity algorithms in an outdoor channel.

5.3.1.6 SINR Outage Probability Performance in an Outdoor Channel

A summary of mean variation, variance and ranges of different FPC algorithms is shown in Figure 5.18. The balanced FPC algorithms still yield better power efficiency and the balanced DM algorithms also yield better tracking ability. However, there is no significant improvement in the BER performance curve. The effect of different multipath components on BER performance curve is that FPC algorithms trigger only the working point of the systems, and the BER is mainly determined by the coding, interleaving and receiver structure, and FPC algorithms attempt to narrow the received SINR levels at the base station. Thus, the BER performance is completely characterized by the pdf of the error signal, and more specifically its mean and variance, and its absolute effect on the overall system performance is a function of the underlying receiver structure (i.e. coding, antenna space diversity and interference cancellation algorithms used).

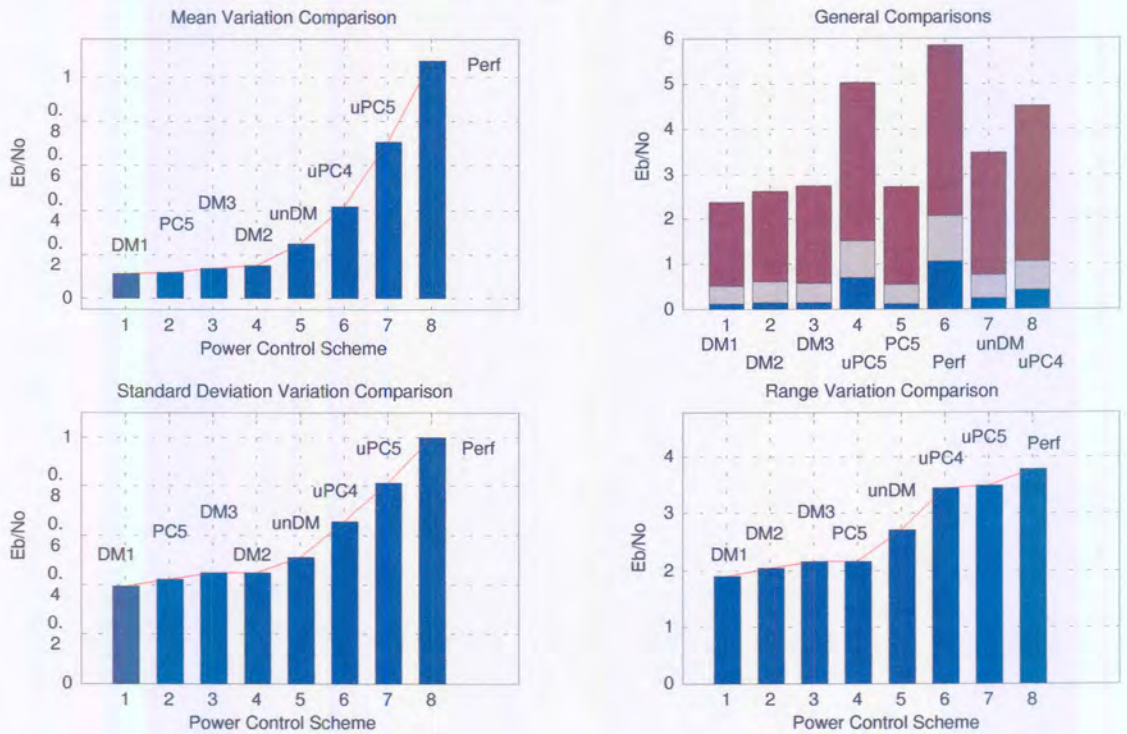

FIGURE 5.18: Mean variation, standard deviation and range comparisons for different FPC pdf algorithms with an outdoor channel, Rx=2, i=1, RAKE fingers=3, N=32 and matched-filtered W-CDMA system.

A perfect FPC algorithm would mean that the receiver structure always operates at the same working point. In reality, power cannot be perfectly controlled due to overshoot, rising time and loop delay. Also, the capacity of a W-CDMA system would be maximized if FPC algorithms were employed and supplementary to other receiver structures.

5.3.1.7 Conclusions of The Influence Of Multipath Components

Figure 5.19 compares the BER performance for different FPC algorithms in three channel conditions.

Unbalanced FPC algorithms do not improve BER performance in AWGN channels significantly because the channel model does not take multipath components and Doppler spread into account. When a frequency-selective, Rayleigh, fast-fading channel is introduced in the channel model, there is a significant improvement in BER performance compared to balanced FPCs. This is primarily due to the fact that the power signals fade more quickly than they rise in a typical Rayleigh distributed channel. Also, unbalanced FPC algorithms outperform balanced FPC algorithms by decreasing the burst-error length. It is also shown that the assumption of Gaussian approximation of FPC error distribution is not valid in frequency-selective fading channels, as seen from SINR outage probability test results.

It is important to note that the BER is mainly determined by the coding, interleaving and receiver structure, and FPC algorithms attempt to narrow the received SINR levels at base station as much as possible. Thus, the performance is completely characterized by the pdf of the error signal, and more specifically its mean and variance, and its absolute effect on the overall system performance is a function of the underlying receiver structure (i.e. coding, antenna-space diversity and interference cancellation algorithms used).

The SINR outage probability simulation results show that balanced FPCs yield the best power efficiency, and balanced and unbalanced DMs yield the best robustness in different channel conditions.

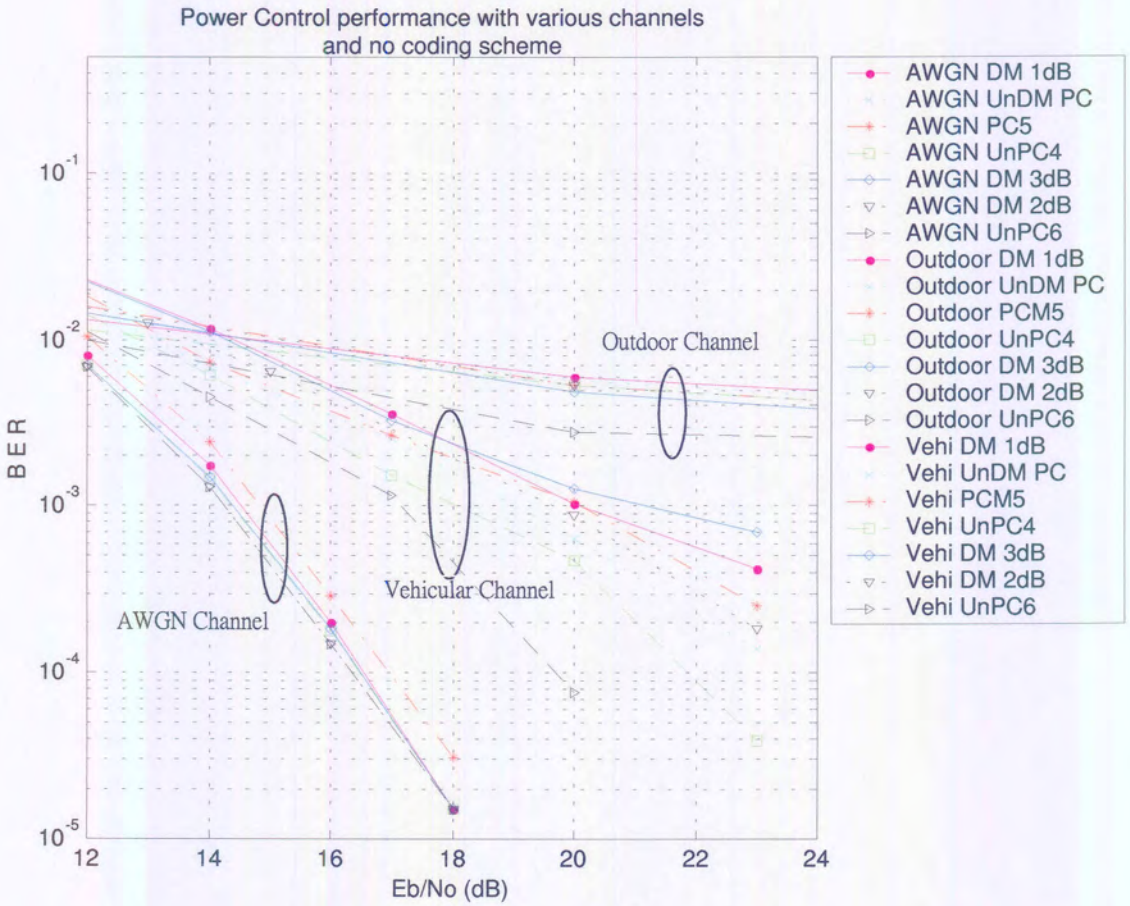

FIGURE 5.19: Comparison of performance for different FPC algorithms in three channel conditions.

5.3.2 Influence of Doppler Spread

Whereas previous sections have investigated the influence of time-dispersion effects on FPC algorithms, the influence of Doppler spread is the theme of this section. Doppler spread is the relative motion between the base station and the handset, which results in random frequency-demodulation of the received signals. This leads to signal distortion. To facilitate these effects in a simulation environment, a fast-fading channel environment in which the coherent time of the channel is less than the symbol period of the transmitter signals is programmed.

Three relative speeds are considered in this simulation, namely v = 10km/h, 120km/h and 200km/h, respectively, in an outdoor channel environment with two-receiver antennae and matched-filter W-CDMA receiver. The BER performance curves of different mobile speeds are shown in Figure 5.3.2. Comparing these BER performance curves for different speeds, it

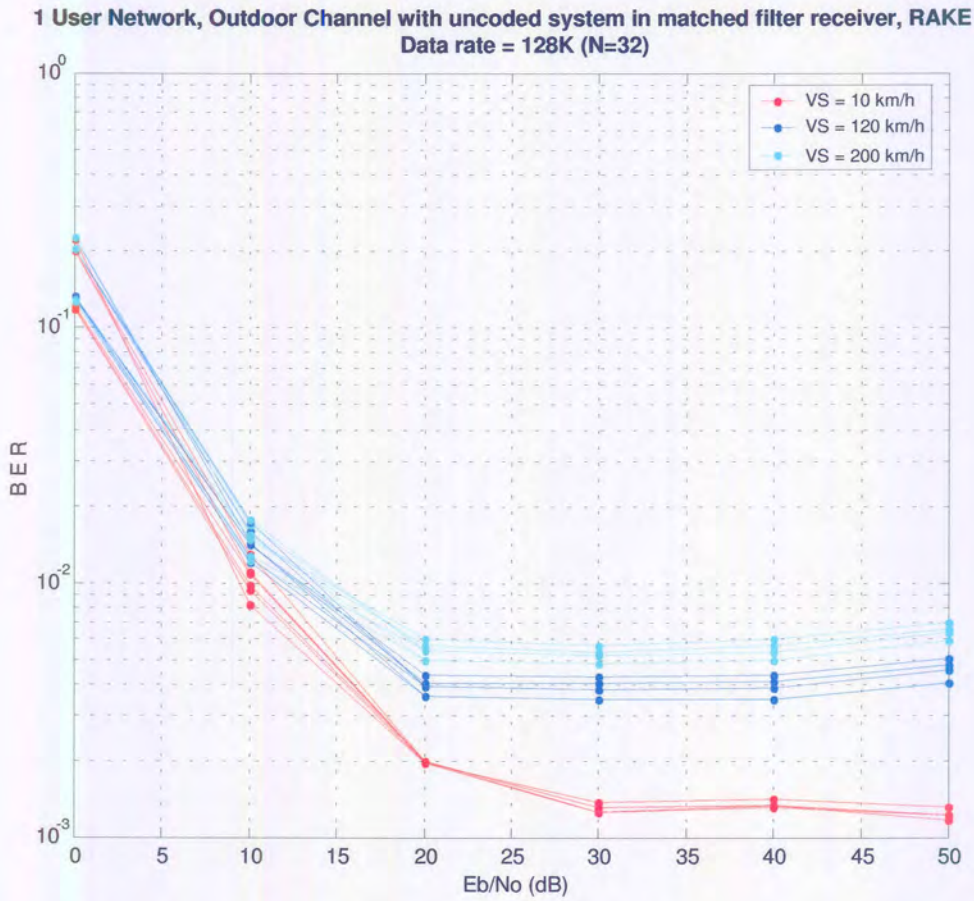

FIGURE 5.20: Influence of Doppler spread. BER performance curves of different FPC algorithms in a uncoded, three-vehicle speed, W-CDMA system with an outdoor channel, Rx=2, i=1, RAKE fingers=3, N=32 and matched-filter detector.

is clear that an increase in the speed of a mobile further degrades the BER performance due to the rapid variation of the transmitted signals, by about 10 dB if mobile speed is 120 km/h and by about 20 dB if mobile speed is 200 km/h.

5.3.3 Influence of Coding Schemes

Using the power-sensitive model outlined above, the spreading gain for each user is equal to 32 and coding gain is three. Simulation is carried out in AWGN, outdoor and vehicular channel conditions with no coding, convolutional and Turbo codes. This section investigates the influence of coding schemes with unbalanced FPC algorithms. Although it has been shown that coding schemes may increase power-efficiency and W-CDMA system capacity [Figures 5.21 to 5.22], this section will focus on how FPC algorithms further improve system capacity in a coded system.

Table 5.4: BER performance of different FPC algorithms in a convolutional-coded W-CDMA system with an AWGN channel at 5 dB.

$E_b/I_0 = 5$ dB	BER
unDM	0.000018
unPCM6	0.000060
unPCM4	0.000086
DM1	0.000098
DM2	0.001181
PCM5	0.001366
DM3	0.008681

Table 5.5: BER performance of different FPC algorithms in a Turbo-coded W-CDMA system with an AWGN channel at 5 dB.

$E_b/I_0 = 5$ dB	BER
unPCM6	0.000024
unPCM4	0.000042
unDM	0.000052
DM1	0.000090
DM2	0.000394
PCM5	0.000810
DM3	0.009653

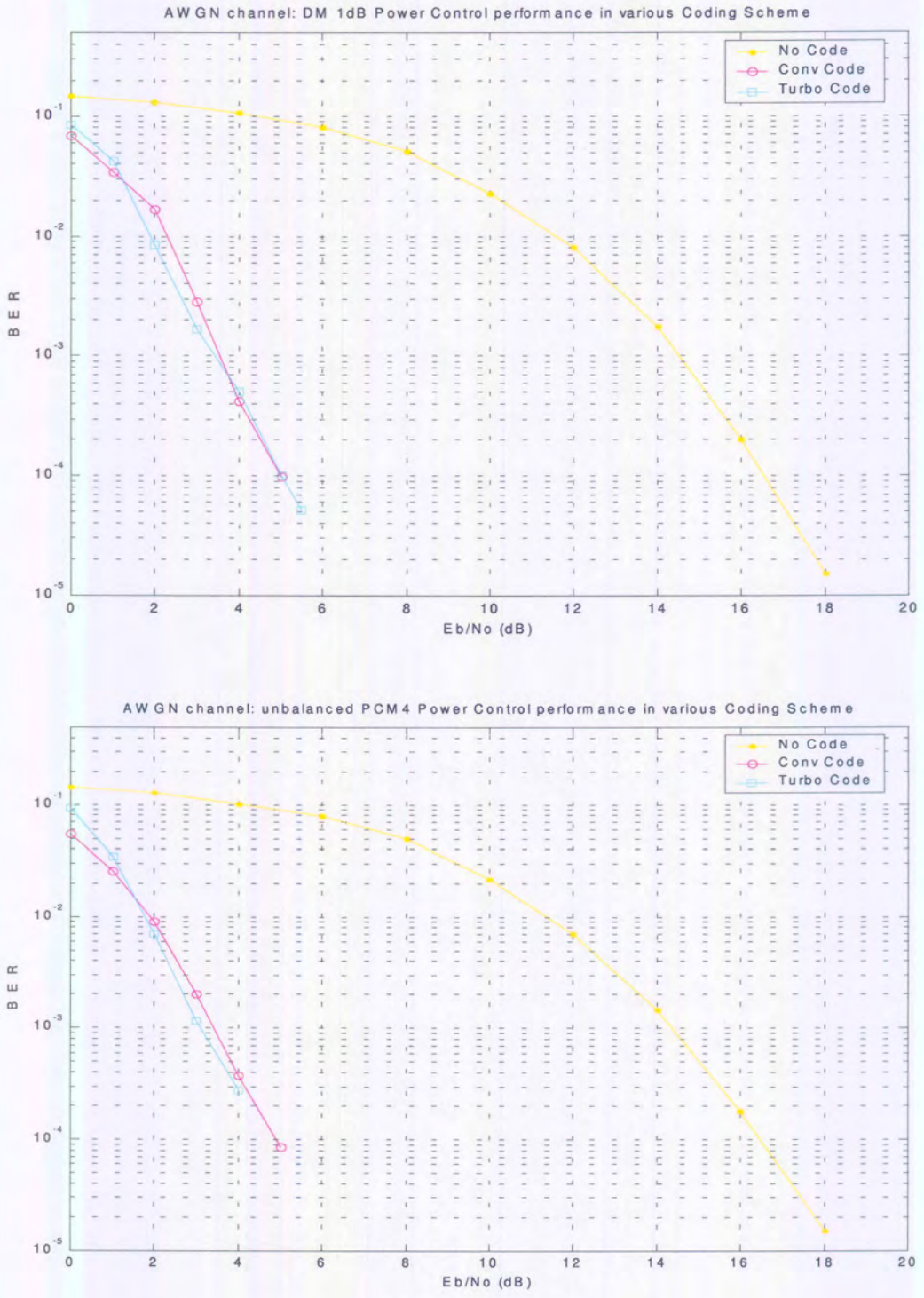

FIGURE 5.21: BER performance for FPC algorithms in an AWGN channel with uncoded, convolutional and Turbo coding. The top figure shows the improvement of BER performance on DM1 FPC with different coding schemes. The bottom figure shows the improvement of BER performance of unPC4 FPC with different coding schemes.

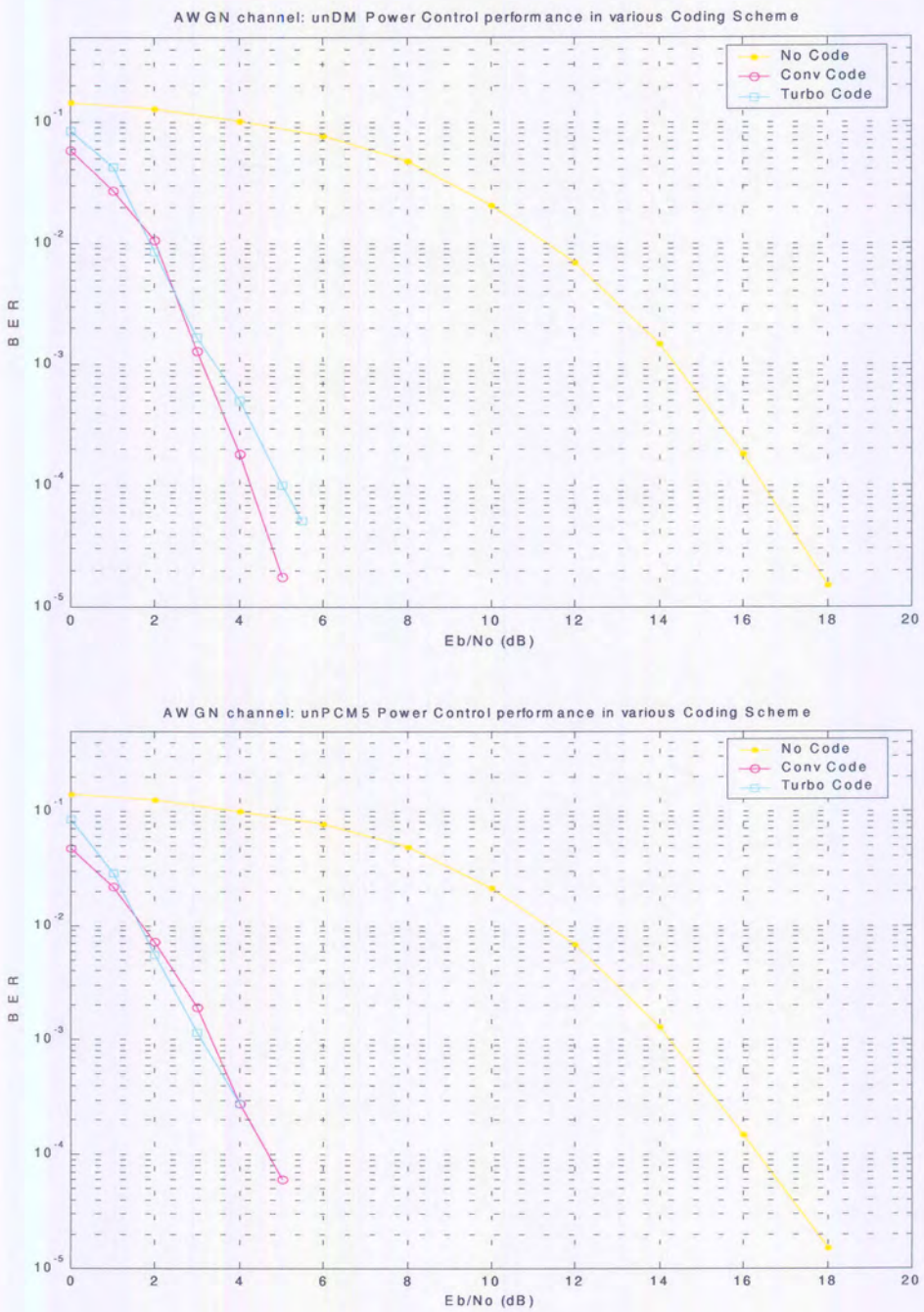

FIGURE 5.22: BER performance for FPC algorithms in an AWGN channel with uncoded, convolutional and Turbo coding. The topional and Turbo coding. The top BER performance on unDM FPC with different coding schemes. The bottom figure shows the improvement of BER performance of unPC6 FPC with different coding schemes.

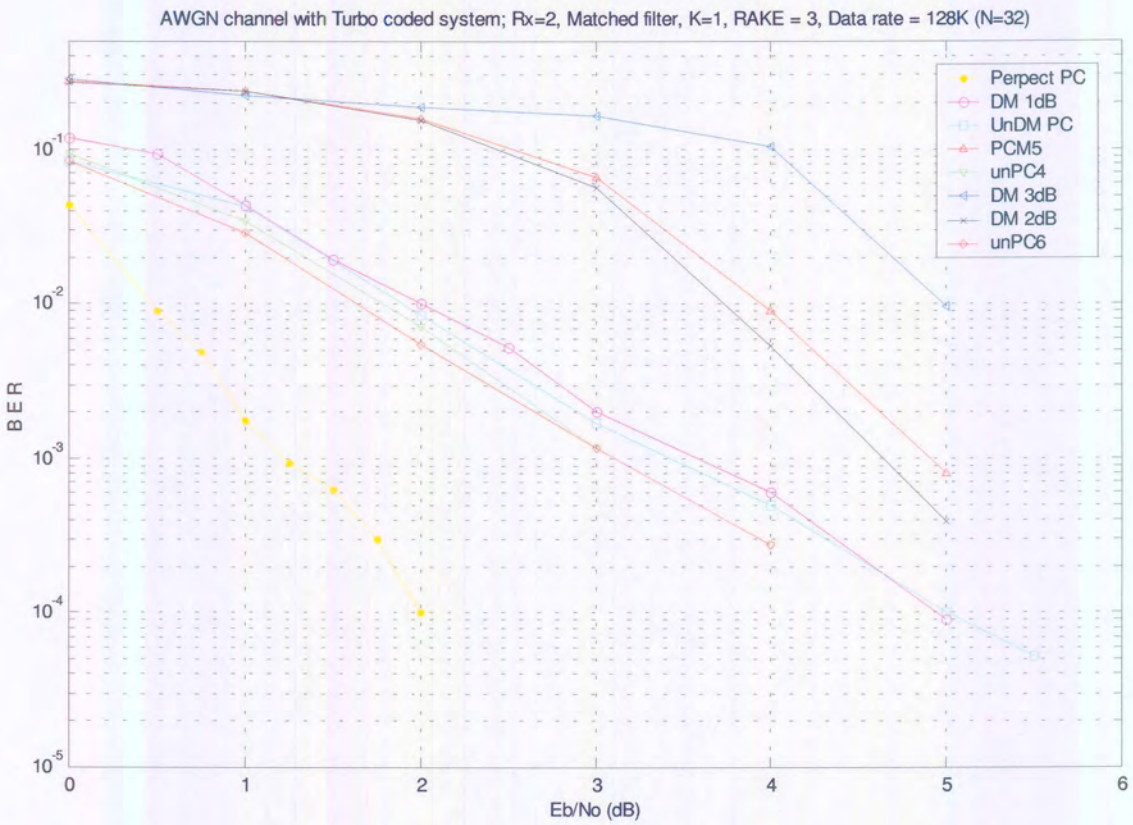

FIGURE 5.23: Influence of coding schemes. BER performance curves of different FPC algorithms in a Turbo-coded W-CDMA system with an AWGN channel, Rx=2, i=1, RAKE fingers=3, N=32 and matched-filter detector.

5.3.3.1 BER Performance for an AWGN Channel

The BER performance of the system in an AWGN channel is shown in Figures 5.21 and 5.22. Significant improvements are observed when coding schemes are incorporated in the simulation package. Generally, a 10 dB coding gain is observed from the simulation results. This is primarily due to the fact that the channel coding protects digital data from errors by selectively introducing redundancies in the transmitted data.

Figure 5.23 shows the BER performance of the eight FPC algorithms in an AWGN channel with Turbo codes. The results show that, generally, the unbalanced DM FPC technique yields a 11 dB coding gain at BER = 10^{-4} when we compare the BER performance curves of an uncoded AWGN channel to that of a Turbo-coded AWGN channel. Comparing the BER performance of unbalanced and balanced PCM FPC algorithms, unbalanced PCM algorithms outperform balanced ones significantly; since the unbalanced FPC algorithms improve and compensate for the burst errors more effectively, it is less probable that errors will occur in a burst sequence which coding schemes cannot detect and correct and the improvement rate increases as the transmitted SINR values increase.

Comparing the BER performance of the eight FPC algorithms at 5 dB, we see that there is a significant improvement with unbalanced FPC algorithms in a channel-coded system [Tables 5.4 and 5.5]. The BER performance of different FPC algorithms yields similar results in both channel-coded systems, but the performance of the Turbo-code system yields better results than the convolutional code system.

From these tables, it can be seen that the unbalanced DM FPC technique yields better power efficiency than the balanced DM FPC technique, but with an improvement of approximately 1 dB only. It is important to note that since the BER performance of the cellular system can also be influenced by spreading gain factors also, it is predicted that the system capacity will increase if spreading gain factors are increased.

5.3.3.2 BER Performance for Outdoor and Vehicular Channels

Thus far, we have shown that convolutional and Turbo codes introduced in the receiver system in an AWGN channel result in a significant improvement on the BER performance of different FPC algorithms. Let us now apply the same system in an outdoor channel condition where previously FPC algorithms failed to bring W-CDMA BER performance to within an acceptable BER.

The inevitable impairment of wireless channel conditions is the result of the numerous multipath components and Doppler spread effects on the transmitted signal. When the number of multipath components increases, the received SINR value of received signals decreases, and the BER performance of the different FPC algorithms also degrades. Whereas the pervious section has shown that coding schemes improve the BER performance in an AWGN channel condition by 11dB, this section will focus on how coding algorithms further improve BER performance in an outdoor channel condition by comparing Figure 5.17 to Figure 5.24.

Significant improvements are observed when coding schemes are incorporated in the outdoor channel condition. Generally, incorporating Turbo coding schemes result in greater QoS since W-CDMA systems provide a more robust service to the subscribers in unpredictable wireless environments.

Figure 5.24 shows the BER performance of the eight FPC algorithms in an outdoor channel with a Turbo-coded system. The results show that, generally, the unbalanced DM FPC technique yields acceptable BER performance at BER = 10^{-4} when we compare the BER performance curves of an uncoded outdoor channel to that of a Turbo-coded outdoor channel. Comparing the BER performance of unbalanced and balanced PCM FPC algorithms, unbalanced PCM algorithms outperform balanced ones significantly: since the unbalanced FPC algorithms improve and compensate for the burst errors more effectively, it is less probable that errors will occur in a burst sequence which coding schemes cannot detect and correct and the improvement rate increases as the transmitted SINR values increase.

Comparing the BER performance of the eight FPC algorithms at 3.5 dB [Tables 5.6], we see that there is a significant improvement with unbalanced FPC algorithms in a channel-coded system. And that the unbalanced DM FPC technique yields better power efficiency than the balanced DM FPC technique.

Figure 5.24 shows the performance of different FPC algorithms in an outdoor channel model with convolutional schemes. Although a convolutional-coded system yields better BER performance than a Turbo-coded system, both coded systems improve the BER

Table 5.6: BER performance of different FPC algorithms in a W-CDMA system with an outdoor channel and Turbo code at 3.5 dB.

$E_b/I_0 = 3.5$ dB	BER
unPCM6	0.000016
unPCM4	0.000046
UnDM	0.000231
DM1	0.000787
PCM5	0.013935
DM2	0.016019
DM3	0.031481

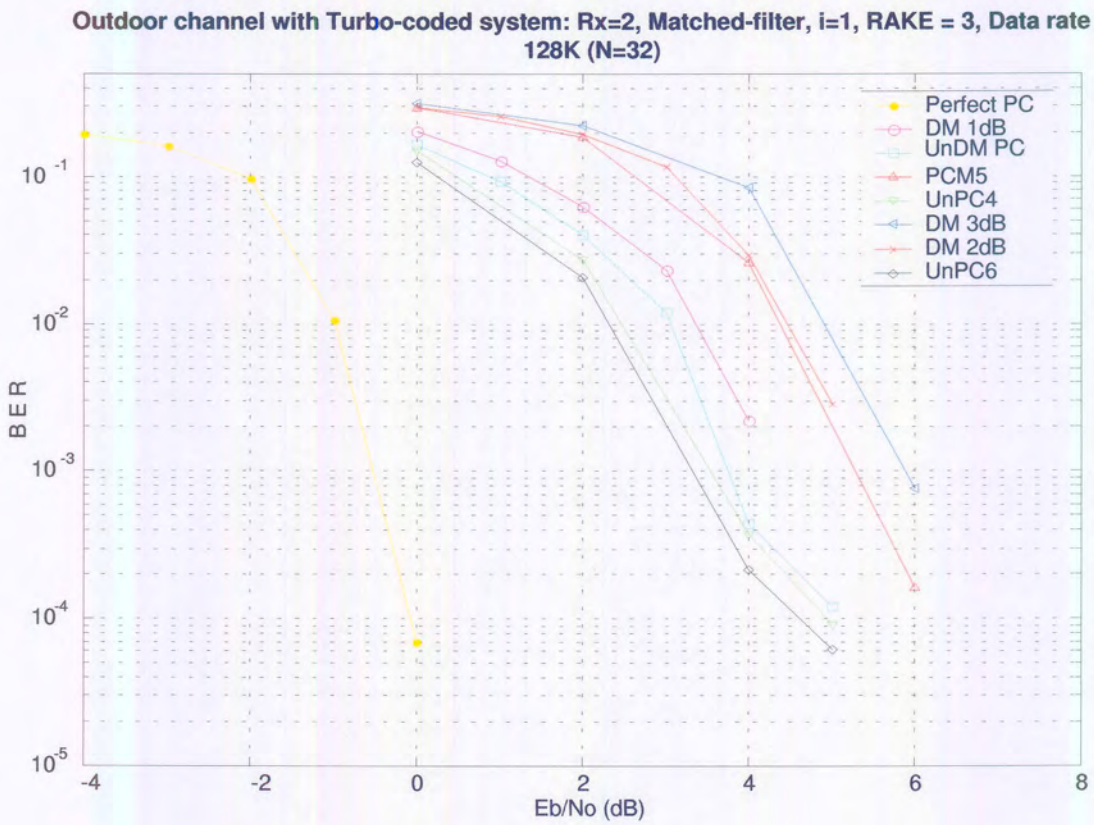

FIGURE 5.24: Influence of coding schemes. BER performance curves of different FPC algorithms in a Turbo-coded, W-CDMA system with an outdoor channel, Rx=2, i=1, RAKE fingers=3, N=32 and matched-filter detector.

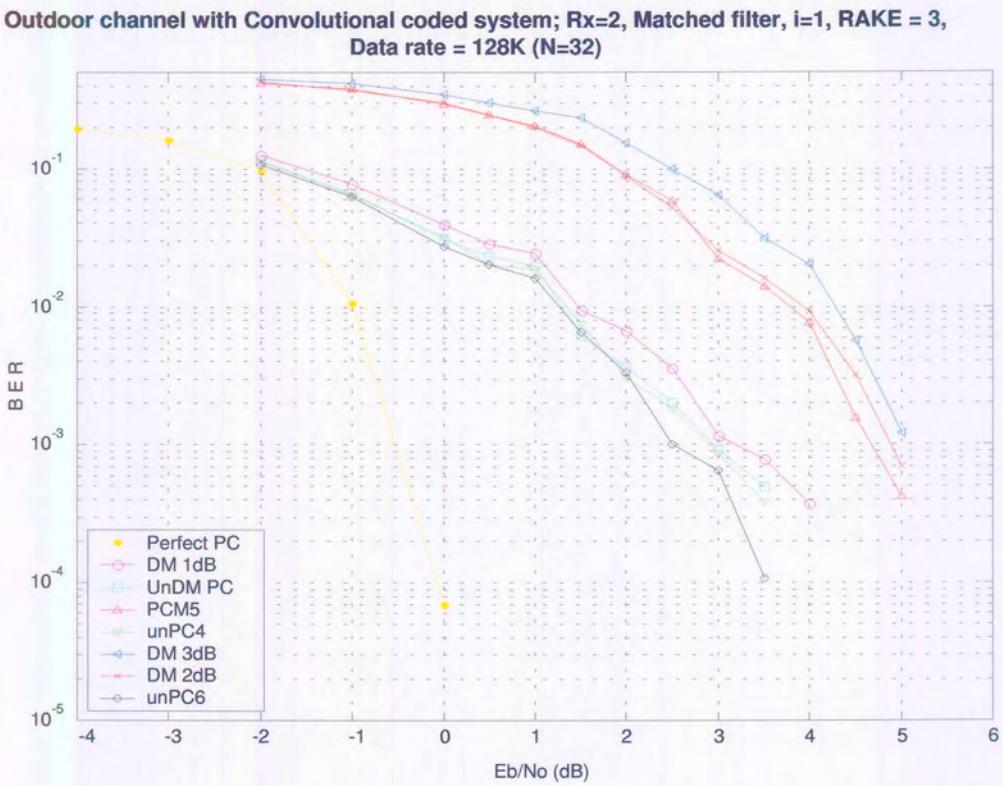

FIGURE 5.25: Influence of coding schemes. BER performance curves of different FPC algorithms in a convolutional-coded W-CDMA system with the outdoor channel, Rx=2, i=1, RAKE fingers=3, N=32 and matched-filter detector.

performance significantly compared to uncoded, outdoor channel systems.

Thus, a significant performance improvement can be achieved if FPC and coding schemes are both incorporated in the W-CDMA systems. It is also expected that FPC algorithms that correspond with other physical receiver structures, such as space-time diversity, multi-user detection and RRM, can further improve the system performance. This section investigates and compares the effects of coding schemes and shows that performance can be improved by combining coding schemes with FPC algorithms in a frequency-selective, Rayleigh, fast-fading environment. This phenomenon is also observed in a vehicular channel [Figure 5.26].

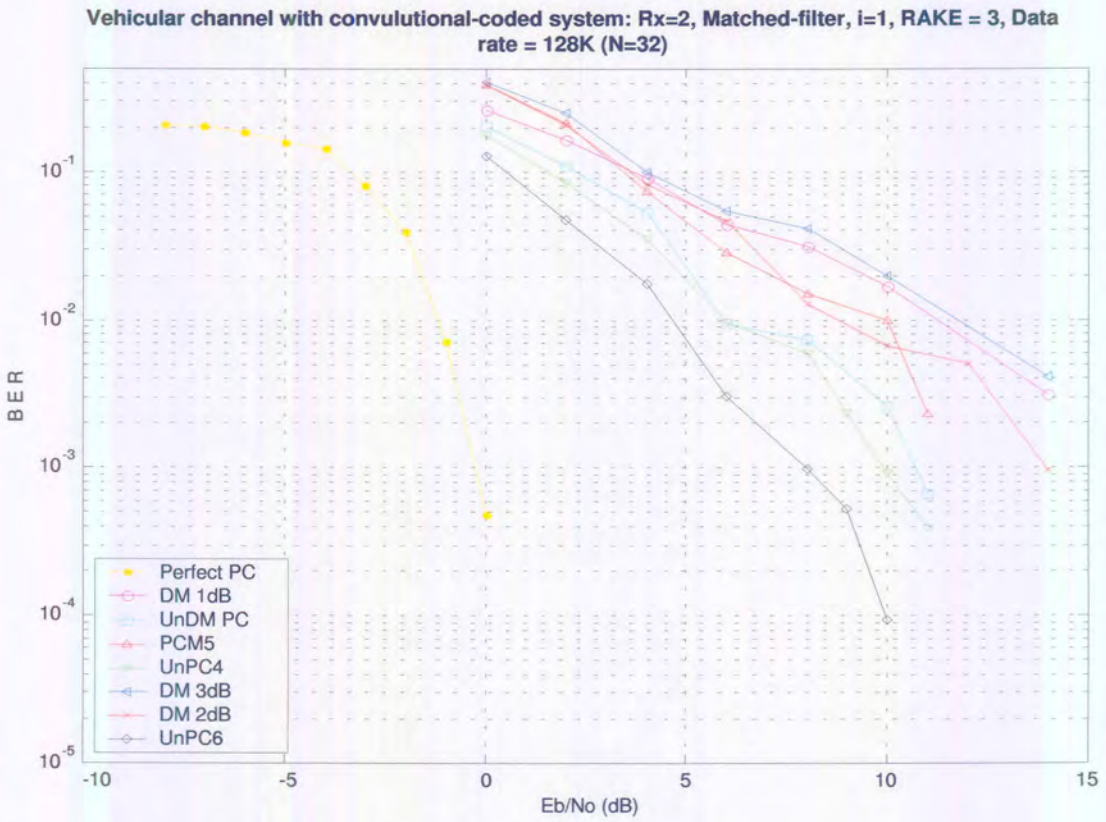

FIGURE 5.26: Influence of coding schemes. BER performance curves of different FPC algorithms in a convolutional-coded W-CDMA system with a vehicular channel, Rx=2, i=1, RAKE fingers=3, N=32 and matched-filter detector.

5.3.3.3 Conclusions Of The Influence Of Coding Schemes

The introduction of convolutional and Turbo-code schemes in AWGN, W-CDMA cellular systems improves power efficiency, generally, by about 10 dB with the different FPC

algorithms. When a frequency-selective, Rayleigh fast-fading channel is introduced in the channel model, there is a significant improvement in BER performance with unbalanced DM and PCM algorithms, especially at high SINR levels. This is primarily due to the fact that the unbalanced FPC algorithms improve and compensate for the burst error of the Rayleigh fading channels more effectively since it is less probable that errors will occur in a burst sequence which coding schemes cannot detect and correct.

Unlike wireline systems where QoS can be predicted and controlled, cellular systems tend to be stochastic and unpredictable. Thus, the emphasis of most wireline systems research is on the layer 2 or higher protocols, such as routing, admission-control, congestion-control and collision-control etc. The challenge of W-CDMA technology is to control wireless communication systems such that QoS to subscribers can be predicted and controlled. Thus, transmitted power and power distribution must be carefully planned. It is important to note that the BER is determined mainly by the coding, interleaving and receiver structure, and FPC algorithms not only attempt to narrow the received SINR levels at the base station, but should also act as a supplementary mechanism for other receiver structures to deliver acceptable QoS levels.

A mediation device is required to provide a physical-layer QoS monitoring facility and network-layer RRM decision-making facility while FPC algorithms do not improve the system performance significantly, they do provide online link QoS monitoring, online resource and interference management, and QoS assurance for adaptation to changes induced by mobility, channel impairment and traffic demand.

5.3.4 Influence Of Number Of Receiver Antennae

In the previous section it was shown that a decrease in the number of multipath components and the mobile speed significantly increase the BER performance of the cellular systems. Because of the large bandwidth of CDMA systems compared to TDMA/FDMA systems, CDMA systems are capable of receiving and exploiting a larger number of multipath components using a RAKE receiver and antenna space-diversity. Therefore, one approach to minimizing the effects of a large number of multipath components and Doppler spread is to increase the number of receiver antennae.

5.3.4.1 BER Performance for Different Number of Receiver Antennae

Thus far, the number of receiver antennae was set at two, and each antenna was assigned three RAKE fingers. Decreasing the number of antennae to one leads to a significant decrease in

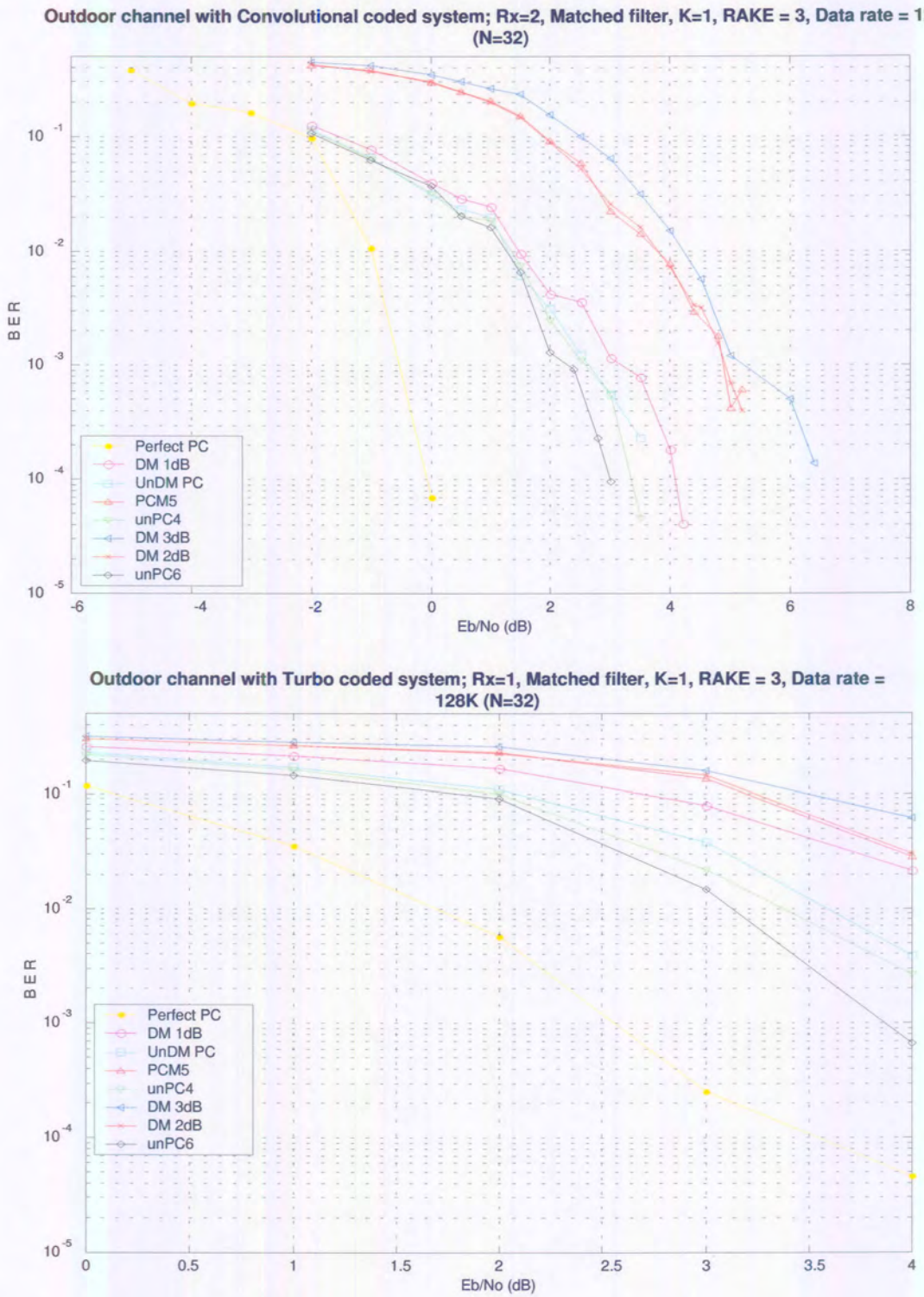

FIGURE 5.27: Different FPC algorithms vs. BER performance. The top figure shows the results with two receiver antennae. The bottom figure shows the results with one receiver-antenna in a convolutional-coded system with a matched-filter detector in an outdoor channel.

system BER performance as shown in Figure 5.27. This decrease in system performance is equally true for all FPC algorithms. Comparing the increase in system performance that can be achieved by increasing the number of branches in the RAKE as well as receiver antennae, it is clear that the increase of number of antennae will lead to a greater increase in system capacity. The same applies to antennae space-time processing techniques.

5.3.5 Influence Of Number Of Users

The power-sensitive model shown in Chapter 2 describes the significant effect of MAI on system capacity, especially in multi-media, multi-user W-CDMA systems. The following derivations show that the system capacity is largely dependent on intra-cell, inter-cell and MAI interference.

For a single-user, W-CDMA system, the outage probability can be denoted by:

$$P_r\left[\left(\frac{E_b}{I_o}\right)_i \geq \gamma_i\right] = P_r\left[\frac{h_{ik}P_i}{\delta^2 W}\frac{W}{R_i} \geq \gamma_i\right] \tag{5.1}$$

where i=1, j=1, and k=1. The outage probability is solely dependent on the channel impairments, processing gain, data rate and transmitted power level, However as the number of users increases, say to N, at cell k, the outage probability can be denoted by:

$$P_r\left[\left(\frac{E_b}{I_o}\right)_i \geq \gamma_i\right] = P_r\left[\frac{h_{ik}P_i}{\sum_{j\neq i}^{N} h_{jk}P_j + \delta^2 W}\frac{W}{R_i} \geq \gamma_i\right] \tag{5.2}$$

where $i = 1, ..., N$, $j = 1, ..., N$, N is the number of active users in cell k, $k = 1, ..., K$,K is the number of cells of the W-CDMA systems, $\gamma_i = \gamma_1, ..., \gamma_N$ and $R_i = R_1, ..., R_N$. Now, the outage probability is largely dependent on intra-cell, inter-cell and MAI interference. This section will focus on the influence of number of users in different channel conditions on the system capacity.

5.3.5.1 BER Performance In An AWGN Channel

The BER performance of a one-user, Turbo-coded W-CDMA system is shown in the top figure of Figure 5.28. The bottom figure of Figure 5.28 shows the BER performance of a two-user, Turbo-coded W-CMA system. Figure 5.29 depicts the BER performance of a four-user system with the same settings. The eight FPC algorithms are simulated in an AWGN channel, Rx=2, RAKE finger=3 and a matched-filter detector. The results show that an increase in number of users increases the BER and as a consequence decreases the system capacity. This is equally true for all eight FPC algorithms. This is primarily due

Table 5.7: BER performance of different FPC algorithms in a one-user, Turbo-coded, W-CDMA system with an AWGN channel at 4 dB.

$E_b/I_0 = 4$ dB	BER
unPCM6	0.000248
unPCM4	0.000278
unDM	0.000500
DM1	0.000600
DM2	0.005301
PCM5	0.008958
DM3	0.103519

Table 5.8: BER performance of different FPC algorithms in a two-users, Turbo-coded, W-CDMA system with an AWGN channel at 4 dB.

$E_b/I_0 = 4$ dB	BER
unPCM6	0.000672
unPCM4	0.000834
unDM	0.001113
DM1	0.001300
DM2	0.014676
PCM5	0.017870
DM3	0.119907

to the fact that since the MAI interference increases [Equ. 5.2], more transmitted power is required to compensate for both h_{ik} and MAI effects. Therefore the noise floor increases, and because cellular handsets need to utilize their battery power in the most efficient way, the handset must regulate its transmitted power at a pre-determined level. Thus, some calls will be dropped since the base station is not competent to sustain good SINR levels to subscribers as the MAI increases.

Table 5.9: BER performance of different FPC algorithms in a four-users, Turbo-coded, W-CDMA system with an AWGN channel at 4 dB.

$E_b/I_0 = 4$ dB	BER
unPCM6	0.035914
unPCM4	0.037830
DM1	0.048426
unDM	0.050289
DM2	0.069867
PCM5	0.084815
DM3	0.177257

Unbalanced FPC algorithms improve the BER performance in a multimedia, multi-user W-CDMA environment as seen in Figure 5.28, but as the number of users increases to four [Figure 5.29] so the rate of degradation of BER performance increases more than with the balanced FPC algorithms. This is primarily due to the fact that the unbalanced FPC algorithms are designed to compensate for the Raleigh fading channel by increasing the average transmitted power level of the handset. As the number of users increases, so the excess average transmitted power level generates more MAI interference to other users. Thus, the rate of BER performance degrades faster in unbalanced FPC algorithms than balanced FPC algorithms. These effects are summarised in Tables 5.7, 5.8 and 5.9.

Figures 5.30 to 5.34 compare the BER performance of a one-user, two-user and four-user system with different FPC algorithms.

5.3.5.2 Conclusions of The Influence Of Number of Users in AWGN Channel

The overall BER performance of different FPC algorithms in AWGN channel, Turbo-coded W-CDMA system is shown in Figure 5.35. As the number of users increases, so the excess

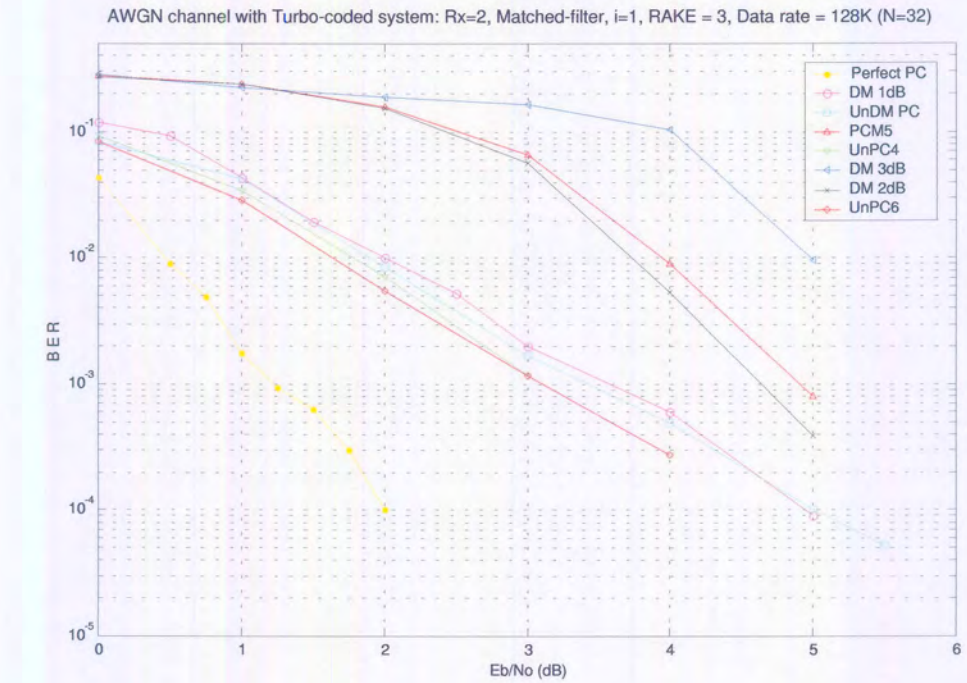

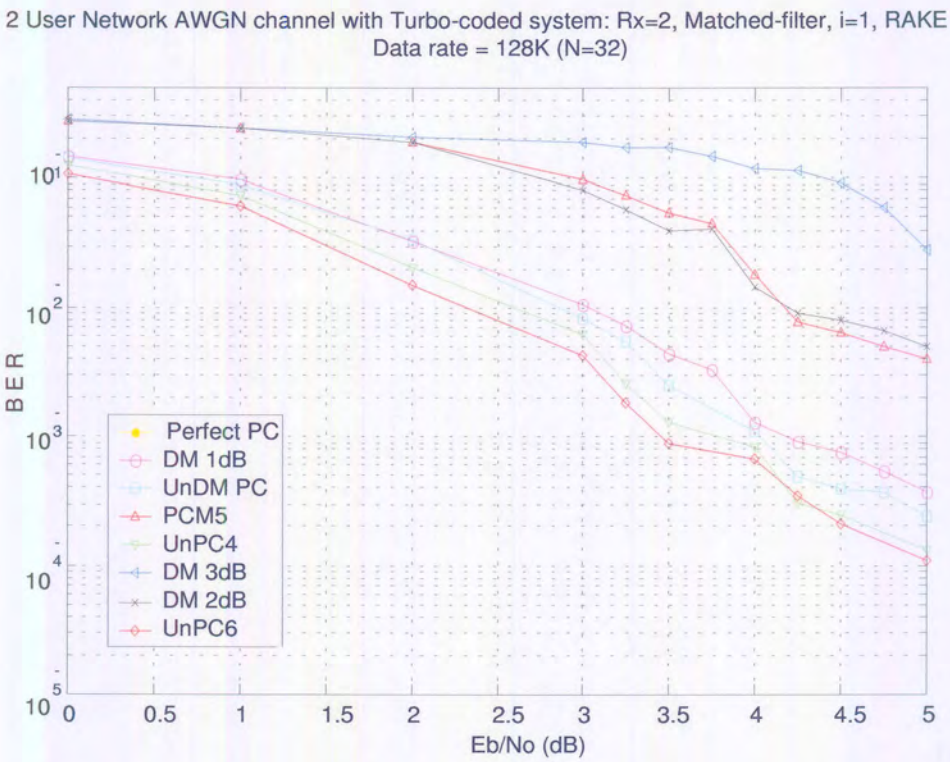

FIGURE 5.28: Influence of number of users. The top figure shows the BER performance results with a one-user, Turbo-coded W-CDMA system with an AWGN channel, Rx=2, RAKE fingers=3, N=32 and matched-filter detector. The bottom figure shows the BER performance results with a two-user, Turbo-coded W-CDMA system and same settings.

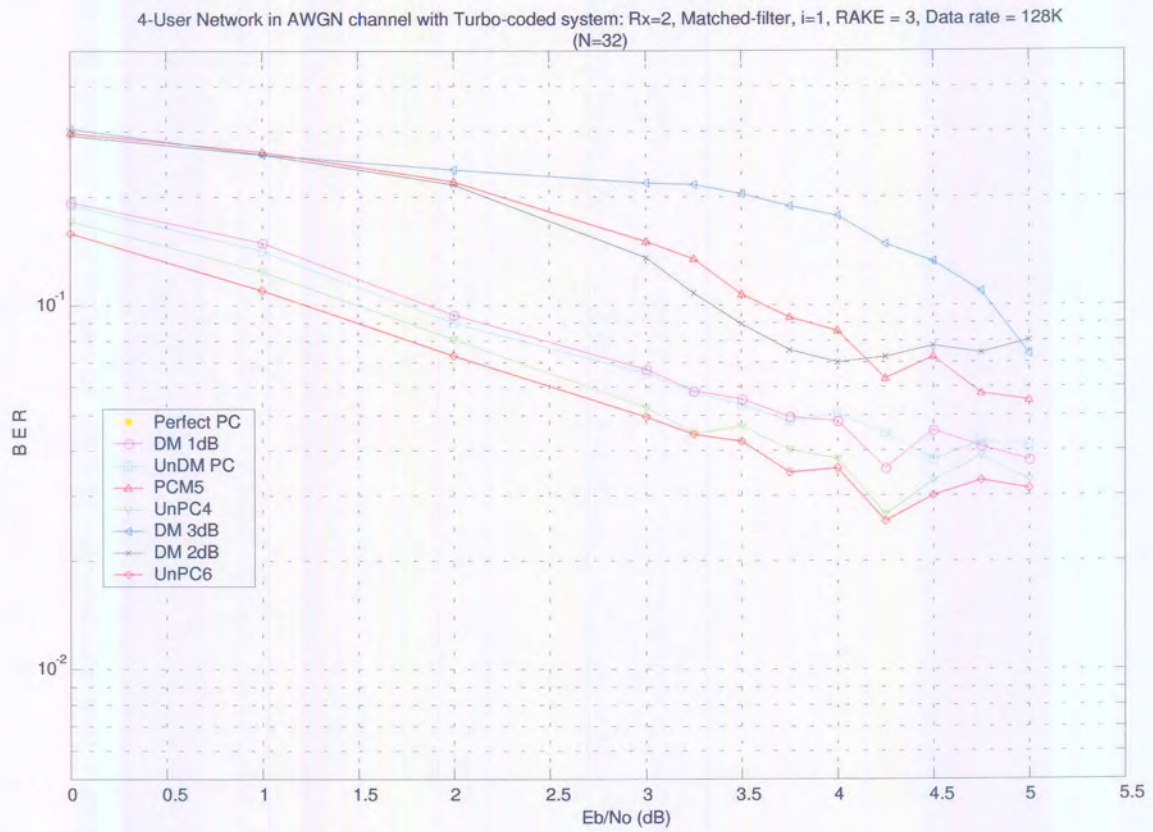

FIGURE 5.29: Influence of number of users. The top figure shows the BER performance results with a four-user, Turbo-coded W-CDMA system with an AWGN channel, Rx=2, RAKE fingers=3, N=32 and matched-filter detector.

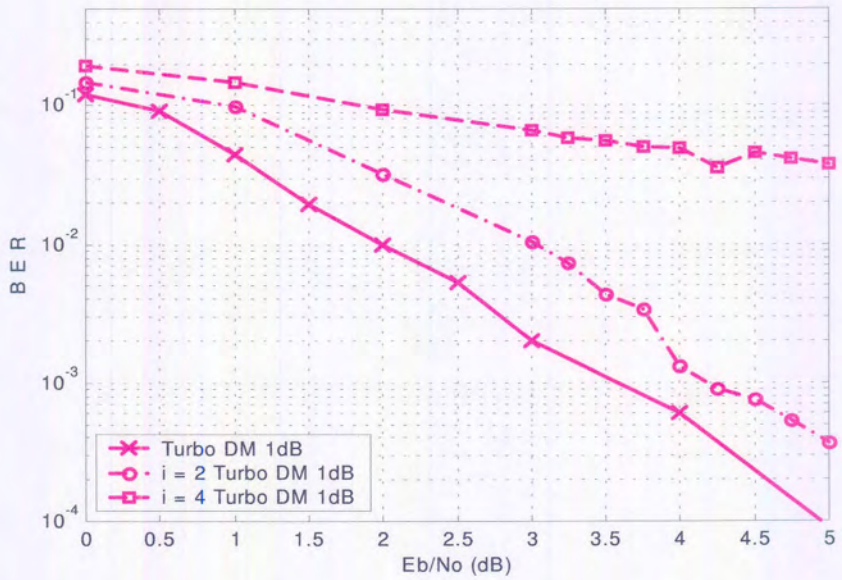

FIGURE 5.30: Influence of number of users. BER performance curve of DM1 FPC algorithm in a Turbo-coded, W-CDMA system with an AWGN channel.

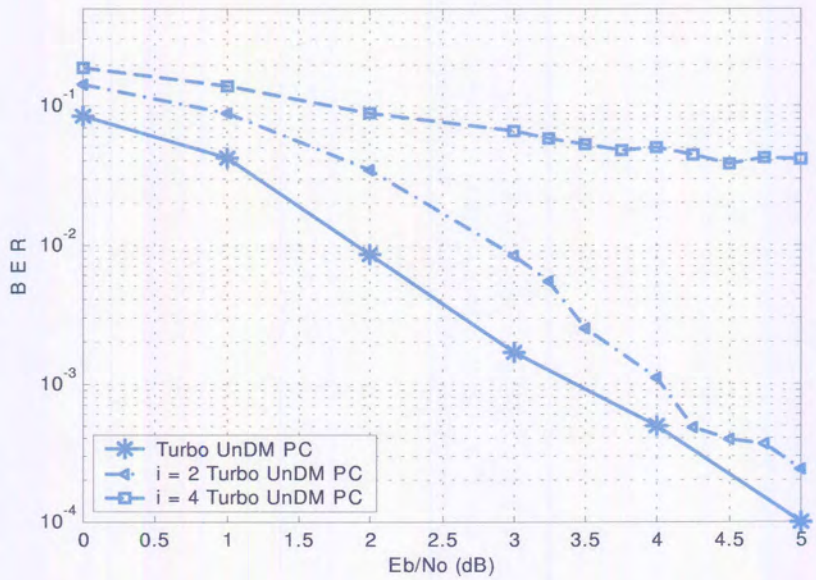

FIGURE 5.31: Influence of number of users. BER performance curve of unDM FPC algorithm in a Turbo-coded, W-CDMA system with an AWGN channel.

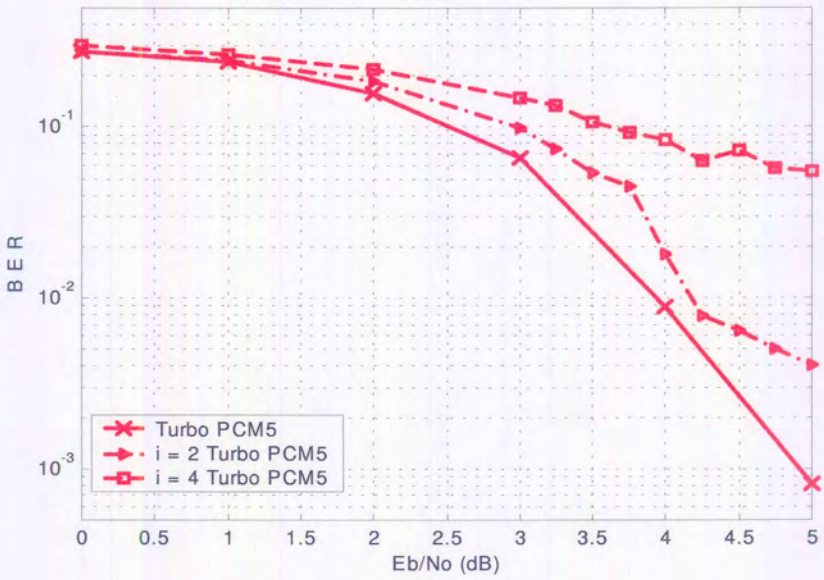

FIGURE 5.32: Influence of number of users. BER performance curve of PCM5 FPC algorithm in a Turbo-coded, W-CDMA system with an AWGN channel.

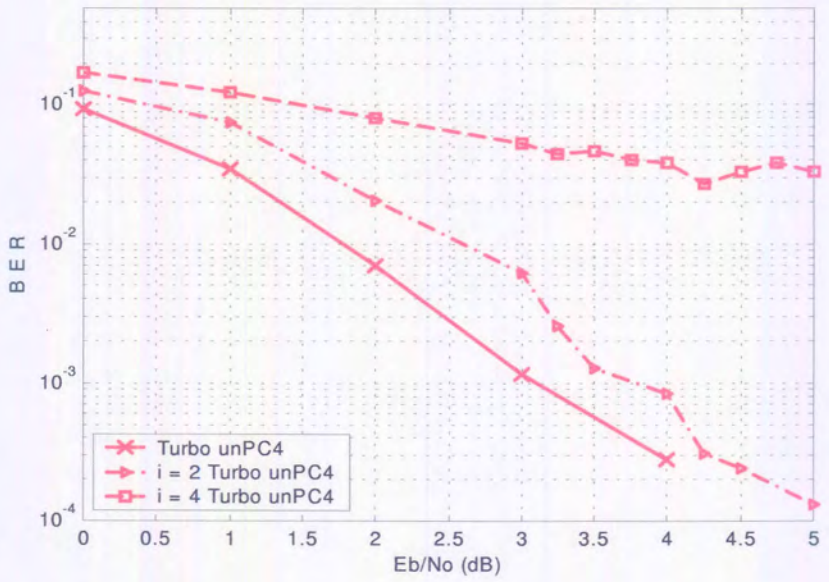

FIGURE 5.33: Influence of number of users. BER performance curve of unPC4 FPC algorithm in a Turbo-coded, W-CDMA system with an AWGN channel.

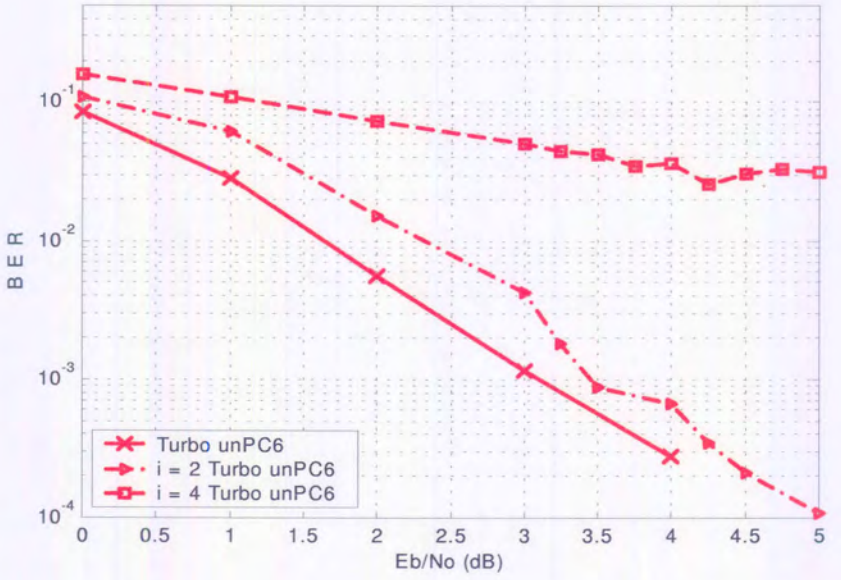

FIGURE 5.34: Influence of number of users. BER performance curve of unPC6 FPC algorithm in a Turbo-coded, W-CDMA system with an AWGN channel.

average transmitted power level will generate more MAI interference to other users. Thus, the rate of BER performance is worsen faster in unbalanced FPC algorithms than balanced FPC algorithms.

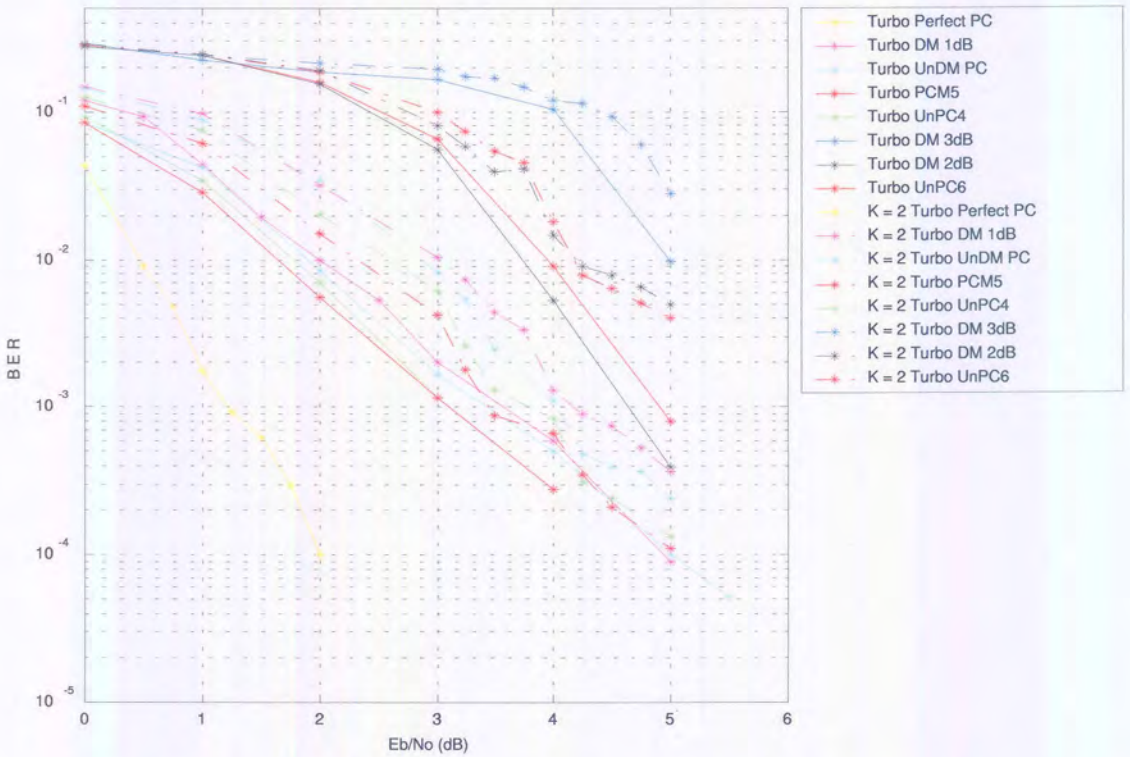

FIGURE 5.35: Influence of number of users. BER performance curve of different FPC algorithms in a Turbo-coded, W-CDMA system with an AWGN channel, Rx=2, i=2, RAKE fingers=3, N=32 and matched-filter detector.

5.3.5.3 BER Performance In An Outdoor Channel

Figure 5.36 depicts the BER performance curve of different FPC algorithms in a one-user, uncoded, W-CDMA system with an outdoor channel. This diagram shows clearly the significant effects of MAI interference on the W-CDMA system capacity, and also shows that either the unbalanced nor the balanced FPC algorithms improve the BER performance in an outdoor channel condition. Later in this section, we describe the effect of incorporating a Turbo code into the W-CDMA system.

Figure 5.37 depicts the BER performance curve of different FPC algorithms in a two-user, Turbo-coded, W-CDMA system with an outdoor channel. By comparing Figure 5.24 with Figure 5.37, we can observe that the BER performance of a two-user, Turbo-coded W-CDMA system degrades compared to a one-user, Turbo-coded W-CDMA system. It is

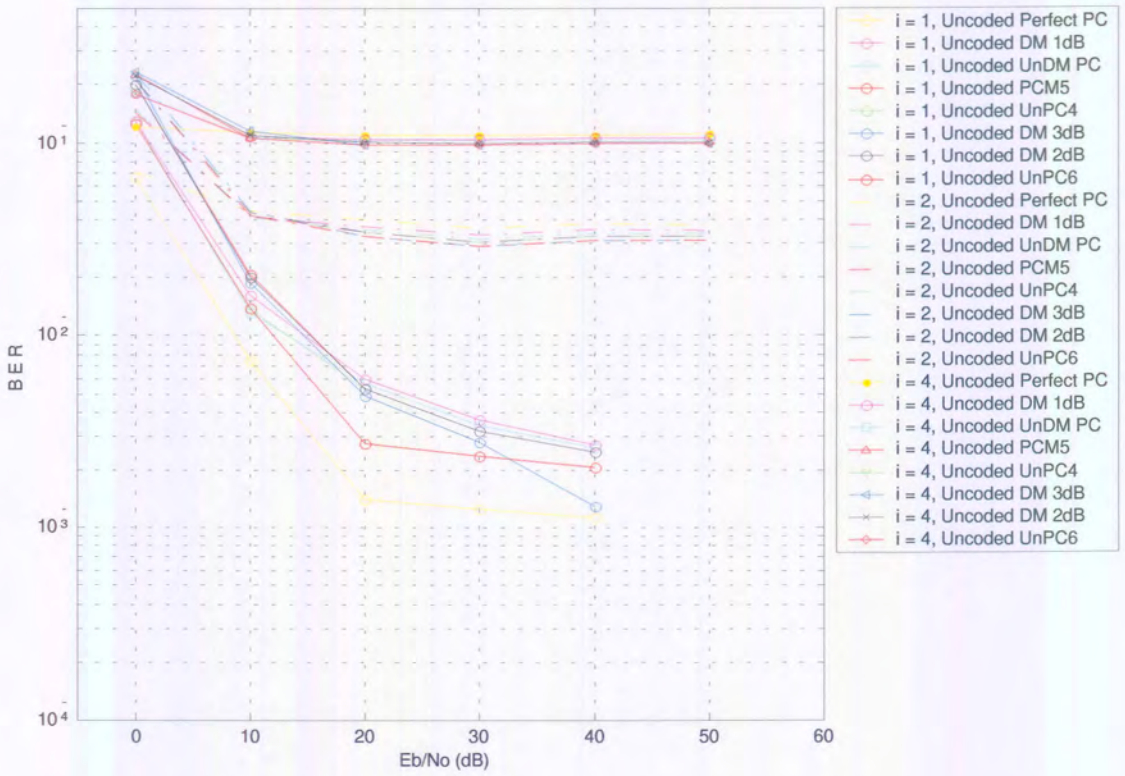

FIGURE 5.36: Influence of number of users. BER performance curve of different FPC algorithms in a uncoded, W-CDMA system with an outdoor channel, Rx=2, i=1, RAKE fingers=3, N=32 and matched-filter detector.

Table 5.10: BER performance of different FPC algorithms in a one-user, Turbo-coded, W-CDMA system with an outdoor channel at 4 dB.

$E_b/I_0 = 4$ dB	BER
unPCM6	0.000248
unPCM4	0.000278
unDM	0.000500
DM1	0.000600
DM2	0.005301
PCM5	0.008958
DM3	0.103519

Table 5.11: BER performance of different FPC algorithms in a two-users, Turbo-coded, W-CDMA system with an outdoor channel at 4 dB.

$E_b/I_0 = 4$ dB	BER
unPCM6	0.000672
unPCM4	0.000834
unDM	0.001113
DM1	0.001300
DM2	0.014676
PCM5	0.017870
DM3	0.119907

also true that the rate of degradation with unbalanced FPC algorithms increases faster than with balanced FPC algorithms. Thus, the rate of BER performance increases are faster with unbalanced FPC algorithms than with balanced FPC algorithms. We can conclude this from the data shown in Table 5.10 and 5.11.

Figures 5.38 to 5.44 depict the BER performance of one-user and two-users systems with different FPC algorithms.

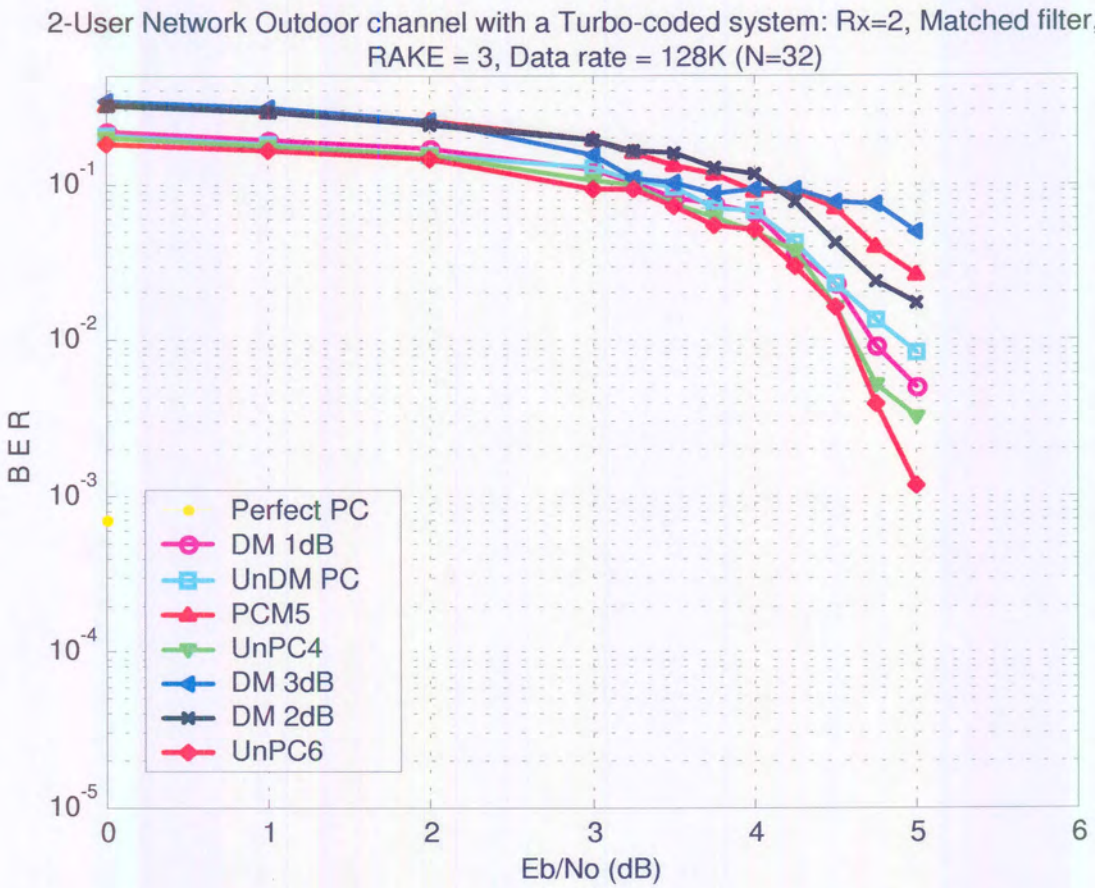

FIGURE 5.37: Influence of number of users. BER performance curve of different FPC algorithms in a Turbo-coded W-CDMA system with an outdoor channel, Rx=2, i=2, RAKE fingers=3, N=32 and matched-filter detector.

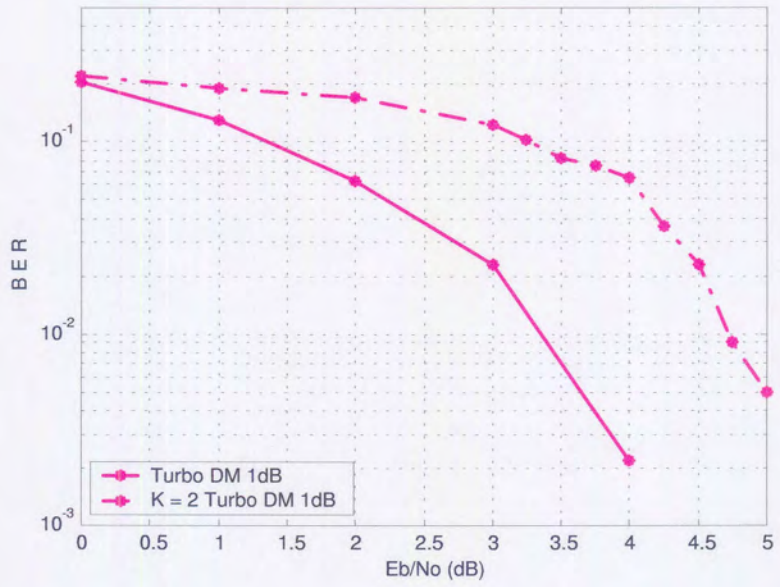

FIGURE 5.38: Influence of number of users. BER performance curve of DM FPC algorithm in a Turbo-coded, W-CDMA system with an outdoor channel.

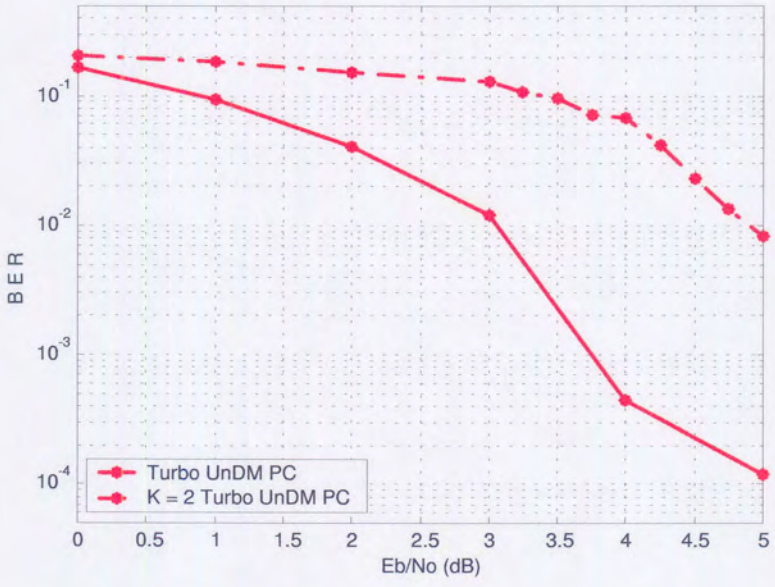

FIGURE 5.39: Influence of number of users. BER performance curve of unDM FPC algorithm in a Turbo-coded W-CDMA system with an outdoor channel.

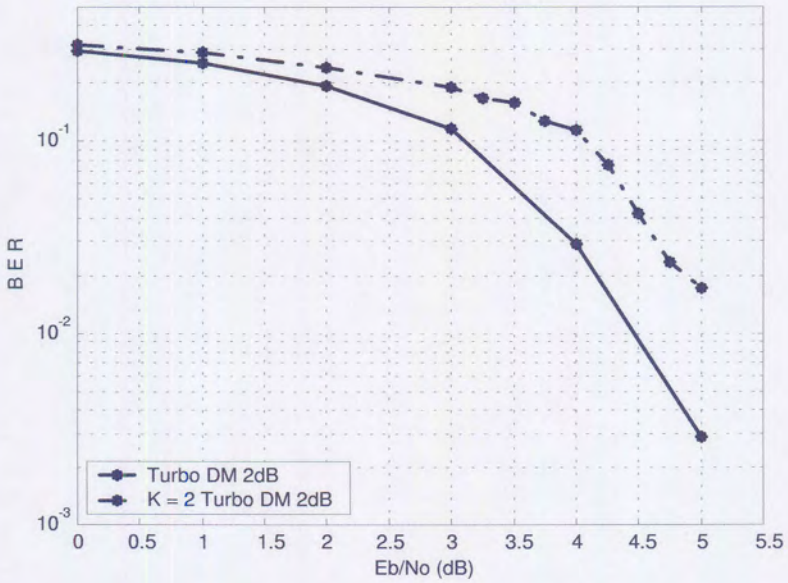

FIGURE 5.40: Influence of number of users. BER performance curve of DM2 FPC algorithm in a Turbo-coded W-CDMA system with an outdoor channel.

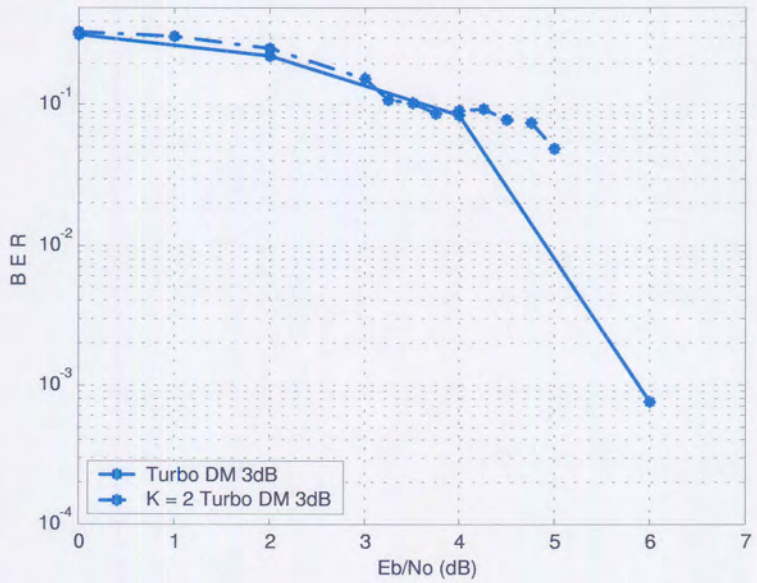

FIGURE 5.41: Influence of number of users. BER performance curve of DM3 FPC algorithm in a Turbo-coded, W-CDMA system with an outdoor channel.

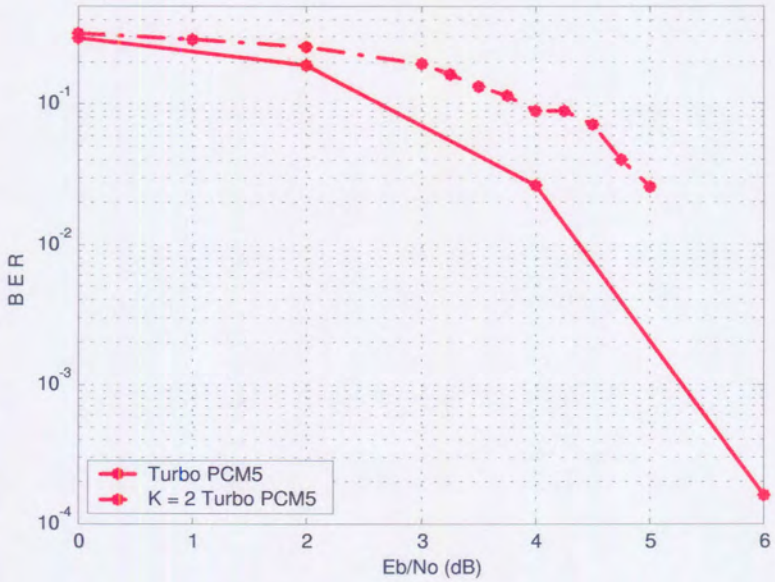

FIGURE 5.42: Influence of number of users. BER performance curve of PCM5 FPC algorithm in a Turbo-coded, W-CDMA system with an outdoor channel.

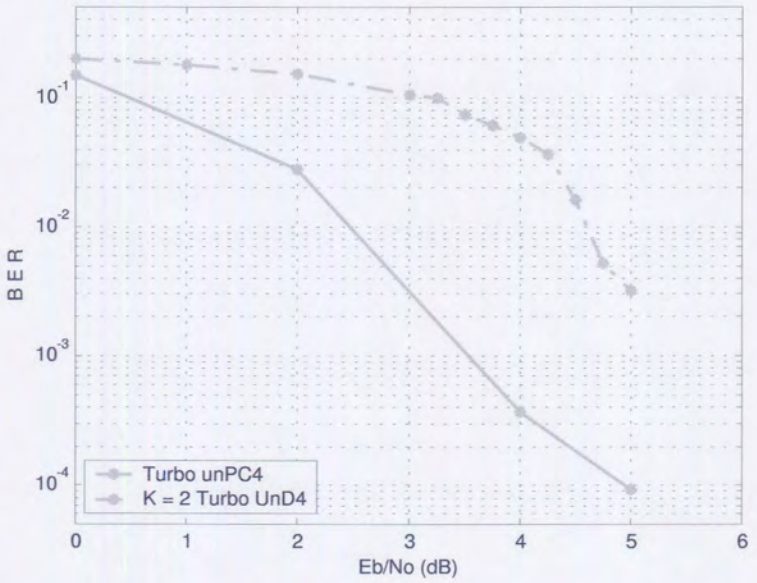

FIGURE 5.43: Influence of number of users. BER performance curve of unPC4 FPC algorithm in a Turbo-coded, W-CDMA system with an outdoor channel.

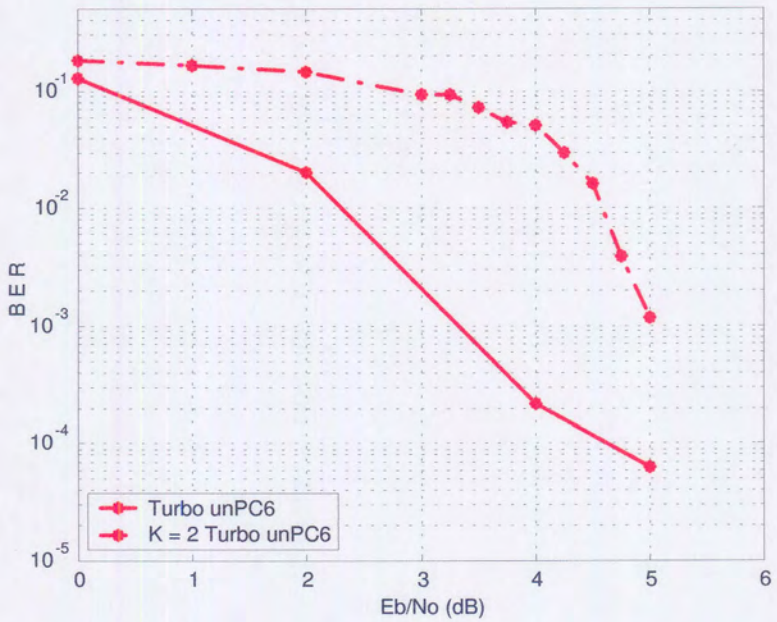

FIGURE 5.44: Influence of number of users. BER performance curve of unPC6 FPC algorithm in a Turbo-coded, W-CDMA system with an outdoor channel.

CHAPTER SIX

CONCLUSION

In this final chapter, the most important results and conclusions of this dissertation are summarized and the goals of the dissertation, as outlined in Chapter 1, are revisited and assessed in terms of whether they have been achieved. Recommendations for future research are also given.

6.1 Goals of The Dissertation

Below is a description of the main goals of the dissertation and the extent to which they have been met.

- To establish a general and mathematically tractable power-sensitive model for multi-media, W-CDMA cellular systems.

  A new power-sensitive model based on capacity analysis for multi-media cellular systems, as described in Chapter 2, has been developed. This model incorporates various physical realities of a cellular network including the influence of:

  - interference on the signal received at the base station (section 2.2.2.1)
  - resource-management on system capacity (section 2.2.2.2)
  - channel effects on the signal received at the base station (section 2.2.2.3)

  Total interference, PC error, traffic demand requirement and transmission rate are amongst the most important factors in defining the capacity limit.

- To establish a general framework structure for PC algorithms in multi-media W-CDMA cellular systems.

The power-sensitive model proposed in Chapter 2 is then used to establish a framework for various APC layers of multi-media CDMA cellular systems as described in Chapter 3. The factors that influence system capacity can be minimized if a complete PC structure is intelligently defined. The APC layers are divided into:

  - NPC (section 3.4)
  - OPC (section 3.5)
  - FPC (section 3.6)

- To propose new QoS-based PC algorithms based on the framework structure established above.
  The power-sensitive model is used to establish a framework for various PC algorithms. The PC layers are divided into:

  - interference management system: QoS-based FPC algorithm (section 4.3.1)
  - service management system: QoS-based OPC algorithm (section 4.3.2) and
  - network management system: QoS-based NPC algorithm (section 4.3.3)

- To program a Turbo-coded, RAKE combining and multi-media uplink W-CDMA simulation platform in a Monte Carlo simulation package with Matlab software.

- To compare balanced, step-size, FPC algorithms with the proposed unbalanced scheme based on BER performance and outage probability with various numbers of multipath components, Doppler spread, number of received antennae and various coding schemes. Using the proposed APC structure presented above, the influence of the following parameters on system performance and capacity is presented in Chapter 5:

  - power profiles (section 5.3.1)
  - diversity schemes (section 5.3.2)
  - coding schemes (section 5.3.3)
  - Doppler spreads (section 5.3.4)
  - number of users (section 5.3.5)

6.2 Overview and Background

After a review of the literature on W-CDMA communication systems in section 1.1, the potential advantages of W-CDMA over TDMA/FDMA for the growing mobile/personal communications market were outlined, the characteristic of *SS waveforms* and *sharing resources* gives CDMA the advantage of providing higher capacity and greater flexibility than TDMA/FDMA. However, the literature revealed at Chapter 1 that SS techniques are broadband in the sense that the entire transmission bandwidth is shared amongst all users at all times. This implies that the system capacity is very much dependent on MAI. Thus, the design of W-CDMA systems is considered as one of power management wireless network architecture, with PC being the central controller for resource allocation and interference management. In this dissertation, a power-sensitive model for the accurate evaluation of W-CDMA system gains has been developed and the influence of various parameters on overall system performance has been determined.

The specific APC structure that was mainly considered in this dissertation is QoS-based PC algorithms. In section 1.2.3, an overview of this APC structure is given with an explanation of how these techniques endeavor to:

- reduce inter-cell and intra-cell interference;
- extend radio resource usage and;
- extend system traffic capacity;

In section 1.3 the limitations of current PC algorithms for future multi-media cellular systems are presented. one of the limitations which is the lack of system treatment of existing APC algorithms is dealt with in more detail in chapters 2 and 3. Chapter 2 presents a newly proposed power-sensitive model for the evaluation of multi-media communication systems using APC structures. Chapter 3 presents a new APC framework for a systematic treatment of APC algorithms.

6.3 A General Power-Sensitive Model for W-CDMA Systems

Chapter 2 describes a mathematical, power-sensitive network model used to evaluate the performance of APC structure in a Turbo-coded, RAKE combining uplink W-CDMA

system. Based on this model, we are able to show that W-CDMA system is a design of interference management network because W-CDMA is interference and resource limited. All the important parameters and basic assumptions, which are important for the simulated-wireless environment, are defined in Chapter 2.

As outlined in section 2.2, the parameters affecting the temporal fading of each multipath signal are orthogonal factor, transmitted power, receiver gains, Doppler spread, channel impairment and traffic demand. Specifically, the channel model assumes that each multipath signal is subject to frequency-selective, Rayleigh fading in indoor-office, outdoor and pedestrian and vehicular environments. All these parameters are combined into a single power-sensitive W-CDMA model.

6.4 Framework for Uplink Power Control Techniques

Chapter 3 formulates on APC framework systematically. Mathematical derivations and comparisons of existing PC algorithms in standard framework are the highlights of this chapter. From our review of the literature, the APC structure (NPC, OPC and FPC) have not previously been considered in such detail and that the concept of linear-receiver unbalanced and non-linear-receiver, unbalanced structures for APC algorithms is unique in the sense that this is the first time this concept has been investigated. All of the existing PC algorithms in publiched literature up to now can be categorize into this proposed framework system.

The main system parameters that are evaluated are:

- NPC (section 3.4)
  - PC and admission-control (section 3.4.2)
  - PC and base station assignment (section 3.4.3)
- OPC (section 3.5)
  - Linear-receiver SINR-balancing (section 3.5.1.1)
  - Linear-receiver SINR-unbalanced (section 3.5.1.2)
- FPC (section 3.6)
  - Iterative convergence to optimal power vector (section 3.6.2)

Previously, PC algorithms were treated as separated mechanisms, However in this dissertation these PC algorithms have been integrated into a state-of-the-art power-sensitive

architecture. The inclusion of iterative decoding techniques was based on a discussion with P.G.W van Rooyen.

6.5 A Multiple-Target Utility-Based PC Strategy

An implementable state-of-the-art QoS-based PC strategy using iterative decoding techniques is presented in Chapter 4. Also included in this chapter are a definition of resources and QoS, and a detailed description of eight FPC algorithms. An analysis of the bounds on the stability of FPC algorithms are also presented.

Two OPC algorithms are also presented with emphasis on the accuracy of the BER-prediction algorithm based on iterative decoding techniques. The Turbo-code algorithm used in the simulation package was programmed by D. van Wyk [126]. The centralized linear-programming optimization problem for OPC algorithms is described, with mathematical equations and block diagrams.

6.6 Numerical Performance Evaluation of Adaptive FPC Algorithms

Having derived the proposed APC structure for the multi-media services of a W-CDMA wireless network, the influence of a number of parameters on each performance measure is described (Chapter 5). Specifically, the influence of power profile, Doppler spread, diversity, coding scheme and number of users in Turbo-coded, RAKE combining and uplink Rayleigh fading channel W-CDMA cellular package of eight FPC algorithms are compared in detailed.

- The influence of the multipath components, Doppler spread, coding scheme, diversity, and number of users was considered in this chapter. The mathematical power-sensitive models used in the evaluation of any adaptive PC system must take all of the mentioned aspects into account in order to obtain an accurate measure of system performance.

- Unbalanced FPC algorithms did not make a significant improvement in AWGN channels because multipath components and Doppler spread were not introduced in the channel model. Unbalanced FPC algorithms outperformed balanced FPC algorithms by decreasing the burst error length.

- Applying convolutional or Turbo-code schemes to AWGN and vehicular, W-CDMA cellular systems improved power efficiency, generally, by about 10 dB with the

different FPC algorithms. When a frequency-selective, Rayleigh, fast-fading channel was introduced in the channel model, there was a significant improvement in BER performance with unbalanced DM and PCM algorithms, especially at high SINR levels.

- It is important to note that the BER is determined mainly by the coding, interleaving and receiver structure, and FPC algorithms not only attempt to narrow the received SINR levels at the base station, but should also correspond to and act as a supplementary mechanism to other receiver structures, to deliver acceptable QoS levels.

- A mediation device is required to provide physical-layer QoS monitoring facility and network-layer RRM decision making facilities. FPC algorithms do not improve the system performance substantially. However, they provide online link QoS monitoring, online resource and interference management, and QoS assurance for adaptation to changes induced by mobility, channel impairment and traffic demand.

- These results show that in a multi-media cellular environment the BER performance at base station is highly unpredictable, stochastic, and the need for a centralized/distributed radio resource management mechanism is a paramount issue.

6.7 Conclusion

This dissertation proposed a new power-sensitive model based on capacity analysis and incorporate APC algorithms to evaluate W-CDMA systems. This model incorporates various physical parameters that influence the performance of power-based W-CDMA cellular systems and makes possible an analytical evaluation of the overall system performance, while at the same time considering a number of physical realities.

Having derived a new PC structure for a multi-media W-CDMA network, the influence of a variety of parameters on each PC structure was determined. Specifically, the number of resolvable multipath components, coding schemes, Doppler spread and number of users were evaluated under a Monte Carlo simulation package in a single-cell, Turbo-coded, RAKE-combining and uplink W-CDMA cellular environment. This dissertation also addressed the trade-off decisions a network operator faces when having to decide whether to implement a physical layer technique or an upper network and management layer scheme to police the link QoS and to increase system capacity. This dissertation shows that optimum performance can be obtained using complete QoS-based PC techniques.

REFERENCES

[1] S. Suda, H. Kawai, and F. Adachi, "A Fast Transmit Power Control based on Markov transition for DS-CDMA Mobile Radio," *Preprint*, 1999.

[2] S. Seo, T. Dohi, and F. Adachi, "SIR-Based Transmit Power Control of Reverse Link for Coherent DS-CDMA Mobile Radio," *IEICE Trans. Commun.*, vol. E81-B, pp. 1508–1516, July 1998.

[3] H. Kawai, H. Suda, and F. Adachi, "Outer-loop control of target SIR for fast transmit power control in turbo-coded W-CDMA mobile radio," *Electronics Letters*, 1999.

[4] F. Adachi and M. Sawahashi, "Wideband Wireless Access Based on DS-CDMA," *IEICE Trans. Commun.*, vol. E81-B, pp. 1305–1316, July 1998.

[5] F. Adachi, M. Sawahashi, and H. Suda, "Wideband DS-CDMA for Next-Generation Mobile Communications Systems," *IEEE Communications Magazine*, pp. 56–69, September 1998.

[6] J. Aein, "Power Balancing in Systems Employing Frequency Reuse," Tech. Rep. 277-299, COMSAT Tech Rev., 1973.

[7] R. Bettketon and H. Alavi, "Power Control for Spread Spectrum Cellular Radio Systems," *IEEE Transactions on Vehicular Technology*, pp. 242–246, 1983.

[8] A. Leon-Garcia, *Probability and Random Processes for Electrical Engineering*. Addison Wesley, 1994.

[9] S. Ariyavisitakul and L. Chang, "Signal and Interference Statistics of a CDMA System with Feedback Power Control," *IEEE Transactions on Communications*, vol. 41, pp. 1626–1634, November 1993.

[10] S. Ariyavisitakul and L. Chang, "Performance of Power Control method for CDMA radio Communications System," *Electronics Letters*, vol. 27, pp. 920–922, May 1991.

[11] S. Ariyavisitakul and L. Chang, "Simulation of CDMA System performance with Feedback Power Control," *Electronics Letters*, vol. 27, pp. 2127–2128, November 1991.

[12] A. Baier, "Design Study for a CDMA-Based Third Generation Mobile Radio Systems," *IEEE Journal on Selected Areas of Communication*, vol. 12, May 1994.

[13] N. Bambos, "Toward Power-Sensitive Network Architectures in Wireless Communications: Concepts, Issues, and Desgin Aspects," *IEEE Personal Communications*, pp. 50–59, June 1998.

[14] P.-R. Chang and B.-C. Wang, "Adaptive Fuzzy Power Control for CDMA Mobile Radio Systems," *IEEE Transactions on Vehicular Technology*, vol. 45, pp. 225–236, May 1996.

[15] C.-J. Chang, J.-H. Lee, and F.-C. Ren, "Design of Power Control Mechanisms with PCM Reallization for the Uplink of a DS-CDMA Cellular Mobile Radio System," *IEEE Transactions on Vehicular Technology*, vol. 45, pp. 522–530, August 1996.

[16] A. Chockalingam, P. D. Laurence, B. Milstein, and R. R. Rao, "Performance of Cosed - Loop Power Control in DS-CDMA Cellular Systems," *IEEE Transactions on Vehicular Technology*, vol. 47, pp. 774–788, August 1998.

[17] J. D. Herdtner and E. K. Chong, "Analysis of a Class of Distributed Asynchronous Power Control Algorithms for Cellular Wireless Systems," *IEEE Journal on Selected Areas of Communication*, vol. 18, pp. 436–446, March 2000.

[18] E. Dahlman, G. Gudmundson, M. Nilsson, and J. Skold, "UMTS/IMT-2000 Based on Wideband CDMA," *IEEE Communications Magazine*, pp. 70–80, September 1998.

[19] E. Dahlman, P. Beming, J. Knutsson, F. Ovesjo, M. Persson, and C. Roobol, "WCDMA-The Radio Interface for Future Mobile Multimedia Communications," *IEEE Transactions on Vehicular Technology*, vol. 47, pp. 1105–1118, November 1998.

[20] A. Ephremides and S. Verdu, "Control and Optimization methods in Communication Network Problems," *IEEE Transaction of Automatic Control*, vol. 34, no. 9, 1992.

[21] A. Ephremides, J. Wieselthier, and D. Baker, "A Design Concept for reliable Mobile Radio Networks with Frequency Hopping Signalling," *Proc. IEEE*, vol. 75, no. 1, 1987.

[22] G. J. Foschini and Z. Miljanic, "Distributed Autonomous Wireless Channel Assignment with Power Control," *IEEE Transactions on Vehicular Technology*, vol. 44, pp. 420–429, August 1995.

[23] G. J. Foschini and Z. Miljanic, "A Simple Distributed Autonomous Power Control Algorithm and its Convergence," *IEEE Transactions on Vehicular Technology*, vol. 42, pp. 641–646, November 1993.

[24] R. L. Freeman, *Radio System Design for Telecommunications*. John Wiley and Sons, Inc., 2nd ed., 1997.

[25] T. Fujii and S. Kozono, "Received Signal level characteristics with Adaptive Transitter Power Control in Mobile Communications," *Trans. IEICE*, vol. J72-B-II, pp. 434–441, Sept 1989.

[26] R. Gejji, "Mobile Multimedia scenario using ATM and Microcellular Technologies," *IEEE Transactions on Vehicular Technology*, vol. 43, pp. 699–703, Aug. 1994.

[27] C.-L. I and R. D. Gitlin, "Multi-code CDMA Wireless Personal Communications Networks," in *Proceedings of IEEE International Conference on Communications,*, (Seattle, WA), pp. 1060–1064, June 1995.

[28] S. Glisic and B. Vucetic, *Spread Spectrum CDMA Systems for Wireless Communications*. Artech House Publisher, 1997.

[29] D. Goodman and N. Mandayam, "Power Control for Wireless Data," *IEEE Personal Communication*, pp. 48–54, April 2000.

[30] S. Grandhi, R. Vijayan, D. Goodman, and J. Zander, "Centralized Power Control in Cellular Radio Systems," *IEEE Transactions on Vehicular Technology*, vol. 42, pp. 466–468, November 1993.

[31] S. Grandhi, R. Vijayan, and D. Goodman, "Distributed Power Control in Cellular Radio Systems," *IEEE Transactions on Communications*, vol. 42, pp. 226–228, Feb/March/Apri; 1994.

[32] S. Hanly and D. Tse, "Power Control and Capacity of Spread Spectrum Wireless Networks." Unpublished, July 1999.

[33] S. V. Hanly, "An Algorithm for Combined Cell-Site Selection and Power Control to Maximize Cellular Spread Spectrum Capacity," *IEEE Journal on Selected Areas of Communication*, vol. 13, pp. 1332–1340, September 1995.

[34] S. Hanly, "Congestion measures in DS-CDMA Networks," *IEEE Transactions on Communications*, vol. 47, pp. 426–437, March 1999.

[35] S. Hanly and D. Tse, "Multi-access Fading Channels: Part ii: Delay-limited Capacities," *IEEE Transactions on Information Theory*, vol. 44, pp. 2816–2831, Nov 1998.

[36] S. Hanly and D. Tse, "Multi-access Fading Channels: Part i: Polymatroid Structure, optimal resource Allocation and Throughput Capacities," *IEEE Transactions on Information Theory*, vol. 44, pp. 2796–2815, Nov. 1998.

[37] S. Haykin, *Communications Systems*. New York: John Wiley and Sons, Third ed., 1994.

[38] C. L. Holloway, M. G. Cotton, and P. Mckenna, "A Model for Predicting the Power Delay Profile Characteristics Inside a Room," *IEEE Transactions on Vehicular Technology*, vol. 48, pp. 1110–1119, July 1999.

[39] H. H. A. Toskala, *W-CDMA for UMTS (Radio Access for Third Generation Mobile Communications)*. John Wiley and Sons, LTD, 2000.

[40] F. Simpson and J. M. Holtzman, "Direct Sequence CDMA Power Control, Interleaving and Coding," *IEEE Journal on Selected Areas of Communication*, vol. 11, pp. 1085–1095, September 1993.

[41] S. Ramakrishna and J. Holtzman, "A Scheme for Throughput Maximization in a Dual-Class CDMA System," *IEEE Journal on Selected Areas of Communication*, vol. 16, no. 6, pp. 830–844, 1998.

[42] P. Kumar and J. Holtzman, "Analysis of Handoff Algorithms using both Bit Error Rate and Relative Signal Strengths," *Proc. ICUPC*, 1994.

[43] T.-H. Hu and M. Liu, "Power Control for Wreless Multimedia CDMA Systems," *Electronics Letters*, vol. 33, pp. 660–663, April 1997.

[44] T. H. Hu and M. K. Liu, "A New Power Control Function for Multirate DS-CDMA Systems," *IEEE Transactions on Communications*, vol. 47, pp. 896–904, June 1999.

[45] C. Kchao and G. Stuber, "Analysis of a Direct-Sequence Spread-Spectrum Cellular Radio System," *IEEE Transactions on Communications*, vol. 41, pp. 1507–1516, October 1993.

[46] D. Kim, K.-N. Chang, and S. Kim, "Efficient Distributed Power Control for Cellular Mobile Systems," *IEEE Transactions on Vehicular Technology*, vol. 46, pp. 313–318, May 1997.

[47] D. Kim, "Rate-Regulated Power Control for Supporting Flexible Transmission in Future CDMA Mobile Networks," *IEEE Journal on Selected Areas of Communication*, vol. 17, pp. 968–977, May 1999.

[48] D. Kim, "Setting SIR Targets for CDMA Mobile Systems in the Presence of SIR Measurement Error," *IEICE Trans. Commun.*, vol. E82-B, pp. 196–199, January 1999.

[49] J. Kim, S. Lee, Y. Kim, M. Chung, and D. Sung, "Performance of Single-Bit Adaptive Step-Size Closed-Loop Power Control scheme in DS-CDMA System," *IEICE Trans, Commun.*, vol. E81-B, pp. 1548–1552, July 1998.

[50] R. Jantti and S.-J. Kim, "Second-Order Power Control with Asymptotically," *IEEE Journal on Selected Areas of Communication*, vol. 18, pp. 447–457, March 2000.

[51] J. Wu and R. Kohno, "A Wireless Multi-Media CDMA System Based on Transmission Power Control," *IEEE Journal on Selected Areas of Communication*, 1996.

[52] W.-M. Tam and C. M. Lau, "Analysis of Power Control and its Imperfections in CDMA Cellular Systems," *IEEE Transactions on Vehicular Technology*, vol. 48, pp. 1706–1717, September 1999.

[53] F. Lau and W. M. Tam, "Intelligent Closed-loop Power Control Algorithm in CDMA Mobile Radio Systems," *Electronics Letters*, vol. 35, pp. 785–786, May 1999.

[54] W. Tam and F. Lau, "Power control mixing C/I balancing and constant-received signal strength in CDMA mobile communications system," *Electronics Letters*, vol. 35, pp. 1609–1610, September 1999.

[55] C. Lee and T. Park, "A Parametric Power Control with Fast Convergence in Cellular Radio Systems," *IEEE Transactions on Vehicular Technology*, vol. 47, pp. 440–449, May 1998.

[56] T.-H. Lee and J.-C. Lin, "A Fully Distributed Power Control Algorithm for Cellular Mobile System," *IEEE Journal on Selected Areas of Communication*, vol. 14, pp. 692–697, May 1996.

[57] T.-H. Lee, J.-C. Lin, and Y.-T. Su, "Downlink Power Control Algorithms for Cellular Radio System," *IEEE Transactions on Vehicular Technology*, vol. 44, pp. 89–94, February 1995.

[58] W. C. Y. Lee, "Overview of Cellular CDMA," *IEEE Transactions on Vehicular Technology*, vol. 40, pp. 291–302, May 1991.

[59] K. K. Leung, "Power Control by Interference Predictions for Wireless IP Networks," *IEEE INFOCOM99,*, vol. New York, NY,, March 1999.

[60] J. Razavilar, F. Rashid-Farrokhi, and K. R. Liu, "Joint Optimal Power Control and Beamforming in Wireless Networks Using Antenna Arrays," *IEEE Transactions on Communications*, vol. 46, pp. 1313–1323, October 1998.

[61] J. Razavilar, F. Rashid-Farrokhi, and K. R. Liu, "Software Radio Architecture with Smart Antennas: A Tutorial on Algorithms and Complexity," *IEEE Journal on Selected Areas of Communication*, pp. 662–676, April 1999.

[62] Y. Lu and R. Brodersen, "Integrating Power Control, Error Correction Coding, and Scheduling for a CDMA Downlink System," *IEEE Journal on Selected Areas of Communication*, vol. 17, pp. 978–989, June 1999.

[63] H. Meyr, M. Moeneclaey, and S. A. Fechtel, *Digital Communication Receivers*. Wiley Series in Telecommunicatins and Signal Processing, John Wiley and Sons Inc., 1998.

[64] R. Rick and L. Milstein, "Parallel Acquisition in Mobile DS-CDMA Systems," *IEEE Transactions on Communications*, vol. 45, pp. 1466–1476, Nov 1997.

[65] R. Rick and L. Milstein, "Optimum Decision Strategies for Acquisition of Spread Spectrum," *IEEE Transactions on Communications*, vol. 46, pp. 686–694, May 1998.

[66] L. B. Milstein, "Wideband Code Division Multiple Access," *IEEE Journal on Selected Areas of Communication*, pp. 1344–1354, 2000.

[67] D. Mitra and J. A. Morrison, "A Distributed Power Control Algorithm for Bursty Transmissions in Cellular, Spread Spectrum Wreless Networks," in *Proc. 5th Winlab Workshop Wireless Info. Networks*, Rutgers University, 1996.

[68] D. Mitra and J. A. Morrison, "A Novel Distributed Power Control Algorithm for Classes of Service in Cellular CDMA Networks," in *Proc. 6th Winlab Workshop Wireless Info. networks*, Rutgers University, 1997.

[69] M. A. Mokhtar and S. C. Gupta, "Power Control Considerations for DS/CDMA Personal Communication Systems," *IEEE Transactions on Vehicular Technology*, vol. 41, pp. 479–487, November 1992.

[70] H. Morikawa, T. Kajiya, T. Aoyama, and A. T. Campbell, "Distributed Power Control for Various QoS in a CDMA Wireless System," *IEEE Journal on Selected Areas of Communication*, pp. 903–907, 1997.

[71] K. Okawa, Y. Okumura, M. Sawahashi, and F. Adachi, "1.92 Mbps data transmission experiments over a coherent W-CDMA mobile radio link," in *IEEE Vehicular Technology Conference*, (Ottawa, Ontario), May 1998.

[72] T. Ottosson and A. Svensson, "Multirate Schemes in DS/CDMA Systems," in *In Proceedings of 45th IEEE Vehicular Technology Conference*, (Chicago, U.S.A.), pp. 1006–1010, July 1995.

[73] S. Park and H. S. Nam, "DS/CDMA closed-loop Power Control with Adaptive Agorithm," *Electronics Letters*, vol. 35, pp. 1425–1427, August 1999.

[74] R. Prasad, *CDMA for Wireless Personal Communications*, vol. Norwood:MA. Artech House, 1996.

[75] R. Prasad, A. Kegel, and M. Jansen, "Effect of Imperfect Power Control on Cellular CDMA System," *Electronics Letters*, vol. 28, pp. 848–849, April 1992.

[76] R. Prasad, J. S. Dasilva, and B. Arroyo-Fernandez, "Air-Interface Access Scheme for Wireless Communication," *IEEE Communications Magazine*, pp. 70–81, December 1999.

[77] T. Ojanpera and R. Prasad, "An Overview of Air Interface Multiple Access for IMT-2000/UMTS," *IEEE Communications Magazine*, pp. 82–95, September 1998.

[78] E. Geraniotis and M. B. Pursley, "Performance of Noncoherent DS-CDMA Communications over Specular Multipath Fading Channels," *IEEE Transactions on Communications*, vol. COM-34, pp. 219–226, March 1986.

[79] M. Pursley, "The Role of Spread Spectrum in Packet Radio Networks," *Proc. IEEE*, vol. 75, no. 1, 1987.

[80] 3rd Generation Partnership Project, Technical Specification Group RAN, Working Group 2, "Radio Resource Management Strategies," tech. rep., 3G TR 25.922 Ver. 0.5.0, September 1999.

[81] T. Rappaport, *Wireless Communications Principles and Practice*. Prentice Hall Communications Engineering and Emerging Technologies, Pretice Hall Inc.: Kluwer Academic Publisher, 1996.

[82] C.-J. Chang and F.-C. Ren, "Centralized and Distributed Downlink Power Control Methods for a DS-CDMA Cellular Mobile Radio System," *IEICE Trans. Commun.*, vol. E80-B, pp. 366–371, Feb 1997.

[83] F. Swarts, P. van Rooyen, I. Oppermann, and M. P. Lotter, *CDMA Techniques for Third Generation Mobile Systems*. Kluwer Academic Publishers, 1999.

[84] P. Alexander, L. Rasmussen, P. van Rooyen, and I. Oppermann, "Multiuser Detectors for the Universal Mobile Telecommunication Systems." Alcatel Research Unit for Wireless Access, 1999.

[85] X. Xia, P. van Rooyen, and I. Craig, "Comparitive study of Power Control Techniques for Cellular CDMA." Alcatel Research Unit for Wireless Access, 1999.

[86] A. Samukic, "UMTS Universal Mobile Telecommunication System: Development of Standards for the Third Generation," *IEEE Transactions on Vehicular Technology*, vol. 47, pp. 1099–1104, November 1998.

[87] M. Saquib, *Quality of Service for Multi-rate DS/CDMA Systems With Multi-user Detection*. PhD thesis, Rutgers, The State University of New Jersey, January 1998.

[88] E. Seneta, *Non Negative Matrices*. Geoge Allen and Unwin., 1973.

[89] D. Famolari, N. Mandayam, D. Goodman, and V. Shah, *A New Framework for Power Control in Wireless Data Networks: Utility and Pricing*. Wireless Multimedia Network Technologies, Kluwer Academic Publishers, 1999.

[90] J. da Silva, B. Arroyo-Fernandez, B. Barani, J. Pereira, and D. Ikonomou, *Mobile and personal communications: ACTS and beyond*. No. 197-414, Kluwer Academic Press, in Wireless communications:TDMA versus CDMA ed., 1997.

[91] M. Sim, E. Gunawan, B.-H. Soong, and C.-B. Soh, "Performance Study of Closed-Loop Power Control Algorithms for a Cellular CDMA System," *IEEE Transactions on Vehicular Technology*, vol. 48, pp. 911–921, May 1999.

[92] F. Simpson and J. M. Holzman, "Direct Sequence CDMA Power Control, Interleaving and Coding," *IEEE Journal on Selected Areas of Communication*, vol. 11, pp. 1085–1095, September 1993.

[93] C. Sung and W. Wong, "The Convergence of an Asynchronous Cooperative Algorithm for Distributed Power Control in Cellular Systems," *IEEE Transactions on Vehicular Technology*, vol. 48, pp. 563–570, March 1999.

[94] C. Sung and W. Wong, "A Distributed Fixed-Step Power Control Algorithm with Quantization and Active Link Quality Protection," *IEEE Transactions on Vehicular Technology*, vol. 48, pp. 553–562, March 1999.

[95] W. Tam and F. Lau, "Analysis of Power Control and Its Imperfections in CDMA Cellular Systems," *IEEE Transactions on Vehicular Technology*, vol. 48, pp. 1706–1717, September 1999.

[96] W. Tam and F. Lau, "Intelligent closed-loop power control algorithm in CDMA mobile radio system," *Electronics Letters*, vol. 35, pp. 785–786, May 1999.

[97] W. Tam and F. Lau, "Power Control mixing C/I balancing and constant-received signal strength in CDMA mobile communication system," *Electronics Letters*, vol. 35, pp. 1609–1610, September 1999.

[98] H. Toskala and P. Group, "ETSI WCDMA for UMTS," *IEEE Communications Magazine*, 1998.

[99] D. Tse, "Optimal Power Allocation over Parallel Gaussian Broadcast Channels," tech. rep., submitted to IEEE Transactions on Information Theory,, Oct. 1998.

[100] T.-C. Song, L. Linder, and X. Xia, "A New W-CDMA Ttransmit Power Control Technique," in *3rd International Conference on Control Theory and Applications* (IEEE, ed.), ICCTA'01, December 2001.

[101] T.-C. Song and L. Linde, "A New W-CDMA Transmit Power Control Technique based on Iterative Coding Techniques," in *SATNAC '00*, Telkom S.A. Ltd., Sep. 2000.

[102] T.-C. Song, P. van Rooyen, and X. Xia, "Comparative Study of Power Control Techniques for Cellular CDMA," in *SATNAC'99 Conference*, Telkom S.A. Ltd., September 1999.

[103] S. Ulukus, *POWER CONTROL, MULTIUSER DETECTION AND INTERFERENCE AVOIDANCE IN CDMA SYSTEMS*. PhD thesis, The State University of New Jersey, October 1998.

[104] G. Ungerboeck, "Channel Coding with Multilevel/Phase Signaling," *IEEE Transactions on Information Theory*, vol. IT-25, pp. 55–67, January 1982.

[105] A. Urie and C. Mourot, "An Advanced TDMA Mobile Access System for UMTS," in *Proc. IEEE PIMRC'94*, 1994.

[106] R. Lupas and S. Verdu, "Near-Far Resistance of Multiuser Detectors in Asynchronous Channels," *IEEE Transactions on Communications*, vol. COM-38, pp. 496–508, April 1990.

[107] K. Gilhousen, I. Jacobs, R. Padovani, J. Viterbi, K. Weaver, and C. Wheatley, "On the capacity of a cellular CDMA systems.," *IEEE Transactions on Vehicular Technology*, vol. 40, pp. 303–312, May 1991.

[108] A. Viterbi and A. M. Viterbi, "Erlang Capacity of Power Controllled CDMA system," *IEEE Journal on Selected Areas of Communication*, vol. 11, pp. 892–900, August 1993.

[109] A. Viterbi, A. M. Viterbi, K. Gilhausen, and E. Zahavi, "Soft Handoff extends CDMA cell coverage and increases reverse link capacity," *IEEE Journal on Selected Areas of Communication*, vol. 12, pp. 1281–1288, October 1994.

[110] A. Viterbi, A. Viterbi, and E. Zehavi, "Performance of Power-Controlled Wideband Terrestrial Digital Commuinication," *IEEE Transactions on Communications*, vol. 41, pp. 559–568, April 1993.

[111] X. Wang and H. V. Poor, "Iterative (Turbo) Soft Interference Cancellation and Decoding for Coding," *IEEE Transactions on Communications*, vol. 47, pp. 1046–1061, July 1999.

[112] J.-H. Wen, L.-C. Yeh, and J.-R. Chiou, "Short-term Fading Prediction-based Power Control Methode for DS/CDMA Cellular Mobile Radio Networks," *IEEE Transactions on Vehicular Technology*, pp. 908–912, 1997.

[113] Q. Wu, W.-L. Wu, and J.-P. Zhou, "Centralised power control in CDMA cellular mobile systems," *Electronics Letters*, vol. 33, pp. 115–116, January 1997.

[114] Y.-J. Yang and J.-F. Chang, "A Strength-and SIR Combined Adaptive Power Control for CDMA Mobile Radio Channels," *IEEE Transactions on Vehicular Technology*, vol. 48, pp. 1996–2004, November 1999.

[115] R. Yates and C.-Y. Huang, "Integrated Power Control and Base Station Assignment," *IEEE Transactions on Vehicular Technology*, vol. 44, pp. 638–644, August 1995.

[116] C.-Y. Huang and R. Yates, "Rate of Convergence for Minimum Power Assignment in Cellular Radio Systems," *ACM/Baltzer Wireless Networks Journal*, vol. 1, pp. 223–231, 1998.

[117] R. Yates, "A Framework for Uplink Power Control in Cellular Radio Systems," *IEEE Journal on Selected Areas of Communication*, vol. 13, pp. 1341–1347, September 1995.

[118] S. Hanly and C. Chan, "Slow Power Control in a CDMA Network," in *Proc. VTC 99*, (vol. 2), pp. 1119–1123, 1999.

[119] S. Ulukus and R. D. Yates, "Stochastic Power Control for Cellular Radio Systems," *IEEE Transactions on Communications*, vol. 46, pp. 784–786, June 1998.

[120] A. Yener, *Efficient Access and Interference Management for CDMA Wireless Systems*. PhD thesis, Rutgers, The State University of New Jersey, May 2000.

[121] J. Zander, "Performance of Optimum Transmitter Power Control in Cellular Radio Systems," *IEEE Transactions on Vehicular Technology*, vol. 41, pp. 57–62, February 1992.

[122] M. Andersin, Z. Rosberg, and J. Zander, "Distributed Discrete Power Control in Cellular PCS," *Wireless Personal Communications*, vol. 6, no. 3, 1998.

[123] J. Zander, "Distributed Cochannel Interference Control in Cellular Radio Systems," *IEEE Transactions on Vehicular Technology*, vol. 41, pp. 305–311, Aug. 1992.

[124] W. Zhuang, "Integrated Error Control and Power Control for DS-CDMA Multimedia Wireless Communications," tech. rep., Department of Electrical and Computer Engineeering, University of Waterloo, Waterloo, ON, Canada, 1998.

[125] M. Medard, "The Effect Upon Channel Capacity in Wireless Communications of Perfect and Imperfect Knowledge of Channel," *IEEE Transactions on Information Theory*, vol. 46, pp. 933–946, May 2000.

[126] E. P. D. van Wyk and P. van Rooyen, "Comparative study and design of Turbo coding techniques for UMTS." Alcatel Research Unit for Wireless Access, 1999.

[127] J. G. Proakis, *Digital Communications*. McGraw-Hill, 2nd ed. ed., 1989.

[128] M. Saquib, A. Ganti, and R. Yates, "Power control for an asynchronous multi-rate decorrelator," in *34th Allerton Conference on Communications, control and Computing*, (Monticello, IL,), September 1997.

[129] J. Whitehead, "Performance and Capacity of Distributed dynamic Channel Assignment and Power Control in shadow fading," in *1993 Int. Commun. Cong.*, (Geneva, Switzerland), May 1993.

APPENDIX A

3G UPLINK/DOWNLINK SIMULATION ENVIRONMENT

This appendix provides a brief description of the MATLAB 3G Uplink/Downlink Simulation Environment. The simulation environment is controlled through a Graphical User Interface (GUI). This has been developed to provide the user with an integrated 3G CDMA simulation platform for performance evaluations. The package has been developed using MATLAB 5.2, running on a WINDOWS 95/98/NT platform.

A.1 Link Level Simulation

This section will describe the MATLAB link-level software implementations of the uplink and downlink. Figure A.1 and A.2 illustrate the general block diagrams of the transmission links.

For both the up- and downlinks, the data sequence is firstly encoded, interleaved and frame converted before data modulation using QPSK. A frame consists of multiple slots. Tme consists of multiple slots. T- and slot- based processing for the receiver and transmit functions. For the transmitter, the frame based processing consists of frame encoding and interleaving. Then each slot is transmitted and received. When a slot is received and placed into the de-interleaver buffer, the power control command is computed for the next transmit slot. Only when the entire de-interleaver input is filled can the receiver frame based processing (consisting of de-interleaving and decoding) commence. For the uplink, a single transmitter antenna is assumed, while the downlink may include M_T transmit antennas, used either in a CDTD or TDTD signalling configuration (see [84] for more details on the different transmit diversity schemes).

In the simulation system the in-phase and quadrature components of the transmitted

signal are multiplied by a random segment of a pre-generated fading channel complex envelope. The channel models under consideration, include the UMTS *indoor*, *outdoor-to-indoor/pedestrian* and *vehicular*. The resulting signals are then summed and finally AWGN of known power is added.

All of the users add their contribution to the centre slot buffer, then each user processes this buffer after the addition of noise, to model AWGN. For each user the data transmitted on the physical channel results from the encoding of an information sequence and the control information transmitted on the channel is randomly generated.

The length of the information sequence and the encoding rate sets the number of binary symbols to be transmitted on the I and Q arms of the modulator. This in turn sets the processing gain of each user. By setting the information sequence length of each user, we may control the processing gain of each user. Users with higher information rates will have correspondingly lower spreading gains. Importantly, the frame interleaver sizes used in the convolutional- and turbo encoding and decoding are also determined by the information data rate.

The receiver first performs chip waveforming matching. Channel estimation is performed on each resolved path, and used in the pilot symbol assisted (PSA) RAKE combiner to resolve each of the transmitted streams from the multiple transmit antennas. The RAKE receiver then consists of a number of correlators (or fingers), operating in parallel. Each finger correlates a shifted version of the received signal with the spreading sequence for the user of interest. The different shifts correspond to the different excess delays for each multipath component received by the mobile terminal. Thus each RAKE finger is synchronized to a different multipath component and picks up the energy associated with that component. The outputs of the RAKE fingers must be combined (once per symbol period) to obtain an estimate of the received symbol.

Closed loop power control is used on the dedicated channels to reduce the imbalance in transmit power (near-far effect). Ideally the base station adjusts the transmitted power such that the mobile terminal observes a prescribed signal-to-interference ratio (SIR). Both pilot and data symbols are used in measuring the instantaneous received signal power, but pilot symbols are used in measuring the instantaneous interference plus background noise power. The measured SIR is then compared with the target value to generate the transmit power control (TPC) command which is sent to the transmitter at the base station at the end of each slot.

A.1.1 Simulation Cases

Three types of users, each having different service requirements, may be considered. The three service types are as indicated in Table A.1.

Parameter	Class 1	Class 2	Class 3
Physical channel rate (uncode)	48 *kbits/*	256 *kbits/*	1024 *kbits/*
Spreading factor, N	32	16	4
FEC rate	1 or 1/3	1 or 1/3	1 or 1/3
Frame Interleaving	10 *ms*	10 *ms*	10 *ms*
DPCCH/DPDCH power	0 *dB*	0 *dB*	0 *dB*

TABLE A.1: Simulation service classes.

Table A.2 provides a summary of the implemented receivers, transmit diversity, and coded techniques and their corresponding labels.

A.2 MATLAB Simulation Software

A.2.1 Getting Started

In order to get the MATLAB simulation platform up and running the following steps should be followed:

Step 1 Create a suitable working directory to which the software will be copied. For example: `'c:\umts_sim'`

Step 2 Copy the downloaded 'p-code' files (`'*.p'`) to the working directory.

Step 3 Create the simulation data directory to which `'error'` and `'log_file'` results will be stored. This directory should be created on the 'C' drive as follows: `'c:\data'`

Step 4 Start MATLAB, and add the directory created under Step 1 to the MATLAB path.

Step 5 You should be able to run the simulation platform. Type in `'umts_sim'` at the MATLAB command line.

Acronym	Description
SICL	Iterated SIC, no clip/linear (3 Iterations)
SICH	Iterated SIC, hard (3 Iterations)
SICL	Iterated SIC, clip (3 Iterations)
PICL	Iterated PIC, no clip/linear (3 Iterations)
PICH	Iterated PIC, hard (3 Iterations)
PICL	Iterated PIC, clip (3 Iterations)
NLMS	Normalized LMS ($\mu = 0.02$)
EMF	Estimated Matched Filter ($\mu = 0.02$)
NO TD	No Transmit-Diversity
O-CDTD	Orthogonal Code-Division Transmit-Diversity
RR-TDTD	Round-Robin Time-Division Transmit-Diversity
AS-TDTD	Antenna-Selection Time-Division
UNC	Uncoded Transmission
RC	Repetition Coding
CC	Convolutional Coding (128 or 256 states)
TC	Turbo Coding (4, 8 or 16 states)
	MAP decoder, 8 Iterations

Table A.2: Implemented single- and multiuser detection, transmit-diversity and channel coding techniques and corresponding labels.

A.2.2 Main Simulation Window

By invoking `'umts_sim.p'` at the MATLAB command line, the main GUI from which different simulation engines are called from will be opened. A screen capture of this GUI window is depicted in Figure A.3.

A.2.3 Simulation Environment Configuration

Figure A.4 shows a screen capture of the simulation environment configuration window. By selecting `'Transceiver/Channel Setup'` button, the configuration window, shown in Figure A.4 will be opened.

The DS/CDMA transceiver and environment parameters controlled through this GUI are given below:

- General transceiver parameters:
  - Number of simultaneous users, K.
  - Users' load in a mixed throughput environment, given as percentage of number of simultaneous transmitting users.
  - Signal-to-Noise ratio range and step increments.
- Channel environment parameters:
  - Type: AWGN, UMTS Indoor, UMTS Outdoor-to-Indoor and Pedestrian, and UMTS Vehicular.
  - Average speed and log-normal shadowing variance.
- Monte-Carlo simulation parameters:
  - Minimum number of bit errors to detect.
  - Minimum and maximum number of frames to receive.
- Parameters common to uplink and downlink:
  - Number of RAKE fingers available.
  - Power control algorithm selection.
- Parameters specific to uplink:
  - Number of receiving antenna.

  - Choice of receiver (choice between single and multi user detectors):
    * Iterated SIC, No clip.
    * Iterated SIC, Clip.
    * Iterated SIC, Hard.
    * Iterated PIC, No clip.
    * Iterated PIC, Clip.
    * Iterated PIC, Hard.
    * Estimated Matched Filter (EMF).
    * Normalized LMS (NLMS).
  - Choice of FEC technique:
    * No coding.
    * Convolutional encoder with soft-input Viterbi decoder.
    * Turbo encoder with iterative MAP decoder (8 Iterations).

- Parameters specific to downlink:
  - Number of transmitting antenna.
  - Transmit diversity selection:
    * No transmit diversity.
    * Orthogonal CDTD.
    * Round-Robin Time-Division Transmit Diversity (RR-TDTD).
    * Antenna-Selection Time-Division Transmit Diversity (AS-TDTD).
  - Choice of receiver:
    * Estimated Matched Filter (EMF).
    * Normalized LMS (NLMS).
  - Choice of FEC technique:
    * No coding.
    * Convolutional encoder with soft-input Viterbi decoder.
    * Turbo encoder with iterative MAP decoder (8 Iterations).

A.2.4 Example

To understand how to use the simulation platform, an example is presented.

Step 1 Type `'umts_sim'` at the MATLAB command line. This will bring up the main interface window (figure), shown in Figure A.3.

Step 2 Click on the `'Transceiver/Channel Setup'` button. This will open the configuration window, as shown in Figure A.4.

Step 3 Select the number of users, K.

Step 4 Change the 'E_b/N_o range in dB' entry to the desired range. Note that this parameter is entered in typical MATLAB style for vectors which is *start:step:end* with *step* defaulting to 1.0 if not specified.

Step 5 Select the desired channel environment.

Step 6 Select the vehicle speed and log-normal shadowing variance.

Step 7 Set up the users' loads as a percentage. Upon exit the entries will be normalized to a total load of 100 %.

Step 8 Change the simulation control parameters.

Step 9 Set up the parameters common to both the uplink and downlink.

Step 10 Set up the uplink specific parameters.

Step 11 Set up the downlink specific parameters. Note that when only a single transmit antenna has selected, that the transmit diversity scheme will be defaulted to the 'No Transmit Diversity (TD)' selection.

Step 12 Click on the `'Continue'` button. This causes the configuration window to close. The theoretical curve for selected uncoded DS/QPSK system will be plotted over the E_b/N_o range in dB.

Step 13 (Optional) Click on the `'Clear'` button to remove the plotted curves.

Step 14 Click on either the `'UPLINK Simulation'` or `'DOWNLINK Simulation'` button to start the simulation. The simulation continuous for each E_b/N_o value specified in the 'E_b/N_o range in dB' entry. Information on 'Simulation Completion'

will be displayed. The plot will be updated as the bit error rate of each evaluation point bit error exceeds has been completed. Note that each point is evaluated until the condition where the bit error count exceed the 'minimum number of errors', and the received frame counter exceeds the 'minimum number of simulation blocks', is reached for that particular value of E_b/N_o. At completion of the simulation, a legend is added and results are displayed on the graph. At this stage, the result can be copied to the clipboard to paste in some other application for recalling purposes.

Step 15 The main figure window can now be exit from by clicking on the `'Exit'` button, or more simulations can be performed.

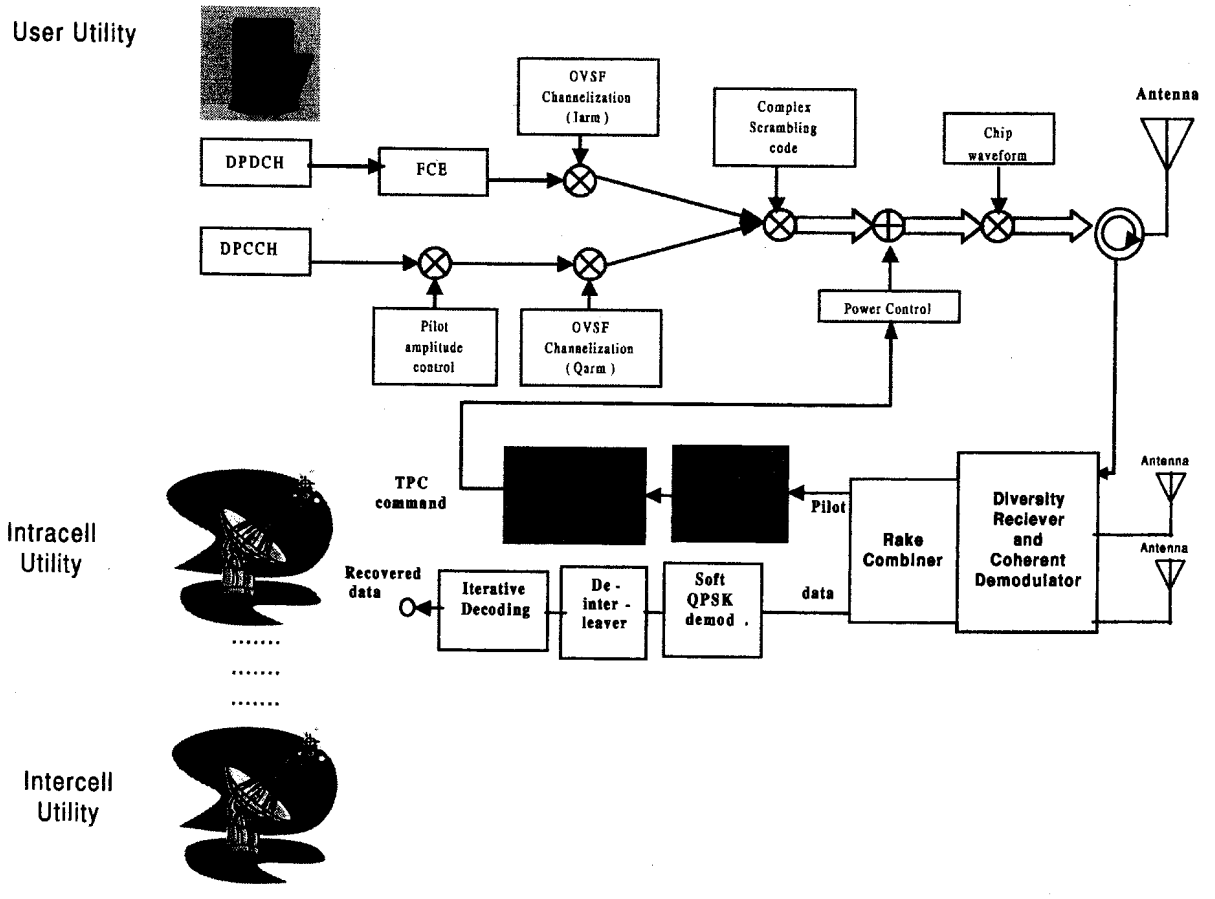

FIGURE A.1: Overall block diagram of the uplink.

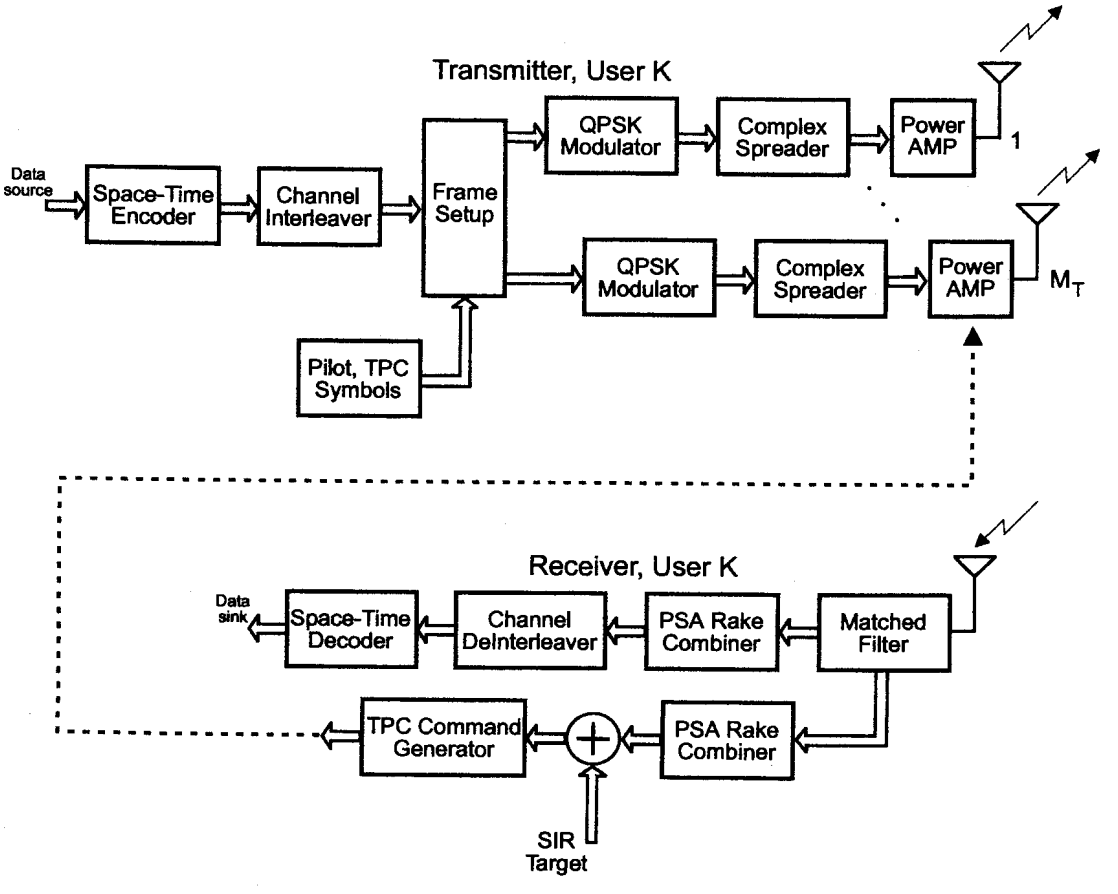

FIGURE A.2: Overall block diagram of the downlink.

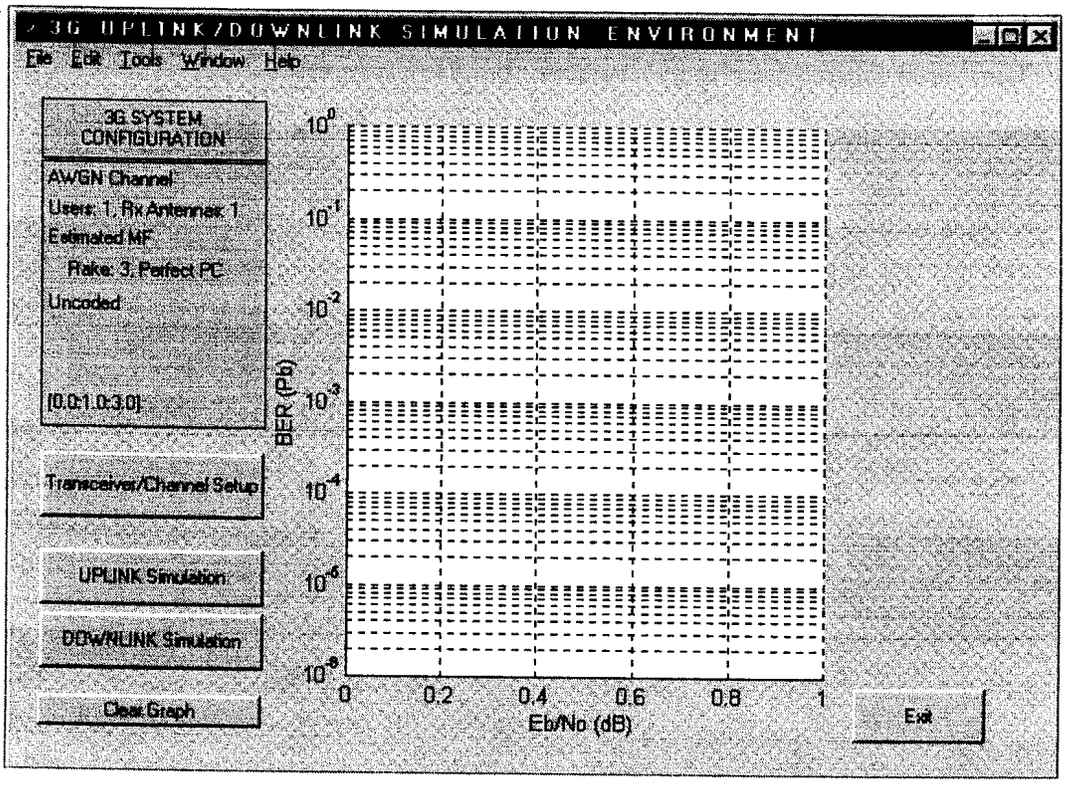

FIGURE A.3: Main interactive simulation platform window.

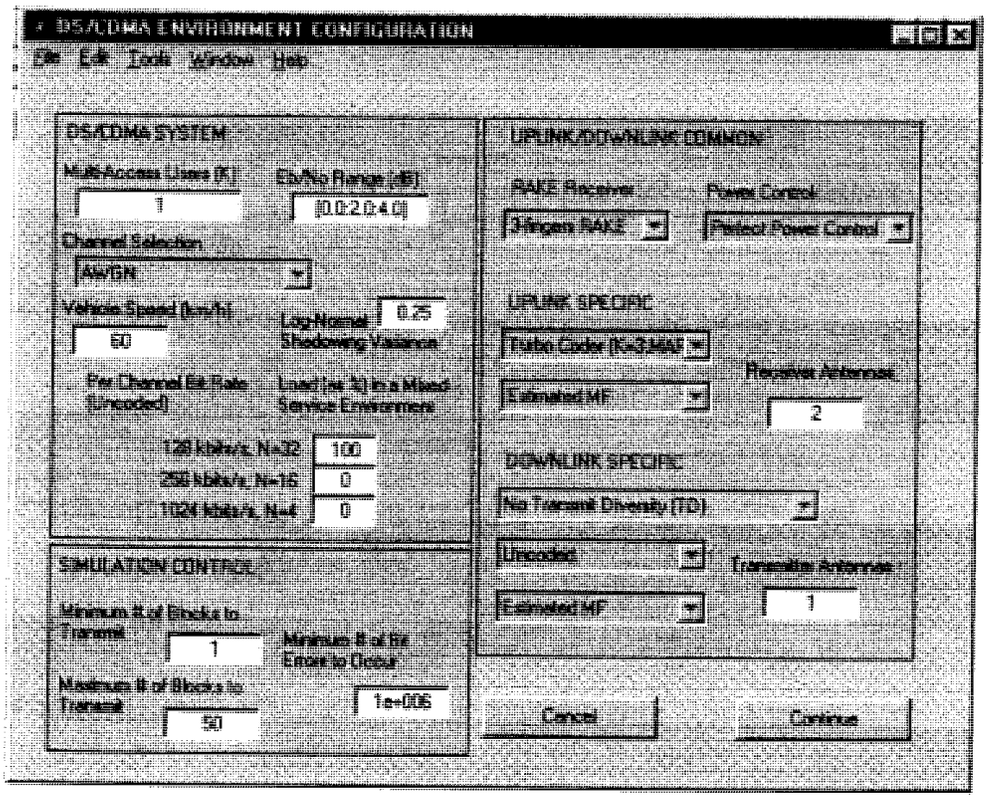

FIGURE A.4: Simulation platform configuration window.

APPENDIX B

SOURCE CODE OF THE ARUWA SIMULATION PACKAGE

```
%function TransOne

global status1; global status2; global status3; global status4;
global status5; status1 = 0; status2 = 0; status3 = 0; status4 =
0; status5 = 0; global AveSigPwr; AveSigPwr = 1;

store = struct(...
   'n'          ,       [],...                          % MAI /simulator
   'h'          ,       [],...                          % channel effect /frame
   'Rayleigh'   ,       [],...                          % Multipath fading /frame
   'shadow',            [],...                          % Shadow /frame
   'userData'   ,       [],...                          % User Data buffer /frame
   'Txsignal',          [],...
                            % Transmitted signal /slot (Text: Transmitted power)
   'Rxsignal',          [],...                          % Received signal /slot
   'profile'    ,       [],...                          % Power Profile /frame
   'PControl'   ,       [],...
                            % Transmitted power & received SIR /slot
   %(Text: Actual SIR & Estimated SIR
   'SIRset',            [],...
   'SIRmea',            [],...
   'PConsump'   ,       [],...                          % Power Consumption /frame
   'ErrorDist',         [],...                          % Error distribution /frame
   'NoisePower',        [],...                          % Noise power at channel
   'AvePw',             [],...                          % Average Transmitted power
   'Pe',                [],...                          % Error Probability /FER
   'iteration',         [],...
   'extrinsic',         [],...
   'iteration1',        [],...
   'extrinsic1',        []);

mud = 8;
                1: SIC with iterations, no clip
                2: SIC with iterations, clip
```

```
                3: SIC with iterations, hard7
                4: PIC with iterations, no clip
                5: PIC with iterations, clip
                6: PIC with iterations, hard
                7: Normalised LMS
                8: estimated  MF

rake = 3;          % Rake fingers
fec = 4;           % selected forward error correction scheme
                1: No error correction coding
                2: Convolutional coding, K=8, Rate-1/3 (128-state)
                3: Convolutional coding, K=9, Rate-1/3 (256-state)
                4: Turbo coding, K=3, Rate-1/3 (4-state)
                5: Turbo coding, K=4, Rate-1/3 (8-state)
                6: Turbo coding, K=5, Rate-1/3 (16-state)
chan = 1;                                          % selected channel
                                1: AWGN Channel, no multipath
                                2: UMTS Indoor
                                3: UMTS Pedestrian
                                4: UMTS Vehicular
                                5: 1-Path Rayleigh
                                6: 2-Path Rayleigh
                                7: 3-Path Rayleigh
logn_s =2;                  % Shadowing variance
v = 60/3.6;                 % speed, convert from km/h to m/s
lRxA = 1;                   % number of receiver antenna
IT = 8;                     % number of iteration to perform for turbo decoder

PwrCtrl = 2;
                                1: Perfect PC
                                2: CLPC (2dB)
                                3: CLPC (1dB)
                                4: Xia1
                                5: Xia2
                                6: fuzzy
%=========================================
% System Parameters: UMTS/UTRA standards
%=========================================
sys = struct(...
   'Nf', 41472,...                  % # of chips in a frame
   'M' , 16,...                     % # of slots in a frame
   'm' , 1,...                      % current slot
   'Nm', 0,...                      % # of chips in a slot
   'S' , 4,...                      % # of samples per chip
   'Sf', 0,...                      % # of samples per frame
   'Sm', 0,...                      % # of samples per slot
   'B' , 1,...                      % # of receive antenna (diversity)
   's' , [],...                     % long code
   'c' ,    [],...                  % chip waveform
   'Q' , 0,...                      % centre tap of chip waveform
   'chan',chan,...                  % AWGN (selected) channel
   'v',v,...                        % vehicle speed (60/3.6 ms^-1)
```

```
    'h',[],...                          % multipath fading profile at chip rate
    'receiver',mud,...                  % type of receiver (SC, MF, PC)
    'rake',rake,...                     % RAKE fingers
    'fec',fec,...                       % fec type
    'pwr_ctrl',PwrCtrl);                % power control
sys.Nm = sys.Nf/sys.M;                  % chips per slot
sys.Sf = sys.Nf*sys.S;                  % samples per frame
sys.Sm = sys.Sf/sys.M;                  % samples per slot

% Long Code
s = 2*(rand(sys.Nf,1)>0.5)-1;
sys.s = [s;s];                          % avoid %Nf by replication of long code

% chip waveform
sys.c = chip(2,sys.S,1);
 type 0 = square, type 1 = root raised cosine
sys.Q = floor(length(sys.c)/2);
 index of centre tap (-1), offset in conv

Multifading

channel = 1;                            % channel
store = Multifading(store,channel,sys);
sys.h = store.h;

%=========================================
% User Required Parameters: Data Rate, QoS,
%=========================================

% Single transmit antenna
channel = channels(sys.S,sys.chan);             % pick type of fading channel
P = size(channel,1);                            % # of multipath delays
if fec == 1
   n = 1;
else
   n = 3;
end

store.profile = channel';

Lu = sys.Nf/32/n; N  = 32;
L  = n*Lu;
                        % # of channel symbols per frame (% # bits out of encoder)
Lm = L/sys.M;                                   % # of channel symbols per slot

Tx(1) = struct(...
   'Lu' , Lu,...        % Data buffer          % # of bits into frame encode
   'L'  , L,...                                % # of bits at encoder output per frame
   'Lm' , Lm,...                               % # of bits at encoder output per slot
   'b'  , [],...                               % User data generate in frame based
   'dI' , zeros(L,1),...                       % Encode user data at output register
   'I'  , [],...                               % bitwise channel interleaver
```

```
   'dQ' , [],...                                % training symbols
   'N'  , N,...                                 % spreading gain
   'cI' , zeros(N,1),...                        % I arm spreading code
   'cQ' , zeros(N,1),...                        % Q arm spreading code
   'n'  , 3,...
   'sIp', 0,...                                 % phase of I arm scramble
   'sQp', 0,...                                 % phase of Q arm scrambl
   'w'  , zeros(sys.B*P,1),...                  % adaptive filter
   'P'  , P,...          % Channel parameter    % # of multipath delays
   'hp', zeros(P,sys.B),...                     % phases of multipath profile
   'ho', zeros(P,sys.B),...
                  % offset into fading array of multipath profile into sys.h
   'delay',0,...                                % group delay (models async to other users
   'power', zeros(P,1),...                      % relative power of fading channels
   'tau', zeros(P,1),...                        % multipath delays measured in samples
   'SINRset',0.5,...    % Receiver parameter    % target received SINR
   'SINR',0,...                                 % measured SINR
   'QoS', 10e-3,...                             % Target received BER
   'Wtx',zeros(sys.M+1,1));                     % Tx scaling to satisfy SINRset
    [Tx(1).cI, Tx(1).cQ] = tree(N);             % binary antipodal channelisation code
   % multipath fading\
   J = sqrt(-1);
   homax = length(sys.h)-sys.Nf;                % max multipath sequence offset%

Tx(1).power = 10.^(channel(:,2)/10);            % convert MP strengths from dB to linear\
Tx(1).tau = channel(:,1);
                           % assign MP delays as a function of the selected channel
Tx(1).delay = floor(rand*10*sys.S);             % asynchronism
Tx(1).hp = exp(J*2*pi*rand(P,sys.B));           % phases of multipath profile
Tx(1).sIp = 0; Tx(1).sQp = 0;%
%=========================================
 Initiate Transmitter Parameters
=========================================
Errs = 0;
EbonNodB = 0;
                           % find the required EbonNodB for various data rate, channel,
run = 0;
% diversity scheme and coding
 Interleaver
 cEbNodB = EbonNodB(1);

I=1:L; for i=1:L, j=ceil(rand*L);
   temp=I(j);
   I(j)=I(i);
   I(i)=temp;
end; Tx(1).I=I;
%        Tx(1).dQ = 2*round(rand(L,1))-1;
        % training symbols
        Tx(1).SINRset = (10^(EbonNodB/10))/Tx(1).n;
        % QoS scaling controls Tx power
        Tx(1).Wtx(1) = 0.5;
                                        % rough initial value for Tx amplitude
```

```
        store.PConsump = Tx(1).Wtx(1);
%=========================================
% Frame-wise encoding and interleaving
%=========================================
while run < 20,
   run = run + 1;
  if fec == 1, Tx(1).b = round(rand(Tx(1).Lu,1));          %Uncoded system
   else Tx(1).b = round(rand(Lu,1)); end;                  %Coded system
   switch fec
       case 1
        Tx(1).dI = 2*Tx(1).b-ones(size(Tx(1).b));
     case {4,5,6} %Turbo Encoder
                % Turbo-encoder
            Rc = 1/3;
            Q=fec-2;
            T_out = turboenc(Q,Tx(1).Lu,Rc,Tx(1).b');
            T_out = T_out';
            % Interleaver
            Tx(1).dI = T_out(I);
     end
store.userData = [store.userData,Tx(1).b];

%=====================================================
% Slot-by-Slot transmission - Enables Utilized-based PC
%=====================================================
      Rx=Tx;
      %save Rx Rx
      %      m=1;
        ebno = 10^(EbonNodB/10);%

      for m=1:sys.M
         sys.m = m;
         Tx(1).ho = m*sys.Nf/16; %ceil(rand(P,sys.B)*homax);
                                        % offset of multipath profile into sys.
            ds = (m-1)*Tx(1).Lm + (1:Tx(1).Lm);
                                        % Index the current user-data buffer
         % Spread spectrum
         dIm= Tx(1).dI(ds);
                                        % User index (ds) to attain slot data
         dQm= Tx(1).dQ(ds);
                                % Training index (ds) to attain slot training symbols
         xI = kron(dIm,Tx(1).cI);
                                        % spread I arm, chip rate
         xQ = kron(dQm,Tx(1).cQ);
                                        % spread Q arm, chip rate, antenuated
         % Check for orthogonality for cI and cQ
         orthogonal=sum(Tx(1).cI+Tx(1).cQ);
                x = Tx(1).Wtx(m)*(xI+J*xQ);
% QPSK symbols to scramble, chip rate, power control
         %Scrambling Code
         sI = (m-1)*sys.Nm + Tx(1).sIp + (1:sys.Nm);
                                       % index I scrambling chip sequence for slot
```

```
sQ = (m-1)*sys.Nm + Tx(1).sQp + (1:sys.Nm);
                                % index Q scrambling chip sequence for slot m
 s1 = sys.s(sI) + J*sys.s(sQ);
                               % get scrambling sequence (The scrambling assigned for

y = s1.*x;
                                % complex scramble, chip rate
                                % initialise observed sequence
e = zeros(sys.Sm,sys.B);


% Diversity
% no diversity yet at this time
   for b=1:sys.B,
                                        % do for each antenna
    for p=1:Tx(1).P,                    % do for each multipath delay
      tau = Tx(1).tau(p);               % no delay first+Tx(1).delay;
      %      w = sqrt(sys.power(p));    % assume average power same on all ants
      sh = Tx(1).ho(p,b) + (m-1)*sys.Nm + (1:sys.Nm);
                                        % indexes of fading sequence
      h = sys.h(sh);                    % get path (p,b) fading profile, chip rat
      e(tau+(1:sys.S:sys.Sm),b)=e(tau+(1:sys.S:sys.Sm),b)+y.*h;% tx times channe
      [mf, vf] = gstat(h);
      ea2 = vf+mf;

      euf(tau+(1:sys.S:sys.Sm),b) = y;
      [meuf, veuf] = gstat(euf(:,1));
      eas = meuf+veuf;
      end;
   end;
 AveSigPwr = abs(eas / ea2);            %Average Signal Power per slot
   % Chip pulse shaping:
   % perform chip waveform convolution (after sum_k) since convolution is linear
   for b=1:sys.B,                       % each antenna
       eb = conv(e(:,b),sys.c);         % convolve with chip waveform
       e(:,b) = eb(sys.Q+(1:size(e,1)));
                                        % slide due to convolution
   end;
if run == 1
      Txsignal = store.Txsignal;
  store.Txsignal = [Txsignal,e];
end

%=====================================================
% Slot-by-Slot transmission - Multi-Access-Interference (MAI)
%=====================================================
       n = randn(size(e))+...
     sqrt(-1)*randn(size(e));           % generate complex AWGN of unit variance%

 No = 0;
 for k=1:K,
   % for every user calculate noise scaling factor to provide desired Eb/No ratio
```

```
        ecno=ebno/(sys.S*sys.B*Tx(1).N*Tx(1).n); % equal transmit power constraint
          Nok = 1/ecno;
                                        % Thermal noise variance per chip for single user
        No = Nok;
           %        end
           No2 = (No/(1*2))*AveSigPwr;
        if sys.pwr_ctrl == 1,
           % for case of perfect power control
                  No = 3^-1*No2/10;              % Noise power (watt)
                n = n*sqrt(No2/2);
        else
              No = 1/3*No2;                      % Noise power (watt)
        end;
        e = e + n;                               % add AWGN to rx samples
store.n = n; store.NoisePower(m,run) = No;
         [mn, var]=gstat(e(:,1));
          Le = length(e);
          AVE=sum(e.*conj(e))/Le;
          Ave1=mn+var;%
          AvePw = store.AvePw;
          store.AvePw = [AvePw,AVE];
          %=====================================================
         % Slot-by-Slot Receiver
         %=====================================================
    if run == 1
        Rxsignal = store.Rxsignal;
      store.Rxsignal = [Rxsignal,e];
   end
   [Rx,store] = slotreceiver(e,sys,Rx,store,Tx,run);
        %=====================================================
        % Slot-by-Slot Power Controller
        %=====================================================%

        if sys.pwr_ctrl > 1
          if sys.pwr_ctrl > 1
                  % power control step size in dB
                  G = 10^(GdB/10);
              g = Rx(1).SINRset/Rx(1).SINR;
              Tx(1).Wtx(m+1) = Tx(1).Wtx(m);       % assume no adjustment
                  if     g > G   Tx(1).Wtx(m+1) = G*Tx(1).Wtx(m);
                  elseif g < 1/G Tx(1).Wtx(m+1) = Tx(1).Wtx(m)/G;
                  end
                Rx(1).Wtx(m+1) = Tx(1).Wtx(m+1);  % copy to Receiver
              else
        % perfect power control
                  Tx(1).Wtx(m+1) = Tx(1).Wtx(m);  % amplification remains fixed
                  Rx(1).Wtx(m+1) = Tx(1).Wtx(m+1);% copy to Receiver
       end;
% Power Consumption   % Transmit Power
PControl = store.PControl; store.PControl = [PControl,
Rx(1).Wtx(m+1)]; store.PControl;
```

```
% Power Consumption    % Transmit Power
PComsump = store.PConsump; store.PConsump = [PComsump,
Rx(1).Wtx(m+1)];
end%
%
            Tx(1).Wtx(1) = Rx(1).Wtx(17);
            Rx(1).dI(1:100) = 1*Tx(1).dI(1:100); % give some symbols to Rx
% Check for Error
sum(gt(Rx(1).dI,0).*2-1==Tx(1).dI);

      %=====================================================
      % Frame Receiver
      %=====================================================
  d = Rx(1).dI;
   switch fec
        case 1
         d = d';
         b = Decide(d,0);                          % return uni-polar array of decisions
         Rx(1).b = b';                             % re-order rows and columns%%
         Err(1) = sum((Rx(1).b)~=(Tx(1).b))        % calculate bit errors
         case {4,5,6}
              d(Rx(1).I) = d; % De-interleaver
                M = fec - 2;
               Rc = 1/3;
                [Errs,store] = TurboMAP(M,Tx(1).Lu,IT,Rc,No,d,Tx(1).b,store,run);
                Err(1) = Errs(IT*2);
      end
   end;
```